

KU Leuven  
Biomedical Sciences Group  
Faculty of Pharmaceutical Sciences  
Department of Pharmaceutical and Pharmacological Sciences



# **SYNTHESIS AND BIOLOGICAL EVALUATION OF HETEROCYCLIC STRUCTURES TARGETING UNDEREXPLORED TARGETS**

Sven Verdonck

Jury:

Promoter: Prof. Piet Herdewijn

Co-promoter: Dr. Steven De Jonghe

Chair: Prof. Pieter Annaert

Jury members: Prof. Wim De Borggraeve

Prof. Matthias D'Hooghe

Prof. Christophe Pannecouque

Prof. Pieter Van Der Veken

Dissertation presented in  
partial fulfilment of the  
requirements for the  
degree of Doctor in  
Pharmaceutical Sciences

April 2020



KU Leuven

Groep Biomedische Wetenschappen

Faculteit Farmaceutische Wetenschappen

Departement Farmaceutische en Farmacologische Wetenschappen



# **SYNTHESE EN BIOLOGISCHE EVALUATIE VAN HETEROCYCLISCHE STRUCTUREN TEGEN WEINIG GEËXPLOREERDE DOELWITTEN**

Sven Verdonck

Promotor: Prof. Piet Herdewijn  
Co-Promotor: Dr. Steven De Jonghe

Proefschrift voorgedragen tot  
het behalen van de graad van  
Doctor in de Farmaceutische  
Wetenschappen

April 2020



## Acknowledgements

*Four years passed since I started my PhD adventure at the lab of medicinal chemistry at the KU Leuven and of course there are a lot of people with whom I shared bliss and sorrows. Therefore, some expressions of gratitude are in order.*

*First of all, I would like to thank **Prof. Piet Herdewijn** for giving me the overall opportunity to start doing a PhD in the lab under his guidance as promotor. I am also greatly indebted to **Dr. Steven De Jonghe**, who was invaluable and involved during all aspects of this journey. His knowledge of the subject of medicinal chemistry and guidance was instrumental to the successful completion of this thesis.*

*I would also like to thank my jury members **Prof. Matthias D'Hooghe**, **Prof. Wim De Borggraeve**, **Prof. Christophe Pannecouque** and **Prof. Pieter Van Der Veken** for extensively proofreading the thesis and being part of the examination committee.*

*Special thanks also go to **Prof. Eveline Lescrinier** and **Luc Baudemprez** for their help in recording and occasional interpretation of NMR spectra. I also thank **Prof. Jef Rozenski** for the mass spectra measurement. I am also indebted to the group of **Prof. Shirit Einav** of the University of Stanford, the group of **Prof. Christa Müller** of the University of Bonn as well as the group of **Prof. Dominique Schols** of the KU Leuven for performing the biological testing of the synthesized compounds.*

*During my stay in the lab of medicinal chemistry, I have come to meet a lot of different people. The first year when I started was the year before we moved to our new building in Gasthuisberg and we were still stationed in the city center in the Minderbroederstraat. I was allowed to start my PhD in the tower at IVAP, the place of the gods (dubbed by **Dr. Piotr Leonczak**) where I was told that I needed to obtain a scholarship to further pursue this career step. A month of studying and general overconfidence in my abilities were quickly crushed by the weekly IWT 'drilling' sessions a.k.a. torture sessions where a lot of sweat was produced and expelled. These were followed by the never ending amusement of my fellow IWT scholar and former torture victim **Dr. Randy Wouters**. Nevertheless, they proved extremely useful as I was able to obtain the scholarship. Therefore I would like to profusely thank all members of IVAP for either taking part in the sessions or for comforting me afterwards: **Dr. Bart Vanderhoydonck**, **Dr. Ling-Jie Gao**, **Dr. Piotr Leonczak**, **Dr. Qiuya Huang**, **Dr. Thierry Louat**, **Dr. Jean Herman**, **Dr. Kristien Van Belle**, **Dr. Yuan Lin** and **Dr. Nastia Parchina**.*

*Because of our isolation in the place of the gods, we rarely came into contact with our colleagues at the Rega institute or N-Blok but thankfully the yearly Christmas party brought change. At this party, my fellow Belgian PhD Students **Dr. Randy Wouters**, **Donaat Kestemont**, **Michiel Vanmeert** and me started forging a tight group which was the starting point of the 'Doctoral Meat-up' which took place monthly (at first just dinner, then talk sessions for our depressions).*

A year into my PhD, the group was expanded with a long lost son who did his first year at the chemistry department **Dries De Ruyscher** and PhD freshman **Charles-Alexandre Mattelaer**. At this point, I would like to thank these five who I can call my friends by now.

A year passed by and then the move came along. This brought us all closer together as all three buildings were now merged on two very connected floors. This change of base brought with it a new office with some new office members. I very much enjoyed our time together in the office and I will take this time to thank **Dr. Puneet Srivastava** and **Dr. Henri-Philippe Mattelaer** for the challenging and nice chemistry discussions (and the occasional card game). I also thank **Dr. Xiaochen Li** for the funny interjections. I also thank my additional lab members **Dr. Shrinivas Dumbre**, **Dr. Elisabetta Groaz** and **Dr. Mikhail (Misha) Abramov** for the nice times and the listening ear in the lab.

I would also like to express my gratitude to **Dr. Joleen Masschelein**, **Dr. Damian Ploschik**, **Shamal Whitanage**, **Paola Handal**, **Prof. Vitor Bernardes Pinheiro** and **Hoai Nguyen** for the daily lunch sessions, to **Guy Schepers** and **Santiago Chaillou** for always being cheerful and optimistic about everything.

Thanks also goes to my other (ex-)colleagues **Dr. Bharat Gadakh**, **Dr. Manesh Nautiyal**, **Dr. Min Luo**, **Dr. Chao Liu**, **Dr. Mengmeng Wang**, **Dr. Jakub Modranka**, **Dr. Paulina Bartos**, **Dr. Peng Nie**, **Qinfeng Li**, **Dr. Junjun Tian**, **Zihua Zheng**, **Dr. Baole Zhang**, **Stijn Lenders**, **Eline Goffin**, **Yuqing Xu**, **Xinlu Li**, **Nikolaos Papastavrou**, **Dr. Belén Martínez Gualda**, **Fabio Da Paixao Soares**, **Dr. Elena Eremeeva**, **Dr. Elzbieta Plebanek**, **Niklas Freund**, **Dr. Marta Gascon**, **Weijie Gu**, **Dr. Rahul Shivaji Patil**, **Dr. Swarup De**, **Hui Yang**, **Dr. Sambasiva Rao Pillalamarri** and **Dr. Kiran Kumar Yalla**.

Many thanks go to **Inge Aerts**, **Cathy De Meyer**, **Christiane Callebaut**, **Patrick Briers**, **Dominique Brabants** and **Myriam Cornelis** for the excellent secretarial work. I would also like to thank **Chantal Biernaux** for the excellent care of the administrative procedures necessary for being part of the lab.

In this last part, I would like to thank all my friends for their support, care, holidays and for providing a listening ear during the past 4 years.

I am also deeply grateful to my girlfriend, **Iris**, for always being there to support me during the good and the bad lab days and further along during the up and downs in thesis-writing. Thank you for your love and support.

Last but not least, I thank my family for their constant support and love since the beginning of my life, for all the opportunities they gave me and for all things they did for me.

In short, thank you all!!!

## Summary

Tremendous improvements in the field of genomics and molecular biology have accelerated the identification of various targets that can be used in drug discovery programs. Over 22000 genes were identified after sequencing of the human genome from which an estimated 5000 have a disease modulating effect. This paved the way for the design and synthesis of drugs against a selected target, instead of relying on the desired effect as in a phenotypic screening. However, only a fraction of the estimated available targets has been explored and is currently pursued as drug target. In this PhD thesis, the synthesis and biological evaluation of small molecule ligands for three underexplored targets is described.

In **Chapter 2**, adaptor protein 2 associated kinase 1 (AAK1) was chosen as a target for the development of antiviral agents. AAK1 plays a crucial role in the regulation of the clathrin mediated endocytosis, which is an integral part of the viral lifecycle of several unrelated viruses like dengue virus and Ebola virus. Since AAK1 is a host protein, AAK1 inhibitors offer the possibility of developing broad spectrum antivirals, and, in addition, the emergence of resistance is less of an issue. A known pyrrolo [2,3-*b*]pyridine analogue was selected as starting point for an optimization campaign for increasing its potency in both the binding and *in vitro* antiviral assay against the dengue and Ebola virus. Furthermore, it was demonstrated that AAK1 inhibition was an important mechanism in the antiviral activity of these compounds. These findings establish the potential of AAK1 inhibitors as treatment of currently untreatable viral threats.

**Chapter 3** relied on Mas-related gene receptor X2 (MRGPRX2) as the target of choice. This G-protein coupled receptor (GPCR) is primarily expressed in the dorsal root ganglia and on mast cells. Stimulation of MRGPRX2 leads to an IgE-independent degranulation of mast cells. Therefore, MRGPRX2 antagonists hold promise for the treatment of various allergic diseases like asthma and chronic urticaria. A compound library of over 1600 heterocycles was screened for MRGPRX2 antagonistic activity yielding four hits based on a benzo[4,5]imidazo[1,2-*a*]pyrimidin-4(10*H*)-one scaffold. These hits were systematically optimized to increase their potency as MRGPRX2 antagonists, affording three new analogues with activity in the low nanomolar range.

Finally, **Chapter 4** introduced the cluster chemokine receptor 8 (CCR8) as drug target. This GPCR is involved in the migration of immune cells (especially regulatory T-cells) to infection hearths. CCR8 is unique amongst its peers that it is the sole receptor for CCL1. Furthermore, it has been established that CCR8 inhibition in the tumor microenvironment correlates with an increased survival of cancer patients. In contrast, in the mouse encephalitis model, a generally accepted *in vivo* model for multiple sclerosis, administration of CCL1 and subsequent activation of CCR8 suppresses this autoimmune disease, underpinning the role of CCR8 in autoimmune modulation. Therefore, a known CCR8 agonist with moderate CCR8 affinity was subjected to a systematic optimization in order to increase its potency in the CCR8 binding and calcium mobilization assay.

## Samenvatting

Enorme vooruitgangen op het gebied van genomics en moleculaire biologie hebben de identificatie van verscheidene doelwitten die gebruikt kunnen worden in het ontdekken van geneesmiddelen, versneld. Meer dan 22000 genen werden geïdentificeerd na de sequentieanalyse van het menselijk genoom waarvan er ongeveer 5000 een rol spelen in verschillende pathologiën. Dit heeft geleid tot het ontwerp en synthese van moleculen die gericht zijn tegen een gekozen doelwit in plaats van te rekenen op een gewenst effect zoals in fenotypische screening. Toch wordt maar een kleine fractie van het totaal aantal doelwitten effectief gebruikt als doelwit voor geneesmiddelen. In deze doctoraatsthesis wordt bijgevolg de synthese en biologische evaluatie van kleine moleculen tegen een aantal weinig onderzochte doelwitten beschreven.

In **Hoofdstuk 2** werd het adaptor proteïne 2 geassocieerde kinase 1 (AAK1) gekozen als doelwit voor de ontwikkeling van antivirale middelen. AAK1 is een cruciale regulator van clathrine gemedieerde endocytose, wat een belangrijke rol speelt in de levenscyclus van een aantal niet-gerelateerde virussen zoals het dengue virus en ebola virus. Daarenboven is AAK1 een cellulaire gastheer factor wat ervoor zorgt dat AAK1 inhibitoren onderzocht kunnen worden als breed spectrum antivirale middelen. Bovendien leidt de toediening van AAK1 inhibitoren minder snel tot de ontwikkeling van resistentie. Een gekend analoog gebaseerd op een pyrrolo[2,3-*b*]pyridine kern werd gekozen als startpunt voor de optimalisatie van zowel de bindingsaffiniteit als de antivirale eigenschappen tegen het dengue virus en ebola virus. Voorts werd aangetoond dat AAK1 inhibitie een belangrijke rol speelt in de antivirale activiteit van deze producten. Deze bevindingen tonen het nut aan van AAK1 inhibitoren voor de behandeling van virale infecties die actueel niet te behandelen zijn.

**Hoofdstuk 3** bracht Mas-related gene receptor X2 (MRGPRX2) naar voren als doelwit proteïne. Deze GPCR komt hoofdzakelijk tot expressie in dorsale ganglia en mastcellen. Stimulatie van MRGPRX2 IgE-onafhankelijke degranulatie van de mastcellen. Bijgevolg zijn MRGPRX2 antagonisten potentieel nuttig voor de behandeling van verschillende allergische aandoeningen zoals astma en chronische netelroos. Een collectie van 1600 heterocyclische verbindingen werd gescreend als potentiële MRGPRX2 antagonisten. Hieruit kwamen vier verbindingen naar voren, allen gebaseerd op een benzo[4,5]imidazo[1,2-*a*]pyrimidin-4(10*H*)-one skelet. Deze hits werden vervolgens systematisch geoptimaliseerd met als bedoeling hun ter verhoging van hun activiteit als MRGPRX2 antagonisten. Dit leverde drie producten op met een laag nanomolaire activiteit.

Tenslotte werd in **Hoofdstuk 4** de cluster chemokine receptor 8 (CCR8) bestudeerd als doelwit. Deze GPCR is betrokken bij de migratie van immuun cellen (vooral regulatoire T-cellen) naar infectiehaarden. CCR8 is de enige receptor die CCL1 kan activeren wat hem uniek maakt onder de chemokine receptoren. Bovendien werd aangetoond dat CCR8 inhibitie in het tumor micromilieu een verhoogde kans geeft op overleving in kankerpatiënten. De toediening van CCL1, daarentegen, in het muis encefalitis model, een algemeen aanvaard *in vivo* model voor multiple sclerose, leidt tot



immunosuppressie en een verbetering van deze autoimmuun aandoening. Dit bevestigt de cruciale rol van CCR8 in de modulatie van immuunsuppressie. Met de bedoeling om nieuwe en potente CCR8 agonisten te ontdekken, werd een gekende CCR8 agonist met een matige CCR8 affiniteit onderworpen aan een systematische studie om zowel de bindingsaffiniteit als de werkzaamheid in de calcium mobilisatie testen te verhogen.

## Abbreviation List

5-HT	Serotonin
AAK1	Adaptor protein 2 associated kinase
Ab	Antibody
ACKR4	Atypical chemokine receptor 4
ADE	Antibody dependent enhancement
ADME	Absorption, distribution, metabolism, excretion
AF647	AlexaFluor™ 647
AP1-5	Adaptor protein 1-5
AP1M1	$\mu_1$ subunit of AP1
AP2M2	$\mu_2$ subunit of AP2
ASCH	Activation-segment C-terminal helix
BIKE	BMP-2 inducible kinase
BOP	Benzotriazol-1-yloxytris(dimethylamino)phosphonium hexafluorophosphate
BRET	Bioluminescence resonance energy transfer
BTK	Bruton's tyrosine kinase
C	Capsid protein
CC <sub>50</sub>	Half maximal cytotoxic concentration
CCR8	Cluster Chemokine Receptor 8
CCV	Clathrin coated vesicles
CHIKV	Chikungunya Virus
CME	Clathrin mediated endocytosis
COPD	Chronic obstructive pulmonary disease
CPME	Cyclopentylmethylether
CT	Clathrin triskelia
DARC	Duffy antigen/chemokine receptor
DENV	Dengue Virus
DIBAL	Diisobutylaluminium hydride
DMF	<i>N,N</i> -Dimethylformamide
DMSO	Dimethylsulfoxide
DRG	Dorsal root ganglion
E	Envelope protein
EBOV	Ebola Virus
EC <sub>50</sub>	Half maximal effective concentration
EC <sub>90</sub>	90% effective concentration
FBS	Fetal bovine serum
FLIPR	Fluorescence imaging plate reader
FRET	Fluorescence resonance energy transfer
GAK	Cyclin G-associated kinase
GPCR	G protein coupled receptor
GRK	G protein coupled receptor kinase
HCV	Hepatitis C virus
HEPES	4-(2-Hydroxyethyl)-1-piperazineethanesulfonic acid
HTRF	Homogenous time resolved fluorescence
HTS	High throughput screening
IC <sub>50</sub>	Half maximal inhibitory concentration
IgD	Immunoglobulin D
IgE	Immunoglobulin E
IgM	Immunoglobulin M
IP <sub>3</sub>	Inositol triphosphate
JAK3	Janus kinase 3
JAK-STAT	Janus Kinase - Signal transducer and activator of transcription proteins
K <sub>D</sub>	Dissociation constant

KOtBu	Potassium <i>tert</i> -butoxide
M	Membrane protein
MC	Mast cell
MC <sub>T</sub>	Tryptase containing mast cell
MC <sub>TC</sub>	Tryptase and chymase containing mast cell
MDDC	Monocyte derived dendritic cell
MgATP	Magnesium bound ATP
MOI	Multiplicity of infection
MPSK1	myristoylated and palmitoylated serine-threonine kinase 1
MRGPR	Mas-related gene receptor
NAK	NUMB-associated kinase
NBS	<i>N</i> -bromosuccinimide
NIS	<i>N</i> -iodosuccinimide
NMP	<i>N</i> -methyl pyrrolidinone
PAMPA	Parallel artificial membrane permeability assay
PBS	Phosphate buffered saline
PI(4,5)P <sub>2</sub>	Phosphatidylinositol (4,5)-bisphosphate.
PIP <sub>4</sub>	Phosphatidylinositol-4-phosphate
<i>p</i> NA	<i>Para</i> -nitroaniline
prM	Proto membrane protein
S Scores	Selectivity scores
SAR	Structure-Activity relationship
SNSR	Sensory neuron specific receptor
THF	tetrahydrofuran
TLR	Toll-like receptor
T <sub>reg</sub>	Regulatory T-cell
WHO	World Health Organization
WNV	West Nile virus
ZIKV	Zika virus

**TABLE OF CONTENTS**

<b>Acknowledgements</b> .....	<b>I</b>
<b>Summary</b> .....	<b>III</b>
<b>Samenvatting</b> .....	<b>V</b>
<b>Abbreviation list</b> .....	<b>VII</b>
<b>CHAPTER 1: GENERAL INTRODUCTION</b> .....	<b>1</b>
1.1. THE DRUG DISCOVERY PROCESS .....	1
1.1.1. <i>The classical process</i> .....	1
1.1.2. <i>Screening methods</i> .....	1
1.2. TARGETS IN DRUG DISCOVERY AND TARGET SELECTION IN THIS THESIS .....	2
1.2.1. <i>What are targets?</i> .....	2
1.2.2. <i>Kinases</i> .....	3
1.2.2.1. Adaptor-associated kinase 1 (AAK1) .....	5
a. AAK1 enzyme.....	5
b. The clathrin mediated endocytosis pathway .....	6
c. Adaptor proteins as key regulators of clathrin-mediated endocytosis .....	7
d. Dengue virus (DENV) and transmission.....	8
e. DENV lifecycle and genome .....	8
f. Dengue illness and current treatment.....	9
g. AAK1 inhibitors.....	10
1.2.3. <i>G-protein coupled receptors</i> .....	11
1.2.3.1. Mas-related gene receptor X2 (MRGPRX2).....	13
a. Mas-related gene (MRGPR) receptor family .....	13
b. Mast cells and MRGPRX2.....	14
c. Allergic diseases and MRGPRX2.....	15
d. Ligands and coupling mechanism of MRGPRX2.....	15
1.2.3.2. Cluster chemokine receptor 8 (CCR8).....	17
a. Chemokines and their receptors .....	17
b. CCL1 and CCR8 .....	17
c. Small molecule CCR8 agonists and antagonists .....	18
1.3. OBJECTIVES.....	19
1.4. REFERENCES.....	21
<b>CHAPTER 2: SYNTHESIS AND STRUCTURE-ACTIVITY RELATIONSHIPS OF 3,5-DISUBSTITUTED-PYRROLO[2,3-B]PYRIDINES AS INHIBITORS OF ADAPTOR ASSOCIATED KINASE 1 (AAK1) WITH ANTIVIRAL ACTIVITY</b> .....	<b>25</b>
2.1. INTRODUCTION.....	25
2.2. SYNTHESIS OF PYRROLO[2,3-B]PYRIDINE ANALOGUES.....	26

2.3.	KINASE PROFILING AND X-RAY CRYSTALLOGRAPHY OF COMPOUND <b>1.15</b> .....	30
2.4.	STRUCTURE-ACTIVITY RELATIONSHIP (SAR) STUDY .....	32
2.4.1.	<i>SAR at position 5 of the 7-aza-indole scaffold</i> .....	33
2.4.2.	<i>SAR of the N-acyl moiety</i> .....	34
2.4.3.	<i>SAR of the linker moiety at position 3</i> .....	35
2.4.4.	<i>SAR of phenylacetylene</i> .....	36
2.4.5.	<i>Scaffold modifications</i> .....	37
2.5.	BROAD-SPECTRUM ANTIVIRAL ACTIVITY .....	38
2.5.1.	<i>Correlation of the antiviral effect with functional AAK1 inhibition</i> .....	39
2.5.2.	<i>Inhibition of DENV infection in human primary monocyte-derived dendritic cells</i> .....	40
2.6.	KINASE SELECTIVITY .....	41
2.7.	CONCLUSIONS .....	42
2.8.	EXPERIMENTAL SECTION .....	43
2.8.1.	<i>Chemistry</i> .....	43
2.8.1.1.	Synthesis of key intermediate <b>2.4</b> .....	43
2.8.1.2.	Synthesis of 3-nitro-5-aryl-pyrrolo[2,3- <i>b</i> ]pyridines ( <b>2.5a-h</b> ) .....	44
2.8.1.3.	Synthesis of 5-aryl-3-amino- and 5-aryl-3- <i>N</i> -acylamino pyrrolo[2,3- <i>b</i> ]pyridines ( <b>2.6a-f</b> and <b>2.7a-o</b> ).....	46
2.8.1.4.	Synthesis of 5-(3,4-dimethoxyphenyl)-3- <i>N</i> -acylamino pyrrolo[2,3- <i>b</i> ]pyridines .....	49
2.8.1.5.	Synthesis of 3-alkynyl-5-bromo-pyrrolo[2,3- <i>b</i> ]pyridines ( <b>2.19a-f</b> ) .....	54
2.8.1.6.	Synthesis of 3-alkynyl-5-(3,4-dimethoxyphenyl)-pyrrolo[2,3- <i>b</i> ]pyridines ( <b>2.20a-f</b> )56	
2.8.2.	<i>Binding-displacement assay for NAK family selectivity</i> .....	61
2.8.3.	<i>Biological assays</i> .....	62
2.8.3.1.	AAK1 expression, purification and crystallization.....	62
2.8.3.2.	Data collection, structure solution and refinement .....	62
2.8.3.3.	Virus construct .....	62
2.8.3.4.	Cells .....	63
2.8.3.5.	Virus Production .....	63
2.8.3.6.	Infection assays .....	63
2.8.3.7.	Viability assays .....	63
2.8.3.8.	Effect of compounds <b>1.15</b> , <b>2.7g</b> and <b>2.20b</b> on AP2 phosphorylation .....	64
2.8.4.	<i>Binding assays</i> .....	64
2.8.4.1.	AAK1 LanthaScreen™ Eu binding assay.....	64
2.8.4.2.	AAK1 K <sub>D</sub> assay.....	64
2.8.4.3.	Kinase Selectivity assay.....	64
2.8.5.	<i>Statistical analysis</i> .....	65

2.8.6.	<i>General safety aspects</i> .....	65
2.9.	REFERENCES.....	66
<b>CHAPTER 3: SYNTHESIS AND STRUCTURE-ACTIVITY RELATIONSHIP STUDIES OF BENZO[4,5]IMIDAZO[1,2-A]PYRIMIDIN-4(10H)-ONES AS MAS-RELATED GENE RECEPTOR X2 ANTAGONISTS .....</b>		
3.1.	INTRODUCTION.....	69
3.2.	SYNTHESIS OF BENZO[4,5]IMIDAZO[1,2-A]PYRIMIDIN-4(10H)-ONE ANALOGUES .....	70
3.2.1.	<i>Structural modifications on the pyrimidine moiety</i> .....	70
3.2.2.	<i>Structural modifications on the benzo moiety</i> .....	71
3.3.	STRUCTURE-ACTIVITY RELATIONSHIP STUDY .....	72
3.3.1.	<i>SAR of the pyrimidine moiety</i> .....	73
3.3.2.	<i>SAR of the benzo moiety</i> .....	75
3.4.	CONCLUSION .....	77
3.5.	EXPERIMENTAL SECTION .....	77
3.5.1.	<i>Chemistry</i> .....	78
3.5.1.1.	Synthesis of 2-alkyl-3-oxoesters .....	78
3.5.1.2.	Synthesis of benzyl-protected 1,2-diaminophenyl derivatives .....	79
3.5.1.3.	Synthesis of 2-aminobenzimidazole derivatives .....	81
3.5.1.4.	Synthesis of 6,(7)-(di)substituted-imidazo[1,2- <i>a</i> ]pyrimidin-5(8H)-ones and 2,(3)-(di)substituted-benzo[4,5]imidazo[1,2- <i>a</i> ]pyrimidin-4(10H)-ones .....	82
3.5.2.	<i>β-arrestin assay</i> .....	85
3.5.3.	<i>General safety aspects</i> .....	86
3.6.	REFERENCES.....	87
<b>CHAPTER 4: SYNTHESIS AND STRUCTURE ACTIVITY RELATIONSHIP STUDIES OF CLUSTER CHEMOKINE RECEPTOR 8 AGONISTS .....</b>		
4.1.	INTRODUCTION.....	89
4.2.	SYNTHESIS OF PHENOXYBENZYL ANALOGUES AS CCR8 AGONISTS.....	90
4.3.	BIOLOGICAL EVALUATION .....	92
4.3.1.	<i>Principle of the assays</i> .....	92
4.3.2.	<i>Structure-activity relationship study</i> .....	93
4.4.	CONCLUSION .....	97
4.5.	EXPERIMENTAL PART .....	98
4.5.1.	<i>Chemistry</i> .....	98
4.5.1.1.	Synthesis of Boc protected ethyl carbamates .....	98
4.5.1.2.	Synthesis of phenoxybenzyl-amine analogues.....	100
4.5.1.3.	Synthesis of phenoxybenzylpyrrolidine-amide derivatives .....	102
4.5.1.4.	Synthesis of phenoxybenzylpyrrolidine urea derivatives.....	104

4.5.1.5. Synthesis of phenoxybenzylpiperazine analogues .....	106
4.5.1.6. Synthesis of phenoxybenzylpiperazine urea analogues .....	109
4.5.2. <i>Biological assays</i> .....	110
4.5.3. <i>General safety aspects</i> .....	111
4.6. REFERENCES.....	113
<b>CHAPTER 5: GENERAL DISCUSSION AND FUTURE PERSPECTIVES .....</b>	<b>115</b>
5.1. GENERAL DISCUSSION.....	115
5.2. REFERENCES.....	121
<b>CHAPTER 6: SCIENTIFIC ACKNOWLEDGEMENTS, PERSONAL CONTRIBUTION AND CONFLICT OF INTEREST STATEMENT.....</b>	<b>123</b>
6.1. SCIENTIFIC ACKNOWLEDGEMENTS .....	123
6.2. PERSONAL CONTRIBUTION .....	123
6.3. CONFLICT OF INTEREST STATEMENT.....	123





## Chapter 1: General introduction

### 1.1. The drug discovery process

#### 1.1.1. The classical process

The development of a drug is a complicated practice that is considered a high-risk, high-reward process, due to the enormous financial investments and the substantial amount of time that is needed to market a drug. The drug discovery process is split into several phases: hit identification, hit-to-lead and lead optimization, preclinical evaluation, clinical trials and finally marketing (**Figure 1.1**). The choice of a suitable target is of critical importance for a drug program to be successful. The major reasons that drug fail during clinical trials are toxicity and/or lack of efficacy.

Different available options can be tapped with the intention of launching a new drug discovery campaign to elucidate biologically active compounds. Through scientific or patent literature or by using virtual screening methods, potential hit compounds can be identified. However, a drug discovery project usually commences with high-throughput screening (HTS) of compound libraries in an appropriate assay. Either a phenotypic or a target-based screening strategy is followed.<sup>1</sup> A recent analysis demonstrated that first-in-class medicines are usually discovered by a phenotypic drug discovery strategy, whereas target-based assays showed supremacy for the development of follower drugs.<sup>2</sup>

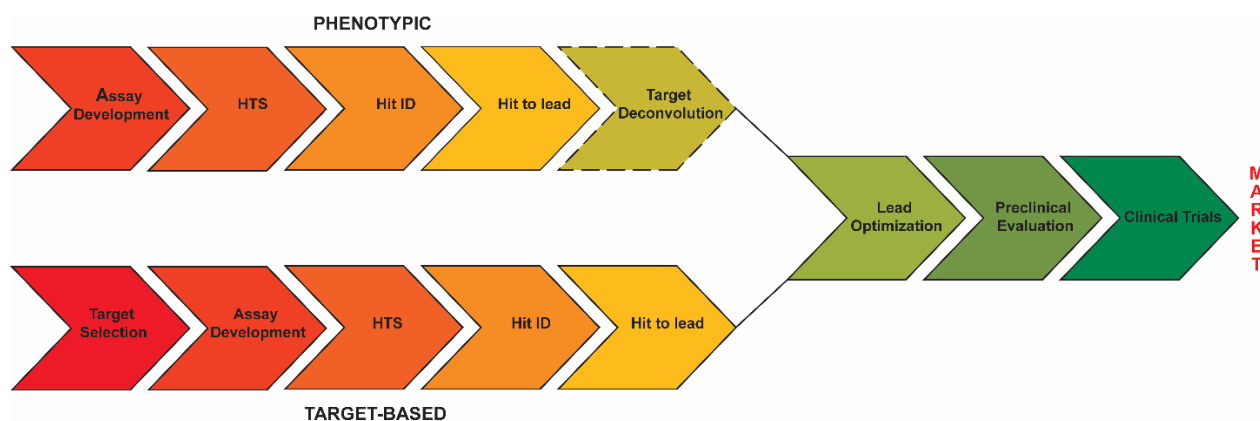


**Figure 1.1.** The drug discovery process

#### 1.1.2. Screening methods

##### a) Phenotypic-based screening

The phenotypic design is the oldest strategy used in drug discovery and has been thriving for many years. The basic concept is the development of an assay that displays a certain phenotype (e.g. killing of bacteria). These assays do not necessitate prior knowledge of the molecular mechanism of action, although this can be optionally deconvoluted later on.<sup>2</sup> Translation into therapeutic impact in a given pathologic phenotype can be achieved more effectively through activity observed in a phenotypic assay

than through a more artificial target-based assay. Additionally, bias towards a particular molecular target is avoided in cellular assays and these assays are therefore not limited to the identification of inhibitors of a specific protein or pathway, but instead may target any key player involved.<sup>1,3</sup> Although phenotypic assays are very powerful, because the starting point is based on a known, clinically relevant, effect and not on the hypothetical involvement of a protein in disease pathology, it has some drawbacks. These include the lack of knowledge of the exact mode-of-action, and the inability to assemble a focused screening library due to the lack of target knowledge.<sup>1,4</sup>

### *b) Target-based design<sup>2</sup>*

The identification of novel druggable targets that play a key role in disease development was significantly advanced by the tremendous improvements in genomics and molecular biology in the 1990's. More than 22,000 human genes emerged<sup>5</sup> after the decoding of the human genome of which an assumed 1,000 are directly involved in the pathogenesis of several diseases. Furthermore, because some of these 1000 genes cannot be modulated directly, they are investigated further through their connection to downstream proteins, therefore coming to the assumption of at least 5,000 – 10,000 susceptible targets for drug design.<sup>6</sup> Keeping both assumptions in mind, modulation of target activity, either directly or indirectly by targeting one of their downstream proteins, offers a rationale to set up new drug discovery programs. A specific biological hypothesis is generated by this target-centric approach and this can subsequently be used as a starting point for the identification of molecules that interact with the target of interest. In the past twenty years, molecular target-based drug screening evolved as the drug discovery concept of choice used in both the pharmaceutical industry and academic laboratories.<sup>1</sup> The fundamental idea of this approach is the development of clinically relevant *in vitro* assays and animal models to essentially validate the target as being druggable and safe.<sup>7</sup> The main disadvantages of target-based design is the bias towards a particular target and the occasional untranslatability to a certain phenotype.<sup>1,3</sup> Despite these challenges, target-based design remains a formidable technique for the future development of drugs.

## **1.2. Targets in drug discovery and target selection in this thesis**

### **1.2.1. What are targets?**

A target can be defined as a single gene, a gene product, a phenotype or a molecular mechanism previously pinpointed based on biological observations and genetic analysis. They can be sorted into two categories: genetic targets and mechanistic targets. Genetic targets are described as mutations within a gene or gene product that leads to the development of specific diseases or increases the likelihood of developing a certain pathological condition.<sup>4</sup> They are validated quite easily through the use of transgenic animals with the observed mutation implemented in their genome. In contrast are the mechanistic targets, usually enzymes, receptors and other gene products which are not genetically different from the normal healthy population. In contrast to the genetic targets are mechanistic targets.

These targets include receptors, genes and enzymes. that play a causative role in a pathological state (e.g. overexpression of HER-2 in breast cancer).<sup>4,8</sup> These targets only emerge through biological observation in a given disease state as their genetic make-up does not differ from the healthy population and their validation is therefore more complex.<sup>4</sup> Over the course of history, an abundant number of targets belonging to both classes have been identified and validated with great success. As of 2017, a total of 695 human targets and 198 microbiological targets are exploited by over 1500 approved drugs for a variety of clinical effects.<sup>9</sup>

### 1.2.2. Kinases

Kinases are the second most explored group of drug targets, following the G-protein coupled receptors (GPCRs), as it has been estimated that one third of target-based drug discovery programs in pharmaceutical industry focus on kinases.<sup>10</sup> The human kinome consists of over 500 members which are phylogenetically classified into nine groups. This resulted in the development of the kinome tree (Figure 1.2).

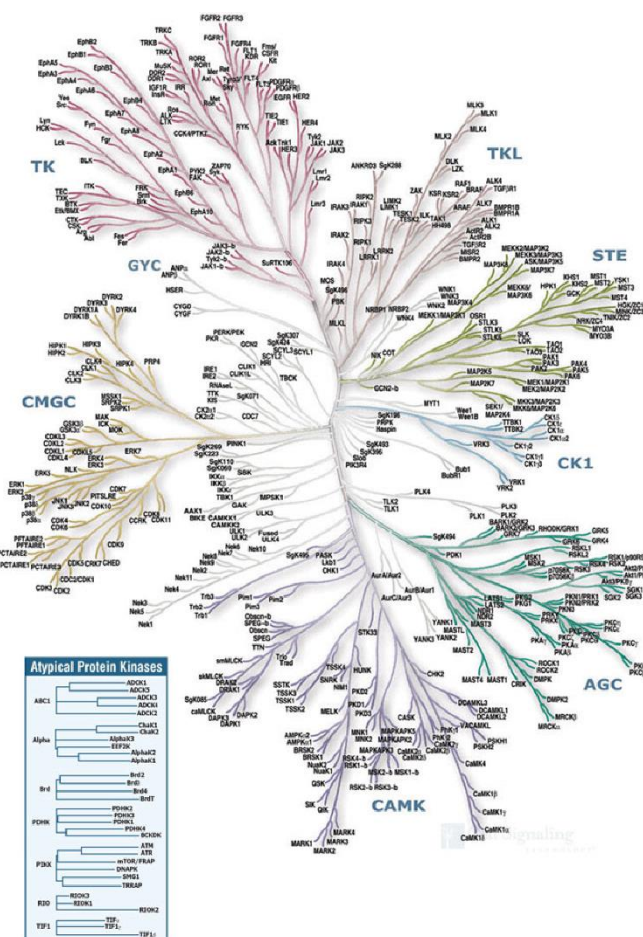


Figure 1.2. Kinome tree.<sup>11</sup>

Kinases can be divided into four groups according to their substrate specificity: tyrosine kinases, serine/threonine kinase, dual specificity kinases and small molecule (lipid or sugar) kinases.<sup>12</sup> The main function of kinases is the phosphorylation of their target proteins on a specific amino acid within the sequence. They achieve this goal by using the  $\gamma$ -phosphate of magnesium bound ATP (MgATP), often

in response to an external stimulus. This phosphorylation usually activates the target protein to exert its cellular function, while the phosphatases dephosphorylate the target protein and suppress this function. This phosphorylation-dephosphorylation cycle tightly regulates the function of cellular proteins.

The huge interest in kinase research led to the marketing approval of 48 small molecule kinase inhibitors, of which 43 are used as drugs for the treatment of malignant tumors ranging from breast cancer to acute myelogenous leukemia.<sup>13</sup> The majority of the currently approved kinase inhibitors target tyrosine kinases (**Figure 1.3**) that consist of 90 members and represent around 17% of the total human kinome. Additionally, 64% of the approved kinase inhibitors acts as multitarget drugs, having little to no selectivity towards a specific kinase. This is attributed to the highly conserved MgATP binding site, where the phosphate transfer occurs, across the kinome, which is the binding pocket for the majority of small-molecule kinase inhibitors. This transfer can happen either directly from MgATP to the target protein (ternary mechanism) or via a phosphoenzyme intermediate (ping-pong mechanism).<sup>14</sup> The success of kinase inhibitors in oncology field is due to the essential role of kinases in regulating intracellular signal transduction and to the ability of protein kinases to regulate cell life by phosphorylating specific proteins.

The remaining 83% of the human kinome has been sparsely explored as drug target. The availability of potent and selective inhibitors of underexplored kinases will allow to study the role of the kinases in different disease areas outside of the oncology field.<sup>13</sup> Especially for auto-immune diseases, several kinases (such as JAK3 and BTK) are being targeted for the treatment of rheumatoid arthritis.<sup>15</sup> Recently, kinases have been identified as regulators of viral infection.<sup>16,17</sup> and therefore the adaptor-associated kinase 1 (AAK1) was pursued as an underexplored antiviral drug target in this PhD thesis.

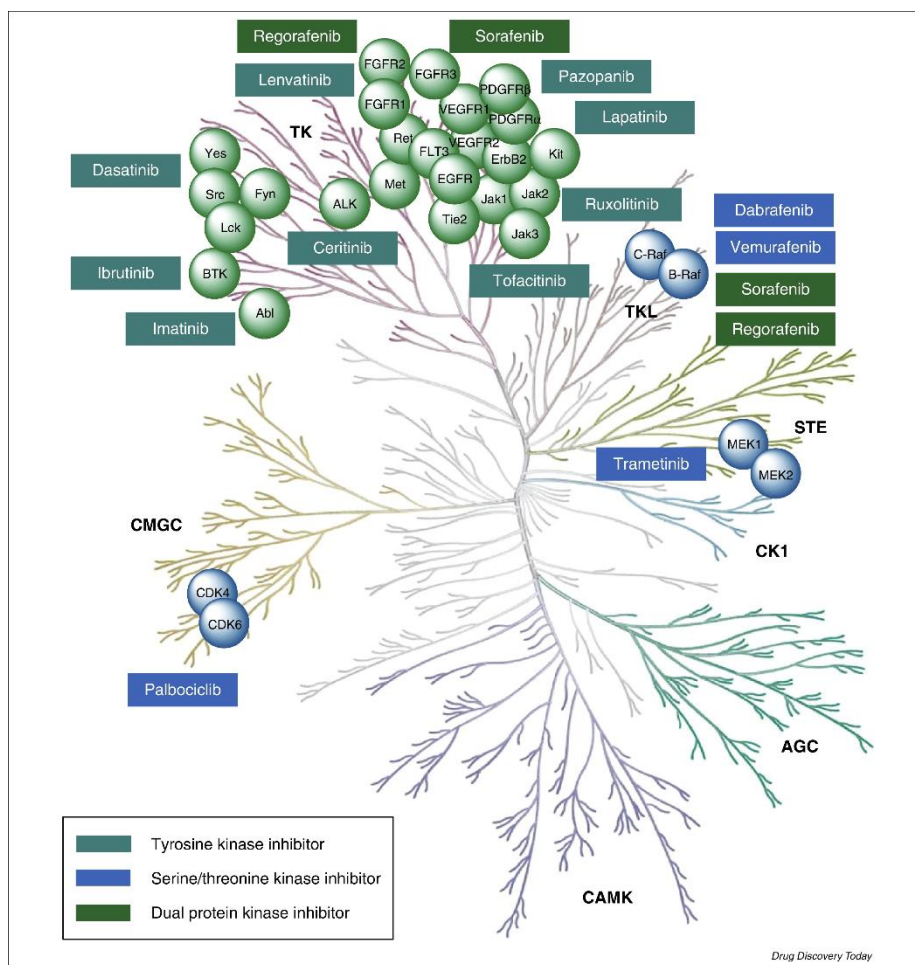


**Figure 1.3.** Current targeted kinases (Figure taken from Wu et al., 2016)<sup>18</sup>

### 1.2.2.1. Adaptor-associated kinase 1 (AAK1)

#### a. AAK1 enzyme

AAK1 is a member of the NUMB-associated kinase (NAK) family, along with cyclin G associated kinase (GAK), BMP-2-inducible kinase (BIKE) and myristoylated and palmitoylated serine/threonine kinase 1 (MPSK1). Despite sharing a similar serine/threonine kinase motif, the NAK family is structurally diverse and exhibits a myriad of downstream effects.<sup>19</sup> AAK1 functions as a key regulator in clathrin mediated endocytosis (CME) through phosphorylation of adaptor protein 2 (AP2) which recognizes cargo proteins and recruits clathrin triskelia (CT). Known broad spectrum kinase inhibitors and approved anticancer drugs erlotinib (**1.1, Figure 1.4**) and sunitinib (**1.2, Figure 1.4**) have potent off-target GAK ( $K_D = 3.1$  nM) and AAK1 ( $K_D = 11$  nM) activity, respectively.<sup>16</sup> Both drugs display *in vitro* antiviral activity against distinct viruses such as hepatitis C virus (HCV), dengue virus (DENV), Chikungunya virus (CHIKV), Zika virus (ZIKV), West Nile virus (WNV) and Ebola virus (EBOV). Combination therapy of both inhibitors protected mice from mortality and morbidity associated with EBOV and DENV infections.<sup>16</sup>

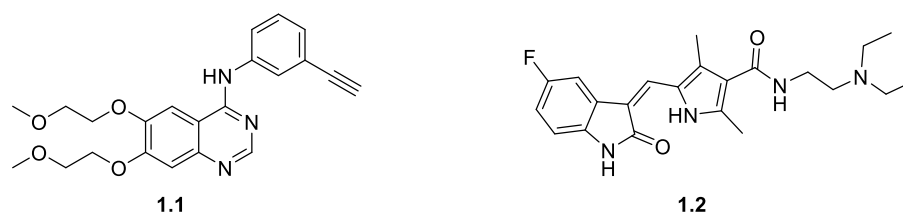


**Figure 1.4.** Structures of erlotinib (**1.1**) and sunitinib (**1.2**)

These data effectively demonstrate that small molecule inhibitors targeting AAK1 and GAK have the potential to act as broad spectrum antiviral agents. However, both erlotinib and sunitinib display little kinase selectivity as they both inhibit an array of other host kinases potentially leading to off-target side effects. Therefore, the need for a selective AAK1 inhibitor, to effectively probe the efficacy and potential of AAK1 inhibition as antiviral strategy arises.<sup>20-22</sup>

#### *b. The clathrin mediated endocytosis pathway*

The importance of clathrin coated vesicles (CCV) for the internalization of viruses can be exploited as target for the development of antiviral drugs. This approach is different from current antiviral strategies that target viral proteins. The disadvantage of targeting viral factors is that it often results in a narrow spectrum drug (the ‘one bug, one drug’ approach). Targeting a host enzyme which is essential for the infectivity of different viruses can lead to a broad spectrum antiviral drug.<sup>17</sup> In addition, targeting host factors may confer a higher genetic barrier for the development of resistance than antiviral agents acting on viral factors. The clathrin-mediated endocytosis pathway is tightly regulated by various proteins and intensive phosphorylation and dephosphorylation by different regulating protein kinases and phosphatases.<sup>16,23,24</sup> The process goes through five stages (initiation, cargo selection, coat assembly, scission and uncoating) in which soluble CT form the lattice of the vesicle after recruitment to the cell membrane. This recruitment requires the use of adaptor proteins, as the CT cannot directly bind to the membrane or cargo receptors.<sup>25</sup>

The exact molecular mechanism of CCV formation is not clearly resolved yet. Recent studies suggest the formation of a nucleation module containing various adaptor proteins such as F-BAR containing proteins FCHO1/2, intersectin 1 and eps15/eps15R. These proteins have a strong affinity for phosphatidylinositol(4,5)diphosphate (PI(4,5)P<sub>2</sub>), which is located within the cell membrane and can form specific endocytic hotspots (**Figure 1.5A**).<sup>25</sup> The nucleation module will directly recruit AP2 via eps15 and intersectin 1 which in turn recruits CT.<sup>25,26</sup> AP2 coordinates the recruitment of cargo molecules (**Figure 1.5B**) and vesicle assembly via phosphorylation.<sup>24</sup> Binding of the nucleation module and AP2 results in the recruitment of CT to the plasma membrane and the formation of a clathrin coated pit (**Figure 1.5C**).<sup>25</sup> After full maturation and budding of the CCV, it is separated from the plasma membrane and released in the cytosol by the dynamin enzyme through an unknown process (**Figure 1.5D**).

After detachment from the plasma membrane, uncoating of the vesicle will occur through the use of the ATPase heat shock cognate 70 along with its cofactors auxilin and GAK (**Figure 1.5E**). This last process takes place at the scission site, where the clathrin cage is incomplete. It releases the enclosed cargo and CT into the cytosol.<sup>25</sup>

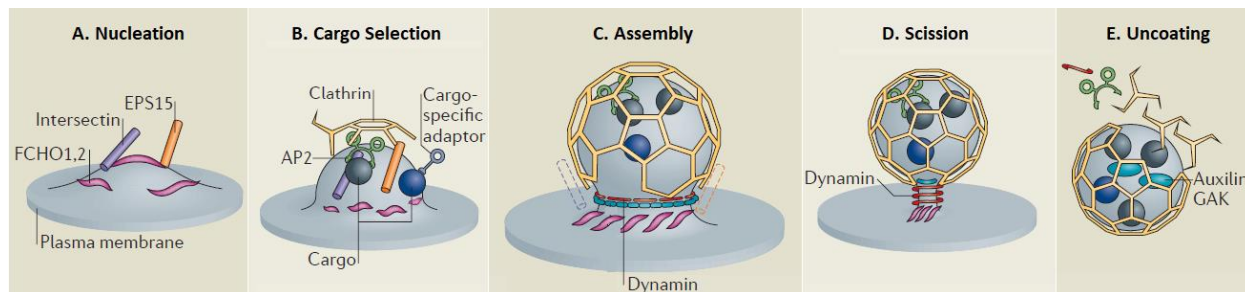


**Figure 1.5.** Clathrin-mediated endocytosis A. Formation of clathrin coated pit; B. Cargo selection; C. Vesicle Assembly; D. Scission and release into cytosol; E. Uncoating and cargo release. (Figure adapted from McMahon et al., 2011)<sup>25</sup>

### c. Adaptor proteins as key regulators of clathrin-mediated endocytosis

Adaptor proteins, existing in five forms (AP1-AP5), are highly conserved within all eukaryotic cells. As AP3-AP5 are not involved in viral particle uptake and secretion, they will not be discussed further. AP1 and AP2 have similar functions despite their different locations. AP2 is predominantly functional at the cell membrane, whereas AP1 mainly operates at the *trans* Golgi network (TGN). AP are heterotetrameric proteins consisting of two large subunits (AP1:  $\gamma$  and  $\beta$ 1, AP2:  $\alpha$  and  $\beta$ 2), one medium subunit (AP1:  $\mu$ 1, AP2:  $\mu$ 2) and one small subunit (AP1:  $\sigma$ 1, AP2:  $\sigma$ 2) with all subunits mutually interchangeable, though possessing a preference for the main subunit partner.<sup>27</sup> Subunits  $\gamma$  and  $\alpha$  are responsible for donor membrane receptor binding through recognition of phosphatidylinositol-4-phosphate (PIP<sub>4</sub>) ( $\gamma$ ) or phosphatidylinositol (4,5)-bisphosphate (PI(4,5)P<sub>2</sub>) ( $\alpha$ ) which explains the locational preference. Subunits  $\gamma$  and  $\alpha$  also contain an appendage domain that is responsible for accessory protein recruitment.<sup>28,29</sup> The  $\beta$ 1 and  $\beta$ 2 subunits recruit CT to the cell membrane via a clathrin binding motif located within the hinge region of its appendage domain.<sup>29,30</sup> The  $\sigma$  subunits are present for structural stability of the AP complex.<sup>30</sup> Tyrosine- or dileucine motifs present on cargo molecules act as sorting signals which are recognized by and bind to the  $\mu$ -subunits of the AP complexes.<sup>31</sup> Phosphorylation of threonine 156 of the  $\mu$  subunit of AP2 (AP2M2) and threonine 144 of the  $\mu$  subunit of AP1 (AP1M1) by either AAK1 or GAK (**Figure 1.6**) increases the efficiency of cargo protein binding through a conformational change. Both these kinases are also regulating the recruitment of CT and AP2 to the plasma membrane.<sup>32</sup>

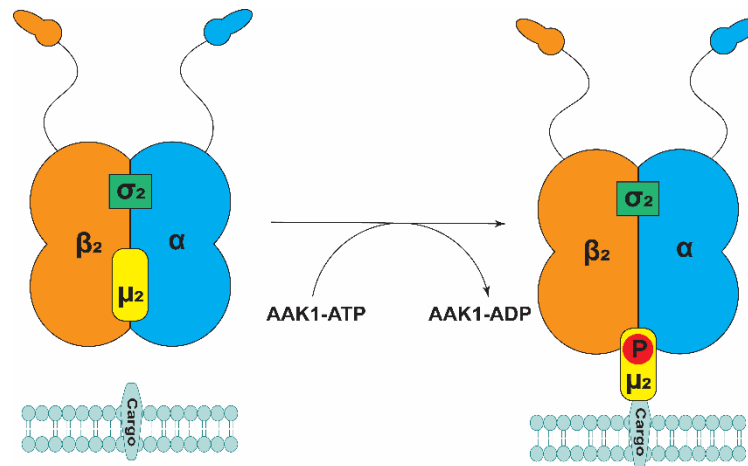


**Figure 1.6.** Activation of AP2 by GAK and AAK1

#### *d. Dengue virus (DENV) and transmission*

The dengue virus (DENV) belongs to the *Flaviviridae*, a family of positive stranded RNA viruses branching into three genera: hepacivirus, pestivirus and flavivirus.<sup>33</sup> Severe diseases with a high mortality rate in humans are associated with infections by these pathogens. DENV, member of the flavivirus genus, possesses the highest mortality rate within its genus, ranking it as one of the worlds most neglected tropical diseases. Yellow fever virus and West Nile virus are examples of other clinically relevant flaviviruses.

The transmission of viral particles occurs via vectors, more specifically the female mosquitoes of the genus *Aedes* with *Aedes Aegypti* being the primary vector. *Aedes albopictus* has also been identified as a carrier for these viruses and acts as the secondary vector.<sup>33,34</sup> This genus of mosquito has evolved to mate, feed and reside within the tropical areas near urban settlements. Feeding peaks right after dawn and before dusk. It has also spread beyond the tropical areas due to trade internationalization and the DENV adapting to the lower temperatures of Europe and North America.<sup>33,35</sup> Infection of the mosquito with DENV occurs when a mosquito feeds on a person in the viremic or acute febrile phase of the disease. After a 8-10 days incubation period, the virus replicates in the salivary glands where it remains transmittable for the rest of the mosquito's life which is on average one week.<sup>36</sup> This infection is highly influenced by regional temperature, as well as the serotype and mosquito competence.<sup>33,36</sup>

There are four antigenically and genetically related serotypes of DENV (DENV1-4), all of which are transmitted by the *Aedes* mosquitoes and can cause the dengue disease. Injection of the virus into the bloodstream by mosquito feeding, leads to infection of macrophages and dendritic cells. Migration of infected cells to the lymph nodes initiates the recruitment of monocytes and other macrophages that become secondary targets for viral infection.

#### *e. DENV lifecycle and genome*

**Figure 1.7** represents the genome of DENV and its viral replication. The mature particle binds on an as of yet unidentified host receptor via the envelope (E) glycoprotein which harbors three domains: domain I, domain II containing the fusion peptide and domain III for receptor binding.<sup>37</sup> Internalization



of the virus occurs via exploiting the clathrin-mediated endocytosis pathway.<sup>17,38</sup> The low pH within the endosome triggers a conformational change within the membrane (M) glycoprotein and enables membrane fusion, releasing the viral capsid (C). The viral RNA is released after uncoating of the capsid (~11 kb). The viral RNA is translated as a single polyprotein containing the three structural proteins: C, M which is first transcribed as proto M (prM) and E. The remaining seven proteins within the polyprotein are non-structural proteins that are necessary for viral replication.<sup>23</sup> After synthesis of the machinery necessary for replication, negative sense RNA is produced to serve as template for replication. After RNA replication and assembly, the immature virus particle will have its prM cleaved by host cell furin and will be secreted as a mature virus by hijacking CME for a second time.<sup>16</sup> Following an incubation period of four to seven days, the onset of illness occurs.<sup>36</sup>

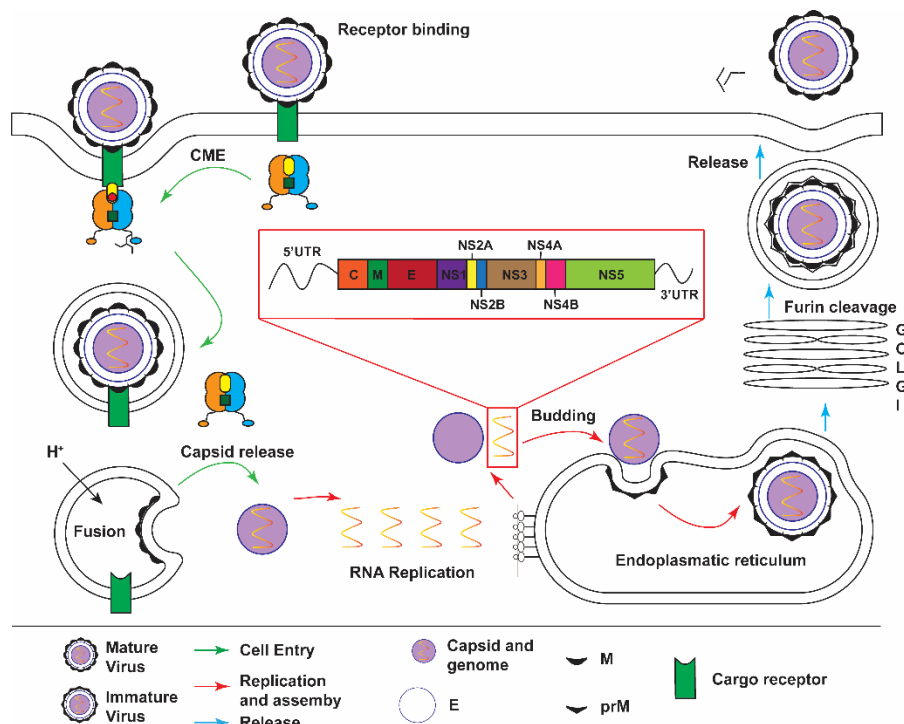


**Figure 1.7.** DENV lifecycle and genome

#### *f. Dengue illness and current treatment*

The illness caused by DENV infection greatly varies between different persons and is clinically classified into three groups: a) dengue with or b) without warning signs or c) severe dengue.<sup>36,39-41</sup> Suspicion of dengue arises when a sudden onset of high fever (39-40°C) is manifested, which is accompanied by at least two of the following symptoms: severe headache, nausea, myalgia, vomiting, joint pain, rash, pain behind the eyes or swollen glands. Decline of the symptoms usually follow within two to seven days after onset. The further flow of the disease can either be paired with or without warning signs. Aside from a decrease in temperature, warning signs include persistent vomiting with or without blood, severe abdominal pain, fatigue, restlessness, bleeding gums and rapid breathing. Early recognition of these warnings is imperative as they increase the risk of developing severe dengue. The severe form of dengue greatly affects the hemostasis and the permeability of the microvascular system.

The increase of the permeability and decrease in hemostasis results in plasma leakage all over the body and severe hemorrhages resulting in hypotension, hypotensive shock and ultimately death.<sup>33</sup> Upon primary infection, the majority of patients remain asymptomatic,<sup>41</sup> however the risk of developing severe dengue upon secondary infection with a different serotype greatly increases due to antibody-dependent enhancement (ADE). After primary infection with one serotype of DENV, the patient develops lifelong homotypical immunity. Upon infection with another serotype, the non-neutralizing antibodies capture the viral particles and guides them to Fcγ receptor bearing cells. These cells include macrophages and monocytes which would be inefficiently infected in the absence of antibodies.<sup>42</sup> This results in an increased infection rate and ultimately in an increased viral load.<sup>39,43</sup>

The current treatment for a disease so complex in its symptoms lies within the early recognition<sup>41</sup> of the symptoms or the warning signs followed by adequate supportive care. This primarily involves the monitoring and adjustment of the blood volume either orally or intravenously. If a patient suffers from severe dengue with hemorrhagic complications, a blood transfusion is imperative.<sup>33,36</sup>

### g. AAK1 inhibitors

AAK1 has been studied before as drug target for the treatment of a variety of neurological disorders, such as Parkinson's disease, schizophrenia, neuropathic pain<sup>44</sup>, Alzheimer's disease and bipolar disorders.<sup>45,46</sup> It led to the discovery of potent AAK1 inhibitors based on various chemotypes that have been divulged in patent literature.

An overview of these inhibitors along with their enzymatic inhibition data is shown in **Figure 1.8**.

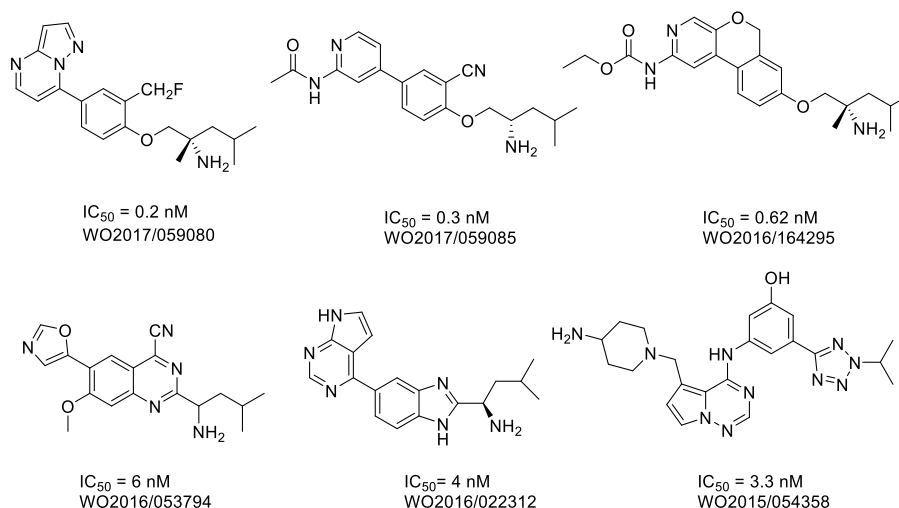


**Figure 1.8.** Known AAK1 Inhibitors

Despite the promise of AAK1 as an antiviral drug target, none of the existing AAK1 inhibitors have been investigated or optimized for antiviral activity. A series of compounds bearing an imidazo[1,2-*b*]pyridazine core, originally developed by Lexicon Pharmaceuticals, is the only exception (**Figure 1.9**).<sup>44</sup> Both compounds **1.3** and **1.4** displayed low nanomolar binding affinity for AAK1 (**1.3**  $K_D = 1.25 \text{ nM}$  and **1.4**  $K_D = 1 \text{ nM}$ ) and were endowed with low micromolar activity against DENV with  $EC_{50}$  values of  $1.5 \text{ } \mu\text{M}$  and  $5.1 \text{ } \mu\text{M}$  for compounds **1.3** and **1.4**, respectively.<sup>16</sup>

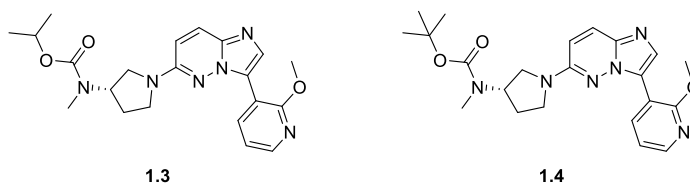


**Figure 1.9.** Imidazo[1,2-*b*]pyridazine based AAK1 inhibitors.

### 1.2.3. G-protein coupled receptors

GPCRs, often labeled as 7-transmembrane receptors or heptahelical receptors, are the largest family of at least 800 membrane receptors in various organisms.<sup>47</sup> The superfamily is divided into six classes: rhodopsin, secretin, frizzled, cAMP, pheromone and the metabotropic glutamate receptors which on their turn are divided into subclasses based on agonist selectivity or biological effect. Two of these classes are not observed within humans and are exclusively present in amoeba (cAMP) and fungi (pheromone)

(**Figure 1.10**).<sup>48,49</sup>

An estimated 36% of all marketed drugs target a GPCR.<sup>50</sup> Notable examples include the  $\beta$ -adrenergic receptors that are exploited for the treatment of hypertension and asthma and serotonin (5-HT) receptors with their broad spectrum of treatable diseases, mainly depression. This historical success of GPCRs as drug targets still makes GPCRs a heavily studied target class in academic laboratories and in pharmaceutical industry.

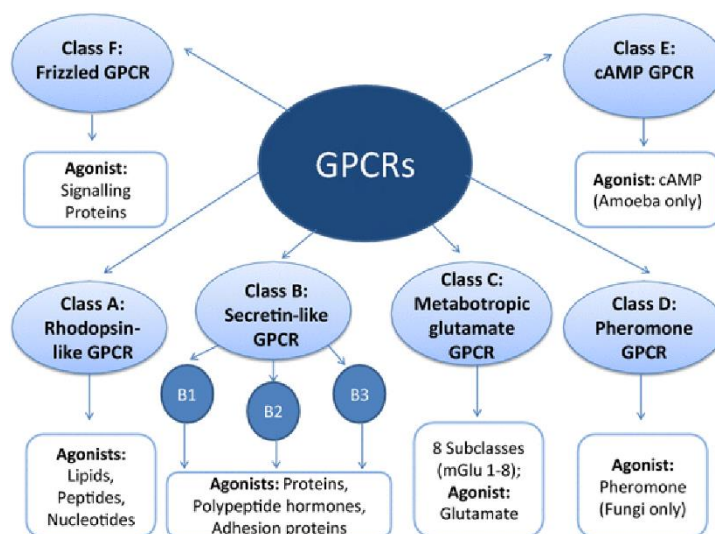


**Figure 1.10.** GPCR classification system (Origin of figure: Moran et al., 2016).<sup>48</sup>

G-proteins are heterotrimeric proteins comprised of a  $G\alpha$  GTPase and a  $G\beta\gamma$  dimer associated with each other forming the G-protein complex that in turn is associated with the cytosolic end of the receptors at the cell membrane.<sup>51</sup> Binding of an agonist to the extracellular part of the receptor causes a conformational change in the cytosolic part of the receptor, leading to an exchange of GDP for GTP in the inactive  $G\alpha$  subunit. This exchange activates the  $G\alpha$  subunit, and leads to its dissociation from the  $G\beta\gamma$  dimer. Both the  $G\alpha$  and  $G\beta\gamma$  dimer can elicit downstream effects via various second messengers, like cAMP or inositol triphosphate ( $IP_3$ ).<sup>48</sup>

The  $G\alpha$  subunit is classified into four classes:  $G_s$ ,  $G_{i/o}$ ,  $G_q$  and  $G_{12/13}$ . Each of these modulates a different second messenger system within the cell (**Figure 1.11**). The majority of GPCRs are capable to associate with different  $G\alpha$  subtypes, and hence are able to activate several signaling pathways.<sup>48</sup> After the intrinsic GTPase activity of  $G\alpha$  hydrolyses GTP to GDP, it reverts back to its inactive state and re-associates with the  $G\beta\gamma$  dimer, ready to enter a new signaling cycle.<sup>48</sup>

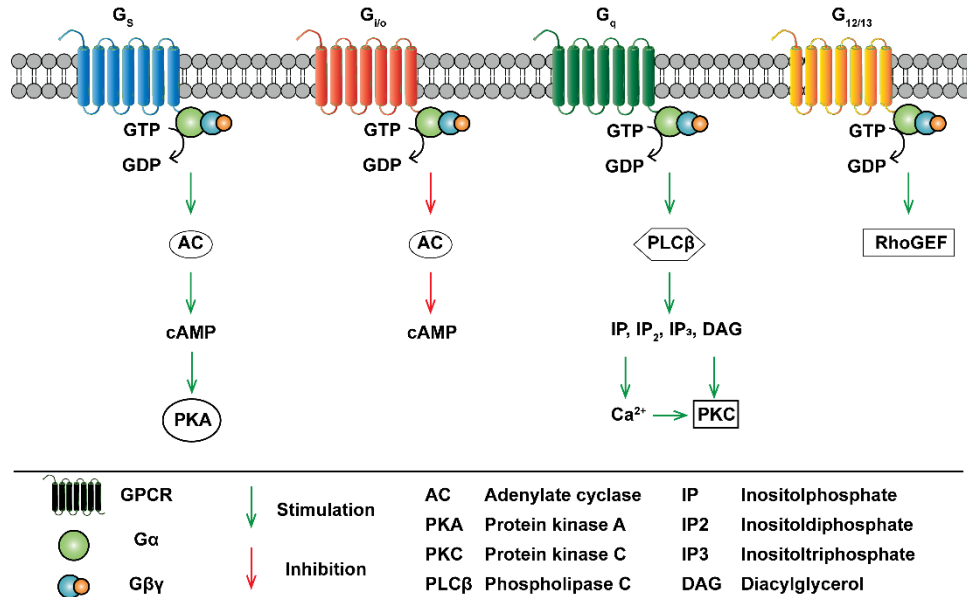


**Figure 1.11.** The different classes of  $\alpha$  subunit associated with a GPCR and their signal pathways (Figure adapted from Williams et al., 2009).<sup>51</sup>

Signal transduction is terminated by phosphorylation of a serine/threonine residue in the cytosolic part of the receptor by G-protein coupled receptor kinases (GRK).<sup>52</sup> The phosphorylated tail acts as a binding site and activator for a  $\beta$ -arrestin protein that blocks the reassociation of the trimeric G-protein and therefore desensitizes the receptor. Furthermore, the  $\beta$ -arrestin proteins facilitate the sequestration or endocytosis of the receptor.<sup>52</sup> After sequestration, the GPCRs are categorized into two classes, depending on their interaction with  $\beta$ -arrestin. Class A GPCRs quickly dissociate from  $\beta$ -arrestin, while class B GPCRs form stable receptor- $\beta$ -arrestin complexes. Following fusion of the GPCR containing vesicle and an acidic endosome, one of two patterns can be pursued. Class A GPCRs release their activating ligand and are dephosphorylated by a GPCR specific phosphatase (PP2A), followed by recycling to the cell membrane. On the other hand, class B GPCRs accumulate within the acidic endosomes. Either, they are degraded resulting in GPCR downregulation or they are slowly recycled back to the cell membrane through an unknown mechanism (**Figure 1.12**).<sup>53</sup> Multiple studies also revealed that  $\beta$ -arrestin proteins are able to initiate signal transduction.<sup>53</sup>

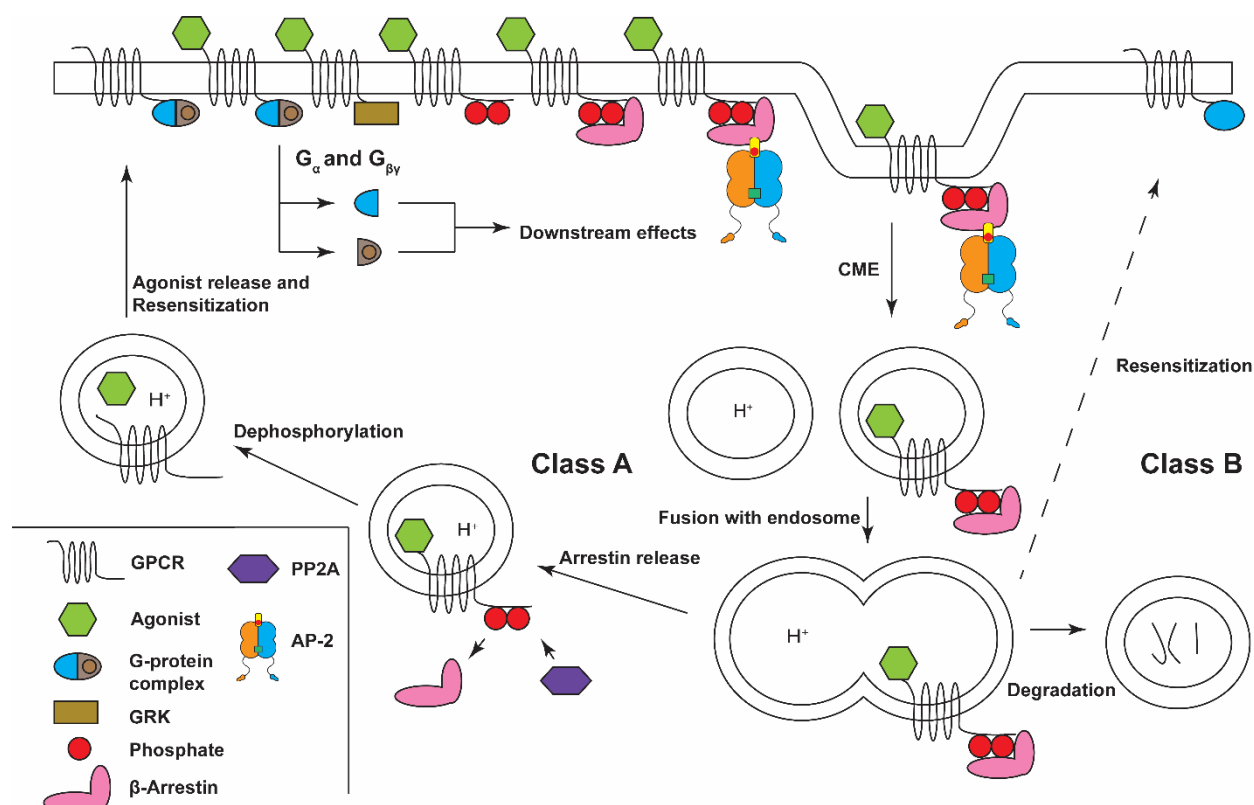


**Figure 1.12.** Signal termination of the activated GPCRs

Despite the fact that GPCRs have been heavily exploited as drug targets, this target class still attracts considerable interest from the drug discovery community due to their role in a broad range of pathophysiological conditions. More than 50% of the human GPCRs are orphan receptors, receptors whose natural ligand and biological function remain poorly understood, hampering further research.<sup>54</sup> The availability of potent and selective small molecule ligands as chemical tools for these underexplored GPCRs will allow to study them in detail. In this doctoral thesis, the mas-related gene receptor X2 (MRGPRX2) and cluster chemokine receptor 8 (CCR8) were selected as representative examples of understudied GPCRs.

### 1.2.3.1. *Mas-related gene receptor X2 (MRGPRX2)*

#### *a. Mas-related gene (MRGPR) receptor family*

The MRGPR receptors are a family of orphan GPCRs discovered in 2001.<sup>55</sup> The family consists of 32 murine members and 4 human receptors.<sup>54,56</sup> All receptors are classified into eight subfamilies. MRGPRA, MRGPRB, MRGPRC and MRGPRH are all rodent specific, whereas MRGPRX is only found in primates.<sup>57</sup> MRGPRD, MRGPRE and MRGPRF are present in both primates and rodents. All MRGPR members exist in multiple forms and their expression pattern is species dependent.<sup>58</sup> The name is derived from their homology with the MAS oncogene. Sometimes, they are also called sensory neuron-specific receptors (SNSR). Human MRGPRX2 is mainly located within dorsal root ganglia (DRG)<sup>59</sup> and adrenal chromaffin cells. Based on this tissue distribution, it was proposed that MRGPRX2

is involved in nociception and catecholamine secretion.<sup>60</sup> Besides their presence on neurons, MRGPRX2 receptors are also expressed on mast cells (MC).<sup>58,61,62</sup>

### *b. Mast cells and MRGPRX2*

MC are an integral part of the immune system and form the first line defense against external threats within healthy tissues near external surfaces.<sup>63</sup> Upon activation and through degranulation, MC secrete plenty of mediators that are essential for the immune response. Based on the content of these granules, MC are divided into two subtypes: the tryptase containing MC (MC<sub>T</sub>) and the tryptase and chymotryptic proteinase containing MC (MC<sub>TC</sub>).<sup>64</sup> Both MC types also vary in the expression of membrane receptors, since MC<sub>TC</sub> stably expresses MRGPRX2, whereas MC<sub>T</sub> does not. MC<sub>T</sub>'s are more prevalent in the lung alveolar wall and the intestinal mucosa, while MC<sub>TC</sub>'s are more widespread near the skin surface.<sup>65</sup> Degranulation of MC mainly occurs via the interaction of an antigen with immunoglobulin E (IgE) and the FcεRI receptor.<sup>61,63</sup> Naive B-cells normally produce immunoglobulin D (IgD) and immunoglobulin M (IgM), but switch to the production of IgE after antigen exposure and subsequent proliferation. These newly produced IgE antibodies bind to the FcεRI receptor on MC and rarely circulate in the bloodstream as free antibodies making the response to an antigen swift and efficient. When IgE is exposed to its antigen a crosslinking bridge between two homologous receptor-bound IgE's is formed, inducing the degranulation of the MC and subsequent release of the immunomodulating agents.<sup>66</sup> These modulators are grouped depending on the time of release after antigen contact. Group 1 modulators are usually released within seconds after antigen contact due to their preformed existence and include histamine, proteoglycans and proteases. Group 2 include newly formed arachidonic acid derived leukotrienes and prostaglandins that are released within minutes. Finally, group 3 modulators are released within hours after antigen contact due to the requirement of gene transcription and include cytokines and chemokines. The result is an inflamed zone with an increased vascular permeability and a remodeled connective tissue matrix, along with mast cells acting as antigen presenting cells ready for further responses of the adaptive immune system.<sup>67</sup> The continued exposure to increasing amounts of antigen leads to a desensitization of the MC for that antigen through an unknown mechanism.<sup>66</sup>

Recently, it was demonstrated that degranulation can also happen in an IgE independent way.<sup>67</sup> This IgE independent degranulation can be initiated by activation of different receptors, such as the Toll-like receptors (TLRs), the adenosine A<sub>3</sub> receptor, the ATP receptor P2X<sub>7</sub> and also the MRGPRX2 receptor. Stimulation of P2X<sub>7</sub>, A<sub>3</sub> and MRGPRX2 receptors induces an IgE-like degranulation, releasing all three groups of MC derived molecules. On the other hand, stimulation of TLRs only leads to the secretion of cytokines and chemokines (**Figure 1.13**).

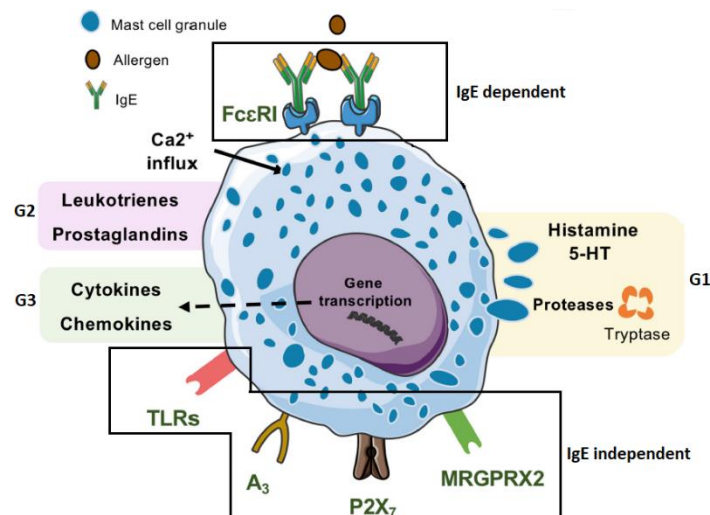


**Figure 1.13.** MC with the IgE dependent and the IgE independent degranulation (Figure adapted from Méndez-Enríquez et al., 2019).<sup>67</sup>

### c. Allergic diseases and MRGPRX2

MC degranulation is a key player in the development of various allergic disorders. It has been demonstrated that in healthy tissue, the numbers of MC<sub>TC</sub> (especially in the skin and to a lesser extent in the lungs) are stable. However, under inflammatory or infectious conditions, the number of MC<sub>TC</sub>, and hence the MRGPRX2 receptors is increased. This increases the likelihood of MC degranulation and MC mediated effects in inflamed tissue.<sup>68</sup> Diseases like allergic asthma, chronic obstructive pulmonary disease (COPD), chronic urticaria, allergic rhinitis and atopic dermatitis are all mediated by MC degranulation, albeit with a different symptomatology.<sup>62,67,68</sup>

### d. Ligands and coupling mechanism of MRGPRX2

The MRGPRX2 receptor is, like the rest of its family members, an orphan receptor. Although the endogenous ligand has not been identified,<sup>58,61</sup> several agonists for the receptor, synthetic and natural alike, have been identified over the years. These are branded as basic secretagogues due to their polycationic qualities and include Substance P, compound 48/80, cathelicidins,<sup>58</sup>  $\beta$ -defensins<sup>61</sup> and the main research ligand cortistatin-14.<sup>59,69</sup> Upon activation of the receptor, the recruitment of G<sub>i/o</sub> and Gq<sup>58</sup> with subsequent release of intracellular calcium is observed, ultimately leading to degranulation of the MC (Figure 1.14).<sup>61</sup>

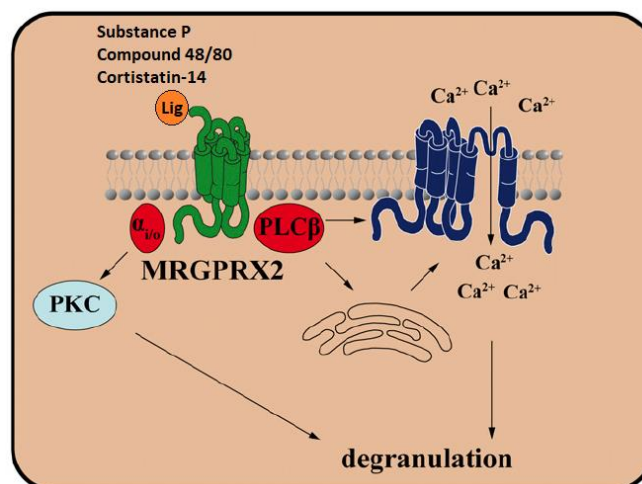


**Figure 1.14.** MRGPRX2 signal transduction within MC (Origin of figure : Solinski et al., 2014).<sup>61</sup>

Apart from the basic secretagogues, a few small molecule MRGPRX2 agonists are known (**1.5** and **1.6** in **Figure 1.15**).<sup>70,71</sup> A classical high-throughput screening led to the discovery of the tetracyclic benzimidazole **1.5** as MRGPRX2 agonist ( $EC_{50}$  value of 316 nM).<sup>71</sup> Very recently, virtual screening by *in silico* docking of over 3 million compounds in a homology model of the MRGPRX2 receptor led to the discovery of pyrazolopyrimidine **1.6** as a promising agonist of MRGPRX2 with an  $EC_{50}$  value of 760 nM in the  $\beta$ -arrestin assay. Furthermore, this compound **1.6** displayed comparable  $EC_{50}$  values in the calcium mobilization and mast cell degranulation assays.<sup>70</sup>

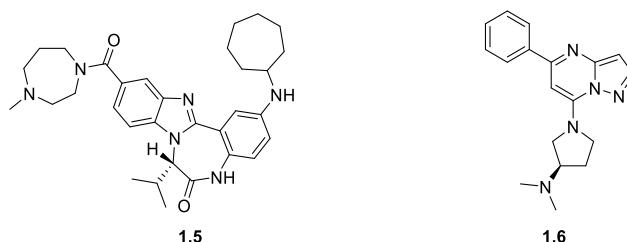


**Figure 1.15.** Known MRGPRX2 agonists.<sup>70,71</sup>

Despite the promise of MRGPRX2 antagonists to treat a variety of allergic disorders, the number of known MRGPRX2 antagonists is very limited. Only very recently, two MRGPRX2 antagonists were reported in literature (**Figure 1.16**). Quinazoline analogue **1.7** and phenazine derivative **1.8** were both discovered by screening a compound library and displayed  $IC_{50}$  values of 1.6  $\mu$ M and 2.5  $\mu$ M, respectively in the calcium mobilization assay. In addition, both compounds are able to block mast cell degranulation induced by basic secretagogues with low micromolar activity.<sup>60</sup>

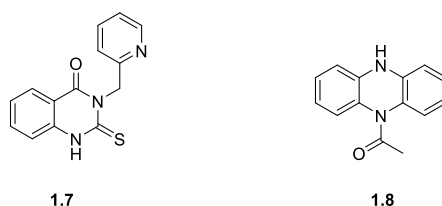


**Figure 1.16.** Known MRGPRX2 antagonists.<sup>60</sup>



### 1.2.3.2. Cluster chemokine receptor 8 (CCR8)

#### a. Chemokines and their receptors

Chemokines (chemoattractant cytokines) are a group of small (8-15 kDa), structurally related proteins with basic characteristics. They represent the largest family of cytokines with over 50 ligands and they govern host defense through regulating the migration and activation of immune cells.<sup>72</sup> Based on the relative positioning of cysteine residues in the amino terminus of the protein, they are classified into four subfamilies.<sup>73</sup> The majority of the chemokines belong to the CXCL or CCL class. In the CXCL subfamily, a variable amino acid (denoted as X) is present between the cysteine residues, whereas in the CCL subfamily these cysteine residues flank each other.<sup>74,75</sup> CX3CL and XCL are two additional subfamilies, where the cysteine residues are separated by three variable amino acids or where only one cysteine residue is present, respectively.<sup>74,75</sup>

Chemokines exert their biological effects by interaction with cell-surface receptors that belong to the rhodopsin class GPCR superfamily. Some chemokines bind to more than one GPCR, and conversely, some GPCRs display overlapping chemokine specificities albeit often with variable affinities. Chemokine GPCRs are divided into two groups. There are 18 conventional chemokine receptors and 4 atypical chemokine receptors. The conventional receptors are classified, in analogy with their corresponding ligands, into four subfamilies: CCR, CXCR, CX<sub>3</sub>CR and XCR and initiate the signaling cascade through G<sub>i/o</sub>,  $\beta$ -arrestin or JAK-STAT.<sup>74</sup> The expression of the different receptors depends on the differentiation and activation stage of the cells.<sup>76</sup> Cells expressing these receptors will be attracted to locations with higher concentrations of the chemokines explaining the chemotactic role of the chemokines.<sup>77</sup> The four atypical chemokine receptors (DARC, CXCR7, D6 and ACKR4) bind their chemokine ligands with high affinity, yet do not couple to any of the signaling pathways with the exception of CXCR7, which can elicit downstream effects via coupling with  $\beta$ -arrestin. The remaining three mainly act as chemokine scavengers to regulate untimely chemokine receptor desensitization by overexposure to the chemokine.<sup>74,75</sup>

#### b. CCL1 and CCR8

Recently, the chemokine receptor CCR8, emerged as a novel promising drug target. CCR8 can be activated by four chemokines (CCL1, CCL8, CCL16, CCL18), whereby CCR8 is the only known receptor for CCL1.<sup>78</sup> CCL1 is secreted mainly by T-cells, monocytes and mast cells and attracts T-helper-cells 2 and immature monocytes along with a subset of regulatory T cells (T<sub>reg</sub>).<sup>79</sup>

CCR8 expression has shown to be specifically augmented in tumor-infiltrating regulatory T (T<sub>reg</sub>) cells that are potent suppressors of effector T-cell responses. CCR8 has a constitutively active state of about 12% of its maximal effect.<sup>80</sup> The presence of CCR8 in the tumor microenvironment correlates with a reduced survival of cancer patients, and T<sub>reg</sub> cell depletion has been reported to enhance anti-tumor immune responses. It is further postulated that inhibiting the migration of CCR8<sup>+</sup> tumor-associated T<sub>reg</sub> cells or modulating their function in the tumor microenvironment by specific CCR8 antagonists represents a valuable therapeutic strategy in cancer immunotherapy.<sup>81</sup>

Regulatory T cells also play pivotal roles in suppressing autoimmunity. In a recent study, CCR8<sup>+</sup> T<sub>reg</sub> cells were identified as key drivers of immunosuppression.<sup>78</sup> In a mouse model of experimental autoimmune encephalomyelitis (which is a model for multiple sclerosis), CCL1-induced potentiation of CCR8<sup>+</sup> T<sub>reg</sub> cells suppressed the disease, underpinning their immune regulating role.<sup>82</sup> The stimulation of CCR8<sup>+</sup> T<sub>reg</sub> cells by CCR8 agonists thus appears a promising approach for the treatment of various autoimmune diseases, such as multiple sclerosis, rheumatoid arthritis and Crohn's disease.<sup>83</sup>

### c. Small molecule CCR8 agonists and antagonists

A number of CCR8 agonists and antagonists have been described in literature (**Figure 1.17**). The phenoxybenzyl moiety is an essential feature in several CCR8 agonists.<sup>84</sup> The introduction of a piperazine ring, from which the second nitrogen is substituted with an ethoxyethanol group afforded compound **1.9**, that displayed an EC<sub>50</sub> value of 254 nM in a calcium mobilization assay.<sup>83</sup> Alternatively, reaction of the piperazine moiety with a variety of isocyanates yielded a series of piperazine – urea analogues with EC<sub>50</sub> values ranging from over 3 nM to 3000 nM. The most potent congener **1.10** was found to be a partial agonist of CCR8.<sup>85</sup> The replacement of piperazine by 4-amino-piperidine, followed by reaction of the exocyclic amino group with a range of carboxylic acids, furnished a series of compounds that were evaluated for their CCR8 binding affinity. Compound **1.11** displayed high affinity for CCR8 (K<sub>i</sub> = 15 nM) and was a potent inhibitor of chemotaxis.<sup>86</sup>

In the late 2000's, a series of naphthalene sulfonamides<sup>87</sup> and oxazolidinones<sup>88</sup> were developed as CCR8 antagonists. Systematic structural variation of the amide and sulfonamide moieties in the naphthalene sulfonamide series afforded compound **1.12** that acted as a potent antagonist (IC<sub>50</sub> = 5 nM) in the calcium mobilization assay. Extensive optimization of the oxazolidinone analogues yielded derivative **1.13** that show nanomolar activity in the calcium mobilization assay.<sup>87,88</sup> The interest of developing small molecule CCR8 antagonists led to the discovery of an allosteric ligand **1.14** based on a diazaspiroundecane scaffold by AstraZeneca in 2010. This compound displays low nanomolar binding affinity for CCR8, combined with oral bioavailability and a good pharmacokinetic profile.<sup>89</sup>

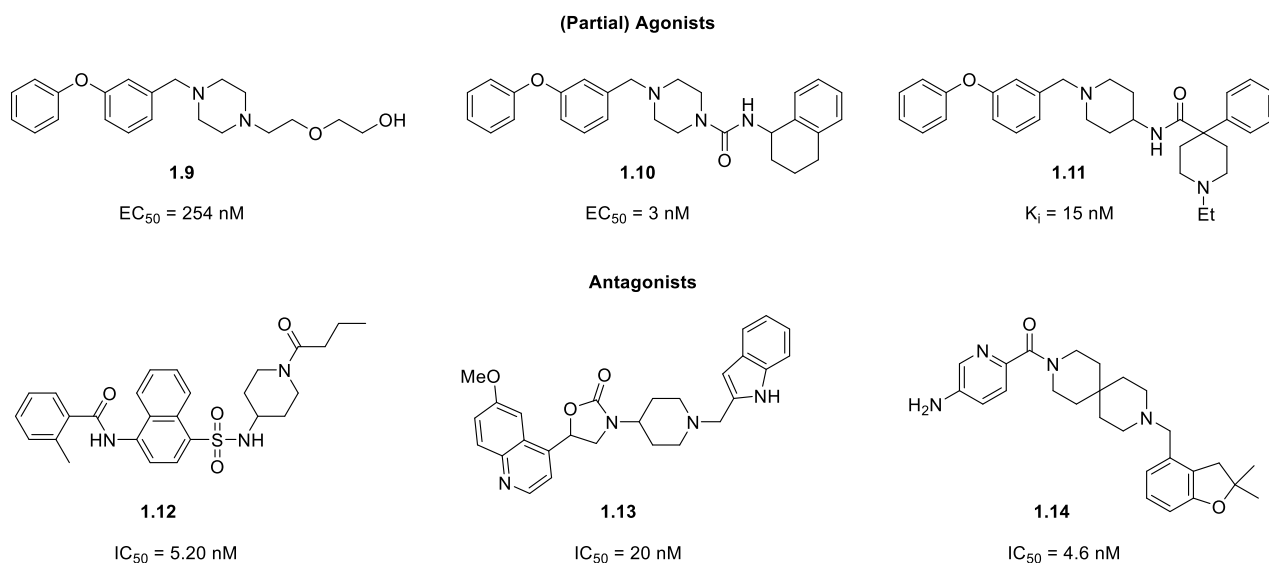


**Figure 1.17.** Ligands of CCR8.<sup>80,85,86</sup>

### 1.3. Objectives

Despite the wealth of drug targets currently pursued, there is still a substantial number of promising drug targets for which no potent and selective ligands are known. Therefore, in this PhD thesis, three underexplored targets (AAK1, MRGPRX2 and CCR8) belonging to the most popular target classes (kinases and GPCRs) were selected. The availability of potent and selective ligands will allow to study the effect of target modulation in different disease areas (i.e. use compounds as chemical tools). Alternatively, these compounds can also function as starting point for a drug discovery program (i.e. use compounds as leads).

Mature viral particles enter host cells by hijacking the CME mechanism.<sup>32</sup> Inhibition of AAK1 and the resulting inhibition of the AP2 phosphorylation prevents AP2 to recognize cargoreceptors and the subsequent clathrin recruitment, and hence has the potential to impede the uptake of viruses in host cells. This hypothesis was confirmed by pharmacological inhibition of AAK1 with sunitinib, an approved broad spectrum kinase inhibitor, as it displayed antiviral activity against several unrelated viruses.<sup>17</sup> In **Chapter 2**, compound **1.15** (Figure **1.18**) was selected as starting point for the discovery of novel and antivirally active AAK1 inhibitors. It was considered as a suitable hit to start an optimization campaign in order to improve its quite strong AAK1 affinity ( $K_D = 53$  nM) and moderate antiviral activity ( $EC_{50} = 8.4$   $\mu$ M).

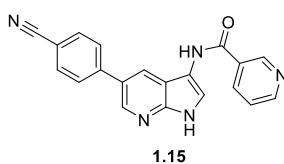


**Figure 1.18.** Potent AAK1 inhibitor.<sup>90</sup>

In **Chapter 3**, MRGPRX2 was selected as drug target. Activation of this orphan GPCR, leads to degranulation of mast cells in the absence of IgE.<sup>67</sup> Moreover, MRGPRX2 is overexpressed on MC<sub>TC</sub> cells which are upregulated in inflamed tissue. Therefore, MRGPRX2 antagonism represents a potential new approach in the treatment of allergic diseases.<sup>62</sup> At the onset of this PhD, no MRGPRX2 antagonists were known in literature and only in July 2019 the first MRGPRX2 antagonists were published.<sup>60</sup> Initial screening of a 1600-membered commercial compound library in a  $\beta$ -arrestin assay, followed by testing of a focused library, led to the discovery of four pyrimido[1,2-*a*]benzimidazoles (**1.16-1.19**, **Figure 1.19**) displaying low micromolar activity. In Chapter 3, structural variation of the pyrimidine and the phenyl moiety of pyrimido[1,2-*a*]benzimidazoles **1.16-1.19** was carried out, aiming at the improvement of the MRGPRX2 antagonism.

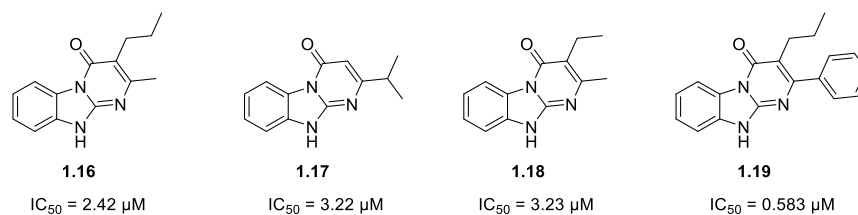


**Figure 1.19.** MRGPRX2 hits

Finally, in **Chapter 4**, drug discovery efforts towards CCR8 are described. It has been postulated that CCR8 agonism represents a new strategy for the treatment of autoimmune disorders. Despite the fact that some small molecule CCR8 agonists are known in literature, none of them has been assessed for immunosuppressive properties nor have they been evaluated in preclinical animal models of autoimmune diseases. As the phenoxybenzyl moiety is a common structural feature (such as in compounds **1.9-1.11**) of the different CCR8 agonists, focus was given on the synthesis of phenoxybenzyl analogues with a different substitution pattern (**Figure 1.20**) in order to discover novel and potent CCR8 agonists.

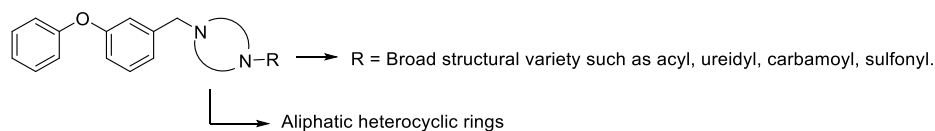


**Figure 1.20.** CCR8 agonist design strategy

## 1.4. References

- (1) Kubota, K.; Funabashi, M.; Ogura, Y., Target deconvolution from phenotype-based drug discovery by using chemical proteomics approaches. *Biochim. Biophys. Acta, Proteins Proteomics* **2019**, *1867* (1), 22-27.
- (2) Swinney, D. C.; Anthony, J., How were new medicines discovered? *Nat. Rev. Drug. Discov.* **2011**, *10*, 507-519.
- (3) Croston, G. E., The utility of target-based discovery. *Expert Opin. on Drug Discovery* **2017**, *12* (5), 427-429.
- (4) Sams-Dodd, F., Target-based drug discovery: is something wrong? *Drug Discov. Today* **2005**, *10* (2), 139-147.
- (5) Pertea, M.; Salzberg, S. L., Between a chicken and a grape: estimating the number of human genes. *Genome Biology* **2010**, *11* (5), 206.
- (6) Drews, J., Drug discovery: a historical perspective. *Science* **2000**, *287*, 1960-1964.
- (7) Hughes, J. P.; Rees, S.; Kalindjian, S. B.; Philpott, K. L., Principles of early drug discovery. *Br. J. Pharmacol.* **2011**, *162* (6), 1239-1249.
- (8) Ooi, A.; Takehana, T.; Li, X.; Suzuki, S., et al., Protein overexpression and gene amplification of HER-2 and EGFR in colorectal cancers: an immunohistochemical and fluorescent in situ hybridization study. *Modern Pathology* **2004**, *17* (8), 895-904.
- (9) Santos, R.; Ursu, O.; Gaulton, A.; Bento, A. P., et al., A comprehensive map of molecular drug targets. *Nat. Rev. Drug. Discov.* **2016**, *16*, 19-34.
- (10) Bhullar, K. S.; Lagarón, N. O.; McGowan, E. M.; Parmar, I., et al., Kinase-targeted cancer therapies: progress, challenges and future directions. *Mol. Cancer* **2018**, *17* (48).
- (11) Protein Kinases: Human Protein Kinases Overview. <https://www.cellsignal.com/contents/science-protein-kinases/protein-kinases-human-protein-kinases-overview/kinases-human-protein> (accessed August 4).
- (12) Fabbro, D.; Cowan-Jacob, S. W.; Moebitz, H., Ten things you should know about protein kinases: IUPHAR Review 14. *Br. J. Pharmacol.* **2015**, *172* (11), 2675-2700.
- (13) Roskoski, R., Properties of FDA-approved small molecule protein kinase inhibitors. *Pharmacol. Res.* **2019**, *144*, 19-50.
- (14) Wang, Z.; Cole, P. A., Catalytic mechanisms and regulation of protein kinases. *Method. Enzymol* **2014**, *548*, 1-21.
- (15) Ferguson, F. M.; Gray, N. S., Kinase inhibitors: the road ahead. *Nat. Rev. Drug. Discov.* **2018**, *17* (5), 353-377.
- (16) Bekerman, E.; Neveu, G.; Shulla, A.; Brannan, J., et al., Anticancer kinase inhibitors impair intracellular viral trafficking and exert broad-spectrum antiviral effects. *J. Clin. Invest.* **2017**, *127* (4), 1338-1352.
- (17) Bekerman, E.; Einav, S., Combating emerging viral threats. *Science* **2015**, *348* (6232), 282-283.
- (18) Wu, P.; Nielsen, T. E.; Clausen, M. H., Small-molecule kinase inhibitors: an analysis of FDA-approved drugs. *Drug Discov. Today* **2016**, *21* (1), 5-10.
- (19) Sorrell, Fiona J.; Szklarz, M.; Abdul Azeez, Kamal R.; Elkins, Jon M., et al., Family-wide Structural Analysis of Human Numb-Associated Protein Kinases. *Structure* **2016**, *24* (3), 401-411.
- (20) Karaman, M. W.; Herrgard, S.; Treiber, D. K.; Gallant, P., et al., A quantitative analysis of kinase inhibitor selectivity. *Nat. Biotechnol.* **2008**, *26* (1), 127-132.
- (21) Davis, M. I.; Hunt, J. P.; Herrgard, S.; Ciceri, P., et al., Comprehensive analysis of kinase inhibitor selectivity. *Nat. Biotechnol.* **2011**, *29* (11), 1046-1051.
- (22) Fedorov, O.; Marsden, B.; Pogacic, V.; Rellos, P., et al., A systematic interaction map of validated kinase inhibitors with Ser/Thr kinases. *Proc. Natl. Acad. Sci. U. S. A.* **2007**, *104* (51), 20523-20528.
- (23) Mukhopadhyay, S.; Kuhn, R. J.; Rossmann, M. G., A structural perspective of the flavivirus life cycle. *Nat. Rev. Microbiol.* **2005**, *3* (1), 13-22.

- (24) Neveu, G.; Ziv-Av, A.; Barouch-Bentov, R.; Berkerman, E., et al., AP-2-Associated Protein Kinase 1 and Cyclin G-Associated Kinase Regulate Hepatitis C Virus Entry and Are Potential Drug Targets. *J. Virol.* **2015**, *89* (8), 4387-4404.
- (25) McMahon, H. T.; Boucrot, E., Molecular mechanism and physiological functions of clathrin-mediated endocytosis. *Nat. Rev. Mol. Cell Biol.* **2011**, *12*, 517.
- (26) Henne, W. M.; Boucrot, E.; Meinecke, M.; Evergren, E., et al., FCHO Proteins Are Nucleators of Clathrin-Mediated Endocytosis. *Science* **2010**, *328*, 1281-1284.
- (27) Keyel, P. A.; Thieman, J. R.; Roth, R.; Erkan, E., et al., The AP-2 adaptor beta2 appendage scaffolds alternate cargo endocytosis. *Mol. Biol. Cell* **2008**, *19* (12), 5309-5326.
- (28) Traub, L. M., Clathrin-associated adaptor proteins; putting it all together. *Trends Cell Biol.* **1997**, *7* (2), 43-46.
- (29) Park, S. Y.; Guo, X., Adaptor protein complexes and intracellular transport. *Biosci. Rep.* **2014**, *34* (4), 381-390.
- (30) Lee, M. H.; Hwang, I., Adaptor proteins in protein trafficking between endomembrane compartments in plants. *J. Plant Biol.* **2014**, *57* (5), 265-273.
- (31) Korolchuk, V.; Banting, G., Kinases in clathrin-mediated endocytosis. *Biochem. Soc. Trans.* **2003**, *31* (4), 857-860.
- (32) Pu, S.-Y.; Wouters, R.; Schor, S.; Rozenski, J., et al., Optimization of Isothiazolo[4,3-*b*]pyridine-Based Inhibitors of Cyclin G Associated Kinase (GAK) with Broad-Spectrum Antiviral Activity. *J. Med. Chem.* **2018**, *61* (14), 6178-6192.
- (33) Gubler, D. J.; Ooi, E. E.; Vasudevan, S.; Farrar, J., *Dengue and Dengue Hemorrhagic Fever*. 2 ed.; CABI: 2014.
- (34) Behnam, M. A. M.; Nitsche, C.; Boldescu, V.; Klein, C. D., The Medicinal Chemistry of Dengue Virus. *J. Med. Chem.* **2016**, *59* (12), 5622-5649.
- (35) Gubler, D. J., Epidemic dengue/dengue hemorrhagic fever as a public health, social and economic problem in the 21st century. *Trends Microbiol.* **2002**, *10* (2), 100-103.
- (36) Guzman, M. G.; Gubler, D. J.; Izquierdo, A.; Martinez, E., et al., Dengue infection. *Nat. Rev. Dis. Primers* **2016**, *2*.
- (37) Bäck, A. T.; Lundkvist, A., Dengue viruses - an overview. *Infection ecology & epidemiology* **2013**, *3*, 10.3402/iee.v3i0.19839.
- (38) Rodenhuis-Zybert, I. A.; Wilschut, J.; Smit, J. M., Dengue virus life cycle: viral and host factors modulating infectivity. *Cell. Mol. Life Sci.* **2010**, *67* (16), 2773-2786.
- (39) Whitehead, S. S.; Blaney, J. E.; Durbin, A. P.; Murphy, B. R., Prospects for a dengue virus vaccine. *Nat. Rev. Microbiol.* **2007**, *5*, 518-528.
- (40) WHO, Dengue vaccine: WHO position paper. *Weekly Epidemiological Record* **2018**, *93* (36), 457-476.
- (41) WHO; TDR, *Dengue: Guidelines for Diagnosis, Treatment, Prevention and Control*. WHO: France, 2009; p 147.
- (42) Schmid, M. A.; Diamond, M. S.; Harris, E., Dendritic Cells in Dengue Virus Infection: Targets of Virus Replication and Mediators of Immunity. *Front. Immunol.* **2014**, *5*, 1-10.
- (43) Guzman, M. G.; Alvarez, M.; Halstead, S. B., Secondary infection as a risk factor for dengue hemorrhagic fever/dengue shock syndrome: an historical perspective and role of antibody-dependent enhancement of infection. *Arch. Virol.* **2013**, *158* (7), 1445-1459.
- (44) Kostich, W.; Hamman, B. D.; Li, Y. W.; Naidu, S., et al., Inhibition of AAK1 Kinase as a Novel Therapeutic Approach to Treat Neuropathic Pain. *J. Pharmacol. Exp. Ther.* **2016**, *358* (3), 371-386.
- (45) Bronson, J.; Chen, L.; Ditta, J.; Dzierba, C. D., et al. Biaryl Kinase Inhibitors. 2017.
- (46) Kuai, L.; Ong, S.-E.; Madison, J. M.; Wang, X., et al., AAK1 identified as an inhibitor of neuregulin-1/ErbB4-dependent neurotrophic factor signaling using integrative chemical genomics and proteomics. *Chem. Biol.* **2011**, *18* (7), 891-906.
- (47) Tang, X.-l.; Wang, Y.; Li, D.-l.; Luo, J., et al., Orphan G protein-coupled receptors (GPCRs): biological functions and potential drug targets. *Acta Pharmacol. Sin.* **2012**, *33*, 363-371.
- (48) Moran, B. M.; Flatt, P. R.; McKillop, A. M., G protein-coupled receptors: signalling and regulation by lipid agonists for improved glucose homeostasis. *Acta Diabetol.* **2016**, *53* (2), 177-188.

- (49) Lagerström, M. C.; Schiöth, H. B., Structural diversity of G protein-coupled receptors and significance for drug discovery. *Nat. Rev. Drug. Discov.* **2008**, *7*, 339-357.
- (50) Sriram, K.; Insel, P. A., GPCRs as targets for approved drugs: How many targets and how many drugs? *Mol. Pharmacol.* **2018**, *93*, 251-258.
- (51) Williams, C.; Hill, S. J., GPCR Signaling: Understanding the Pathway to Successful Drug Discovery. In *G-Protein Coupled Receptors in Drug Discovery*, Leifert, W. R., Ed. Humana Press: Totowa, NJ, 2009; pp 39-50.
- (52) Luttrell, L. M.; Lefkowitz, R. J., The role of  $\beta$ -arrestins in the termination and transduction of G-protein-coupled receptor signals. *J. Cell Sci.* **2002**, *115* (3), 455-465.
- (53) Walther, C.; Ferguson, S. S. G., Chapter Four - Arrestins: Role in the Desensitization, Sequestration, and Vesicular Trafficking of G Protein-Coupled Receptors. In *Prog. Mol. Biol. Transl. Sci.*, Luttrell, L. M., Ed. Academic Press: 2013; Vol. 118, pp 93-113.
- (54) Burstein, E. S.; Ott, T. R.; Feddock, M.; Ma, J.-N., et al., Characterization of the Mas-related gene family: structural and functional conservation of human and rhesus MrgX receptors. *Br. J. Pharmacol.* **2006**, *147* (1), 73-82.
- (55) Dong, X.; Han, S.-k.; Zylka, M. J.; Simon, M. I., et al., A Diverse Family of GPCRs Expressed in Specific Subsets of Nociceptive Sensory Neurons. *Cell* **2001**, *106* (5), 619-632.
- (56) Wu, H.; Zeng, M.; Cho, E. Y. P.; Jiang, W., et al., The Origin, Expression, Function and Future Research Focus of a G Protein-coupled Receptor, Mas-related Gene X2 (MrgX2). *Prog. Histochem. Cytochem.* **2015**, *50* (1), 11-17.
- (57) Subramanian, H.; Gupta, K.; Ali, H., Roles of Mas-related G protein-coupled receptor X2 on mast cell-mediated host defense, pseudoallergic drug reactions, and chronic inflammatory diseases. *J. Allergy Clin. Immunol.* **2016**, *138* (3), 700-710.
- (58) Bader, M.; Alenina, N.; Andrade-Navarro, M. A.; Santos, R. A., Mas and Its Related G Protein-Coupled Receptors, Mrgprs. *Pharmacol. Rev.* **2014**, *66* (4), 1080-1105.
- (59) Robas, N.; Mead, E.; Fidock, M., MrgX2 Is a High Potency Cortistatin Receptor Expressed in Dorsal Root Ganglion. *J. Biol. Chem.* **2003**, *278* (45), 44400-44404.
- (60) Ogasawara, H.; Furuno, M.; Edamura, K.; Noguchi, M., Novel MRGPRX2 antagonists inhibit IgE-independent activation of human umbilical cord blood-derived mast cells. *J. Leukocyte Biol* **2019**, 1-9.
- (61) Solinski, H. J.; Gudermann, T.; Breit, A., Pharmacology and Signaling of MAS-Related G Protein-Coupled Receptors. *Pharmacol. Rev.* **2014**, *66* (3), 570.
- (62) Manorak, W.; Idahosa, C.; Gupta, K.; Roy, S., et al., Upregulation of Mas-related G Protein coupled receptor X2 in asthmatic lung mast cells and its activation by the novel neuropeptide hemokinin-1. *Respir. Res.* **2018**, *19* (1), 1-5.
- (63) Metcalfe, D. D.; Baram, D.; Mekori, Y. A., Mast cells. *Physiol. Rev.* **1997**, *77* (4), 1033-1079.
- (64) Oskeritzian, C. A.; Zhao, W.; Min, H.-K.; Xia, H.-Z., et al., Surface CD88 functionally distinguishes the MCTC from the MCT type of human lung mast cell. *J. Allergy Clin. Immunol.* **2005**, *115* (6), 1162-1168.
- (65) Irani, A. A.; Schechter, N. M.; Craig, S. S.; DeBlois, G., et al., Two types of human mast cells that have distinct neutral protease compositions. *Proc. Natl. Acad. Sci. U. S. A.* **1986**, *83* (12), 4464-4468.
- (66) Krystel-Whittemore, M.; Dileepan, K. N.; Wood, J. G., Mast Cell: A Multi-Functional Master Cell. *Front. Immunol.* **2016**, *6*, 1-9.
- (67) Méndez-Enríquez, E.; Hallgren, J., Mast Cells and Their Progenitors in Allergic Asthma. *Front. Immunol.* **2019**, *10*.
- (68) Okayama, Y.; Saito, H.; Ra, C., Targeting Human Mast Cells Expressing G-Protein-Coupled Receptors in Allergic Diseases. *Allergol. Int.* **2008**, *57* (3), 197-203.
- (69) McNeil, B. D.; Pundir, P.; Meeker, S.; Han, L., et al., Identification of a mast-cell-specific receptor crucial for pseudo-allergic drug reactions. *Nature* **2014**, *519*, 237.
- (70) Lansu, K.; Karpiak, J.; Liu, J.; Huang, X.-P., et al., In silico design of novel probes for the atypical opioid receptor MRGPRX2. *Nat. Chem. Biol.* **2017**, *13*, 529-536.
- (71) Malik, L.; Kelly, N. M.; Ma, J.-N.; Currier, E. A., et al., Discovery of non-peptidergic MrgX1 and MrgX2 receptor agonists and exploration of an initial SAR using solid-phase synthesis. *Bioorg. Med. Chem. Lett.* **2009**, *19* (6), 1729-1732.

- (72) Griffith, J. W.; Sokol, C. L.; Luster, A. D., Chemokines and Chemokine Receptors: Positioning Cells for Host Defense and Immunity. *Annu. Rev. Immunol.* **2014**, *32* (1), 659-702.
- (73) Koelink, P. J.; Overbeek, S. A.; Braber, S.; de Kruijf, P., et al., Targeting chemokine receptors in chronic inflammatory diseases: An extensive review. *Pharmacol. Ther.* **2012**, *133* (1), 1-18.
- (74) Hughes, C. E.; Nibbs, R. J. B., A guide to chemokines and their receptors. *The FEBS Journal* **2018**, *285* (16), 2944-2971.
- (75) Turner, M. D.; Nedjai, B.; Hurst, T.; Pennington, D. J., Cytokines and chemokines: At the crossroads of cell signalling and inflammatory disease. *Biochim. Biophys. Acta, Mol. Cell Res.* **2014**, *1843* (11), 2563-2582.
- (76) Iellem, A.; Mariani, M.; Lang, R.; Recalde, H., et al., Unique Chemotactic Response Profile and Specific Expression of Chemokine Receptors Ccr4 and Ccr8 by Cd4+Cd25+Regulatory T Cells. *J. Exp. Med.* **2001**, *194* (6), 847-853.
- (77) Dembic, Z., Chapter 7 - Cytokines of the Immune System: Chemokines. In *The Cytokines of the Immune System*, Academic Press: Amsterdam, 2015; pp 241-262.
- (78) Barsheshet, Y.; Wildbaum, G.; Levy, E.; Vitsenshtein, A., et al., CCR8+ FOXP3+Tregcells as master drivers of immune regulation. *Proc. Natl. Acad. Sci. U. S. A.* **2017**, *114* (23), 6086-6091.
- (79) Denis, C.; Deiteren, K.; Mortier, A.; Tounsi, A., et al., C-Terminal Clipping of Chemokine CCL1/I-309 Enhances CCR8-Mediated Intracellular Calcium Release and Anti-Apoptotic Activity. *PLOS ONE* **2012**, *7* (3), 1-9.
- (80) Rummel, P.; Arfelt, K.; Baumann, L.; Jenkins, T., et al., Molecular requirements for inhibition of the chemokine receptor CCR8 – probe-dependent allosteric interactions. *Br. J. Pharmacol.* **2012**, *167* (6), 1206-1217.
- (81) Villarreal, D. O.; Huillier, A.; Armington, S.; Mottershead, C., et al., Targeting CCR8 induces protective antitumor immunity and enhances vaccine-induced responses in colon cancer. *Cancer Res.* **2018**, *78* (18), 5340-5348.
- (82) Karin, N., Chemokines and cancer: new immune checkpoints for cancer therapy. *Curr. Opin. Immunol.* **2018**, *51*, 140-145.
- (83) Haskell, C. A.; Horuk, R.; Liang, M.; Rosser, M., et al., Identification and Characterization of a Potent, Selective Nonpeptide Agonist of the CC Chemokine Receptor CCR8. *Mol. Pharmacol.* **2006**, *69* (1), 309-316.
- (84) Onuffer, J. J.; Horuk, R., Chemokines, chemokine receptors and small-molecule antagonists: recent developments. *Trends Pharmacol. Sci.* **2002**, *23* (10), 459-467.
- (85) Petersen, T. P.; Mirsharghi, S.; Rummel, P. C.; Thiele, S., et al., Multistep Continuous-Flow Synthesis in Medicinal Chemistry: Discovery and Preliminary Structure–Activity Relationships of CCR8 Ligands. *Chem. Eur. J.* **2013**, *19* (28), 9343-9350.
- (86) Ghosh, S.; Elder, A.; Guo, J.; Mani, U., et al., Design, Synthesis, and Progress toward Optimization of Potent Small Molecule Antagonists of CC Chemokine Receptor 8 (CCR8). *J. Med. Chem.* **2006**, *49* (9), 2669-2672.
- (87) Jenkins, T. J.; Guan, B.; Dai, M.; Li, G., et al., Design, Synthesis, and Evaluation of Naphthalene-Sulfonamide Antagonists of Human CCR8. *J. Med. Chem.* **2007**, *50* (3), 566-584.
- (88) Jin, J.; Wang, Y.; Wang, F.; Kerns, J. K., et al., Oxazolidinones as novel human CCR8 antagonists. *Bioorg. Med. Chem. Lett.* **2007**, *17* (6), 1722-1725.
- (89) Connolly, S.; Skrinjar, M.; Rosendahl, A., Orally bioavailable allosteric CCR8 antagonists inhibit dendritic cell, T cell and eosinophil migration. *Biochem. Pharmacol.* **2012**, *83* (6), 778-787.
- (90) Bamborough, P.; Drewry, D.; Harper, G.; Smith, G. K., et al., Assessment of Chemical Coverage of Kinome Space and Its Implications for Kinase Drug Discovery. *J. Med. Chem.* **2008**, *51* (24), 7898-7914.



## ***Chapter 2: Synthesis and structure-activity relationships of 3,5-disubstituted-pyrrolo[2,3-b]pyridines as inhibitors of adaptor associated kinase 1 (AAK1) with antiviral activity***

This chapter is based on the published paper: Verdonck, S.; Pu, S.-Y.; Sorrell, F. J.; Elkins, J. M., et al., Synthesis and Structure–Activity Relationships of 3,5-Disubstituted-pyrrolo[2,3-b]pyridines as Inhibitors of Adaptor-Associated Kinase 1 with Antiviral Activity. *J. Med. Chem.* **2019**, 62 (12), 5810-5831. The PhD candidate performed the synthesis of all described compounds along with their characterization.

### **2.1. Introduction**

Dengue virus (DENV) is an enveloped, positive-sense, single-stranded RNA virus belonging to the *Flaviviridae* family. DENV is transmitted by the mosquitoes *Aedes aegypti* and *Aedes albopictus*, which mainly reside in (sub)tropical climates.<sup>1</sup> In 2013, the WHO reported 3.2 million cases of severe dengue and more than 9,000 dengue-related deaths worldwide.<sup>2</sup> Up to 80% of DENV-infected patients remain asymptomatic. The likelihood of progression to severe dengue, manifesting by shock, hemorrhage and organ failure, is greater upon secondary infection with a heterologous dengue serotype (of four that circulate) due to antibody-dependent enhancement.<sup>3</sup>

Current efforts in search for drugs active against DENV focus primarily on viral targets.<sup>4</sup> However, targeting viral functions is often associated with the rapid emergence of drug resistance and usually provides a ‘one drug, one bug’ approach. DENV relies extensively on host factors for their replication and survival. These cellular factors represent attractive candidate targets for antiviral agents, potentially with a higher barrier for resistance.<sup>5,6</sup>

Intracellular membrane trafficking is an example of a cellular process that is hijacked by various viruses.<sup>7</sup> Adaptor complexes mediate the sorting of cargo proteins to specific membrane compartments within the cell. While AP2 sorts in the endocytic pathway, AP1 and AP4 sort in the secretory pathway.<sup>8</sup> The activity of AP2 and AP1 is regulated by two host cell kinases, adaptor-associated kinase 1 (AAK1) and cyclin G associated kinase (GAK). Phosphorylation of specific threonine residues in the  $\mu$  subunits of AP2 and AP1 by these kinases is known to stimulate their binding to tyrosine signals in cargo proteins and enhance vesicle assembly and internalization. Both AAK1 and GAK regulate clathrin-mediated endocytosis by recruiting clathrin and AP2 to the plasma membrane. AAK1 also regulates clathrin-mediated endocytosis of cellular receptors via alternative sorting adaptors that collaborate with AP2, e.g. by phosphorylation of NUMB.<sup>8</sup> AAK1 and GAK regulate hepatitis C (HCV) entry and assembly by modulating the activity of AP2<sup>8,9</sup> while also playing a role in the viral release and cell-to-cell spread via regulation of AP1 activity.<sup>5,10</sup> AAK1 and GAK are also required in the life cycle of DENV.<sup>5</sup>

The approved anticancer drugs sunitinib and erlotinib that potently inhibit AAK1 and GAK, respectively, demonstrate broad-spectrum *in vitro* antiviral activity against different members of the *Flaviviridae* family (HCV, DENV, ZIKV, WNV), as well as against various unrelated families of RNA viruses.<sup>5</sup> It also has been demonstrated that the combination of these two drugs effectively reduces viral load, morbidity and mortality in mice infected with DENV and EBOV.<sup>5,11</sup> These data provide a proof-of-concept that small molecule inhibition of AAK1 and GAK can yield broad-spectrum antiviral agents.<sup>5,11</sup> Moreover, using single-cell transcriptomic analysis, AAK1 has been validated as a particularly attractive target since it is overexpressed specifically in DENV-infected and not bystander cells (uninfected cells from the same cell culture), and its expression level increases with cellular virus abundance.<sup>5</sup>

Potent AAK1 inhibitors have been developed for the treatment of different neurological disorders, However, rather than starting from a potent AAK1 inhibitor, a structurally simple compound with reasonable AAK1 activity was selected as starting point as it allows for easy structural variation. A screening campaign of 577 structurally diverse compounds (representing kinase inhibitor chemical space) across a panel of 203 protein kinases using the DiscoverX binding assay format previously identified a pyrrolo[2,3-*b*]pyridine or 7-aza-indole derivative (**1.15**, **Figure 2.1**) as a potent AAK1 inhibitor ( $K_D = 53$  nM).<sup>12</sup> In this chapter, the efforts to optimize the AAK1 affinity and anti-DENV activity of compound **1.15** are described.

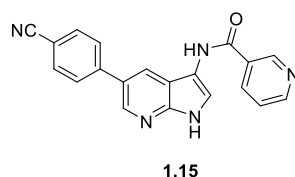


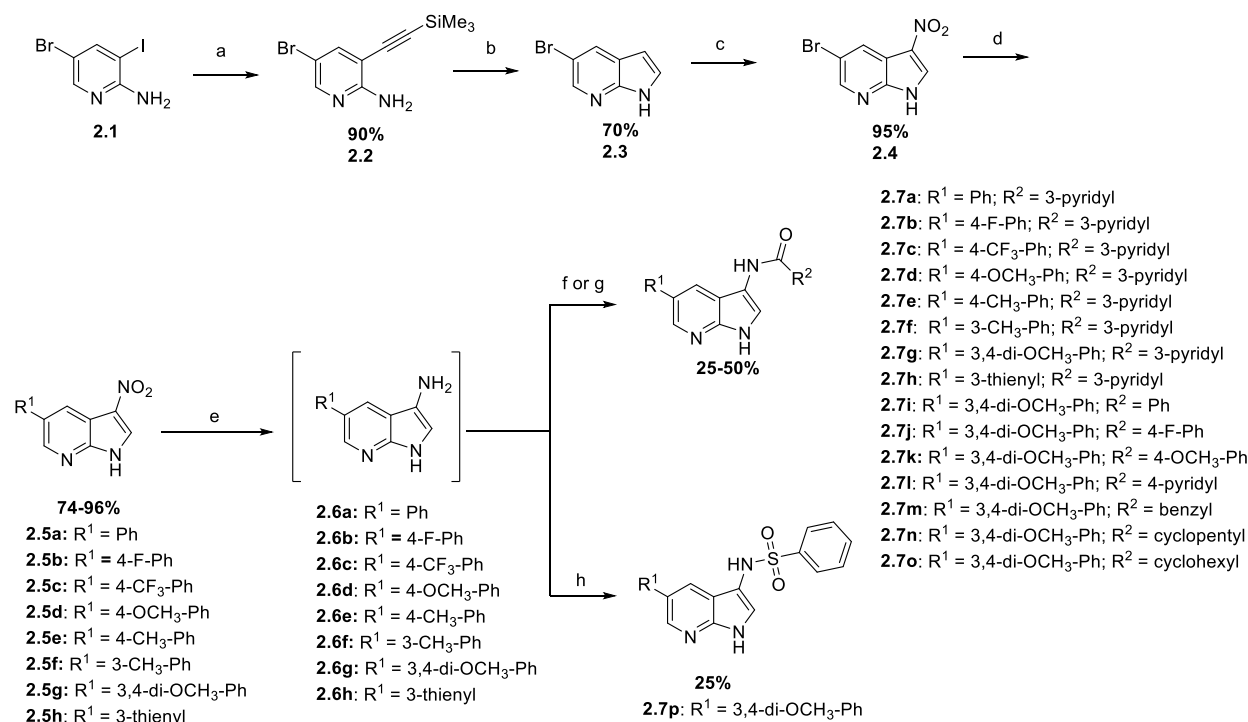
**Figure 2.1.** A pyrrolo[2,3-*b*]pyridine (7-aza-indole) based AAK1 inhibitor

## 2.2. Synthesis of pyrrolo[2,3-*b*]pyridine analogues

### *Synthesis of 3-substituted-5-aryl pyrrolo[2,3-*b*]pyridines*

A regioselective Sonogashira coupling of trimethylsilylacetylene (TMSA) with commercially available 2-amino-5-bromo-3-iodopyridine **2.1** afforded the alkynyl derivative **2.2** (**Scheme 2.1**).<sup>13</sup> Compound **2.2** was then reductively ring closed with a strong base yielding pyrrolo[2,3-*b*]pyridine **2.3**. Initially, NaH was used as base<sup>13</sup>, but later on potassium *tert*-butoxide (KO*t*Bu)<sup>14</sup> was applied as this gave a cleaner reaction outcome and an improved yield. Initial attempts to nitrate position 3 of the 7-azaindole scaffold employed a mixture of a 65% HNO<sub>3</sub> solution and sulfuric acid.<sup>15</sup> However, the desired product was difficult to isolate from this reaction mixture and therefore, the nitration was performed by treatment of compound **2.3** with fuming nitric acid.<sup>16</sup> The 3-nitro derivative **2.4** precipitated from the reaction mixture and was conveniently isolated by filtration. Suzuki coupling of compound **2.4** with a number of arylboronic acids yielded the 3-nitro-5-aryl-pyrrolo[2,3-*b*]pyridines **2.5a-h** in yields ranging from 65 to 85%.<sup>17</sup> Catalytic hydrogenation of the nitro moiety yielded the corresponding amino

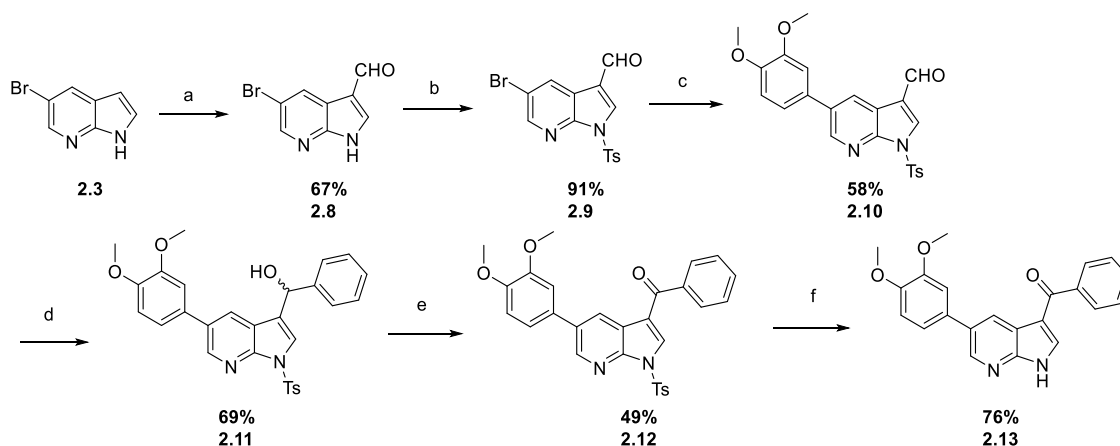
derivatives **2.6a-h**. Because of the instability of the 3-amino-pyrrolo[2,3-*b*]pyridines, these were not purified and used as such for further reaction. Coupling with an acid chloride in a mixture of pyridine and dichloromethane<sup>18</sup> or alternatively, reaction with a carboxylic acid using (benzotriazol-1-yloxy)tris(dimethylamino)phosphonium hexafluorophosphate (BOP) as coupling reagent<sup>19</sup> yielded a small library of pyrrolo[2,3-*b*]pyridines **2.7a-o**. A sulfonamide derivative **2.7p** was prepared via reaction of **2.6g** with phenylsulfonyl chloride in pyridine.



**Scheme 2.1. Reagents and conditions.** a) TMSA, Pd(PPh<sub>3</sub>)<sub>2</sub>Cl<sub>2</sub>, CuI, Et<sub>3</sub>N, THF, rt, 3h; b) KO<sup>t</sup>Bu, NMP, 80°C, 1h; c) HNO<sub>3</sub>, 0°C to rt, 40 min; d) Pd(PPh<sub>3</sub>)<sub>4</sub>, K<sub>2</sub>CO<sub>3</sub>, ArB(OH)<sub>2</sub>, H<sub>2</sub>O, dioxane, 105°C, overnight; e) H<sub>2</sub>, Pd/C, THF, rt, 3-4h; f) RCOCl, **2.6a-h**, pyridine, THF, 1M NaOH, rt, 3h; g) RCOOH, **2.6d**, BOP, Et<sub>3</sub>N, DMF, rt, overnight; h) PhSO<sub>2</sub>Cl, pyridine, rt, overnight.

### Synthesis of 3-benzoyl-5-(3,4-dimethoxyphenyl)-pyrrolo[2,3-*b*]pyridine (**2.13**)

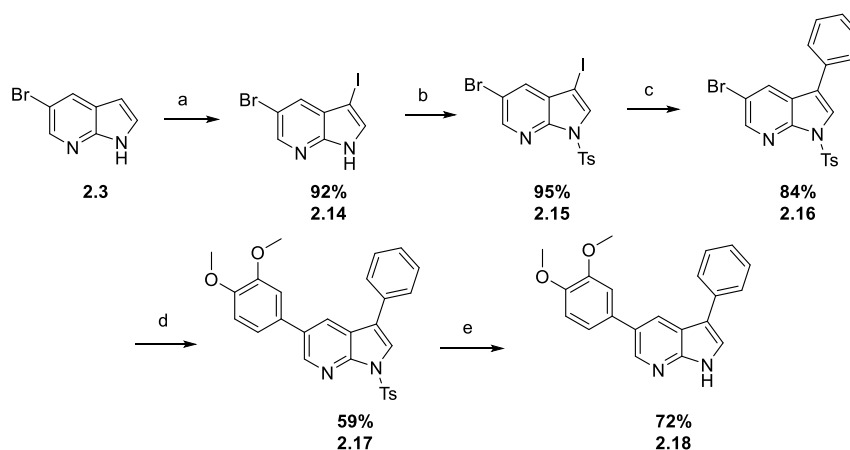
To construct a ketone linker, a first direct attempt was carried out in the form of a Friedel-Crafts reaction. As this reaction was unsuccessful a different approach was devised. Formylation of compound **2.3** by a Duff reaction<sup>20</sup> yielded 5-bromo-3-formyl-azaindole **2.8** (**Scheme 2.2**). The pyrrole nitrogen was protected<sup>21</sup> using NaH and tosylchloride (*p*TsCl) yielding compound **2.9**. Suzuki coupling reaction with 3,4-dimethoxyphenylboronic acid furnished compound **2.10**. Nucleophilic addition<sup>22</sup> of phenylmagnesium bromide to the aldehyde furnished the secondary alcohol **2.11**. Oxidation<sup>23</sup> of the benzylic alcohol using MnO<sub>2</sub> afforded ketone **2.12**. Finally, alkaline deprotection<sup>24</sup> of the tosyl group yielded the desired compound **2.13**.



**Scheme 2.2.** Reagents and conditions. a) hexamine, H<sub>2</sub>O, CH<sub>3</sub>COOH, 120°C, overnight; b) NaH, *p*TsCl, 0°C to rt, 3h; c) 3,4-dimethoxyphenylboronic acid, Pd(PPh<sub>3</sub>)<sub>4</sub>, 2M K<sub>2</sub>CO<sub>3</sub>, toluene, EtOH, 105°C, 4h; d) 3M PhMgBr, THF, rt, 1h; e) MnO<sub>2</sub>, THF, rt, overnight; f) KOH, EtOH, 80°C, 3h.

#### Synthesis of 3-phenyl-5-(3,4-dimethoxyphenyl)-pyrrolo[2,3-*b*]pyridine (2.18)

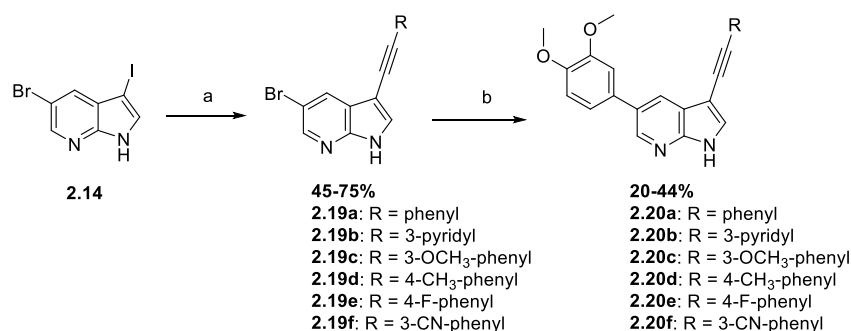
Iodination of compound 2.3 with *N*-iodosuccinimide (NIS)<sup>25</sup> afforded compound 2.14 (Scheme 2.3). Reaction of compound 2.14 with phenylboronic acid led only to recovery of unreacted starting material. Therefore, the pyrrole nitrogen of the 7-azaindole scaffold was protected with a tosyl group<sup>21</sup>, affording compound 2.15. A regioselective Suzuki coupling reaction using phenylboronic acid furnished the 3-phenyl-pyrrolo[2,3-*b*]pyridine analogue 2.16. A subsequent Suzuki reaction<sup>17</sup> with 3,4-dimethoxyphenylboronic acid yielded compound 2.17. Finally, alkaline cleavage of the tosyl protecting group afforded the desired target compound 2.18.



**Scheme 2.3.** Reagents and conditions. a) NIS, acetone, rt, 2h; b) NaH, *p*TsCl, THF, 0°C to rt, 2.5h; c) PhB(OH)<sub>2</sub>, Pd(PPh<sub>3</sub>)<sub>4</sub>, K<sub>2</sub>CO<sub>3</sub>, toluene, EtOH, H<sub>2</sub>O, 90°C, 3h; d) 3,4-dimethoxyphenylboronic acid, Pd(PPh<sub>3</sub>)<sub>4</sub>, K<sub>2</sub>CO<sub>3</sub>, toluene, EtOH, H<sub>2</sub>O, 105°C, 4h; e) KOH, EtOH, 80°C, 2h.

#### Synthesis of 3-alkynyl-5-(3,4-dimethoxyphenyl)-pyrrolo[2,3-*b*]pyridines (2.20a-f)

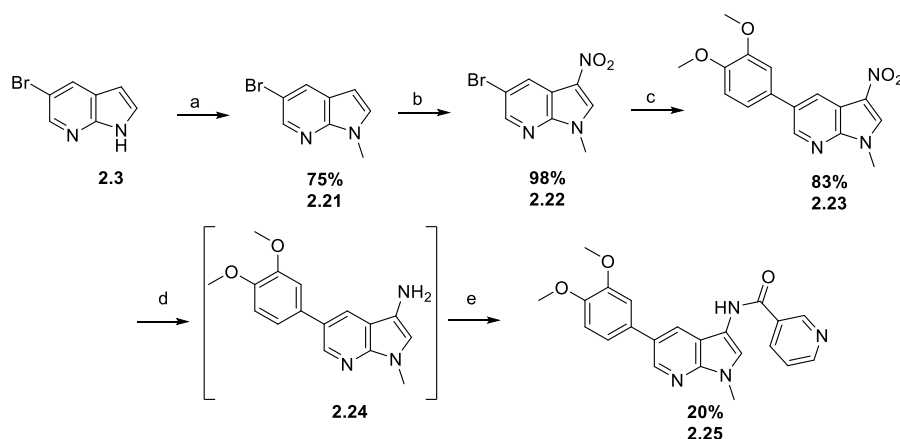
Sonogashira reaction of compound 2.14 with a number of (hetero)arylacetylenes yielded regioselectively compounds 2.19a-f in yields varying from 20-70% (Scheme 2.4).<sup>13</sup> In contrast to Suzuki couplings at position 3 presented in Scheme 2.3, protection of the pyrrole nitrogen was not necessary. Subsequent Suzuki coupling<sup>17</sup> at position 5 of the pyridine moiety with 3,4-dimethoxyphenylboronic acid gave access to final compounds 2.20a-f.



**Scheme 2.4.** *Reagents and conditions.* a)  $\text{RC}\equiv\text{CH}$ ,  $\text{Pd}(\text{PPh}_3)_2\text{Cl}_2$ ,  $\text{CuI}$ , THF,  $\text{Et}_3\text{N}$ , rt, 4h; b) 3,4-dimethoxyphenylboronic acid,  $\text{Pd}(\text{PPh}_3)_4$ ,  $\text{K}_2\text{CO}_3$ ,  $\text{H}_2\text{O}$ , dioxane, 105 °C, 3h.

#### Synthesis of 1-methyl-1H-pyrrolo[2,3-b]pyridine (2.25)

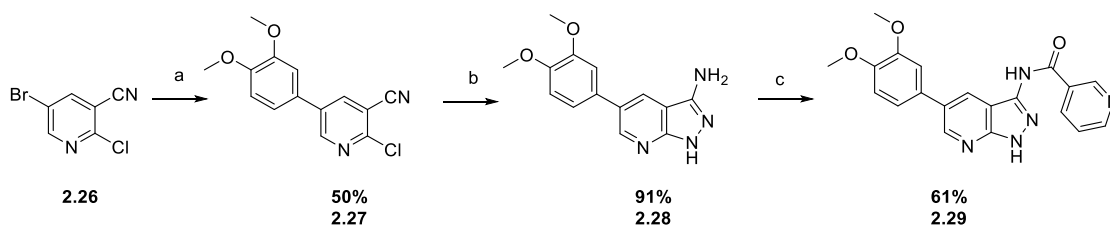
Methylation<sup>26</sup> of compound **2.3** using NaH and MeI furnished compound **2.21** (Scheme 2.5). Nitration<sup>16</sup>, followed by Suzuki coupling<sup>17</sup> gave access to compound **2.23**. Finally, catalytic reduction of the nitro group, followed by condensation<sup>18</sup> of the exocyclic amino group of compound **2.24** with nicotinoyl chloride yielded target compound **2.25**.



**Scheme 2.5.** *Reagents and conditions.* a) NaH, MeI, THF, 0°C to rt, 3h; b)  $\text{HNO}_3$ , 0°C to rt, 30 min; c) 3,4-dimethoxyphenylboronic acid,  $\text{Pd}(\text{PPh}_3)_4$ ,  $\text{K}_2\text{CO}_3$ ,  $\text{H}_2\text{O}$ , dioxane, 105°C, overnight; d)  $\text{H}_2$ , THF, rt, 3h; e) nicotinoyl chloride, pyridine, THF, 1M NaOH, rt, 3h.

#### Synthesis of N-(5-(3,4-dimethoxyphenyl)-1H-pyrazolo[3,4-b]pyridin-3-yl)nicotinamide(2.29)

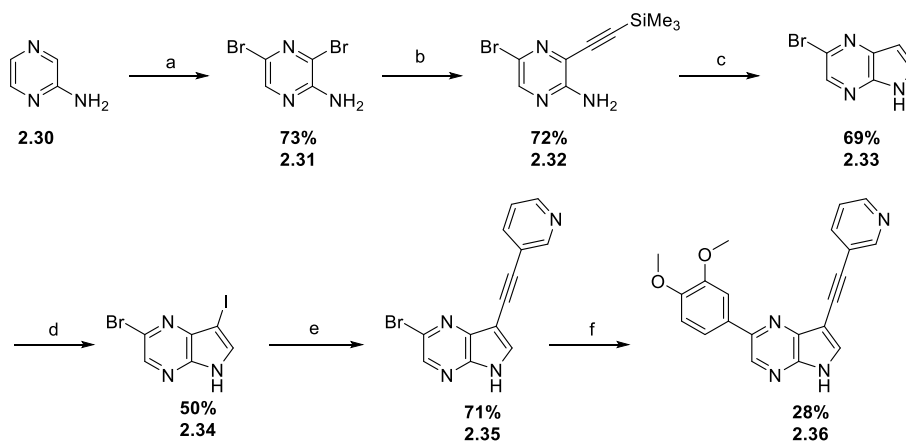
Suzuki coupling<sup>17</sup> between commercially available 5-bromo-2-chloronicotinonitrile **2.26** and 3,4-dimethoxyphenylboronic acid yielded regioselectively compound **2.27** (Scheme 2.6). Nucleophilic displacement of the chlorine by hydrazine, with a concomitant nucleophilic addition at the cyano group<sup>27</sup> allowed to construct the pyrazole moiety, yielding compound **2.28**. Finally, amide formation<sup>28</sup> using nicotinoyl chloride yielded the final compound **2.29**.



**Scheme 2.6.** *Reagents and conditions.* a) 3,4-dimethoxyphenylboronic acid, Pd(PPh<sub>3</sub>)<sub>4</sub>, K<sub>2</sub>CO<sub>3</sub>, H<sub>2</sub>O, dioxane, 105°C, 2,5h; b) 35% hydrazine hydrate, EtOH, 80°C, overnight; c) nicotinoyl chloride, pyridine, rt, overnight.

#### *Synthesis of 2-(3,4-dimethoxyphenyl)-7-(pyridin-3-ylethynyl)-5H-pyrrolo[2,3-b]pyrazine (2.36)*

Treatment of 2-aminopyrazine **2.30** with *N*-bromosuccinimide (NBS) yielded the 3,5-dibromopyrazine intermediate **2.31** (Scheme 2.7).<sup>29</sup> A regioselective Sonogashira coupling with TMSA, followed by a reductive ring closure with KOtBu furnished pyrrolo[2,3-*b*]pyrazine **2.33**.<sup>30</sup> Iodination<sup>31</sup> with *N*-iodosuccinimide yielded the dihalogenated intermediate **2.34** that was subsequently treated with 3-ethynylpyridine<sup>13</sup> and 3,4-dimethoxyphenylboronic acid<sup>17</sup> leading to the desired pyrrolo[2,3-*b*]pyrazine **2.36**.



**Scheme 2.7.** *Reagents and conditions.* a) NBS, DMSO, rt, 3h; b) Me<sub>3</sub>SiC≡CH, Pd(PPh<sub>3</sub>)<sub>2</sub>Cl<sub>2</sub>, CuI, THF, Et<sub>3</sub>N, rt, overnight; c) KOtBu, NMP, 100°C, 3h; d) NIS, acetone, rt, 2h; e) 3-ethynylpyridine, Pd(PPh<sub>3</sub>)<sub>2</sub>Cl<sub>2</sub>, CuI, THF, Et<sub>3</sub>N, rt, 4h; f) 3,4-dimethoxyphenylboronic acid, Pd(PPh<sub>3</sub>)<sub>4</sub>, K<sub>2</sub>CO<sub>3</sub>, H<sub>2</sub>O, dioxane, 105 °C, 3h.

### 2.3. Kinase profiling and X-ray crystallography of compound 1.15

AAK1 is a serine-threonine kinase that belongs to the NUMB-associated family of protein kinases (NAKs). Other members of this kinase family include BIKE/BMP2K (BMP-2 inducible kinase), GAK (cyclin G associated kinase) and MPSK1 (myristoylated and palmitoylated serine-threonine kinase 1, also known as STK16). As part of an early profiling of hit compound **1.15**, its selectivity was assessed by a binding-displacement assay against each of the four NAK family kinases (Figure 2.2). Conversion of the experimentally determined IC<sub>50</sub> values to K<sub>i</sub> values to allow estimation of the selectivity showed that compound **1.15** was 3-fold more selective for AAK1 over GAK, and 8-fold and 22-fold more selective for AAK1 over BMP2K and STK16, respectively (Table 2.1).

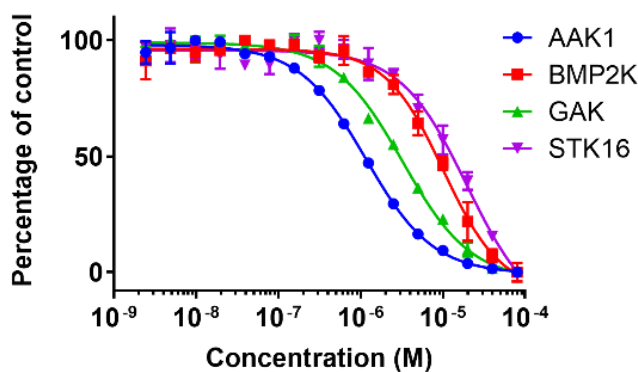
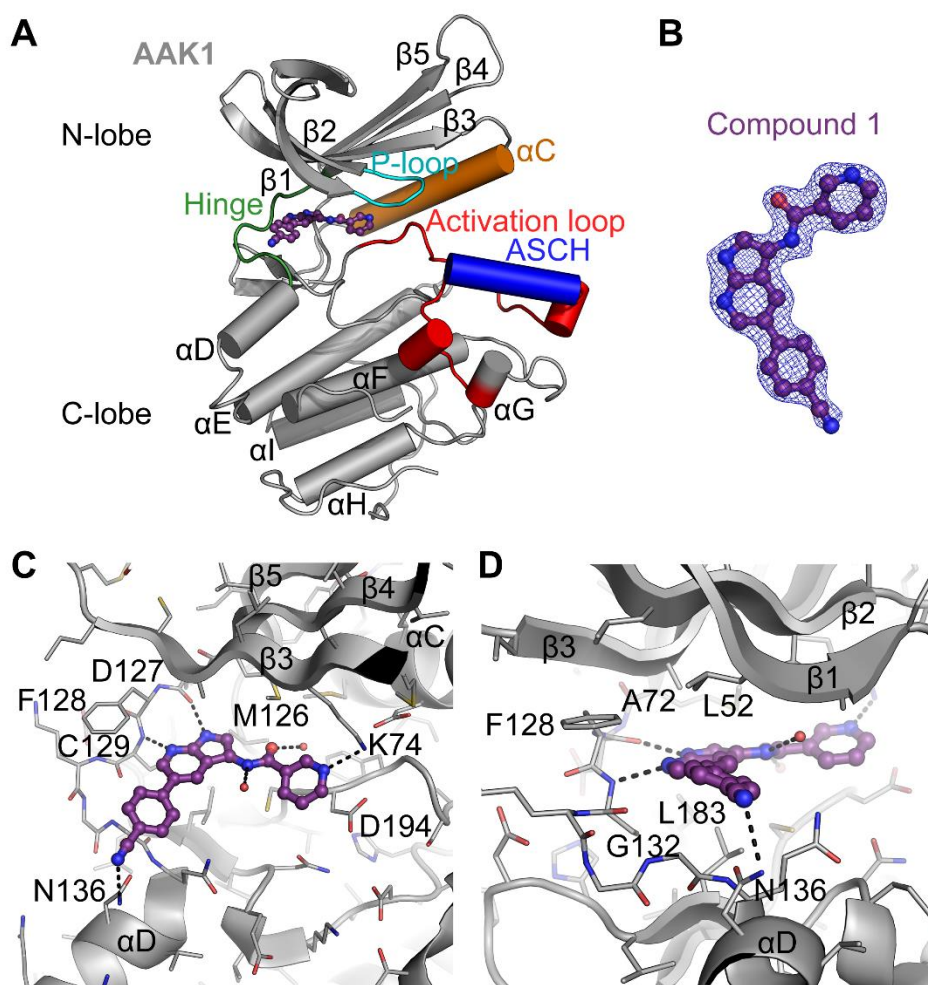


**Figure 2.2.** Binding displacement assay of compound **1.15** against the NAK family members.

Binding Displacement Assay			
NAK	IC <sub>50</sub> (μM)	K <sub>i</sub> (μM)	K <sub>i</sub> / K <sub>i</sub> (AAK1)
AAK1	1.17	0.541	1.0
BMP2K	10.1	4.40	8.13
GAK	3.25	1.75	3.23
STK16	20.0	11.9	22.0

**Table 2.1.** Selectivity of compound **1.15** for AAK1 against the NAK family kinases

To analyse the binding mode of compound **1.15**, the crystal structure of compound **1.15** bound to AAK1 to 2.0 Å resolution was determined (Figure 5). Compound **1.15** binds in the ATP-binding site of AAK1 in a relatively planar manner (Figure 2.3), with the pyrrolo[2,3-*b*]pyridine moiety bound directly between the side-chains of two highly conserved residues: Ala72 from β2 in the kinase N-lobe and Leu183 of the C-lobe, the location where the adenine ring of ATP would bind. The nitrogen atoms of the pyrrolo[2,3-*b*]pyridine moiety form two hydrogen bonds to the peptide backbone of residues Asp127 and Cys129 at the kinase hinge region (Figure 2.3). The 4-cyanophenyl moiety is oriented towards the solvent with the phenyl ring directly sandwiched between the backbone of Gly132 of the hinge and Leu52 of β1 in the N-lobe, and the nitrogen of the cyano moiety forming a polar interaction with the side-chain of Asn136. The nicotinamide moiety is bound against the “gatekeeper” residue Met126, and forms a hydrogen bond to the side chain of Lys74, another highly conserved residue that normally links the phosphate of ATP to the αC-helix and required for correct positioning of the N-lobe for efficient catalysis. Compound **1.15** also interacts with two water molecules, one situated at the back of the ATP pocket that bridges between the oxygen of the amide moiety and the backbone nitrogen of Asp194, and a second at the front of the adenosine binding site directly below Val60 in the β1 strand that interacts with the amide nitrogen and surrounding solvent. The DFG motif (Asp194) is in the conformation expected of active AAK1 (Figure 2.3), with the activation loop of AAK1 in the same conformation as seen in previous AAK1 and BMP2K crystal structures, including the activation-segment C-terminal helix (ASCH), a structural element that is rare amongst other protein kinases, but conserved across the NAK family.<sup>32</sup>



**A:** Overview of the crystal structure of AAK1. Highlighted are areas that are important for kinase function. Compound **1.15** bound at the hinge is shown. ASCH = Activation Segment C-terminal Helix, a feature unique to kinases of the NAK family. **B:**  $2F_o - F_c$  Electron density map contoured at  $1\sigma$  around compound **1.15**, showing the fit of the model to the map. **C and D:** Detailed views of the interactions of compound **1.15** in the ATP-binding site from two orientations. Black dotted lines indicate polar interactions, red spheres indicate water molecules. Note that residues 48-63 from  $\beta 1$  and  $\beta 2$  are removed from C for clarity.

**Figure 2.3.** Crystal structure of AAK1 (grey) in complex with compound **1.15** (purple)

## 2.4. Structure-activity relationship (SAR) study

All compounds synthesized in this study were evaluated for AAK1 affinity using two different, commercially available AAK1 binding assays. In the early stage of the program, the proprietary KINOMEscan screening platform of DiscoverX was used. In this assay, compounds that bind the kinase active site prevent kinase binding to an immobilized ligand and reduce the amount of kinase captured on the solid support. Hits are then identified by measuring the amount of kinase captured in test versus control samples via qPCR that detects an associated DNA label.<sup>33</sup> Later on in the project, compounds were evaluated by the LanthaScreen™ Eu Kinase Binding Assay (ThermoFisher Scientific), in which binding of an Alexa Fluor™ conjugate or “tracer” to a kinase is detected by addition of a Eu-labeled



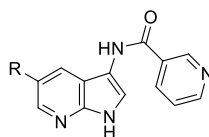
anti-tag antibody. Binding of the tracer and antibody to a kinase results in a high degree of fluorescence resonance energy transfer (FRET), whereas displacement of the tracer with a kinase inhibitor results in loss of FRET.<sup>34</sup>

The compounds were also assessed for antiviral activity in human hepatoma cells (Huh7) infected with DENV2. Their effect on overall infection was measured at 48 hours post infection with DENV2 via luciferase assays and the half-maximal effective concentration and the 90% effective concentrations (EC<sub>50</sub> and EC<sub>90</sub> values, respectively) were calculated. In parallel, the cytotoxicity of the compounds (expressed as the half-maximal cytotoxic concentration or CC<sub>50</sub> value) was measured via an AlamarBlue assay<sup>35</sup> in the DENV-infected Huh7 cells. In all these enzymatic and antiviral assays, sunitinib was included as a positive control (**Tables 2.2, 2.3, 2.4, 2.5 and 2.6**). Sunitinib has potent AAK1 affinity as measured by the KINOMEscan format ( $K_D = 11$  nM) and LanthaScreen assay (IC<sub>50</sub> = 47 nM) and displayed potent activity against DENV with an EC<sub>50</sub> value of 1.35  $\mu$ M.

#### 2.4.1. SAR at position 5 of the 7-aza-indole scaffold

The AAK1 binding affinity of hit compound **1.15** was confirmed, yet a  $K_D$  value of 120 nM was measured (vs. the reported  $K_D = 53$  nM).<sup>12</sup> This hit demonstrated antiviral activity, although rather weak (EC<sub>50</sub> = 8.37  $\mu$ M). Substitution of the 5-(4-cyanophenyl) moiety of compound **1.15** by phenyl (compound **2.7a**), thienyl (compound **2.7h**) and substituted phenyl rings with electron-withdrawing groups (compound **2.7c**), electron-donating substituents (compounds **2.7d-g**) and a halogen (compound **2.7b**) gave rise to a series of analogues with structural variety that were at least equipotent to compound **1.15**, suggesting that structural modification at this position is tolerated for AAK1 binding (**Table 2.2**). The synthesis of this limited number of analogues allowed to quickly identify the 5-(3,4-dimethoxyphenyl) congener (compound **2.7g**) with low nanomolar AAK1 binding affinity in both the KINOMEscan and LanthaScreen assay, indicating an excellent correlation between the two assays. As compound **2.7g** showed stronger AAK1 affinity than the positive control sunitinib, no additional efforts were done to further explore the SAR at this position of the 7-aza-indole scaffold.

All analogues within this series had an improved antiviral activity against DENV, relative to the original hit **1.15**. The compound with the highest binding affinity for AAK1 (compound **2.7g**) also demonstrated the most effective anti-DENV activity, with EC<sub>50</sub> and EC<sub>90</sub> values of 1.64  $\mu$ M and 7.46  $\mu$ M, respectively (**Figure 2.4**).



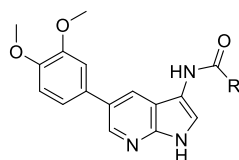
Cmpd#	R	AAK1 enzymatic data		DENV antiviral activity		Cytotoxicity CC <sub>50</sub>
		AAK1 <i>K<sub>D</sub></i> ( $\mu$ M) (DiscoverX)	AAK1 IC <sub>50</sub> ( $\mu$ M) (LanthaScreen)	EC <sub>50</sub> ( $\mu$ M)	EC <sub>90</sub> ( $\mu$ M)	
<b>1.15</b>	4-cyanophenyl	0.120	ND <sup>a</sup>	8.37	46.8	703
<b>2.7a</b>	phenyl	0.0822	ND <sup>a</sup>	5.29	87.1	NE <sup>b</sup>
<b>2.7b</b>	4-F-phenyl	0.141	ND <sup>a</sup>	6.43	25.2	NE <sup>b</sup>
<b>2.7c</b>	4-CF <sub>3</sub> -phenyl	ND <sup>a</sup>	0.23	2.94	12.0	57.0
<b>2.7d</b>	4-OCH <sub>3</sub> -phenyl	0.0194	ND <sup>a</sup>	4.39	25.8	NE <sup>b</sup>
<b>2.7e</b>	4-Me-phenyl	0.0532	ND <sup>a</sup>	2.60	33.6	129
<b>2.7f</b>	3-Me-phenyl	ND <sup>a</sup>	0.0186	4.86	10.8	16.0
<b>2.7g</b>	3,4-di-OCH <sub>3</sub> -phenyl	0.00673	0.00432	1.64	7.46	39.7
<b>2.7h</b>	3-thienyl	0.0161	ND <sup>a</sup>	3.01	66.8	NE <sup>b</sup>
<b>Sunitinib</b>	-	0.0110	0.0474	1.35	2.71	246

<sup>a</sup>ND: not determined; <sup>b</sup>NE: No effect (no apparent effect on cellular viability up to 10  $\mu$ M).

**Table 2.2.** SAR at position 5 of the 7-aza-indole scaffold

### 2.4.2. SAR of the *N*-acyl moiety

Given the improved AAK1 affinity and antiviral activity of compound **2.7g**, the SAR of this compound was further examined through the replacement of the 3-pyridyl group by a number of (hetero)aromatics and cycloaliphatic groups, while the 3,4-dimethoxyphenyl residue was kept fixed (**Table 2.3**). The following findings indicate that the 3-pyridyl moiety is critical for AAK1 binding as all analogues showed a 100-fold decreased AAK1 affinity, when compared to compound **2.7g**, giving rise to AAK1 IC<sub>50</sub> values in the 0.1-0.6  $\mu$ M range. Only the congener with a 4-methoxyphenyl residue (compound **2.7k**) was endowed with an enhanced AAK1 affinity with an IC<sub>50</sub> value of 0.072  $\mu$ M. In correlation with their weaker affinity for AAK1, these compounds had a diminished antiviral activity relative to compound **2.7g**.



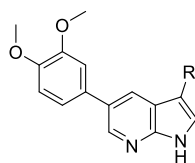
Cmpd#	R	AAK1 enzymatic	DENV antiviral activity		Cytotoxicity
		data	EC <sub>50</sub> (μM)	EC <sub>90</sub> (μM)	CC <sub>50</sub> (μM)
LanthaScreen					
<b>2.7g</b>	3-pyridyl	0.00432	1.64	7.46	39.7
<b>2.7i</b>	phenyl	0.108	4.07	50.5	17.3
<b>2.7j</b>	4-F-phenyl	0.161	8.34	30.2	15.9
<b>2.7k</b>	4-OCH <sub>3</sub> -phenyl	0.0721	NE <sup>a</sup>	NE <sup>a</sup>	23.6
<b>2.7l</b>	4-pyridyl	0.381	12.6	26.8	NE <sup>a</sup>
<b>2.7m</b>	benzyl	0.612	142	NE <sup>a</sup>	NE <sup>a</sup>
<b>2.7n</b>	cyclopentyl	0.398	3.42	8.34	15.2
<b>2.7o</b>	cyclohexyl	0.319	4.27	10.8	14.7

<sup>a</sup>NE: No effect (no apparent antiviral effect or effect on cellular viability up to 10 μM).

**Table 2.3.** SAR of the *N*-acyl moiety

### 2.4.3. SAR of the linker moiety at position 3

To evaluate the importance of the amide linker, a number of surrogates were prepared (**Table 2.4**). For synthetic feasibility reasons, compound **2.7i**, having a phenyl residue instead of a 3-pyridyl ring, and endowed with quite potent AAK1 affinity and moderate antiviral activity, was selected as a reference compound. Removing the amide linker furnished the 3-phenyl substituted analogue **2.18**, which was 4-fold more potent as AAK1 ligand than compound **2.7i**, and showed a slightly improved antiviral activity against DENV (EC<sub>50</sub> and EC<sub>90</sub> values of 3.02 μM and 8.34 μM, respectively). When the amide linker of compound **2.7i** was replaced by a ketone (compound **2.13**) or alkyne (compound **2.20a**) functionality, AAK1 affinity was retained. Compound **2.13** exhibited an improved antiviral activity in comparison with compound **2.7i**. Finally, replacement of the amide moiety by a sulfonamide linker was not well-tolerated, as compound **2.7p** showed close to 200-fold drop in AAK1 affinity.



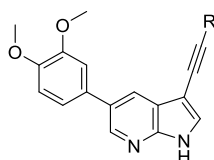
Cmpd#	R	AAK1 enzymatic	DENV antiviral activity		Cytotoxicity
		data	EC <sub>50</sub> (μM)	EC <sub>90</sub> (μM)	CC <sub>50</sub> (μM)
LanthaScreen					
2.7i		0.108	4.07	50.5	17.3
2.7p		4.44	8.14	106	NE <sup>a</sup>
2.13		0.184	1.07	3.73	35.3
2.18		0.0236	3.02	8.34	990
2.20a		0.209	5.64	10.58	20.1

<sup>a</sup>NE: No effect (no apparent effect on cellular viability up to 10 μM).

**Table 2.4.** SAR of the linker moiety at position 3

#### 2.4.4. SAR of phenylacetylene

The data in **Table 2.4** suggest that the amide moiety is not essential for AAK1 binding and can be replaced. Although the 3-phenyl derivative **2.18** displayed potent AAK1 affinity, 3,5-diaryl pyrrolo[2,3-*b*]pyridines are well known in the literature as kinase inhibitors. In contrast, 3-alkynyl-7-aza-indoles are studied to a much less extent. Therefore the acetylene derivate **2.20a** was selected to decipher if it was possible to improve AAK1 affinity and antiviral activity by further modifying the substitution pattern. A number of substituted phenylacetylene derivatives was prepared (compounds **2.20b-f**). The SAR in this series was quite flat, as all compounds displayed very similar AAK1 affinity with IC<sub>50</sub> values in the 0.1-0.4 μM range (**Table 2.5**). In contrast, the introduction of a 3-pyridylacetylene (compound **2.20b**) led to a substantial improvement in AAK1 affinity (IC<sub>50</sub> = 0.0042 μM) with a concomitant improvement in antiviral activity (**Figure 2.4**).



Cmpd#	R	AAK1	DENV antiviral activity		Cytotoxicity
		enzymatic data			
		IC <sub>50</sub> (μM)	EC <sub>50</sub>	EC <sub>90</sub>	CC <sub>50</sub>
		LanthaScreen	(μM)	(μM)	(μM)
<b>2.20a</b>	phenyl	0.209	5.64	10.58	20.1
<b>2.20b</b>	3-pyridyl	0.00402	0.72	4.16	17.0
<b>2.20c</b>	3-OCH <sub>3</sub> -phenyl	0.149	NE <sup>a</sup>	NE <sup>a</sup>	19.6
<b>2.20d</b>	4-CH <sub>3</sub> -phenyl	0.420	7.45	20.5	NE <sup>a</sup>
<b>2.20e</b>	4-F-phenyl	0.387	4.21	8.57	19.9
<b>2.20f</b>	3-CN-phenyl	0.381	10.2	41.2	NE <sup>a</sup>

<sup>a</sup>NE : No effect (no apparent antiviral effect or effect on cellular viability up to 10 μM).

**Table 2.5.** SAR of phenylacetylene moiety

### 2.4.5. Scaffold modifications

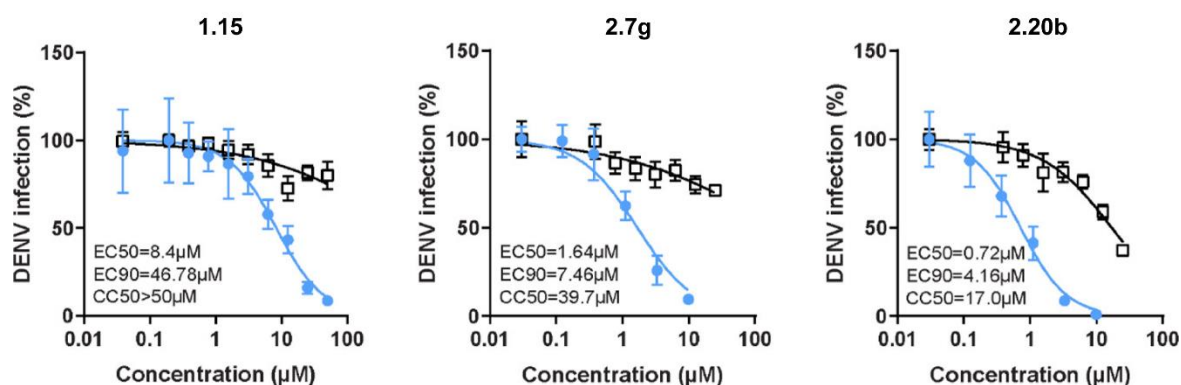
Lastly, the SAR exploration focused on the 7-aza-indole scaffold itself (**Table 2.6**). Methylation of the pyrrole nitrogen afforded compound **2.25**, displaying a greatly decreased AAK1 affinity (>800-fold loss in activity relative to compound **2.7g**) and antiviral activity (EC<sub>50</sub> > 10 μM). Insertion of an additional nitrogen atom in the pyrrole moiety yielded the pyrazolo[3,4-*b*]pyridine analogue **2.29** that is 100-fold less active as an AAK1 ligand relative to the parent compound **2.7g**. When the pyridine moiety of compound **2.20b** was replaced by a pyrazine ring, the pyrrolo[2,3-*b*]pyrazine analogue **2.36** was obtained. This compound was endowed with very potent AAK1 affinity (IC<sub>50</sub> = 0.00927 μM), comparable to its 7-aza-indole counterpart **2.20b**. Unfortunately, compound **2.36** demonstrated greater cytotoxicity than compound **2.20b** in Huh7 cells with CC<sub>50</sub>'s of 4.81 μM vs. 17.0 μM, respectively.

Cmpd#	Structure	AAK1	DENV antiviral activity		Cytotoxicity
		enzymatic data			
		IC <sub>50</sub> (μM)	EC <sub>50</sub>	EC <sub>90</sub>	CC <sub>50</sub>
		LanthaScreen	(μM)	(μM)	(μM)
<b>2.25</b>		3.39	NE <sup>a</sup>	NE <sup>a</sup>	NE <sup>a</sup>
<b>2.29</b>		0.462	2.09	19.0	16.0



<sup>a</sup>NE: No effect (no apparent antiviral effect or effect on cellular viability up to 10  $\mu$ M).

**Table 2.6.** Scaffold modifications

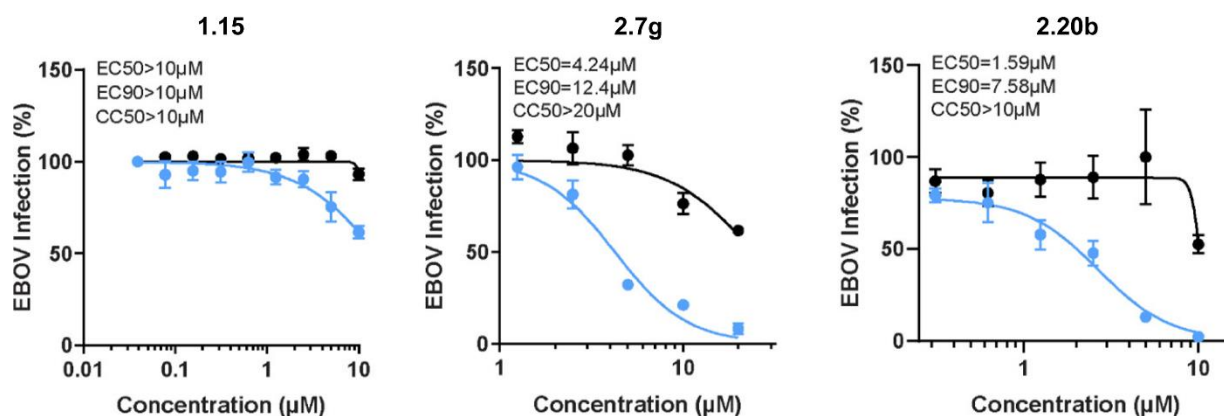


Dose response of DENV infection (blue) and cell viability (black) to compounds **1.15**, **2.7g**, and **2.20b** measured by luciferase and alamarBlue assays, respectively, 48 hours after infection. Data are plotted relative to vehicle control. Shown are representative experiments from at least two conducted, each with 5 biological replicates; shown are means  $\pm$  SD.

**Figure 2.4.** Compounds **2.7g** and **2.20b** suppress DENV infection more effectively than compound **1.15**.

## 2.5. Broad-spectrum antiviral activity

To evaluate for potential broad-spectrum antiviral coverage beyond DENV infection, hit compound **1.15** and the optimized congeners (compounds **2.7g** and **2.20b**) were tested for their activity against the unrelated EBOV. Huh7 cells were infected with EBOV and treated for 48 hours with each compound (**Figure 2.5**). Whereas compound **1.15** did not show effective activity against EBOV, the more potent AAK1 inhibitors **2.7g** and **2.20b** displayed anti-EBOV activity with EC<sub>50</sub> values in the low  $\mu$ M range and CC<sub>50</sub>> 10-20  $\mu$ M.

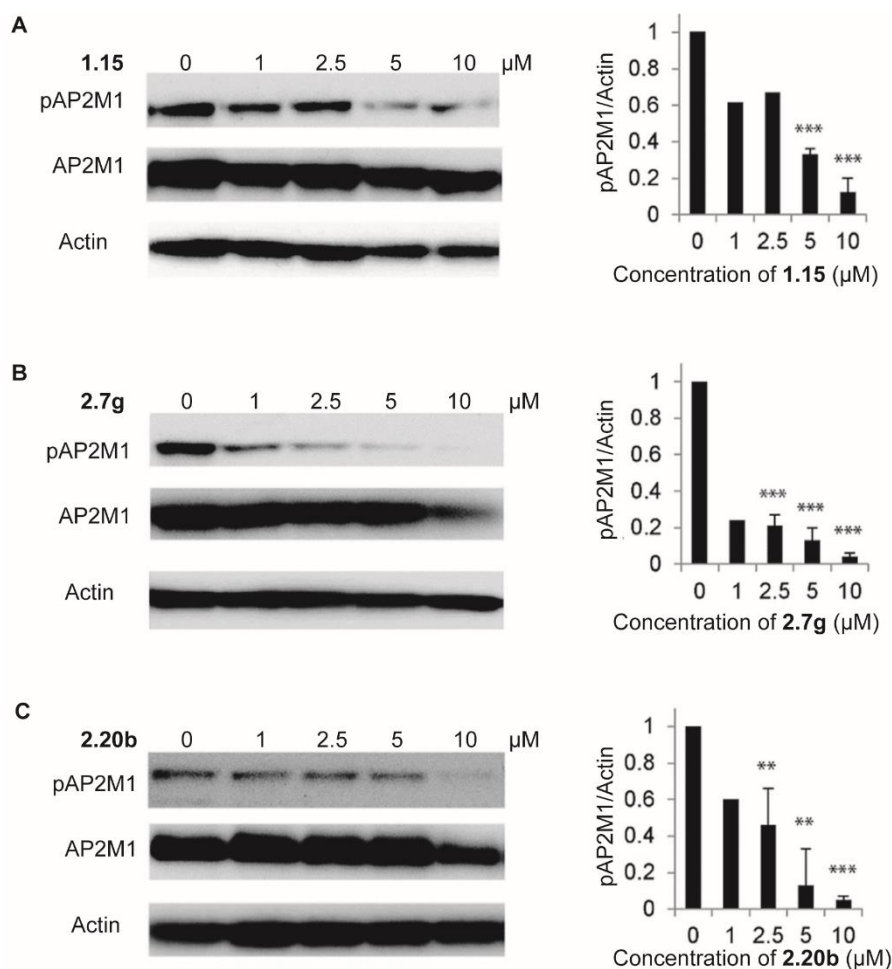


Dose response of EBOV infection (blue) and cell viability (black) to compounds **1.15**, **2.7g** and **2.20b** measured by plaque assay (for compound **1.15**) or immunofluorescence assays (for compounds **2.7g** and **2.20b**) and CellTiter-Glo luminescent cell viability assay in Huh7 cells 48 hours after infection. Data are plotted relative to vehicle control. Shown are representative experiments from at least two conducted, each with 3 biological replicates; shown are means  $\pm$  SD.

**Figure 2.5.** Compounds **1.15**, **2.7g** and **2.20b** suppress EBOV infection.

### 2.5.1. Correlation of the antiviral effect with functional AAK1 inhibition

To confirm that the observed antiviral activity is correlated with functional inhibition of AAK1 activity, levels of the phosphorylated form of the  $\mu$  subunit of the AP2 complex, AP2M1, upon treatment with compounds **1.15**, **2.20b** and **2.7g**, were measured. Since AP2M1 phosphorylation is transient (due to phosphatase PP2A activity)<sup>22</sup>, to allow capturing of the phosphorylated state, Huh7 cells were incubated for 30 minutes in the presence of the PP2A inhibitor calyculin A prior to lysis. Treatment with compounds **1.15**, **2.20b** and **2.7g** reduced AP2M1 phosphorylation (**Figure 2.6**), indicating modulation of AP2M1 phosphorylation via AAK1 inhibition.



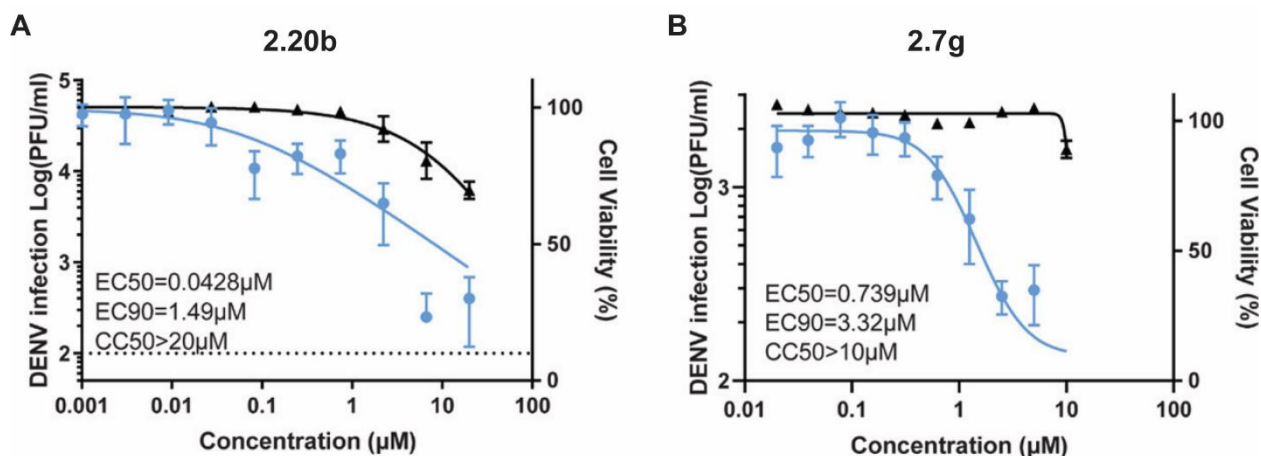
Dose response of AP2M1 phosphorylation to treatment with **1.15** (A), **2.7g** (B), and **2.20b** (C) by Western analysis in lysates derived from Huh7 cells. Representative membranes (from two independent experiments) blotted with anti-phospho-AP2M1 (pAP2M1), anti-AP2M1 (AP2M1), and anti-Actin (Actin) antibodies and quantified data of pAP2M1/actin protein ratio normalized to DMSO controls are shown. \*\*  $p < 0.01$ , \*\*\*  $p < 0.001$  by 2-tailed unpaired  $t$  test.

**Figure 2.6.** Antiviral effect of compounds **1.15**, **2.7g** and **2.20b** correlates with functional inhibition of AAK1.

### 2.5.2. Inhibition of DENV infection in human primary monocyte-derived dendritic cells

To determine the therapeutic potential of the AAK1 inhibitors, their antiviral activity was studied in human primary dendritic cells (MDDC). Primary cells are a physiologically more relevant model for DENV infection than immortalized cell lines, and are considered an *ex vivo* model for DENV infection.<sup>36</sup> Compounds **2.20b** and **2.7g** showed a dose-dependent inhibition of DENV infection with  $EC_{50}$  and  $EC_{90}$  values of 0.0428  $\mu$ M and 1.49  $\mu$ M and 0.739  $\mu$ M and 3.32  $\mu$ M, respectively (**Figure 2.7**). This very potent activity in MDDCs associated with minimal cytotoxicity ( $CC_{50} > 20$   $\mu$ M), particularly of compound **2.20b** demonstrates the potential of AAK1 inhibitors as antiviral agents.





Dose response of DENV infection (blue) and cell viability (black) to compounds **2.20b** (A) and **2.7g** (B) measured by plaque assays and alamarBlue assays, respectively, 72 hours after infection of primary human monocyte-derived dendritic cells (MDDCs). Shown is a representative experiment with cells from a single donor, out of 2 independent experiments conducted with cells derived from 2 donors, each with 6 biological replicates; shown are means  $\pm$  SD.

**Figure 2.7.** *Ex vivo* antiviral activity of **2.20b** and **2.7g** in human primary dendritic cells.

## 2.6. Kinase selectivity

To assess the kinase selectivity of the optimized AAK1 inhibitors, compound **2.20b** was screened against 468 kinases via the KINOMEScan assay (DiscoverX) at a single concentration of 10  $\mu\text{M}$ . As can be derived from the kinase interaction map (**Figure 2.8**), compound **2.20b** cannot be considered as a selective AAK1 inhibitor. Beyond AAK1, compound **2.20b** targets multiple other kinases (including the other members of the NAK family), which might contribute to its antiviral effect.

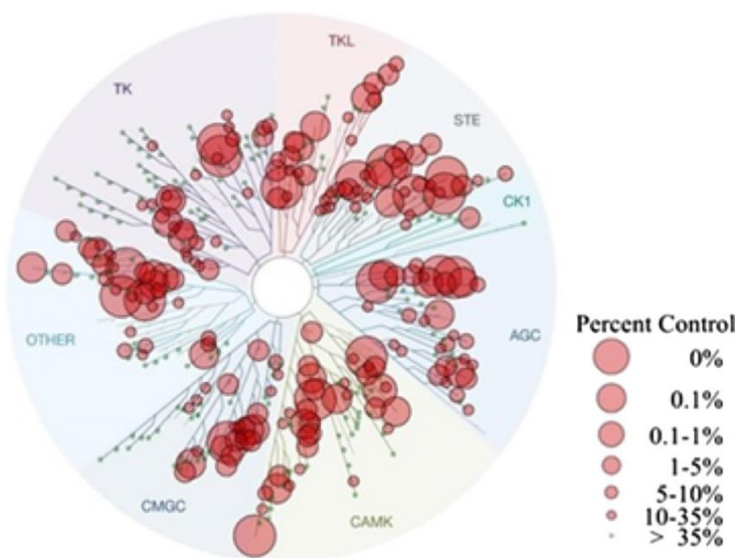


**Figure 2.8.** Kinome tree of compound **2.20b**. Kinases that bind compound **2.20b** are marked with red circles. The larger the circle, the stronger the binding affinity.

To quantitatively characterize the selectivity of compound **2.20b**, selectivity scores (S-scores) were calculated<sup>37</sup> (**Table 2.7**). The S-score is calculated by dividing the number of kinases that compounds bind to by the total number of distinct kinases tested, excluding mutant variants. Up to now, the AAK1

inhibitor that often has been used for antiviral activity studies is sunitinib. The S(3  $\mu$ M)-score of sunitinib, which is the number of kinases found to bind with a dissociation constant less than 3  $\mu$ M divided by the total number of non-mutant kinases tested, is 0.57.<sup>37</sup> The S (3  $\mu$ M) score is comparable with the S(10) score and therefore it can be deduced that the 7-aza-indole based AAK1 inhibitor **2.20b**, although still not very selective, has an improved kinase selectivity profile, relative to that of sunitinib, and it may therefore represent an improved pharmacological tool to probe the role of AAK1 in viral infection.

S-score type	Number of Hits	Number of Non-Mutant Kinases	Selectivity Score
S(35) <sup>a</sup>	212	403	0.526
S(10) <sup>b</sup>	138	403	0.342
S(1) <sup>c</sup>	49	403	0.122

<sup>a</sup>S(35) = (number of non-mutant kinases with %Ctrl <35)/(number of non-mutant kinases tested)

<sup>b</sup>S(10) = (number of non-mutant kinases with %Ctrl <10)/(number of non-mutant kinases tested)

<sup>c</sup>S(1) = (number of non-mutant kinases with %Ctrl <1)/(number of non-mutant kinases tested)

**Table 2.7.** Selectivity scores (S scores) for compound **2.20b** at 10  $\mu$ M

## 2.7. Conclusions

AAK1 is a promising host target for the development of broad-spectrum antiviral agents. In this chapter, the first systematic SAR study of AAK1 inhibitors as antiviral agents is presented. Starting from a known ligand with moderate AAK1 binding affinity and anti-DENV activity (**1.15**), a systematic SAR study was carried out. It led to the discovery of AAK1 ligands with low nanomolar AAK1 binding affinity that display improved antiviral activity against DENV (**2.7g** and **2.20b**). Moreover, the optimized AAK1 inhibitors exhibit very potent activity in DENV-infected primary dendritic cells and anti-EBOV activity, supporting the potential to develop broad-spectrum antiviral agents based on AAK1 inhibition. Kinase profiling revealed that these compounds have an improved selectivity profile relative to sunitinib, yet further research is necessary to improve their kinase selectivity.

## 2.8. Experimental section

All commercial reagents were obtained from Acros Organics, Sigma-Aldrich, AK Scientific and Fluorochem at at least 99% purity unless indicated otherwise. All dry solvents were purchased from Acros Organics with an AcroSeal system and regular solvents were obtained via Fisher Scientific at analytical grade. Thin layer chromatography (TLC) was performed on silica gel on aluminum foils with fluorescent indicator (254 nm) (60 Å pore diameter) obtained from Sigma-Aldrich and visualized using ultraviolet light (254 nm). Recording of the NMR spectra was performed using a Bruker 300 MHz, 500 MHz or 600 MHz spectrometer. The chemical shifts are reported in ppm relative to tetramethylsilane (TMS) or the residual solvent signal for  $^1\text{H}$ , the residual solvent signal for  $^{13}\text{C}$ . Spectra recorded in  $\text{D}_2\text{O}$  and for  $^{19}\text{F}$  are uncorrected. Coupling constants ( $J$ ) are reported in hertz. Mass spectra were acquired on a quadrupole orthogonal acceleration time-of-flight mass spectrometer (Synapt G2 HDMS, Waters, Milford, MA). Samples were infused at 3  $\mu\text{L}/\text{min}$  and spectra were obtained in positive or negative ionization mode with a resolution of 15000 (FWHM) using leucine enkephalin as lock mass. Purity of the compounds was determined on a Waters 600 HPLC system equipped with a Waters 2487 Dual  $\lambda$  absorbance detector set at 256 nm using a 5  $\mu\text{m}$  4.6x150 mm XBridge Reversed Phase ( $\text{C}_{18}$ ) column. The mobile phase was a gradient over 30 minutes starting from 95% A and 5% B and finishing at 5% A and 95% B with a flow rate of 1 ml per minute (solvent A: MilliQ water; solvent B: acetonitrile). All synthesized final compounds had a purity of at least 95 %. Compound **2.7o** was synthesized according to literature procedure.<sup>17</sup>

### 2.8.1. Chemistry

#### 2.8.1.1. Synthesis of key intermediate 2.4

##### 5-Bromo-3-((trimethylsilyl)ethynyl)pyridin-2-amine (2.2)

To a stirring suspension of **2.1** (520 mg, 1.74 mmol) in degassed triethylamine (10 ml) was added copper(I) iodide (6.63 mg, 0.034 mmol) and  $\text{Pd}(\text{PPh}_3)_2\text{Cl}_2$  (12 mg, 0.017 mmol). The system was flushed with nitrogen and trimethylsilylacetylene (188 mg, 265  $\mu\text{l}$ , 1.91 mmol) was added dropwise over 5 minutes. The reaction was allowed to stir for 3 hours at room temperature. After reaction completion, the solvent was evaporated and water was added. The resulting suspension was extracted three times using ethyl acetate. The combined organic phases were washed with water and brine, dried over  $\text{MgSO}_4$  and evaporated *in vacuo*. The crude residue was purified by silica gel flash column chromatography using a mixture of heptane and ethyl acetate (in a ratio of 80:20) as mobile phase, yielding the title compound as a yellow-beige solid (420 mg, 90%).  $^1\text{H}$  NMR (300 MHz,  $\text{DMSO}-d_6$ ):  $\delta$  8.03 (s, 1H), 7.69 (s, 1H), 6.37 (s, 2H), 0.24 (s, 9H,  $\text{Si}(\text{CH}_3)_3$ ).

##### 5-Bromo-1H-pyrrolo[2,3-b]pyridine (2.3)

**2.2** (200 mg, 0.743 mmol) in dry NMP (5 ml) was added portionwise  $\text{KO}t\text{Bu}$  (100 mg, 0.891 mmol). The reaction mixture was heated to 80°C and stirred for 1 hour. After reaction completion, the mixture was diluted with water and extracted with ethyl acetate three times. The combined organic phases were

washed twice with water and once with brine, dried over MgSO<sub>4</sub> and evaporated *in vacuo*. The crude residue was purified using silica gel flash column chromatography (using heptane and ethyl acetate in a ratio of 5:1 as mobile phase) yielding the title compound as a white solid (103 mg, 70%). <sup>1</sup>H NMR (300 MHz, DMSO-*d*<sub>6</sub>): δ 10.33 (bs, 1H), 8.37 (d, *J* = 2.1 Hz, 1H), 8.09 (d, *J* = 2.1 Hz, 1H), 7.37 (m, 1H), 6.47 (m, 1H).

### 5-Bromo-3-nitro-1*H*-pyrrolo[2,3-*b*]pyridine (2.4)

**2.3** (730 mg, 3.7 mmol) was added portionwise to a stirring solution of fuming nitric acid (2 ml) at 0°C over 10 minutes. The reaction was allowed to stir for 30 minutes at 0°C. The mixture was poured into ice water and the formed precipitate was collected via vacuum filtration. The filter cake was washed generously with water and heptane yielding the title compound as a yellow solid (853 mg, 95%). <sup>1</sup>H NMR (300 MHz, DMSO-*d*<sub>6</sub>): δ 13.48 (bs, 1H), 8.87 (s, 1H), 8.51 (s, 2H). <sup>13</sup>C NMR (75 MHz, DMSO-*d*<sub>6</sub>): δ 145.98, 145.26, 132.13, 129.96, 126.32, 115.17, 114.32.

#### 2.8.1.2. Synthesis of 3-nitro-5-aryl-pyrrolo[2,3-*b*]pyridines (2.5a-*h*)

##### General procedure

To a solution of **2.4** (1 eq) in dioxane (8 ml) was added the appropriate boronic acid (1.2 eq) and 2 ml of a K<sub>2</sub>CO<sub>3</sub> (3 eq) solution in water. The system was purged three times with argon and heated to 105°C. After stirring for 10 minutes, Pd(PPh<sub>3</sub>)<sub>4</sub> (0.1 eq) was added and the reaction was purged once more with argon. The reaction mixture was stirred at 105°C overnight. After completion, the reaction mixture was cooled to room temperature and filtered through Celite®. The filtrate was partitioned between water and ethyl acetate and the water layer was extracted with ethyl acetate. The combined organic phases were washed with brine, dried over MgSO<sub>4</sub> and evaporated *in vacuo*. Purification of the crude residue was achieved by silica gel flash column chromatography using the appropriate solvent mixture.

The following compounds were made according to this procedure:

### 3-Nitro-5-phenyl-1*H*-pyrrolo[2,3-*b*]pyridine (2.5a)

The title compound was synthesized according to the general procedure using **2.4** (100 mg, 0.413 mmol), phenylboronic acid (61 mg, 0.496 mmol) and K<sub>2</sub>CO<sub>3</sub> (171 mg, 1.24 mmol). Purification by silica gel flash column chromatography using a mixture of dichloromethane and ethyl acetate (in a ratio of 9:1) as the mobile phase, yielded the desired compound as a white solid (83 mg, 84%). <sup>1</sup>H NMR (300 MHz, DMSO-*d*<sub>6</sub>): δ 13.39 (bs, 1H), 8.89 (s, 1H), 8.76 (d, *J* = 2.1 Hz, 1H), 8.60 (d, *J* = 2.2 Hz, 1H), 7.79 (d, *J* = 7.2 Hz, 2H), 7.54 (t, *J* = 7.4 Hz, 2H), 7.45 (t, *J* = 7.3 Hz, 1H).

### 5-(4-Fluorophenyl)-3-nitro-1*H*-pyrrolo[2,3-*b*]pyridine (2.5b)

The title compound was synthesized according to the general procedure using **2.4** (100 mg, 0.413 mmol), 4-fluorophenylboronic acid (69 mg, 0.496 mmol) and K<sub>2</sub>CO<sub>3</sub> (171 mg, 1.24 mmol). Purification by silica gel flash column chromatography using a mixture of dichloromethane and ethyl acetate (in a ratio of 9:1) as the mobile phase yielded the desired compound as a light brown solid (98 mg, 92%).

<sup>1</sup>H NMR (300 MHz, DMSO-*d*<sub>6</sub>): δ 13.37 (bs, 1H), 8.90 (s, 1H), 8.82 (d, *J* = 2.9 Hz, 1H), 8.68 (d, *J* = 3.0 Hz, 1H), 8.01 (m, 4H).

#### **5-(4-(Trifluoromethyl)phenyl)-3-nitro-1H-pyrrolo[2,3-*b*]pyridine (2.5c)**

The title compound was synthesized according to the general procedure using **2.4** (100 mg, 0.413 mmol), 4-trifluoromethylphenylboronic acid (94 mg, 0.496 mmol) and K<sub>2</sub>CO<sub>3</sub> (171 mg, 1.24 mmol). Purification by silica gel flash column chromatography using a mixture of dichloromethane and ethyl acetate (in a ratio of 9:1) as the mobile phase yielded the desired compound as a white solid (110 mg, 87%). <sup>1</sup>H NMR (300 MHz, DMSO-*d*<sub>6</sub>): δ 13.45 (bs, 1H), 8.93 (s, 1H), 8.84 (d, *J* = 3.2 Hz, 1H), 8.70 (d, *J* = 3.1 Hz, 1H), 8.45 (m, 1H), 8.05 (d, *J* = 8.8 Hz, 2H), 7.89 (d, *J* = 8.9 Hz, 1H).

#### **5-(4-Methoxyphenyl)-3-nitro-1H-pyrrolo[2,3-*b*]pyridine (2.5d)**

The title compound was synthesized according to the general procedure using **2.4** (100 mg, 0.413 mmol), 4-methoxyphenylboronic acid (75 mg, 0.496 mmol) and K<sub>2</sub>CO<sub>3</sub> (171 mg, 1.24 mmol). Purification by silica gel flash column chromatography using a mixture of dichloromethane and ethyl acetate (in a ratio of 9:1) as the mobile phase yielded the desired compound as a yellow solid (104 mg, 94%). <sup>1</sup>H NMR (300 MHz, DMSO-*d*<sub>6</sub>): δ 13.32 (bs, 1H), 8.86 (s, 1H), 8.72 (d, *J* = 2.8 Hz, 1H), 8.55 (d, *J* = 3.0 Hz, 1H), 7.73 (d, *J* = 8.5 Hz, 2H), 7.10 (d, *J* = 8.5 Hz, 2H), 3.83 (s, 3H).

#### **3-Nitro-5-(*p*-tolyl)-1H-pyrrolo[2,3-*b*]pyridine (2.5e)**

The title compound was synthesized according to the general procedure using **2.4** (100 mg, 0.413 mmol), *p*-tolylboronic acid (67 mg, 0.496 mmol) and K<sub>2</sub>CO<sub>3</sub> (171 mg, 1.24 mmol). Purification by silica gel flash column chromatography using a mixture of dichloromethane and ethyl acetate (in a ratio of 9:1) as the mobile phase yielded the desired compound as a white solid (83 mg, 74%). <sup>1</sup>H NMR (300 MHz, DMSO-*d*<sub>6</sub>): δ 13.35 (bs, 1H), 8.88 (s, 1H), 8.74 (d, *J* = 3.2 Hz, 1H), 8.58 (d, *J* = 3.1 Hz, 1H), 7.68 (d, *J* = 7.8 Hz, 2H), 7.35 (d, *J* = 7.8 Hz, 2H), 2.38 (s, 3H).

#### **3-Nitro-5-(*m*-tolyl)-1H-pyrrolo[2,3-*b*]pyridine (2.5f)**

The title compound was synthesized according to the general procedure using **2.4** (100 mg, 0.413 mmol), *m*-tolylboronic acid (67 mg, 0.496 mmol) and K<sub>2</sub>CO<sub>3</sub> (171 mg, 1.24 mmol). Purification by silica gel flash column chromatography using a mixture of dichloromethane and ethyl acetate (in a ratio of 9:1) as the mobile phase yielded the desired compound as a white solid (83 mg, 74%). <sup>1</sup>H NMR (300 MHz, DMSO-*d*<sub>6</sub>): δ 13.35 (bs, 1H), 8.88 (s, 1H), 8.74 (d, *J* = 3.1 Hz, 1H), 8.59 (d, *J* = 3.1 Hz, 1H), 7.58 (t, *J* = 7.2 Hz, 2H), 7.42 (t, *J* = 7.3 Hz, 1H), 7.26 (d, *J* = 3.3 Hz, 1H), 2.42 (s, 3H).

#### **5-(3,4-Dimethoxyphenyl)-3-nitro-1H-pyrrolo[2,3-*b*]pyridine (2.5g)**

The title compound was synthesized according to the general procedure using **2.4** (100 mg, 0.413 mmol), 3,4-dimethoxyphenylboronic acid (63 mg, 0.496 mmol) and K<sub>2</sub>CO<sub>3</sub> (171 mg, 1.24 mmol). The compound precipitated as a yellow solid that was washed twice with dioxane, followed by washing with water yielding the pure title compound (88 mg, 89%). <sup>1</sup>H NMR (300 MHz, DMSO-*d*<sub>6</sub>): δ 8.82 (s, 1H),

8.72 (d,  $J = 2.1$  Hz, 1H), 8.54 (d,  $J = 2.2$  Hz, 1H), 7.30 (m, 2H), 7.10 (d,  $J = 8.3$  Hz, 1H), 3.88 (s, 3H), 3.82 (s, 3H).

### 3-Nitro-5-(3-thienyl)-1H-pyrrolo[2,3-*b*]pyridine (2.5h)

The title compound was synthesized according to the general procedure using **2.4** (100 mg, 0.413 mmol), 3-thienylboronic acid (69 mg, 0.496 mmol) and  $K_2CO_3$  (171 mg, 1.24 mmol). Purification by silica gel flash column chromatography using a mixture of dichloromethane and ethyl acetate (in a ratio of 9:1) as the mobile phase yielded the title compound as a brown solid (97 mg, 96%).  $^1H$  NMR (300 MHz,  $DMSO-d_6$ ):  $\delta$  13.41 (bs, 1H), 8.89 (d,  $J = 3.0$  Hz, 1H), 8.83 (d,  $J = 3.1$  Hz, 1H), 8.57 (d,  $J = 3.0$  Hz, 1H), 7.69 (m, 2H), 7.22 (t,  $J = 4.4$  Hz, 1H) ppm.

### 2.8.1.3. Synthesis of 5-aryl-3-amino- and 5-aryl-3-*N*-acylamino pyrrolo[2,3-*b*]pyridines (2.6a-f and 2.7a-o)

#### General procedure

To a solution of a 5-aryl-3-nitro-pyrrolo[2,3-*b*]pyridine **2.5a-h** (100 mg) in THF (5 ml) was added a slurry of Raney nickel in water in catalytic amounts. The reaction vessel was flushed three times with hydrogen gas and was stirred under a hydrogen atmosphere for 3-4 hours. Upon completion of the reaction, the catalyst was removed by filtration through Celite<sup>®</sup> and the solvent evaporated *in vacuo*. The crude residue was used in the next reaction without any purification, due to the rapid decomposition of the 3-amino-pyrrolo[2,3-*b*]pyridine intermediates **2.6a-h**. To a solution of crude compounds **2.6a-h** (1 eq) in dry pyridine (3 ml) was added a solution of nicotinoyl chloride hydrochloride (1.2 eq) in  $CH_2Cl_2$  (2 ml). The reaction mixture was allowed to stir at room temperature for 3 hours. The solvent was evaporated *in vacuo*. THF (5 ml) was added and the resulting solution was stirred for 5 minutes, followed by the addition of a 1M NaOH solution in water (5 ml). The resulting suspension was stirred for an additional 10 minutes. The precipitate was collected via vacuum filtration and purified using flash column chromatography with the appropriate solvent mixture as mobile phase. Compounds **2.7a-h** were synthesized according to this procedure.

#### *N*-(5-Phenyl-1H-pyrrolo[2,3-*b*]pyridin-3-yl)nicotinamide (2.7a)

The title compound was synthesized according to the general procedure, using **2.5a** (84 mg, 0.351 mmol). Purification by silica gel flash column chromatography (eluting with a mixture of dichloromethane and methanol in a gradient gradually ranging from 98:2 to 9:1) afforded the title compound as a dark brown solid (47 mg, 36%). Purity of 99%.  $^1H$  NMR (300 MHz,  $DMSO-d_6$ )  $\delta$  11.62 (bs, 1H), 10.58 (bs, 1H), 9.19 (s, 1H), 8.79 (d,  $J = 3.0$  Hz, 1H), 8.66 (s, 1H), 8.58 (s, 1H), 8.36 (d,  $J = 6.1$  Hz, 1H), 7.98 (s, 1H), 7.75 (d,  $J = 8.8$  Hz, 2H), 7.60 (t,  $J = 6.0$  Hz, 1H), 7.51 (t,  $J = 7.3$  Hz, 2H), 7.38 (t,  $J = 7.4$  Hz, 1H) ppm.  $^{13}C$  NMR (75 MHz,  $DMSO-d_6$ )  $\delta$  163.46, 152.01, 148.87, 145.52, 142.23, 139.16, 135.60, 131.63, 130.52, 129.13, 127.06, 126.93, 125.49, 123.61, 117.52, 114.10, 113.45 ppm. HRMS  $m/z$   $[M+H]^+$  calcd for  $C_{19}H_{15}N_4O$  315.1240, found 315.1237.

***N*-[5-(4-Fluorophenyl)-1*H*-pyrrolo[2,3-*b*]pyridin-3-yl]nicotinamide (2.7b)**

The title compound was synthesized according to the general procedure using **2.5b** (98 mg, 0.381 mmol). Purification by silica gel flash column chromatography (using a mixture of dichloromethane/methanol in a ratio gradually ranging from 98:2 to 9:1 as mobile phase) afforded the title compound as a brown solid (44 mg, 34%). Purity of 99%. <sup>1</sup>H NMR (300 MHz, DMSO-*d*<sub>6</sub>) δ 11.63 (bs, 1H), 10.57 (bs, 1H), 9.17 (s, 1H), 8.78 (d, *J* = 5.8 Hz, 1H), 8.62 (s, 1H), 8.56 (s, 1H), 8.36 (d, *J* = 8.9 Hz, 1H), 7.98 (d, *J* = 3.2 Hz, 1H), 7.77 (t, *J* = 7.6 Hz, 2H), 7.61 (d, *J* = 9.0 Hz, 1H), 7.35 (t, *J* = 7.5 Hz, 2H) ppm. <sup>13</sup>C NMR (75 MHz, DMSO-*d*<sub>6</sub>) δ 162.24, 161.77 (d, *J*<sub>CF</sub> = 242 Hz), 150.23, 148.62, 148.62, 145.58, 142.05, 138.10, 135.66, 128.86 (d, *J*<sub>CF</sub> = 8.0 Hz), 126.77, 126.72, 125.74, 122.38, 117.74, 116.00, 115.85 (d, *J*<sub>CF</sub> = 20.4), 113.75, 113.47 ppm. HRMS *m/z* [M+H]<sup>+</sup> calcd for C<sub>19</sub>H<sub>13</sub>N<sub>4</sub>O 333.11460, found 333.1145. HRMS *m/z* [M+Na]<sup>+</sup> calcd for C<sub>19</sub>H<sub>13</sub>N<sub>4</sub>O 355.0965, found 355.0950.

***N*-[5-(4-Trifluoromethylphenyl)-1*H*-pyrrolo[2,3-*b*]pyridin-3-yl]nicotinamide (2.7c)**

The title compound was synthesized according to the general procedure using **2.5c** (116 mg, 0.377 mmol). Purification by silica gel flash column chromatography using a mixture of dichloromethane and methanol (in a ratio gradually ranging from 98:2 to 9:1) as mobile phase afforded the title compound as a white solid (49 mg, 36%). Purity of 99%. <sup>1</sup>H NMR (300 MHz, DMSO-*d*<sub>6</sub>) δ 11.73 (bs, 1H), 10.62 (bs, 1H), 9.19 (d, *J* = 3.2 Hz, 1H), 8.78 (t, *J* = 6.1 Hz, 2H), 8.67 (d, *J* = 3.1 Hz, 1H), 8.36 (d, *J* = 3.0 Hz, 1H), 7.99 (d, *J* = 8.9 Hz, 3H), 7.87 (d, *J* = 9.0 Hz, 2H), 7.61 (q, *J* = 5.9 Hz, 1H) ppm. <sup>13</sup>C NMR (75 MHz, DMSO-*d*<sub>6</sub>) δ 163.52, 152.05, 148.85, 145.88, 143.25, 142.35, 135.58, 130.46, 127.48, 126.09, 123.61, 122.80, 117.84, 114.28, 113.52 ppm; missing peaks were observed in an APT spectrum. HRMS *m/z* [M+H]<sup>+</sup> calcd for C<sub>20</sub>H<sub>14</sub>N<sub>4</sub>F<sub>3</sub>O 383.1114; found 383.1114.

***N*-[5-(4-Methoxyphenyl)-1*H*-pyrrolo[2,3-*b*]pyridin-3-yl]nicotinamide (2.7d)**

The title compound was synthesized according to the general procedure using **2.5d** (105 mg, 0.390 mmol). Purification by silica gel flash column chromatography using a mixture of dichloromethane and methanol (in a ratio gradually ranging from 98:2 to 9:1) as mobile phase afforded the title compound as a pink solid (43 mg, 34%). Purity of 99%. <sup>1</sup>H NMR (300 MHz, DMSO-*d*<sub>6</sub>) δ 11.56 (bs, 1H), 10.56 (bs, 1H), 9.18 (s, 1H), 8.78 (d, *J* = 6.1 Hz, 1H), 8.58 (s, 1H), 8.52 (s, 1H), 8.36 (d, *J* = 9.0 Hz, 1H), 7.96 (s, 1H), 7.62 (m, 3H), 7.08 (d, *J* = 8.9 Hz, 2H), 3.82 (s, 3H) ppm. <sup>13</sup>C NMR (75 MHz, DMSO-*d*<sub>6</sub>) δ 163.45, 158.74, 151.99, 148.85, 145.22, 141.99, 135.59, 131.54, 130.50, 128.00, 127.55, 124.87, 123.60, 117.43, 114.64, 113.94, 113.45, 55.34 ppm. HRMS *m/z* [M+H]<sup>+</sup> calcd for C<sub>20</sub>H<sub>16</sub>N<sub>4</sub>O<sub>2</sub> 345.13459, found 345.1343. HRMS *m/z* [M+Na]<sup>+</sup> calcd for C<sub>20</sub>H<sub>17</sub>N<sub>4</sub>O<sub>2</sub> 367.1165; found 367.1153.

***N*-[5-(*p*-Tolyl)-1*H*-pyrrolo[2,3-*b*]pyridin-3-yl]nicotinamide (2.7e)**

The title compound was synthesized according to the general procedure using **2.5e** (96 mg, 0.379 mmol). Purification by silica gel flash column chromatography using a mixture of dichloromethane and methanol (in a ratio gradually ranging from 98:2 to 9:1) as mobile phase afforded the title compound as a beige solid (48 mg, 37%). Purity of 98%. <sup>1</sup>H NMR (300 MHz, DMSO-*d*<sub>6</sub>) δ 11.60 (bs, 1H), 10.59 (bs, 1H), 9.19 (s, 1H), 8.78 (d, *J* = 2.9 Hz, 1H), 8.63 (s, 1H), 8.56 (s, 1H), 8.36 (d, *J* = 6.0 Hz, 1H), 7.99

(s, 1H), 7.59 (m, 3H), 7.31 (d,  $J = 9.3$  Hz, 2H), 2.35 (s, 3H) ppm.  $^{13}\text{C}$  NMR (75 MHz, DMSO- $d_6$ )  $\delta$  163.49, 151.99, 148.85, 145.41, 142.10, 136.28, 136.22, 135.59, 130.51, 129.73, 127.68, 126.73, 125.12, 123.60, 117.50, 114.03, 113.47, 20.77 ppm. HRMS  $m/z$   $[\text{M}+\text{H}]^+$  calcd for  $\text{C}_{20}\text{H}_{17}\text{N}_4\text{O}$  329.1397; found 329.1398.

#### ***N*-[5-(*m*-Tolyl)-1*H*-pyrrolo[2,3-*b*]pyridin-3-yl]nicotinamide (2.7f)**

The title compound was synthesized according to the general procedure using **2.5f** (77 mg, 0.304 mmol). Purification by silica gel flash column chromatography using a mixture of dichloromethane and methanol (in a ratio gradually ranging from 98:2 to 9:1) as mobile phase afforded the title compound as a beige solid (22 mg, 25% yield). Purity of 98%.  $^1\text{H}$  NMR (300 MHz, DMSO- $d_6$ )  $\delta$  11.61 (bs, 1H), 10.59 (bs, 1H), 9.19 (s, 1H), 8.79 (d,  $J = 2.8$  Hz, 1H), 8.64 (s, 1H), 8.57 (s, 1H), 8.37 (d,  $J = 9.0$  Hz, 1H), 7.99 (s, 1H), 7.59 (m, 3H), 7.39 (t,  $J = 7.4$  Hz, 1H), 7.19 (d,  $J = 6.1$  Hz, 1H), 2.41 (s, 3H) ppm.  $^{13}\text{C}$  NMR (75 MHz, DMSO- $d_6$ )  $\delta$  163.49, 151.99, 148.84, 145.47, 142.25, 139.08, 138.27, 135.59, 130.50, 129.02, 127.84, 127.71, 127.53, 125.39, 124.06, 123.60, 117.47, 114.07, 113.42, 21.28 ppm. HRMS  $m/z$   $[\text{M}+\text{H}]^+$  calcd for  $\text{C}_{20}\text{H}_{17}\text{N}_4\text{O}$  329.1397; found 329.1397.

#### ***N*-[5-(3,4-Dimethoxyphenyl)-1*H*-pyrrolo[2,3-*b*]pyridin-3-yl]nicotinamide (2.7g)**

The title compound was synthesized according to the general procedure using **2.5g** (80 mg, 0.297 mmol). Purification by silica gel flash column chromatography using a mixture of dichloromethane and methanol (in a ratio gradually ranging from 98:2 to 9:1) as mobile phase afforded the title compound as a beige solid (56 mg, 50%). Purity of 97%.  $^1\text{H}$  NMR (300 MHz, DMSO- $d_6$ )  $\delta$  11.57 (bs, 1H), 10.56 (bs, 1H), 9.20 (s, 1H), 8.78 (d,  $J = 6.1$  Hz, 1H), 8.58 (d,  $J = 3.2$  Hz, 2H), 8.37 (d,  $J = 9.1$  Hz, 1H), 7.97 (s, 1H), 7.60 (t,  $J = 6.0$  Hz, 1H), 7.27 (t,  $J = 7.4$  Hz, 2H), 7.09 (d,  $J = 9.0$  Hz, 1H), 3.88 (s, 3H), 3.81 (s, 3H) ppm.  $^{13}\text{C}$  NMR (75 MHz, DMSO- $d_6$ )  $\delta$  163.45, 152.00, 149.40, 148.88, 148.43, 145.28, 142.26, 135.61, 132.04, 130.51, 127.84, 124.96, 123.61, 119.23, 117.47, 113.93, 113.39, 112.70, 111.09, 55.92, 55.82 ppm. HRMS  $m/z$   $[\text{M}+\text{H}]^+$  calcd for  $\text{C}_{21}\text{H}_{18}\text{N}_4\text{O}_3$  375.14515, found 375.1447, HRMS  $m/z$   $[\text{M}+\text{Na}]^+$  calcd for  $\text{C}_{21}\text{H}_{19}\text{N}_4\text{O}_3$  397.1271; found 397.1264.

#### ***N*-[5-(3-Thienyl)-1*H*-pyrrolo[2,3-*b*]pyridin-3-yl]nicotinamide (2.7h)**

The title compound was synthesized according to the general procedure using **2.5h** (97 mg, 0.395 mmol). Purification by silica gel flash column chromatography using a mixture of dichloromethane and methanol (in a ratio gradually ranging from 98:2 to 9:1) as mobile phase, afforded the title compound as a brown solid (48 mg, 37%). Purity of 99%.  $^1\text{H}$  NMR (300 MHz, DMSO- $d_6$ )  $\delta$  11.58 (bs, 1H), 10.54 (bs, 1H), 9.20 (d,  $J = 2.8$  Hz, 1H), 8.79 (d,  $J = 2.9$  Hz, 1H), 8.67 (d,  $J = 2.9$  Hz, 1H), 8.64 (d,  $J = 3.0$  Hz, 1H), 8.36 (m, 1H), 7.93 (s, 1H), 7.84 (s, 1H), 7.71 (m, 1H), 7.60 (t,  $J = 5.9$  Hz, 2H) ppm.  $^{13}\text{C}$  NMR (75 MHz, DMSO- $d_6$ )  $\delta$  163.48, 152.02, 148.86, 145.30, 142.03, 140.21, 135.58, 130.49, 127.30, 126.37, 124.61, 123.60, 123.18, 119.78, 117.63, 113.94, 113.49 ppm. HRMS  $m/z$   $[\text{M}+\text{H}]^+$  calcd for  $\text{C}_{17}\text{H}_{13}\text{N}_4\text{OS}$  321.0804; found 321.0804.



***N*-(5-(3,4-Dimethoxyphenyl)-1*H*-pyrrolo[2,3-*b*]pyridin-3-yl)benzamide (2.7i)**

To a solution of **2.5g** (100 mg, 0.334 mmol) in THF (4 ml) was added a catalytic amount of a slurry of Raney nickel in water. The vessel was flushed three times with hydrogen gas and kept under a hydrogen atmosphere for 4 hours. After complete conversion, the catalyst was removed by filtration and the solvent was evaporated *in vacuo*. The crude product was immediately used for further reaction without purification. To a solution of the crude residue from the previous reaction in pyridine (5 ml) was added a solution of benzoyl chloride (47  $\mu$ l, 0.401 mmol) in dichloromethane (0.5 ml). The reaction was stirred overnight at room temperature. After reaction completion, the solvent was evaporated *in vacuo* and the crude residue was partitioned between water and ethyl acetate and the water phase was subsequently extracted with ethyl acetate. The combined organic layers were dried over MgSO<sub>4</sub> and evaporated to dryness. Purification was achieved by silica gel flash column chromatography (using a mixture of dichloromethane and methanol in a ratio of 97:3 as mobile phase), followed by precipitation of the residue from acetone, yielding the title compound as a white solid (27 mg, 22%). Purity of 98%. <sup>1</sup>H NMR (300 MHz, DMSO-*d*<sub>6</sub>)  $\delta$  11.52 (bs, 1H), 10.37 (bs, 1H), 8.56 (d, *J* = 6.5, 2H), 8.00 (m, 3H), 7.56 (d, *J* = 7.6 Hz, 3H), 7.25 (m, 2H), 7.08 (d, *J* = 8.2 Hz, 1H), 3.87 (s, 3H), 3.80 (s, 3H) ppm. <sup>13</sup>C NMR (75 MHz, DMSO-*d*<sub>6</sub>)  $\delta$  165.07, 149.30, 148.30, 145.25, 142.12, 134.88, 132.01, 131.42, 128.48, 127.87, 127.70, 125.04, 119.14, 117.27, 114.22, 113.44, 112.52, 110.87, 55.83, 55.74 ppm. HRMS *m/z* [M+H]<sup>+</sup> calcd for C<sub>22</sub>H<sub>20</sub>N<sub>3</sub>O<sub>3</sub> 374.1499; found 374.1493.

**2.8.1.4. Synthesis of 5-(3,4-dimethoxyphenyl)-3-*N*-acylaminopyrrolo[2,3-*b*]pyridines****General procedure**

Compound **2.5g** (100 mg, 0.334 mmol) was hydrogenated with a catalytic amount of Raney nickel as a slurry in water in THF (5 ml) for 3 hours. The solvents were evaporated *in vacuo* yielding crude 3-amino-5-(3,4-dimethoxyphenyl)-1*H*-pyrrolo[2,3-*b*]pyridine which was used in the next reaction without further purification (90 mg, 99%). To a solution of 3-amino-5-(3,4-dimethoxyphenyl)-1*H*-pyrrolo[2,3-*b*]pyridine (90 mg, 0.334 mmol) in DMF (3 ml) was added the appropriate carboxylic acid (1 eq.), benzotriazol-1-yloxytris(dimethylamino)phosphonium hexafluorophosphate (BOP, 177 mg, 0.401 mmol) and triethylamine (140  $\mu$ l, 1 mmol). The mixture was stirred overnight at room temperature. When the reaction reached completion, water was added and the mixture was extracted three times with ethyl acetate. The combined organic layers were washed with brine, dried over Na<sub>2</sub>SO<sub>4</sub> and evaporated *in vacuo*. The crude residue was purified by silica gel flash chromatography using an appropriate solvent system as mobile phase. An additional purification was performed by preparative TLC using a mixture of dichloromethane and acetone (in a ratio of 8:2) as eluent. Compounds **2.7j-m** were prepared according to this procedure.

***N*-(5-(3,4-Dimethoxyphenyl)-1*H*-pyrrolo[2,3-*b*]pyridin-3-yl)-4-fluorobenzamide (2.7j)**

The title compound was synthesized according to the general procedure using 4-fluorobenzoic acid (47 mg, 0.334 mmol). Purification by silica gel flash column chromatography (using a mixture of

dichloromethane and methanol as mobile phase in a ratio of 99:1) yielded the desired compound as a white solid (56 mg, 43%). Purity of 99%. <sup>1</sup>H NMR (300 MHz, DMSO-*d*<sub>6</sub>) δ 11.53 (bs, 1H), 10.39 (bs, 1H), 8.56 (d, *J* = 8.5 Hz, 2H), 8.12 (m, 2H), 7.93 (s, 1H), 7.38 (t, *J* = 8.7 Hz, 2H), 7.26 (m, 2H), 7.08 (d, *J* = 8.3 Hz, 1H), 3.87 (s, 3H), 3.81 (s, 3H) ppm. <sup>13</sup>C NMR (75 MHz, DMSO-*d*<sub>6</sub>) δ 164.07 (*J*<sub>CF</sub> = 245 Hz), 163.93, 149.30, 148.30, 145.25, 142.12, 131.99, 131.27, 130.57 (*J*<sub>CF</sub> = 9.0 Hz), 127.69, 125.05, 119.12, 117.35, 115.39 (*J*<sub>CF</sub> = 22 Hz), 114.11, 113.46, 112.53, 110.88, 55.84, 55.75 ppm. HRMS *m/z* [M+H]<sup>+</sup> calcd for C<sub>22</sub>H<sub>19</sub>FN<sub>3</sub>O<sub>3</sub> 392.1405; found 392.1399.

***N*-(5-(3,4-Dimethoxyphenyl)-1*H*-pyrrolo[2,3-*b*]pyridin-3-yl)-4-methoxybenzamide (2.7k)**

The title compound was synthesized according to the general procedure using 4-methoxybenzoic acid (51 mg, 0.334 mmol). Purification by silica gel flash column chromatography (using a mixture of dichloromethane and methanol as mobile phase in a ratio of 99:1) yielded the desired compound as a white solid (64 mg, 47%). Purity of 97%. <sup>1</sup>H NMR (600 MHz, DMSO-*d*<sub>6</sub>) δ 11.46 (s, 1H), 10.16 (s, 1H), 8.55 (d, *J* = 1.9 Hz, 1H), 8.53 (d, *J* = 2.2 Hz, 1H), 8.01 (m, 2H), 7.90 (d, *J* = 2.5 Hz, 1H), 7.28 (d, *J* = 2.2 Hz, 1H), 7.22 (dd, *J* = 8.2, 2.2 Hz, 2H), 7.08 (m, 3H), 3.87 (s, 3H), 3.85 (s, 3H), 3.80 (s, 3H) ppm. <sup>13</sup>C NMR (150 MHz, DMSO-*d*<sub>6</sub>) δ 164.43, 161.77, 149.25, 148.24, 145.21, 142.00, 131.99, 129.69, 127.58, 126.92, 124.98, 119.08, 117.14, 114.27, 113.65, 113.48, 112.48, 110.82, 55.78, 55.70, 55.50 ppm. HRMS *m/z* [M+H]<sup>+</sup> calcd for C<sub>23</sub>H<sub>22</sub>N<sub>3</sub>O<sub>4</sub> 404.16047; found 404.1603.

***N*-(5-(3,4-Dimethoxyphenyl)-1*H*-pyrrolo[2,3-*b*]pyridin-3-yl)-2-phenylacetamide (2.7m)**

The title compound was synthesized according to the general procedure using phenylacetic acid (45 mg, 0.334 mmol). Purification by silica gel flash column chromatography (using a mixture of dichloromethane and methanol as mobile phase in a ratio of 99:1) yielded the desired compound as a white solid (49 mg, 54%). Purity of 99%. <sup>1</sup>H NMR (300 MHz, DMSO-*d*<sub>6</sub>) δ 11.36 (s, 1H), 10.45 (s, 1H), 8.53 (m, 2H), 7.79 (d, *J* = 2.3 Hz, 1H), 7.31 (m, 7H), 7.09 (d, *J* = 8.4 Hz, 1H), 3.88 (s, 3H), 3.81 (s, 3H), 3.76 (s, 2H, CH<sub>2</sub>) ppm. <sup>13</sup>C NMR (75 MHz, DMSO-*d*<sub>6</sub>) δ 168.21, 157.37, 149.33, 148.30, 145.01, 142.09, 136.54, 131.94, 129.28, 128.38, 127.55, 126.56, 124.40, 119.00, 115.78, 114.37, 112.78, 112.55, 110.80, 55.83, 55.76, 42.41 ppm. HRMS *m/z* [M+H]<sup>+</sup> calcd for C<sub>23</sub>H<sub>22</sub>N<sub>3</sub>O<sub>3</sub> 388.1656; found 388.1660.

***N*-(5-(3,4-Dimethoxyphenyl)-1*H*-pyrrolo[2,3-*b*]pyridin-3-yl)cyclopentanecarboxamide (2.7n)**

To a solution of 3-nitro-5-(3,4-dimethoxyphenyl)-1*H*-pyrrolo[2,3-*b*]pyridine (**2.5g**) (100 mg, 0.334 mmol) in THF (5 ml) was added a catalytic amount of a slurry of Raney nickel in water. The vessel was flushed three times with hydrogen gas and kept under a hydrogen atmosphere for 4 hours. After complete conversion, the catalyst was removed and the solvent was evaporated *in vacuo*. The crude product was immediately used for further reaction without purification. To a solution of the crude residue in pyridine (5 ml) was added a solution of cyclopentylcarbonyl chloride (46 μl, 0.401 mmol) in DCM (2 ml). The reaction was stirred overnight at room temperature. After reaction completion, the solvent was evaporated *in vacuo* and the crude residue was partitioned between water and ethyl acetate followed by extraction of the water layer with ethyl acetate. The combined organic layers were dried

over MgSO<sub>4</sub> and evaporated to dryness. Purification by silica gel flash column chromatography (using a mixture of dichloromethane and methanol in a ratio of 97:3 as mobile phase) yielded the title compound as a white solid (39 mg, 32%). Purity of 99%. <sup>1</sup>H NMR (300 MHz, DMSO-*d*<sub>6</sub>) δ 11.33 (bs, 1H), 9.96 (bs, 1H), 8.51 (s, 1H), 8.44 (s, 1H), 7.82 (d, *J* = 2.2 Hz, 1H), 7.23 (m, 2H), 7.08 (d, *J* = 8.3 Hz, 1H), 3.88 (s, 3H), 3.81 (s, 3H), 2.90 (m, 1H, CH<sub>2</sub>), 1.77 (m, 8H, CH<sub>2</sub>) ppm. <sup>13</sup>C NMR (75 MHz, DMSO-*d*<sub>6</sub>) δ 173.48, 149.31, 148.30, 145.00, 142.05, 132.01, 127.51, 124.19, 119.05, 115.69, 114.50, 112.71, 112.55, 110.80, 55.82, 55.75, 44.55, 30.46, 25.85. HRMS *m/z* [M+H]<sup>+</sup> calcd for C<sub>21</sub>H<sub>24</sub>N<sub>3</sub>O<sub>3</sub> 366.1812; found 366.1808.

#### **N-(5-(3,4-dimethoxyphenyl)-1*H*-pyrrolo[2,3-*b*]pyridin-3-yl)cyclohexanecarboxamide (2.7o)**

The compound was synthesized according to literature procedure.<sup>17</sup>

#### **N-(5-(3,4-dimethoxyphenyl)-1*H*-pyrrolo[2,3-*b*]pyridin-3-yl)benzenesulfonamide (2.7p)**

To a solution of **2.5g** (100 mg, 0.334 mmol) in THF (5 ml) was added a catalytic amount of a slurry of Raney nickel in water. The vessel was flushed with hydrogen gas three times and kept under a hydrogen atmosphere for 4 hours. After complete conversion, the catalyst was removed and the solvent evaporated. The crude was immediately used in the next reaction without further purification because of the rapid decomposition of the amine. To a solution of the crude from the previous reaction in pyridine (5 ml) was added a solution of benzenesulfonyl chloride (47 μl, 0.368 mmol) in DCM (1 ml). The reaction was stirred overnight at room temperature. After reaction completion the solvent was evaporated and the crude was partitioned between water and ethyl acetate. The water phase was extracted with ethyl acetate. The collected organics were dried with MgSO<sub>4</sub> and evaporated to dryness. Flash column chromatography (using a mixture of dichloromethane and methanol as mobile phase in a ratio of 97:3) yielded the desired compound as an off-white solid (34 mg, 25%). Purity of 98%. <sup>1</sup>H NMR (600 MHz, DMSO-*d*<sub>6</sub>) δ 11.64 (bs, 1H), 9.87 (bs, 1H), 8.42 (d, *J* = 1.9 Hz, 1H), 7.73 (s, 1H), 7.72 (s, 2H), 7.55 (t, *J* = 7.5 Hz, 1H), 7.51 (t, *J* = 7.7 Hz, 2H), 7.20 (d, *J* = 2.5 Hz, 1H), 7.05 (m, 2H), 6.99 (d, *J* = 1.7 Hz, 1H), 3.85 (s, 3H), 3.80 (s, 3H) ppm. <sup>13</sup>C NMR (150 MHz, DMSO-*d*<sub>6</sub>) δ 149.18, 148.27, 145.66, 142.15, 140.05, 132.66, 131.55, 129.03, 128.23, 126.96, 123.76, 121.94, 118.96, 115.65, 113.91, 112.46, 111.06, 110.50, 55.70, 55.68 ppm. HRMS *m/z* [M+H]<sup>+</sup> calcd for C<sub>21</sub>H<sub>20</sub>N<sub>3</sub>O<sub>4</sub>S 408.1023; found 408.1024.

#### **5-Bromo-1*H*-pyrrolo[2,3-*b*]pyridine-3-carbaldehyde (2.8)**

To a solution of **2.3** (500 mg, 2.54 mmol) in a mixture of water and acetic acid (in a ratio of 3:1, 10 ml) was added hexamine (712 mg, 5.08 mmol). The reaction mixture was heated to 120°C and refluxed overnight. The formed precipitate was filtered off, affording the title compound (380 mg, 67%). <sup>1</sup>H NMR (300 MHz, DMSO-*d*<sub>6</sub>) δ 12.93 (bs, 1H), 9.93 (s, 1H), 8.55 (s, 1H), 8.53 (d, *J* = 2.3 Hz, 1H), 8.46 (d, *J* = 2.3 Hz, 1H) ppm. <sup>13</sup>C NMR (75 MHz, DMSO-*d*<sub>6</sub>) δ 185.58, 147.92, 145.09, 139.90, 131.01, 118.32, 116.04, 113.86 ppm.

**5-Bromo-1-tosyl-1H-pyrrolo[2,3-b]pyridine-3-carbaldehyde (2.9)**

To a suspension of 60% NaH on mineral oil (80 mg, 2 mmol) in dry THF (6 ml) was added **2.8** (300 mg, 1.33 mmol) at 0°C. After stirring for 20 minutes at room temperature, tosyl chloride (381 mg, 2 mmol) was added and the resulting solution was stirred for another 3 hours at room temperature. After reaction completion, the solvent was evaporated *in vacuo* and the crude residue was partitioned between water and dichloromethane followed by extraction of the water layer with dichloromethane. The combined organic layers were dried over MgSO<sub>4</sub> and evaporated *in vacuo*, affording the title compound (460 mg, 91%). <sup>1</sup>H NMR (300 MHz, DMSO-*d*<sub>6</sub>) δ 10.03 (s, 1H, CHO), 9.02 (s, 1H), 8.59 (d, *J* = 2.2 Hz, 1H), 8.55 (d, *J* = 2.2 Hz, 1H), 8.07 (d, *J* = 8.4 Hz, 2H), 7.48 (d, *J* = 8.2 Hz, 2H), 2.37 (s, 3H) ppm.

**5-(3,4-Dimethoxyphenyl)-1-tosyl-1H-pyrrolo[2,3-b]pyridine-3-carbaldehyde (2.10)**

To a solution of **2.9** (240 mg, 0.633 mmol) in a mixture of toluene and ethanol (in a ratio of 3:1, 4 ml) was added 3,4-dimethoxyphenylboronic acid (138 mg, 0.759 mmol) and a 2M solution of K<sub>2</sub>CO<sub>3</sub> (950 μl, 1.90 mmol). The system was purged with argon and Pd(PPh<sub>3</sub>)<sub>4</sub> (2 % mol) was added. The reaction was stirred at 105°C for 4 hours. After completion, the solvent was evaporated *in vacuo* and the residue was extracted with water and ethyl acetate. Purification by silica gel flash chromatography using a mixture of heptane and ethyl acetate (in a ratio of 7:3) as mobile phase afforded the title compound (160 mg, 58%). <sup>1</sup>H NMR (300 MHz, DMSO-*d*<sub>6</sub>) δ 10.09 (s, 1H, CHO), 9.00 (s, 1H), 8.76 (s, 1H), 8.55 (s, 1H), 8.11 (d, *J* = 7.7 Hz, 2H), 7.49 (d, *J* = 7.4 Hz, 2H), 7.24 (m, 2H), 7.07 (d, *J* = 8.2 Hz, 1H), 3.85 (s, 3H), 3.79 (s, 3H), 2.37 (s, 3H) ppm.

**(5-(3,4-Dimethoxyphenyl)-1-tosyl-1H-pyrrolo[2,3-b]pyridin-3-yl)(phenyl)methanol (2.11)**

To a solution of **2.10** (160 mg, 0.367 mmol) in dry THF (5 ml) at 0°C was added a 3M solution of phenylmagnesium bromide in diethylether (159 μl, 0.477 mmol). The reaction mixture was stirred for 1 hour at 0°C. After reaction completion, the mixture was quenched with a saturated NH<sub>4</sub>Cl solution and extracted with water and ethyl acetate. The combined organic layers were dried over Na<sub>2</sub>SO<sub>4</sub> and evaporated to dryness yielding the title compound (130 mg, 69%). <sup>1</sup>H NMR (300 MHz, DMSO-*d*<sub>6</sub>) δ 8.62 (s, 1H), 7.99 (d, *J* = 8.8 Hz, 3H), 7.70 (s, 1H), 7.59 – 6.99 (m, 10H), 6.13 (d, *J* = 4.4 Hz, 1H), 6.02 (s, 1H), 3.82 (s, 3H), 3.78 (s, 3H), 2.34 (s, 3H) ppm.

**(5-(3,4-Dimethoxyphenyl)-1-tosyl-1H-pyrrolo[2,3-b]pyridin-3-yl)phenylmethanone (2.12)**

To a solution of **2.11** (130 mg, 0.253 mmol) in dichloromethane (8 ml) was added manganese dioxide (220 mg, 2.53 mmol) and the reaction was stirred overnight at room temperature. After completion, the mixture was filtered through Celite® and the filtrate was evaporated to dryness. The crude residue was purified by silica gel flash column chromatography using a mixture of heptane and ethyl acetate (in a ratio of 6:4) as mobile phase yielding the title compound (64 mg, 49%). <sup>1</sup>H NMR (300 MHz, DMSO-*d*<sub>6</sub>) δ 8.78 (d, *J* = 2.1 Hz, 1H), 8.64 (d, *J* = 2.1 Hz, 1H), 8.33 (s, 1H), 8.16 (d, *J* = 8.3 Hz, 2H), 7.96 (d, *J* = 7.2 Hz, 2H), 7.70 (m, 3H), 7.47 (d, *J* = 8.2 Hz, 2H), 7.25 (m, 2H), 7.08 (d, *J* = 8.4 Hz, 1H), 3.86 (s, 3H), 3.81 (s, 3H), 2.37 (s, 3H) ppm.

**(5-(3,4-Dimethoxyphenyl)-1*H*-pyrrolo[2,3-*b*]pyridin-3-yl)phenylmethanone (2.13)**

To a solution of **2.12** (64 mg, 0.124 mmol) in ethanol (10 ml) was added KOH (35 mg, 0.624 mmol) and the mixture was heated to 80°C. The reaction was stirred for 3 hours. After reaction completion, the solvent was evaporated *in vacuo* and the crude residue was partitioned between water and ethyl acetate. The combined organic layers were dried over MgSO<sub>4</sub> and evaporated to dryness, yielding the title compound as a white solid (34 mg, 76%). <sup>1</sup>H NMR (300 MHz, DMSO-*d*<sub>6</sub>) δ 12.74 (bs, 1H), 8.67 (s, 2H), 8.12 (s, 1H), 7.84 (d, *J* = 6.8 Hz, 2H), 7.61 (m, 3H), 7.25 (m, 2H), 7.10 (d, *J* = 8.3 Hz, 1H), 3.88 (s, 3H), 3.82 (s, 3H) ppm. <sup>13</sup>C NMR (75 MHz, DMSO-*d*<sub>6</sub>) δ 190.00, 149.38, 148.64, 148.45, 143.66, 139.77, 136.58, 131.13, 127.30, 119.42, 118.86, 113.88, 112.59, 110.91, 55.77, 55.75 ppm. HRMS *m/z* [M+H]<sup>+</sup> calcd for C<sub>22</sub>H<sub>19</sub>N<sub>2</sub>O<sub>3</sub> 359.1390; found 359.1393.

**5-Bromo-3-iodo-1*H*-pyrrolo[2,3-*b*]pyridine (2.14)**

To a solution of **2.3** (1.00 g, 5.08 mmol) in acetone (16 ml) was added portionwise *N*-iodosuccinimide (1.26 g, 5.58 mmol). The reaction mixture was stirred for 2 hours at room temperature. The formed precipitate was collected via filtration, yielding the title compound as an off-white solid (1.50 g, 92%). <sup>1</sup>H NMR (300 MHz, DMSO-*d*<sub>6</sub>) δ 12.36 (s, 1H), 8.32 (d, *J* = 2.0 Hz, 1H), 7.87 (d, *J* = 1.7 Hz, 1H), 7.81 (d, *J* = 2.4 Hz, 1H) ppm.

**5-Bromo-3-iodo-1-tosyl-1*H*-pyrrolo[2,3-*b*]pyridine (2.15)**

To a solution of **2.14** (300 mg, 0.929 mmol) in dry THF (10 ml) was added portionwise NaH (41 mg, 1.02 mmol) at 0°C. After stirring for 20 minutes at room temperature, tosyl chloride (230 mg, 1.21 mmol) was added and the reaction was allowed to stir for another 2 hours at room temperature. After reaction completion, the reaction was quenched with water and extracted with ethyl acetate. The combined organic phases were dried over MgSO<sub>4</sub> and concentrated *in vacuo*, yielding the title compound as a white solid (420 mg, 95%). <sup>1</sup>H NMR (300 MHz, DMSO-*d*<sub>6</sub>) δ 8.51 (d, *J* = 2.1 Hz, 1H), 8.22 (s, 1H), 8.00 (m, 3H, /TsH), 7.43 (d, *J* = 8.5 Hz, 2H), 2.34 (s, 3H) ppm.

**5-Bromo-3-phenyl-1-tosyl-1*H*-pyrrolo[2,3-*b*]pyridine (2.16)**

To a solution of **2.15** (200 mg, 0.419 mmol) in a mixture of toluene and ethanol (in a ratio of 3:1) was added phenylboronic acid (51 mg, 0.419 mmol) and a 2M solution of K<sub>2</sub>CO<sub>3</sub> (420 μl, 0.838 mmol). The reaction was flushed with argon three times, followed by the addition of Pd(PPh<sub>3</sub>)<sub>4</sub> (10 mg, 0.008 mmol). The reaction mixture was stirred at 90°C for 3 hours. After reaction completion, the reaction mixture was filtered through Celite® and the filtrate was partitioned between water and ethyl acetate followed by extraction of the water layer with ethyl acetate. The combined organic phases were dried over MgSO<sub>4</sub> and evaporated *in vacuo*. Purification by silica gel flash column chromatography using a mixture of heptane and ethyl acetate (in a ratio of 4:1) as mobile phase yielded the title compound as a white solid (150 mg, 84%). <sup>1</sup>H NMR (300 MHz, DMSO-*d*<sub>6</sub>) δ 8.54 (d, *J* = 2.1 Hz, 1H), 8.50 (d, *J* = 2.1 Hz, 1H), 8.29 (s, 1H), 8.04 (d, *J* = 8.4 Hz, 2H), 7.79 (d, *J* = 7.2 Hz, 2H), 7.45 (m, 5H), 2.35 (s, 3H) ppm.

**5-(3,4-Dimethoxyphenyl)-3-phenyl-1-tosyl-1H-pyrrolo[2,3-b]pyridine (2.17)**

To a solution of **2.16** (150 mg, 0.351 mmol) in a mixture of toluene and ethanol (in a ratio of 3:1) was added 3,4-dimethoxyphenylboronic acid (77 mg, 0.421 mmol) and a 2M solution of K<sub>2</sub>CO<sub>3</sub> in water (351  $\mu$ l, 0.702 mmol). The system was flushed with argon and Pd(PPh<sub>3</sub>)<sub>4</sub> (2 mol%) was added. The reaction was stirred for 4 hours at 105°C. Upon reaction completion, the solvents were evaporated *in vacuo* and the crude residue was partitioned between water and ethyl acetate followed by extraction of the water layer with ethyl acetate. Purification by silica gel flash chromatography using a mixture of heptane and ethyl acetate (in a ratio of 8:2) as mobile phase yielded the desired compound (100 mg, 59%). <sup>1</sup>H NMR (300 MHz, DMSO-*d*<sub>6</sub>)  $\delta$  8.71 (d, *J* = 2.0 Hz, 1H), 8.37 (d, *J* = 2.0 Hz, 1H), 8.23 (s, 1H), 8.08 (d, *J* = 8.4 Hz, 2H), 7.85 (d, *J* = 7.2 Hz, 2H), 7.46 (m, 5H), 7.29 (m, 2H), 7.06 (d, *J* = 8.3 Hz, 1H), 3.84 (s, 3H), 3.80 (s, 3H), 2.35 (s, 3H) ppm.

**5-(3,4-Dimethoxyphenyl)-3-phenyl-1H-pyrrolo[2,3-b]pyridine (2.18)**

To a solution of **2.17** (100 mg, 0.309 mmol) in ethanol (5 ml) was added KOH (87 mg, 1.55 mmol). The reaction was allowed to stir for 2 hours at 80°C. After completion, the solvent was evaporated *in vacuo* and the crude residue was purified by silica gel flash chromatography using a mixture of heptane and ethyl acetate (in a ratio of 7:3) as mobile phase, affording the title compound (49 mg, 72%). <sup>1</sup>H NMR (300 MHz, DMSO-*d*<sub>6</sub>)  $\delta$  11.98 (s, 1H), 8.56 (s, 1H), 8.39 (s, 1H), 7.90 (d, *J* = 2.3 Hz, 1H), 7.79 (d, *J* = 7.5 Hz, 2H), 7.45 (t, *J* = 7.6 Hz, 2H), 7.28 (m, 3H), 7.06 (d, *J* = 8.3 Hz, 1H), 3.87 (s, 3H), 3.80 (s, 3H) ppm. <sup>13</sup>C NMR (75 MHz, DMSO-*d*<sub>6</sub>)  $\delta$  149.32, 148.56, 148.37, 142.16, 135.18, 132.07, 129.15, 129.06, 126.57, 125.83, 124.63, 119.50, 117.37, 114.73, 112.54, 111.27, 55.84, 55.76 ppm. HRMS *m/z* [M+H]<sup>+</sup> calcd for C<sub>21</sub>H<sub>19</sub>N<sub>2</sub>O<sub>2</sub> 331.1440; found 331.1437.

**2.8.1.5. Synthesis of 3-alkynyl-5-bromo-pyrrolo[2,3-b]pyridines (2.19a-f)**General procedure

To a degassed solution of **2.14** (1 eq) in THF and triethylamine (3 eq) was added CuI (0.02 eq) and Pd(PPh<sub>3</sub>)<sub>2</sub>Cl<sub>2</sub> (0.01 eq). The resulting mixture was stirred under an inert atmosphere for 10 minutes at room temperature. A solution of the appropriate alkyne (0.95 eq) in THF was added to the mixture. The reaction mixture was stirred for an additional 4 hours at room temperature. After completion, the reaction was filtered through Celite<sup>®</sup>. The filtrate was diluted with water and extracted with ethyl acetate. The combined organic layers were washed with brine and dried over MgSO<sub>4</sub>. The crude residue was purified by silica gel flash column chromatography with an appropriate mobile phase.

**5-Bromo-3-(phenylethynyl)-1H-pyrrolo[2,3-b]pyridine (2.19a)**

The title compound was synthesized according to the general procedure using **2.14** (200 mg, 0.619 mmol) and phenylacetylene (60 mg, 0.588 mmol). The crude residue was purified by silica gel flash column chromatography using a mixture of heptane and ethyl acetate (in a ratio of 4:1) as mobile phase yielding the title compound as a white solid (85 mg, 51%). <sup>1</sup>H NMR (300 MHz, DMSO-*d*<sub>6</sub>)  $\delta$  12.40 (bs, 1H), 8.39 (d, *J* = 2.2 Hz, 1H), 8.32 (d, *J* = 2.1 Hz, 1H), 8.01 (s, 1H), 7.60 (m, 2H), 7.42 (m, 3H) ppm.

**5-Bromo-3-(pyridin-3-ylethynyl)-1H-pyrrolo[2,3-*b*]pyridine (2.19b)**

The title compound was synthesized according to the general procedure using **2.14** (200 mg, 0.619 mmol) and 3-ethynylpyridine (61 mg, 0.588 mmol). The crude residue was purified by silica gel flash column chromatography using a mixture of heptane and ethyl acetate (in a ratio of 7:3) as mobile phase yielding the title compound as a white solid (140 mg, 75%). <sup>1</sup>H NMR (300 MHz, DMSO-*d*<sub>6</sub>) 12.49 (bs, 1H), 8.81 (s, 1H), 8.56 (d, *J* = 4.8 Hz, 1H), 8.40 (s, 2H), 8.04 (m, 2H), 7.46 (m, 1H) ppm.

**5-Bromo-3-((3-methoxyphenyl)ethynyl)-1H-pyrrolo[2,3-*b*]pyridine (2.19c)**

The title compound was synthesized according to the general procedure using **2.14** (200 mg, 0.619 mmol) and 3-methoxyphenylacetylene (60 mg, 0.588 mmol). The crude residue was purified by silica gel flash column chromatography using a mixture of heptane and ethyl acetate (in a ratio of 7:3) as mobile phase, yielding the title compound as a white solid (105 mg, 51%). <sup>1</sup>H NMR (300 MHz, DMSO-*d*<sub>6</sub>) δ 12.41 (bs, 1H), 8.39 (d, *J* = 2.2 Hz, 1H), 8.34 (d, *J* = 2.1 Hz, 1H), 8.00 (s, 1H), 7.33 (t, *J* = 8.1 Hz, 1H), 7.16 (m, 2H), 6.96 (m, 1H), 3.81 (s, 3H) ppm.

**5-Bromo-3-(*p*-tolylethynyl)-1H-pyrrolo[2,3-*b*]pyridine (2.19d)**

The title compound was synthesized according to the general procedure using **2.14** (200 mg, 0.619 mmol) and *p*-tolylacetylene (68 mg, 0.588 mmol). The crude residue was purified by silica gel flash column chromatography using a mixture of heptane and ethyl acetate (in a ratio of 7:3) as mobile phase, yielding the title compound as a white solid (130 mg, 67%). <sup>1</sup>H NMR (300 MHz, DMSO-*d*<sub>6</sub>) δ 12.36 (bs, 1H), 8.38 (d, *J* = 2.2 Hz, 1H), 8.30 (d, *J* = 2.2 Hz, 1H), 7.98 (s, 1H), 7.48 (d, *J* = 8.1 Hz, 2H), 7.23 (d, *J* = 7.9 Hz, 2H), 2.34 (s, 3H) ppm.

**5-Bromo-3-((4-fluorophenyl)ethynyl)-1H-pyrrolo[2,3-*b*]pyridine (2.19e)**

The title compound was synthesized according to the general procedure using 5-bromo-3-iodo-1H-pyrrolo[2,3-*b*]pyridine **2.14** (200 mg, 0.619 mmol) and 4-fluorophenylacetylene (60 mg, 0.588 mmol). The crude residue was purified by silica gel flash column chromatography using a mixture of heptane and ethyl acetate (in a ratio of 4:1) as mobile phase yielding the title compound as a white solid (110 mg, 56%). <sup>1</sup>H NMR (300 MHz, DMSO-*d*<sub>6</sub>) δ 12.41 (bs, 1H), 8.38 (d, *J* = 2.1 Hz, 1H), 8.34 (d, *J* = 2.1 Hz, 1H), 8.00 (s, 1H), 7.66 (dd, *J* = 8.7, 5.6 Hz, 2H), 7.27 (t, *J* = 8.9 Hz, 2H) ppm.

**3-((5-Bromo-1H-pyrrolo[2,3-*b*]pyridin-3-yl)ethynyl)benzotrile (2.19f)**

The title compound was synthesized according to the general procedure using **2.14** (200 mg, 0.619 mmol) and 3-cyanophenylacetylene (75 mg, 0.588 mmol). The crude residue was purified by silica gel flash column chromatography using a mixture of heptane and ethyl acetate (in a ratio of 7:3) as mobile phase, yielding the title compound as a white solid (90 mg, 45%). <sup>1</sup>H NMR (300 MHz, DMSO-*d*<sub>6</sub>) δ 8.45 (d, *J* = 2.2 Hz, 1H), 8.40 (d, *J* = 2.1 Hz, 1H), 8.14 (s, 1H), 8.05 (s, 1H), 7.91 (d, *J* = 8.0 Hz, 1H), 7.84 (d, *J* = 7.5 Hz, 1H), 7.63 (t, *J* = 7.9 Hz, 1H) ppm.

### 2.8.1.6. Synthesis of 3-alkynyl-5-(3,4-dimethoxyphenyl)-pyrrolo[2,3-*b*]pyridines (2.20a-f)

#### General procedure

To a solution of a 5-bromo-3-arylethynyl-1*H*-pyrrolo[2,3-*b*]pyridine derivative (**2.19a-f**) (1 eq) in dioxane (4 ml) was added 3,4-dimethoxyphenylboronic acid (1.2 eq) and 1 ml of a K<sub>2</sub>CO<sub>3</sub> (3 eq) solution. The system was purged three times with argon and heated to 105 °C. After stirring for 10 minutes, Pd(PPh<sub>3</sub>)<sub>4</sub> (0.1 eq) was added and the reaction was purged once more with argon. The reaction mixture was stirred at 105°C for 3 hours. After completion, the reaction mixture was cooled to room temperature and filtered through Celite®. The filtrate was extracted with water and ethyl acetate. The combined organic layers were washed with brine, dried over MgSO<sub>4</sub> and evaporated *in vacuo*. The crude residue was purified by silica gel flash column chromatography with an appropriate mobile phase. Compounds **2.20a-f** were made according to this procedure.

#### 5-(3,4-Dimethoxyphenyl)-3-(phenylethynyl)-1*H*-pyrrolo[2,3-*b*]pyridine (2.20a)

The title compound was synthesized according to the general procedure using **2.19a** (80 mg, 0.269 mmol). The crude residue was purified by silica gel flash column chromatography using a mixture of dichloromethane and ethyl acetate (in a ratio of 9:1) as mobile phase yielding the title compound as a brown solid (36 mg, 38%). <sup>1</sup>H NMR (300 MHz, DMSO-*d*<sub>6</sub>) δ 12.21 (bs, 1H), 8.61 (s, 1H), 8.25 (s, 1H), 7.96 (d, *J* = 2.2 Hz, 1H), 7.60 (d, *J* = 6.5 Hz, 1H), 8.01 (m, 2H), 7.35 (m, 6H), 7.06 (d, *J* = 8.3 Hz, 1H), 3.88 (s, 3H), 3.81 (s, 3H) ppm. <sup>13</sup>C NMR (75 MHz, DMSO-*d*<sub>6</sub>) δ 149.33, 148.49, 147.24, 143.12, 131.42, 131.27, 131.17, 129.60, 128.80, 128.13, 124.93, 123.48, 120.29, 119.44, 112.48, 111.11, 95.31, 90.75, 83.53, 55.82, 55.73 ppm. HRMS *m/z* [M+H]<sup>+</sup> calcd for C<sub>23</sub>H<sub>19</sub>N<sub>2</sub>O<sub>2</sub> 355.1441; found 355.1435.

#### 5-(3,4-Dimethoxyphenyl)-3-(pyridin-3-ylethynyl)-1*H*-pyrrolo[2,3-*b*]pyridine (2.20b)

The title compound was synthesized according to the general procedure using **2.19b** (140 mg, 0.470 mmol). The crude residue was purified by silica gel flash column chromatography using a mixture of dichloromethane and ethyl acetate (in a ratio of 9:1) as mobile phase, yielding the title compound as a white solid (75 mg, 44%). <sup>1</sup>H NMR (300 MHz, DMSO-*d*<sub>6</sub>) δ 12.30 (s, 1H), 8.81 (s, 1H), 8.63 (d, *J* = 2.0 Hz, 1H), 8.55 (d, *J* = 4.9 Hz, 1H), 8.30 (d, *J* = 1.9 Hz, 1H), 8.01 (m, 2H), 7.46 (m, 1H), 7.31 (m, 2H), 7.07 (d, *J* = 8.3 Hz, 1H), 3.89 (s, 3H), 3.81 (s, 3H) ppm. <sup>13</sup>C NMR (75 MHz, DMSO-*d*<sub>6</sub>) δ 151.46, 149.33, 148.52, 148.34, 147.24, 143.24, 138.19, 131.78, 131.33, 129.73, 125.03, 123.68, 120.59, 120.28, 119.46, 112.47, 111.13, 94.77, 87.69, 86.87, 55.83, 55.74 ppm. HRMS *m/z* [M+H]<sup>+</sup> calcd for C<sub>22</sub>H<sub>18</sub>N<sub>3</sub>O<sub>2</sub> 356.1393; found 356.1393.

#### 5-(3,4-Dimethoxyphenyl)-3-(3-methoxyphenylethynyl)-1*H*-pyrrolo[2,3-*b*]pyridine (2.20c)

The title compound was synthesized according to the general procedure using **2.19c** (110 mg, 0.353 mmol). The crude residue was purified by silica gel flash column chromatography using a mixture of dichloromethane and ethyl acetate (in a ratio of 9:1). Further purification by preparative TLC (the mobile phase being a mixture of nitromethane:toluene in a ratio of 6:4) yielded the title compound as a



white solid (25 mg, 20%).  $^1\text{H}$  NMR (300 MHz, DMSO- $d_6$ )  $\delta$  12.21 (s, 1H), 8.61 (d,  $J = 1.9$  Hz, 1H), 8.25 (d,  $J = 1.9$  Hz, 1H), 7.96 (d,  $J = 2.6$  Hz, 1H), 7.32 (m, 3H), 7.16 (m, 2H), 7.07 (d,  $J = 8.3$  Hz, 1H), 6.96 (m, 1H), 3.89 (s, 3H), 3.81 (s, 3H), 3.80 (s, 3H) ppm.  $^{13}\text{C}$  NMR (75 MHz, DMSO- $d_6$ )  $\delta$  159.33, 149.33, 148.50, 147.24, 143.12, 131.41, 131.34, 129.91, 129.60, 124.97, 124.56, 123.61, 120.28, 119.44, 115.95, 114.58, 112.49, 111.12, 95.24, 90.74, 83.43, 55.82, 55.75, 55.34 ppm. HRMS  $m/z$   $[\text{M}+\text{H}]^+$  calcd for  $\text{C}_{24}\text{H}_{21}\text{N}_2\text{O}_3$  385.1547; found 385.1541.

### 5-(3,4-Dimethoxyphenyl)-3-(*p*-tolylethynyl)-1*H*-pyrrolo[2,3-*b*]pyridine (2.20d)

The title compound was synthesized according to the general procedure using **2.19d** (110 mg, 0.353 mmol). The crude residue was purified by silica gel flash column chromatography using a mixture of dichloromethane and ethyl acetate (in a ratio of 9:1) as mobile phase, yielding the title compound as a white solid (25 mg, 20%). Purity of 95%.  $^1\text{H}$  NMR (300 MHz, DMSO- $d_6$ )  $\delta$  12.18 (bs, 1H), 8.60 (d,  $J = 2.0$  Hz, 1H), 8.22 (d,  $J = 1.8$  Hz, 1H), 7.93 (d,  $J = 2.6$  Hz, 1H), 7.49 (d,  $J = 8.0$  Hz, 2H), 7.27 (m, 4H), 7.03 (m, 2H), 3.88 (s, 3H), 3.81 (s, 3H), 2.34 (s, 3H) ppm.  $^{13}\text{C}$  NMR (75 MHz, DMSO- $d_6$ )  $\delta$  149.33, 148.48, 147.23, 143.07, 137.78, 131.45, 131.11, 131.04, 129.54, 129.42, 124.91, 120.46, 120.27, 119.43, 112.49, 111.11, 95.49, 90.81, 82.77, 55.83, 55.74, 21.14 ppm. HRMS  $m/z$   $[\text{M}+\text{H}]^+$  calcd for  $\text{C}_{24}\text{H}_{21}\text{N}_2\text{O}_2$  369.1597; found 369.1593.

### 5-(3,4-Dimethoxyphenyl)-3-(4-fluorophenylethynyl)-1*H*-pyrrolo[2,3-*b*]pyridine (2.20e)

The title compound was synthesized according to the general procedure using **2.19e** (80 mg, 0.269 mmol). The crude residue was purified by silica gel flash column chromatography using a mixture of dichloromethane and ethyl acetate (in a ratio of 9:1), yielding the desired compound as a brown solid (34 mg, 36%).  $^1\text{H}$  NMR (300 MHz, DMSO- $d_6$ )  $\delta$  12.21 (bs, 1H), 8.61 (s, 1H), 8.25 (s, 1H), 7.95 (d,  $J = 2.4$  Hz, 1H), 7.65 (m, 2H), 7.28 (m, 4H), 7.06 (d,  $J = 8.5$  Hz, 1H), 3.88 (s, 3H), 3.81 (s, 3H) ppm.  $^{13}\text{C}$  NMR (150 MHz, DMSO- $d_6$ )  $\delta$  161.68 (d,  $J_{\text{CF}} = 247$  Hz) 149.27, 148.44, 147.17, 143.07, 133.36 (d,  $J_{\text{CF}} = 8.3$  Hz), 131.35, 131.20, 129.54, 124.91, 120.23, 119.90, 119.89, 119.38, 115.95 (d,  $J_{\text{CF}} = 22$  Hz), 112.42, 111.05, 95.11, 89.60, 83.20, 55.76, 55.68 ppm. HRMS  $m/z$   $[\text{M}+\text{H}]^+$  calcd for  $\text{C}_{23}\text{H}_{18}\text{FN}_2\text{O}_2$  373.1347; found 373.1333.

### 3-((5-(3,4-Dimethoxyphenyl)-1*H*-pyrrolo[2,3-*b*]pyridin-3-yl)ethynyl)benzotrile (2.20f)

The title compound was synthesized according to the general procedure using **2.19f** (100 mg, 0.310 mmol). The crude residue was purified by silica gel flash column chromatography using a mixture of dichloromethane and ethyl acetate (in a ratio of 9:1) as mobile phase, yielding the title compound as a brown solid (44 mg, 37%).  $^1\text{H}$  NMR (300 MHz, DMSO- $d_6$ )  $\delta$  12.31 (bs, 1H), 8.62 (d,  $J = 2.0$  Hz, 1H), 8.32 (d,  $J = 1.9$  Hz, 1H), 8.11 (s, 1H), 8.00 (d,  $J = 2.5$  Hz, 1H), 7.91 (d,  $J = 7.9$  Hz, 1H), 7.82 (d,  $J = 7.9$  Hz, 1H), 7.62 (t,  $J = 7.9$  Hz, 2H), 7.31 (m, 2H), 7.07 (d,  $J = 8.3$  Hz, 1H), 3.89 (s, 3H), 3.81 (s, 3H) ppm.  $^{13}\text{C}$  NMR (75 MHz, DMSO- $d_6$ )  $\delta$  149.33, 148.54, 147.25, 143.28, 135.52, 134.37, 131.91, 131.43, 131.35, 130.10, 129.81, 125.11, 124.93, 120.34, 119.51, 118.33, 112.48, 112.17, 111.17, 94.64, 89.01, 86.05, 55.84, 55.75 ppm. HRMS  $m/z$   $[\text{M}+\text{H}]^+$  calcd for  $\text{C}_{24}\text{H}_{18}\text{N}_3\text{O}_2$  380.1393; found 380.1390.

**5-Bromo-1-methyl-1H-pyrrolo[2,3-b]pyridine (2.21)**

To a solution **2.3** (200 mg, 1.02 mmol) in THF (5 ml) at 0°C was added 60% NaH on mineral oil (49 mg, 1.22 mmol). The reaction was stirred at 0°C for 1.5 hour. Methyl iodide (70  $\mu$ l, 1.12 mmol) was added and the mixture was allowed to warm at ambient temperature and then stirred at room temperature for 3 hours. After completion, the mixture was quenched with water and extracted three times with ethyl acetate. The combined organic layers were washed with brine, dried over MgSO<sub>4</sub>, filtered and evaporated. The crude residue was purified by silica gel flash column chromatography using a mixture of heptane and ethyl acetate (in a ratio of 4:1) as mobile phase, yielding the title compound as an oil that subsequently solidified to an off-white solid (160 mg, 75%). <sup>1</sup>H NMR (300 MHz, DMSO-*d*<sub>6</sub>)  $\delta$  8.31 (d, *J* = 2.1 Hz, 1H), 8.20 (d, *J* = 2.1 Hz, 1H), 7.59 (d, *J* = 3.4 Hz, 1H), 6.46 (d, *J* = 3.4 Hz, 1H), 3.81 (s, 3H) ppm. HRMS *m/z* [M+H]<sup>+</sup> calcd for C<sub>8</sub>H<sub>8</sub>N<sub>2</sub>Br 210.9866; found 210.9866.

**5-Bromo-1-methyl-3-nitro-1H-pyrrolo[2,3-b]pyridine (2.22)**

**2.21** (130 mg, 0.615 mmol) was added portionwise to a stirring solution of fuming nitric acid (1 ml) at 0°C over 10 minutes. The reaction was allowed to stir for 30 minutes at 0°C. The mixture was poured out in ice water and the formed precipitate was collected via vacuum filtration. The filter cake was washed generously with water and heptane yielding the title compound as a pink solid (155 mg, 98%). <sup>1</sup>H NMR (300 MHz, DMSO-*d*<sub>6</sub>)  $\delta$  8.99 (s, 1H), 8.61 (s, 1H), 8.57 (m, 1H), 3.92 (s, 3H) ppm.

**5-(3,4-Dimethoxyphenyl)-1-methyl-3-nitro-1H-pyrrolo[2,3-b]pyridine (2.23)**

To a solution of **2.22** (100 mg, 0.391 mmol) in dioxane (4 ml) was added 3,4-dimethoxyphenylboronic acid (69 mg, 0.469 mmol) and 1 ml of a K<sub>2</sub>CO<sub>3</sub> solution (161 mg, 1.17 mmol). The system was purged three times with argon and heated to 105°C. After stirring for 10 minutes, Pd(PPh<sub>3</sub>)<sub>4</sub> (10 mol%) was added and the reaction was purged once more with argon. The reaction mixture was stirred at 105°C overnight. After completion, the reaction mixture was cooled to room temperature and filtered through Celite<sup>®</sup>. Extraction was performed with water and ethyl acetate. The combined organic layers were washed with brine, dried over MgSO<sub>4</sub> and evaporated. Purification by silica gel flash chromatography using a mixture of dichloromethane and ethyl acetate (in a ratio of 9:1) as mobile phase yielded the title compound as a yellow solid (90 mg, 83%). <sup>1</sup>H NMR (300 MHz, DMSO-*d*<sub>6</sub>)  $\delta$  8.96 (s, 1H), 8.79 (d, *J* = 2.1 Hz, 1H), 8.56 (d, *J* = 2.0 Hz, 1H), 7.30 (m, 2H), 7.10 (d, *J* = 8.2 Hz, 1H), 3.96 (s, 3H), 3.88 (s, 3H), 3.82 (s, 3H) ppm.

**N-(5-(3,4-Dimethoxyphenyl)-1-methyl-1H-pyrrolo[2,3-b]pyridin-3-yl)nicotinamide (2.25)**

The title compound was synthesized according to the general procedure described for the synthesis of compounds **2.7a-h**, starting from 5-(3,4-dimethoxyphenyl)-1-methyl-3-nitro-1H-pyrrolo[2,3-b]pyridine **2.23** (90 mg, 0.287 mmol). Purification by silica gel flash column chromatography using a mixture of dichloromethane and methanol (in a ratio gradually ranging from 98:2 to 95:5) yielded the title compound as a red solid (22 mg, 20%). <sup>1</sup>H NMR (300 MHz, DMSO-*d*<sub>6</sub>)  $\delta$  10.60 (bs, 1H), 9.19 (bs, 1H), 8.77 (d, *J* = 2.6 Hz, 1H), 8.60 (s, 2H), 8.36 (d, *J* = 8.0 Hz, 1H), 8.07 (s, 1H), 7.59 (m, 1H), 7.26 (m, 2H), 7.08 (d, *J* = 8.3 Hz, 1H), 3.87 (s, 6H), 3.80 (s, 3H) ppm. <sup>13</sup>C NMR (75 MHz, DMSO-*d*<sub>6</sub>)  $\delta$

163.33, 152.03, 149.33, 148.87, 148.39, 144.19, 142.14, 135.65, 131.81, 130.43, 127.77, 125.22, 123.63, 121.31, 119.21, 113.40, 113.14, 112.54, 110.93, 55.83, 55.75, 30.91 ppm. HRMS  $m/z$   $[M+H]^+$  calcd for  $C_{22}H_{21}N_4O_3$  389.1608; found 389.1604.

### **2-Chloro-5-(3,4-dimethoxyphenyl)nicotinonitrile (2.27)**

To a solution of 3,4-dimethoxyphenylboronic acid (460 mg, 2.53 mmol) and **2.26** (500 mg, 2.3 mmol) in isopropanol (12 ml) was added a solution of  $K_2CO_3$  (953 mg, 6.9 mmol) in water (4 ml). The reaction mixture was flushed three times with argon and heated to 90°C. Then,  $Pd(PPh_3)_4$  (10 mol%) was added and the system was flushed once more with argon. After stirring at 90°C for 2.5 hours, the reaction was concentrated under reduced pressure. The crude residue was partitioned between ethyl acetate and water and extracted three times. The combined organic phases were washed with brine and dried over  $MgSO_4$ . The solvent was removed under reduced pressure and the crude residue was purified by silica gel flash column chromatography using a mixture of heptane and ethylacetate (in a ratio of 7:3) as mobile phase. This was followed by a second purification by silica gel flash column chromatography using a mixture of dichloromethane, heptane and ethylacetate (in a ratio of 70:25:5) as mobile phase, yielding the title compound as a white solid (320 mg, 50%).  $^1H$  NMR (300 MHz,  $DMSO-d_6$ )  $\delta$  9.06 (d,  $J = 2.5$  Hz, 1H), 8.85 (d,  $J = 2.5$  Hz, 1H), 7.41 (m, 2H), 7.10 (m, 1H), 3.87 (s, 3H), 3.82 (s, 3H) ppm.

### **5-(3,4-Dimethoxyphenyl)-1H-pyrazolo[3,4-b]pyridin-3-amine (2.28)**

To a solution of **2.27** (100 mg, 0.364 mmol) in pyridine (3 ml) was added a hydrazine monohydrate solution (65% in water, 103  $\mu$ l, 0.728 mmol). The reaction was refluxed overnight and after completion the solvent was evaporated. The crude residue was purified by silica gel flash column chromatography using a mixture of dichloromethane and methanol (in a ratio of 95:5) yielding the title compound as a yellow solid (90 mg, 91%).  $^1H$  NMR (300 MHz,  $DMSO-d_6$ )  $\delta$  11.97 (bs, 1H), 8.66 (d,  $J = 2.1$  Hz, 1H), 8.36 (d,  $J = 2.0$  Hz, 1H), 7.21 (m, 2H), 7.07 (d,  $J = 8.4$  Hz, 1H), 3.86 (s, 3H), 3.80 (s, 3H) ppm.

### **N-(5-(3,4-Dimethoxyphenyl)-1H-pyrazolo[3,4-b]pyridin-3-yl)nicotinamide (2.29)**

To a solution of **2.28** (90 mg, 0.332 mmol) in pyridine (3 ml) at 0°C was added nicotinoyl chloride hydrochloride (71 mg, 0.400 mmol). The reaction was stirred at 0°C for 1 hour and then stirred at room temperature overnight. After reaction completion, water was added and the mixture was extracted three times with ethyl acetate. The combined organic phases were washed with brine, dried over  $MgSO_4$  and evaporated to dryness. The crude residue was purified by silica gel flash chromatography using a mixture of dichloromethane and methanol (in a ratio gradually ranging from 98:2 to 96:4) yielding the title compound as a beige solid (76 mg, 61%).  $^1H$  NMR (300 MHz,  $DMSO-d_6$ )  $\delta$  13.47 (s, 1H), 11.33 (s, 1H), 9.24 (s, 1H), 8.85 (d,  $J = 2.1$  Hz, 1H), 8.79 (d,  $J = 3.4$  Hz, 1H), 8.50 (d,  $J = 2.0$  Hz, 1H), 8.42 (d,  $J = 8.1$  Hz, 1H), 7.59 (dd,  $J = 7.7, 4.8$  Hz, 1H), 7.28 (s, 1H), 7.23 (d,  $J = 8.4$  Hz, 1H), 7.07 (d,  $J = 8.4$  Hz, 1H), 3.86 (s, 3H), 3.80 (s, 3H) ppm.  $^{13}C$  NMR (75 MHz,  $DMSO-d_6$ )  $\delta$  164.30, 152.57, 151.36, 149.35, 149.22, 148.89, 148.67, 139.54, 135.92, 130.86, 129.45, 129.25, 129.13, 123.66, 119.50, 112.54, 111.08, 108.70, 55.84, 55.74 ppm. HRMS  $m/z$   $[M+H]^+$  calcd for  $C_{20}H_{17}N_5O_3$  376.1404; found 376.1400.

**2-Amino-3,5-dibromopyrazine (2.31)**

To a solution of aminopyrazine (**2.30**) (1 g, 10.52 mmol) in DMSO (10 ml) was added *N*-bromosuccinimide (3.94 g, 22.08 mmol) portionwise over 45 minutes. The resulting mixture was stirred for 3 hours at room temperature. The reaction was poured in ice water and extracted five times with ethyl acetate. The combined organic phases were washed with brine, dried over MgSO<sub>4</sub> and evaporated to dryness. The crude residue was purified by silica gel flash column chromatography using a mixture of heptane and ethyl acetate (in a ratio of 7:3) as mobile phase, yielding the desired compound as a fluffy white solid (1.94 g, 73%). <sup>1</sup>H NMR (300 MHz, DMSO-*d*<sub>6</sub>) δ 8.13 (s, 1H), 6.99 (bs, 2H) ppm. HRMS *m/z* [M+H]<sup>+</sup> calcd for C<sub>4</sub>H<sub>4</sub>N<sub>3</sub>Br<sub>2</sub> 251.8768; found 251.8765.

**5-Bromo-3-((trimethylsilyl)ethynyl)pyrazin-2-amine (2.32)**

To a solution of **2.31** (1 g, 3.95 mmol) in degassed THF (15 ml) was added copper iodide (7.53 mg, 0.040 mmol), Pd(PPh<sub>3</sub>)<sub>2</sub>Cl<sub>2</sub> (45mg, 0.040 mmol) and triethylamine (1.65 ml, 11.86 mmol). The system was flushed with nitrogen and trimethylsilylacetylene (534 μl, 1.91 mmol) was added dropwise over 5 minutes. The reaction was stirred overnight at room temperature. After reaction completion, the solvent was evaporated and water was added. The resulting suspension was extracted three times with ethyl acetate. The combined organic phases were washed with water and brine, dried over MgSO<sub>4</sub> and evaporated to dryness. The crude residue was purified by silica gel flash column chromatography using a mixture of heptane and ethylacetate (in a ratio of 4:1) as mobile phase, yielding the title compound as a bright yellow solid (769 mg, 72%). <sup>1</sup>H NMR (300 MHz, DMSO-*d*<sub>6</sub>) δ 8.12 (s, 1H), 6.82 (s, 2H), 0.27 (s, 9H) ppm.

**2-Bromo-5*H*-pyrrolo[2,3-*b*]pyrazine (2.33)**

To a solution of **2.32** (1 g, 3.7 mmol) in dry NMP (10 ml) was added portionwise KOtBu (498 mg, 4.44 mmol). The reaction mixture was flushed with nitrogen and stirred for 3 hours at 80°C. After reaction completion, the mixture was diluted with water and extracted with ethyl acetate. The combined organic layers were washed twice with water and once with brine, dried over MgSO<sub>4</sub> and evaporated *in vacuo*. The crude residue was then purified by silica gel flash column chromatography using a mixture of heptane and ethyl acetate (in a ratio of 7:3) as mobile phase, yielding the title compound as a yellow solid (502 mg, 69%). <sup>1</sup>H NMR (300 MHz, DMSO-*d*<sub>6</sub>) δ 12.42 (br s, 1H), 8.35 (s, 1H), 7.97 (d, *J* = 3.48 Hz, 1H), 6.63 (d, *J* = 3.48 Hz, 1H) ppm.

**5-Bromo-3-iodo-1*H*-pyrrolo[2,3-*b*]pyrazine (2.34)**

To a solution of **2.33** (500 mg, 2.52 mmol) in a minimal volume of acetone was added portionwise *N*-iodosuccinimide (625 g, 2.78 mmol). The reaction mixture was stirred for 2 hours at room temperature. The formed precipitate was collected via filtration, yielding the title product as an off-white solid (408 mg, 50%). <sup>1</sup>H NMR (300 MHz, DMSO-*d*<sub>6</sub>) δ 12.82 (br s, 1H), 8.40 (d, *J* = 1.8 Hz, 1H), 8.19 (s, 1H) ppm.

**2-Bromo-7-(pyridin-3-ylethynyl)-5H-pyrrolo[2,3-*b*]pyrazine (2.35)**

To a degassed solution of **2.34** (200 mg, 0.617 mmol) in THF (10 ml) were added triethylamine (238  $\mu$ l, 1.85 mmol), Pd(PPh<sub>3</sub>)<sub>2</sub>Cl<sub>2</sub> (4.33 mg, 1% mol) and CuI (2.35 mg, 2% mol). The resulting mixture was stirred under inert atmosphere for 10 minutes at room temperature. Then, a solution of 3-ethynylpyridine (61 mg, 0.586 mmol) in THF (1 ml) was added to the reaction mixture. The reaction was stirred for 4 hours at room temperature. After completion, the reaction was filtered through Celite<sup>®</sup>, water was added and the mixture was extracted with ethyl acetate. The combined organic layers were washed with brine, dried over MgSO<sub>4</sub> and evaporated *in vacuo*. The crude product was purified by silica gel flash column chromatography using a mixture of heptane and ethyl acetate (in a ratio of 3:2) as mobile phase, yielding the title compound as a white solid (130 mg, 71%). <sup>1</sup>H NMR (300 MHz, DMSO-*d*<sub>6</sub>)  $\delta$  12.94 (bs, 1H), 8.76 (s, 1H), 8.59 (d, *J* = 3.2 Hz, 1H), 8.51 (s, 1H), 8.45 (s, 1H), 7.99 (dt, *J* = 7.9, 1.8 Hz, 1H), 7.47 (dd, *J* = 7.8, 4.8 Hz, 1H). HRMS *m/z* [M+H]<sup>+</sup> calcd for C<sub>13</sub>H<sub>8</sub>N<sub>4</sub>Br 298.9927; found 298.9930.

**2-(3,4-Dimethoxyphenyl)-7-(pyridin-3-ylethynyl)-5H-pyrrolo[2,3-*b*]pyrazine (2.36)**

To a solution of **2.35** (110 mg, 0.368 mmol) in dioxane (4 ml) was added 3,4-dimethoxyphenylboronic acid (80 mg, 0.441 mmol) and 1 ml of a K<sub>2</sub>CO<sub>3</sub> solution (152 mg, 1.1 mmol). The system was purged three times with argon and heated to 105°C. After stirring for 10 minutes, Pd(PPh<sub>3</sub>)<sub>4</sub> (10% mol) was added and the reaction was purged once more with argon. The reaction mixture was stirred at 105°C for 3 hours. After completion, the reaction mixture was cooled to room temperature and filtered through Celite<sup>®</sup>. The filtrate was diluted with water and extracted with ethyl acetate. The combined organic layers were washed with brine, dried over MgSO<sub>4</sub> and evaporated *in vacuo*. Purification by silica gel flash column chromatography using a mixture of dichloromethane and ethyl acetate (in a ratio of 1:1) as mobile phase, yielded the title compound as a white solid (37 mg, 28%). <sup>1</sup>H NMR (300 MHz, DMSO-*d*<sub>6</sub>)  $\delta$  12.63 (bs, 1H), 8.96 (s, 1H), 8.78 (s, 1H), 8.58 (d, *J* = 3.3 Hz, 1H), 8.35 (s, 1H), 8.00 (d, *J* = 7.8 Hz, 1H), 7.76 (m, 2H), 7.48 (m, 1H), 7.11 (d, *J* = 9.0 Hz, 1H), 3.90 (s, 3H), 3.83 (s, 3H) ppm. <sup>13</sup>C NMR (75 MHz, DMSO-*d*<sub>6</sub>)  $\delta$  151.44, 149.97, 149.32, 148.57, 146.70, 139.95, 138.27, 137.69, 136.06, 135.59, 130.21, 123.77, 120.46, 119.60, 112.33, 110.46, 95.69, 88.10, 85.92, 55.88, 55.81 ppm. HRMS *m/z* [M+H]<sup>+</sup> calcd for C<sub>21</sub>H<sub>17</sub>N<sub>4</sub>O<sub>2</sub> 357.1346; found 357.1346.

**2.8.2. Binding-displacement assay for NAK family selectivity**

Inhibitor binding to NAK family kinase domain proteins was determined using a binding-displacement assay which tests the ability of the inhibitors to displace a fluorescent tracer compound from the ATP binding site of the kinase domain. Inhibitors were dissolved in DMSO and dispensed as 16-point, 2x serial dilutions in duplicate into black multiwell plates (Greiner) using an Echo dispenser (Labcyte Inc). Each well contained 1nM biotinylated AAK1, BMP2K, GAK or STK16 kinase domain protein ligated to streptavidin-Tb-cryptate (Cisbio), either 12.5nM (for AAK1 or BMP2K) or 25nM (for GAK or STK16) Kinase Tracer 236 (ThermoFisher Scientific), 10mM Hepes pH 7.5, 150mM NaCl, 2mM DTT,

0.01% BSA, 0.01% Tween-20. Final assay volume for each data point was 5  $\mu$ L, and final DMSO concentration was 1%. The plate was incubated at room temperature for 1.5 hours and then read using a TR-FRET protocol on a PheraStarFS plate reader (BMG Labtech). The data was normalized to 0% and 100% inhibition control values and fitted to a four parameter dose-response binding curve in GraphPad Software. For the purpose of estimating the selectivity between each kinase domain, the determined IC<sub>50</sub> values were converted to K<sub>i</sub> values using the Cheng-Prusoff equation and the concentration and K<sub>D</sub> values for the tracer (previously determined).

### 2.8.3. Biological assays

#### 2.8.3.1. AAK1 expression, purification and crystallization

AAK1 (UniProtKB: Q2M2I8) residues T27-A365 was cloned, expressed and purified as described<sup>32</sup>, except that the protein was expressed in a cell line together with lambda phosphatase to produce the unphosphorylated protein. The purified protein was concentrated to 12 mg/mL and compound **1.15** dissolved in 100% DMSO was added to a final concentration of 1.5 mM (3% final DMSO concentration). The protein-ligand solution was incubated on ice for 30 minutes, then centrifuged at 14,000 rpm for 10 minutes at 4 °C, immediately prior to setting up sitting-drop vapour diffusion crystallization plates. The best-diffracting crystals of the AAK1 - compound **1.15** complex were obtained using a reservoir solution containing 26% PEG 3350, 0.1 M Bis-Tris pH 5.5 by spiking drops with 20 nL of seed-stock solution immediately prior to incubation at 18°C. Seed stock was prepared from poorly-formed crystals of AAK1 compound **1.15** grown during previous rounds of crystal optimization, which were diluted in 50-100  $\mu$ L reservoir solution and vortexed for 2 min in an Eppendorf containing a seed bead. A 1:1 dilution series of seeds was prepared in order to find the optimal seed concentration. Prior to mounting, crystals were cryo-protected *in situ* by addition of reservoir solution containing an additional 25% ethylene glycol. Crystals were then flash frozen in liquid nitrogen.

#### 2.8.3.2. Data collection, structure solution and refinement

Data was collected at Diamond beamline I02 using monochromatic radiation at wavelength 0.9795 Å. Diffraction data were processed using XDS<sup>38</sup> as part of the xia2 pipeline<sup>39</sup> and scaled using AIMLESS<sup>40</sup>, molecular replacement was carried out in Phaser<sup>41</sup> with PDB ID 4WSQ as a search model. REFMAC5<sup>42</sup>, PHENIX<sup>43</sup> and Coot<sup>44</sup> were used for model building and refinement. Coordinates were submitted to the PDB under accession code 5L4Q.

#### 2.8.3.3. Virus construct

DENV2 (New Guinea C strain)<sup>45,46</sup> *Renilla* reporter plasmid used for *in vitro* assays was a gift from Pei-Yong Shi (The University of Texas Medical Branch). DENV 16681 plasmid (pD2IC-30P-NBX) used for *ex vivo* experiments was a gift from Claire Huang (CDC).<sup>47</sup>

#### 2.8.3.4. Cells

Huh7 (Apath LLC) cells were grown in DMEM (Mediatech) supplemented with 10% fetal bovine serum (FBS) (Omega Scientific), nonessential amino acids, 1% L-glutamine, and 1% penicillin-streptomycin (ThermoFisher Scientific) and maintained in a humidified incubator with 5% CO<sub>2</sub> at 37°C. MDDCs were prepared as described with slight modifications.<sup>36</sup> Buffy coats were obtained from the Stanford Blood Center. CD14<sup>+</sup> cells were purified by EasySep™ Human Monocyte Enrichment Kit without CD16 Depletion (Stemcell Technologies). Cells were seeded in 6-well plates (2x10<sup>6</sup> cells per well), stimulated with 500 U/ml granulocyte-macrophage colony-stimulating and 1,000 U/ml interleukin-4 (Pepro tech), and incubated at 37°C for 6 days prior to DENV infection (MOI 1).

#### 2.8.3.5. Virus Production

DENV2 RNA was transcribed *in vitro* using mMessage/mMachine (Ambion) kits. DENV was produced by electroporating RNA into BHK-21 cells, harvesting supernatants on day 10 and titering via standard plaque assays on BHK-21 cells. In parallel, on day 2 post-electroporation, DENV-containing supernatant was used to inoculate C6/36 cells to amplify the virus. EBOV (Kikwit isolate) was grown in Vero E6 cells, supernatants were collected and clarified and stored at -80°C until further use. Virus titers were determined via standard plaque assay on Vero E6 cells.

#### 2.8.3.6. Infection assays

Huh7 cells were infected with DENV in replicates ( $n = 5$ ) at a multiplicity of infection (MOI) of 0.05. Overall infection was measured after 48 hours using a *Renilla* luciferase substrate. MDDCs were infected with DENV2 (16881) at an MOI of 1. Standard plaque assays were conducted following a 72-hour incubation. Huh7 cells were infected with EBOV at an MOI of 1 or 0.1 under biosafety level 4 conditions. Forty-eight hours after infection, supernatants were collected and stored at -80 °C until further use. Cells were formalin-fixed for twenty-four hours prior to removal from biosafety level 4. Infected cells were detected using an EBOV glycoprotein specific monoclonal antibody (KZ52), and quantitated by automated fluorescence microscopy using an Operetta High Content Imaging System and the Harmony software package (Perkin Elmer). For select experiments, supernatants were assayed by standard plaque assay, as described previously. Briefly, supernatants were thawed, serially diluted in growth media, added to VeroE6 cells and incubated for 1 hour at 37°C in a humidified 5% CO<sub>2</sub> incubator, prior to being overlaid with agarose. Infected cells were incubated for 7 days, then stained with neutral red vital dye (Gibco). Plaques were counted, and titers were calculated.

#### 2.8.3.7. Viability assays

Viability was assessed using AlamarBlue® reagent (Invitrogen) or Cell-Titer-Glo® reagent (Promega) assay according to manufacturer's protocol. Fluorescence was detected at 560 nm on InfiniteM1000 plate reader and luminescence on InfiniteM1000 plate reader (Tecan) or a Spectramax 340PC.

#### 2.8.3.8. Effect of compounds **1.15**, **2.7g** and **2.20b** on AP2 phosphorylation

Huh7 cells were kept in serum free medium for 1 hour and then treated with the compounds or DMSO in complete medium for 4 hours at 37°C. To allow capturing of phosphorylated AP2M1, 100 nM of the PP2A inhibitor calyculin A (Cell Signalling) was added 30 min prior to lysis in M-PER lysis buffer (ThermoFisher Scientific) with 1X Halt Protease & phosphatase inhibitor cocktail (ThermoFisher Scientific). Samples were then subjected to SDS-PAGE and blotting with antibodies targeting phospho-AP2M1 (Cell Signaling), total AP2M1 (Santa Cruz Biotechnology), and actin (Sigma-Aldrich). Band intensity was measured with NIH ImageJ.

### 2.8.4. Binding assays

#### 2.8.4.1. AAK1 LanthaScreen™ Eu binding assay

The compounds were subjected to a LanthaScreen™ binding assay in which 10 titrations of dissolved test compound in DMSO are transferred to a 384-well plate. Sequential addition of the kinase buffer (50 mM HEPES pH 7.5, 0.01% BRIJ-35, 10 mM MgCl and 1 mM EGTA), the 2X kinase antibody (Eu Anti GST) mixture and the 4X Tracer 222 solution was performed. After shaking for 30 seconds and a one hour incubation period at room temperature, the plate was read on a fluorescence plate reader. When the bound tracer in the active site was displaced by the test compound, fluorescence was not observed. The collected data were then compared to a 0% displacement control with pure DMSO and a 100% displacement control with sunitinib, a known inhibitor of AAK1, and plotted against the logarithmic concentration parameter. The IC<sub>50</sub> was subsequently extracted.

#### 2.8.4.2. AAK1 K<sub>D</sub> assay

K<sub>D</sub> values for AAK1 were determined as previously described.<sup>33</sup> Briefly, the DNA-tagged AAK1, an immobilized ligand on streptavidin-coated magnetic beads, and the test compound were combined. When binding occurred between AAK1 and a test compound, no binding can occur between AAK1 and the immobilized ligand. Upon washing, the compound-bound, DNA-tagged AAK1 was washed away. The beads carrying the ligands were then resuspended in elution buffer and the remaining kinase concentration was measured by qPCR on the eluate. K<sub>D</sub> values were determined using dose-response curves.

#### 2.8.4.3. Kinase Selectivity assay

Compound **2.20b** was screened against a diverse panel of 468 kinases (DiscoverX, KINOMEscan) using an *in vitro* ATP-site competition binding assay at a concentration of 10 μM. The results are reported as the percentage of kinase/phage remaining bound to the ligands/beads, relative to a control. High affinity compounds have % of control values close to zero, while weaker binders have higher % control values.



### 2.8.5. Statistical analysis

All data were analyzed with GraphPad Prism software. Fifty percent effective concentration ( $EC_{50}$ ),  $EC_{90}$  and  $CC_{50}$  values were measured by fitting data to a three-parameter logistic curve.  $P$  values were calculated by two-way ANOVA with Bonferroni's multiple comparisons tests or by 2-tailed unpaired  $t$  test.

### 2.8.6. General safety aspects

In context of health and safety, documents provided by the lab of medicinal chemistry and the HSE department of the KU Leuven were signed: Binding rules – Laboratory of medicinal chemistry. Based on the European Regulation (EC) No. 1272/2008) on classification, labeling and packaging of chemicals and mixtures, chemicals are classified according to their hazardous properties to humans and the environment into 5 categories (E4+, E4, E3, E2 and E1). Chemical operations were carried out in compliance with these documents and risk analyses were created according to the template provided by the HSE department and the information retrieved from the respective material safety data sheet (MSDS) for every used chemical and solvent. Additionally, personal safety measures were enforced at all times: wearing lab coats, safety goggles, long trousers and closed shoes. Furthermore, special precautions like wearing gloves or a dust mask were taken in case of handling especially hazardous reagents or devices to guarantee optimal safety.

## 2.9. References

- (1) Anne, N. E., Epidemiology of dengue : past , present and future prospects. *Clin. Epidemiol.* **2013**, *5*, 299-309.
- (2) Weekly epidemiological record. *World Health Organization* **2016**, *91* (30), 349-364.
- (3) Sanyal, S.; Sinha, S.; Halder, K. K., Pathogenesis of dengue haemorrhagic fever. *J Indian Med Assoc* **2013**, *89* (6), 152-153.
- (4) Behnam, M. A. M.; Nitsche, C.; Boldescu, V.; Klein, C. D., The Medicinal Chemistry of Dengue Virus. *J. Med. Chem.* **2016**, *59* (12), 5622-5649.
- (5) Bekerman, E.; Neveu, G.; Shulla, A.; Brannan, J., et al., Anticancer kinase inhibitors impair intracellular viral trafficking and exert broad-spectrum antiviral effects. *J. Clin. Invest.* **2017**, *127* (4), 1338-1352.
- (6) Bekerman, E.; Einav, S., Combating emerging viral threats. *Science* **2015**, *348* (6232), 282-283.
- (7) Grove, J.; Marsh, M., The cell biology of receptor-mediated virus entry. *J. Cell Biol.* **2011**, *195* (7), 1071-82.
- (8) Neveu, G.; Ziv-Av, A.; Barouch-Bentov, R.; Berkerman, E., et al., AP-2-Associated Protein Kinase 1 and Cyclin G-Associated Kinase Regulate Hepatitis C Virus Entry and Are Potential Drug Targets. *J. Virol.* **2015**, *89* (8), 4387-4404.
- (9) Neveu, G.; Barouch-Bentov, R.; Ziv-Av, A.; Gerber, D., et al., Identification and Targeting of an Interaction between a Tyrosine Motif within Hepatitis C Virus Core Protein and AP2M1 Essential for Viral Assembly. *PLoS Pathogens* **2012**, *8* (8), e1002845-e1002845.
- (10) Xiao, F.; Wang, S.; Barouch-Bentov, R.; Neveu, G., et al., Interactions between the Hepatitis C Virus Nonstructural 2 Protein and Host Adaptor Proteins 1 and 4 Orchestrate Virus Release. *mBio* **2018**, *9* (2), 1-21.
- (11) Pu, S.-Y.; Xiao, F.; Schor, S.; Bekerman, E., et al., Feasibility and biological rationale of repurposing sunitinib and erlotinib for dengue treatment. *Antivir. Res.* **2018**, *155*, 67-75.
- (12) Bamborough, P.; Drewry, D.; Harper, G.; Smith, G. K., et al., Assessment of Chemical Coverage of Kinome Space and Its Implications for Kinase Drug Discovery. *J. Med. Chem.* **2008**, *51* (24), 7898-7914.
- (13) Barl, N. M.; Sansiaume-Dagousset, E.; Karaghiosoff, K.; Knochel, P., Full Functionalization of the 7-Azaindole Scaffold by Selective Metalation and Sulfoxide/Magnesium Exchange. *Angew. Chem., Int. Ed.* **2013**, *52* (38), 10093-10096.
- (14) Brumsted, C. J.; Moorlag, H.; Radinov, R. N.; Ren, Y., et al. Method for preparation of N-{3-[5-(4-chlorophenyl)-1H-pyrrolo[2,3-b]pyridine-3-carbonyl]-2,4-difluorophenyl} propane-1-sulfonamide. 2012.
- (15) Han, C.; Green, K.; Pfeifer, E.; Gosselin, F., Highly Regioselective and Practical Synthesis of 5 - Bromo-4-chloro-3- nitro-7-azaindole. *Org. Process Res. Dev.* **2017**, *21* (4), 664-668.
- (16) Stokes, S.; Graham, C. J.; Ray, S. C.; Stefaniak, E. J. 1H-Pyrrolo[2,3-b]pyridine derivatives and their use as kinase inhibitors. 2013.
- (17) Gao, L.-j.; Kovackova, S.; Ramadori, A. T.; Jonghe, S. D., et al., Discovery of Dual Death-Associated Protein Related Apoptosis Inducing Protein Kinase 1 and 2 Inhibitors by a Scaffold Hopping Approach. *J. Med. Chem.* **2014**, *57* (18), 7624-7643.
- (18) Le Huerou, Y.; Blake, J.; Gunwardana, I.; Mohr, P., et al. Pyrrolopyridines as kinase inhibitors. 2009.
- (19) Stavenger, R.; Witherington, J.; Rawlings, D.; Holt, D., et al. CHK1 Kinase Inhibitors. 2003.
- (20) Bahekar, R. H.; Jain, M. R.; Jadav, P. A.; Prajapati, V. M., et al., Synthesis and antidiabetic activity of 2,5-disubstituted-3-imidazol-2-yl-pyrrolo[2,3-b]pyridines and thieno[2,3-b]pyridines. *Bioorg. Med. Chem.* **2007**, *15* (21), 6782-6795.
- (21) Chavan, N. L.; Nayak, S. K.; Kusurkar, R. S., A rapid method toward the synthesis of new substituted tetrahydro  $\alpha$ -carbolines and  $\alpha$ -carbolines. *Tetrahedron* **2010**, *66* (10), 1827-1831.
- (22) Chinta, B. S.; Baire, B., Reactivity of indole-3-alkoxides in the absence of acids: Rapid synthesis of homo-bisindolylmethanes. *Tetrahedron* **2016**, *72* (49), 8106-8116.

- (23) McCoull, W.; Hennessy, E. J.; Blades, K.; Box, M. R., et al., Identification and optimisation of 7-azaindole PAK1 inhibitors with improved potency and kinase selectivity. *MedChemComm* **2014**, *5* (10), 1533-1539.
- (24) Gourdain, S.; Dairou, J.; Denhez, C.; Bui, L. C., et al., Development of DANDYs, new 3,5-diaryl-7-azaindoles demonstrating potent DYRK1A kinase inhibitory activity. *J. Med. Chem.* **2013**, *56* (23), 9569-9585.
- (25) Gelbard, H.; Dewhurst, S.; Goodfellow, V.; Wiemann, T., et al. Bicyclic heteroaryl kinase inhibitors and methods of use. 2011.
- (26) Knauber, T.; Tucker, J., Palladium Catalyzed Monoselective  $\alpha$ -Arylation of Sulfones and Sulfonamides with 2,2,6,6-Tetramethylpiperidine·ZnCl<sub>2</sub>·LiCl Base and Aryl Bromides. *J. Org. Chem.* **2016**, *81* (13), 5636-5648.
- (27) Zhao, B.; Li, Y.; Xu, P.; Dai, Y., et al., Discovery of Substituted 1*H*-Pyrazolo[3,4-*b*]pyridine Derivatives as Potent and Selective FGFR Kinase Inhibitors. *ACS Med. Chem. Lett.* **2016**, *7* (6), 629-634.
- (28) Shi, J.; Xu, G.; Zhu, W.; Ye, H., et al., Design and synthesis of 1,4,5,6-tetrahydropyrrolo[3,4-*c*]pyrazoles and pyrazolo[3,4-*b*]pyridines for Aurora-A kinase inhibitors. *Bioorg. Med. Chem. Lett.* **2010**, *20* (14), 4273-4278.
- (29) Van Mileghem, S.; Egle, B.; Gilles, P.; Veryser, C., et al., Carbonylation as a novel method for the assembly of pyrazine based oligoamide alpha-helix mimetics. *Org. Biomol. Chem.* **2017**, *15* (2), 373-378.
- (30) McCormick, S.; Storck, P.-H.; Mertimore, M.; Charrier, J.-D., et al. Compounds useful as inhibitors of ATR kinase. 2012.WO 2012/178123
- (31) Gelbard, H.; Dewhurst, S.; Goodfellow, V.; Wiemann, T., et al. MLK inhibitors and methods of use. 2010.WO 2010/068483
- (32) Sorrell, Fiona J.; Szklarz, M.; Abdul Azeez, Kamal R.; Elkins, Jon M., et al., Family-wide Structural Analysis of Human Numb-Associated Protein Kinases. *Structure* **2016**, *24* (3), 401-411.
- (33) Fabian, M. A.; Biggs, W. H.; Treiber, D. K.; Atteridge, C. E., et al., A small molecule-kinase interaction map for clinical kinase inhibitors. *Nat. Biotechnol.* **2005**, *23* (3), 329-336.
- (34) Lebakken, C. S.; Riddle, S. M.; Singh, U.; Frazee, W. J., et al., Development and Applications of a Broad-Coverage, TR-FRET-Based Kinase Binding Assay Platform. *J. Biomol. Screen.* **2009**, *14* (8), 924-935.
- (35) O'Brien, J.; Wilson, I.; Orton, T.; Pognan, F., Investigation of the Alamar Blue (resazurin) fluorescent dye for the assessment of mammalian cell cytotoxicity. *Eur. J. Biochem.* **2000**, *267* (17), 5421-5426.
- (36) Rodriguez-Madoz, J. R.; Bernal-Rubio, D.; Kaminski, D.; Boyd, K., et al., Dengue virus inhibits the production of type I interferon in primary human dendritic cells. *J. Virol.* **2010**, *84* (9), 4845-50.
- (37) Karaman, M. W.; Herrgard, S.; Treiber, D. K.; Gallant, P., et al., A quantitative analysis of kinase inhibitor selectivity. *Nat. Biotechnol.* **2008**, *26* (1), 127-132.
- (38) Kabsch, W., *XDS. Acta Crystallogr., Sect. D: Biol. Crystallogr.* **2010**, *66* (2), 125-132.
- (39) Winter, G., xia2 : an expert system for macromolecular crystallography data reduction. *J. Appl. Crystallogr.* **2010**, *43*, 186-190.
- (40) Winn, M. D.; Charles, C.; Cowtan, K. D.; Dodson, E. J., et al., Overview of the CCP 4 suite and current developments. **2011**, *D67*, 235-242.
- (41) McCoy, A. J.; Grosse-kunstleve, R. W.; Adams, P. D.; Winn, M. D., et al., Phaser crystallographic software research papers. *J. Appl. Crystallogr.* **2007**, *40*, 658-674.
- (42) Murshudov, G. N.; Vagin, A. A.; Dodson, E. J., Refinement of macromolecular structures by the maximum-likelihood method. *Acta Crystallogr., Sect. D: Biol. Crystallogr.* **1997**, *53* (3), 240-255.
- (43) Adams, P. D.; Afonine, P. V.; Bunkóczi, G.; Chen, V. B., et al., *PHENIX* : a comprehensive Python-based system for macromolecular structure solution. *Acta Crystallogr., Sect. D: Biol. Crystallogr.* **2010**, *66* (2), 213-221.
- (44) Emsley, P.; Lohkamp, B.; Scott, W. G.; Cowtan, K., et al., Features and development of *Coot*. *Acta Crystallogr., Sect. D: Biol. Crystallogr.* **2010**, *66* (4), 486-501.

- (45) Perera, R.; Khaliq, M.; Kuhn, R. J., Closing the door on flaviviruses: entry as a target for antiviral drug design. *Antivir. Res.* **2008**, *80* (1), 11-22.
- (46) Xie, X.; Gayen, S.; Kang, C.; Yuan, Z., et al., Membrane topology and function of dengue virus NS2A protein. *J. Virol.* **2013**, *87* (8), 4609-22.
- (47) Huang, C. Y. H.; Butrapet, S.; Moss, K. J.; Childers, T., et al., The dengue virus type 2 envelope protein fusion peptide is essential for membrane fusion. *Virology* **2010**, *396* (2), 305-315.

## Chapter 3: Synthesis and structure-activity relationship studies of benzo[4,5]imidazo[1,2-*a*]pyrimidin-4(10*H*)-ones as Mas-related gene receptor X2 antagonists

This chapter is based on a manuscript in preparation.

### 3.1. Introduction

Degranulation of MCs plays a crucial role in the development of various allergic disorders, such as asthma, chronic urticaria and atopic dermatitis.<sup>1-3</sup> Especially the MC<sub>TC</sub> subset which is overexpressed in inflamed tissue, is a major contender in the exacerbations of these allergic diseases.<sup>2</sup> MCs can degranulate either via an IgE mediated<sup>4,5</sup> or via an IgE independent mechanism<sup>3</sup>. It has been demonstrated that the orphan receptor MRGPRX2 is involved in the IgE independent degranulation. This receptor, with an unknown endogenous natural ligand, can be activated by a wide array of natural and synthetic ligands, collectively known as the basic secretagogous.<sup>4,6-8</sup> The MRGPRX2 receptor transduces its signal through a G<sub>q</sub> subunit, ultimately leading to the release of intracellular Ca<sup>2+</sup>.<sup>6</sup> Over the years, several small molecule MRGPRX2 agonists<sup>9,10</sup> have been reported, but despite their potential therapeutic use, no small molecule antagonists have been disclosed until very recently.<sup>11</sup>

Screening of a 1600-membered commercial compound library (purchased by Prof. P. Herdewijn, KU Leuven, Belgium) as MRGPRX2 antagonists in a  $\beta$ -arrestin assay (by the group of Prof. C. Muller, University of Bonn, Germany) led to the discovery of a single hit (compound **1.16**), based on a benzo[4,5]imidazo[1,2-*a*]pyrimidin-4(10*H*)-one scaffold. Subsequent screening of a series of commercially available benzo[4,5]imidazo[1,2-*a*]pyrimidin-4(10*H*)-one analogues afforded three more derivatives (compounds **1.17-1.19**) with low micromolar activity (**Figure 3.1**).

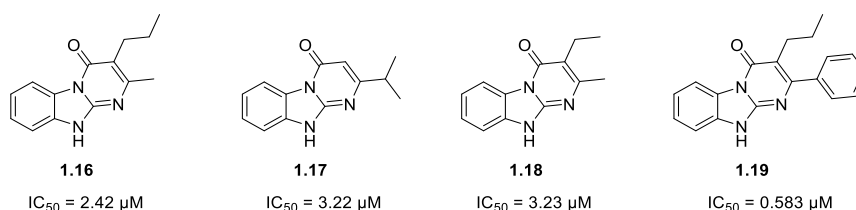


**Figure 3.1.** Hits of MRGPRX2 antagonist screening

In order to study the SAR in a systematic way, the hit scaffold was divided into three fragments (**Figure 3.2**): the benzo, imidazole and pyrimidine moiety.

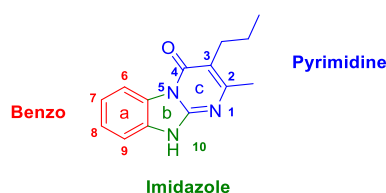
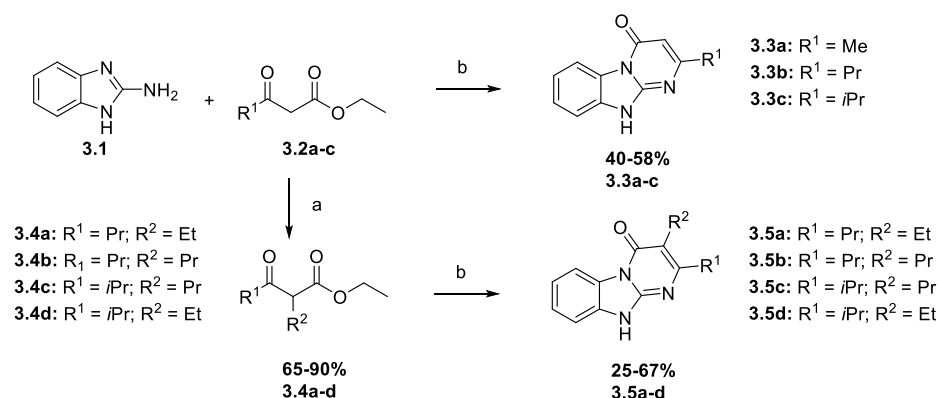


**Figure 3.2.** Subdivision of the benzo[4,5]imidazo[1,2-*a*]pyrimidin-4(10*H*)-one scaffold into three structural parts

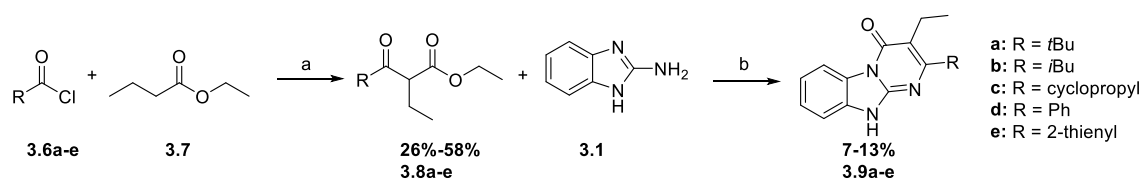
## 3.2. Synthesis of benzo[4,5]imidazo[1,2-*a*]pyrimidin-4(10*H*)-one analogues

### 3.2.1. Structural modifications on the pyrimidine moiety

At the onset of this PhD thesis, the Lab of Medicinal Chemistry at the KU Leuven already prepared a number of benzo[4,5]imidazo[1,2-*a*]pyrimidin-4(10*H*)-one analogues with structural variation on the benzo, imidazole and, to a lesser extent, the pyrimidine moiety. To synthesize the pyrimidine modified analogues, commercially available 2-aminobenzimidazole (**3.1**) was treated with  $\beta$ -ketoesters (**3.2a-c** and **3.4a-d**) to generate the benzo[4,5]imidazo[1,2-*a*]pyrimidin-4(10*H*)-one derivatives (**3.3a-c** and **3.5a-d**).<sup>12</sup> The  $\beta$ -ketoesters were either commercially available (**3.2a-c**) or they were synthesized via alkylation of the  $\alpha$ -position (**3.4a-d**) of the deprotonated  $\beta$ -ketoester with an appropriate alkyl halide (**Scheme 3.1**).<sup>13</sup> The disadvantage of this method, however, was that the reaction does not always reach completion and that starting material and product are difficult to separate and multiple rounds of flash chromatography are required to obtain the pure 3-oxoesters **3.4a-d**.

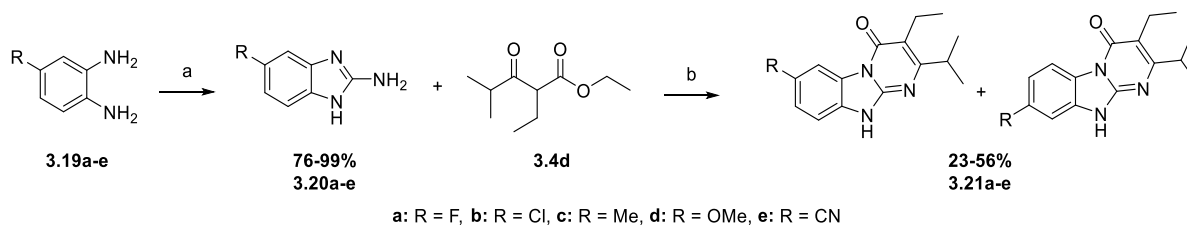


**Scheme 3.1. Reagents and conditions.** a) NaH, R<sub>2</sub>I, THF, 0°C to rt, 3h; b) **3.1**, DMF, reflux, overnight. Therefore, an alternative method was applied to gain access to more  $\beta$ -ketoesters (**Scheme 3.2**). A modified Claisen condensation<sup>14</sup> between an appropriate acid chloride (**3.6a-e**) and ethyl butyrate (**3.7**) yielded the desired  $\beta$ -ketoesters (**3.8a-e**). Subsequent reaction with 2-aminobenzimidazole (**3.1**) afforded benzo[4,5]imidazo[1,2-*a*]pyrimidin-4(10*H*)-ones **3.9a-e**. Although self-condensation of ethyl butyrate could not be avoided, the crude reaction mixtures were much easier to purify, making this Claisen condensation the method of choice for the synthesis of  $\beta$ -ketoesters. In addition, the commercial availability of a wide range of acid chlorides allows to easily introduce structural variety on the benzo[4,5]imidazo[1,2-*a*]pyrimidin-4(10*H*)-one scaffold.



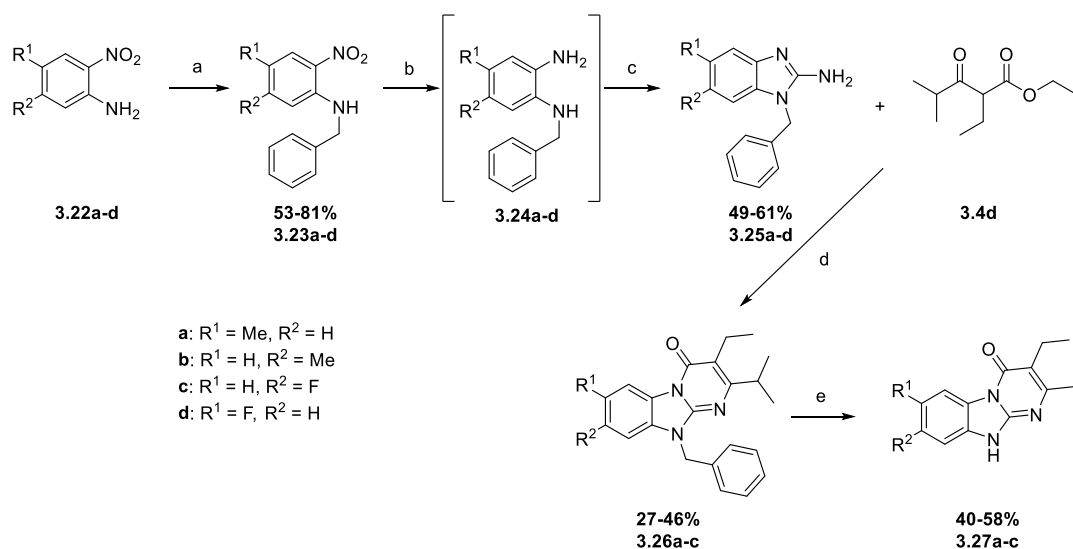
**Scheme 3.2. Reagents and conditions.** a) *n*BuLi, *i*Pr<sub>2</sub>NH, THF, -78°C to rt, 3h; b) DMF, reflux, overnight.





**Scheme 3.5.** *Reagents and conditions.* a) BrCN, EtOH, 50°C, overnight; b) DMF, reflux, overnight.

For a selected number of analogues, a regioselective synthesis method was established (**Scheme 3.6**). Reaction of commercially available substituted 2-nitroanilines **3.22a-d** with benzyl bromide yielded the benzyl protected anilines (**3.23a-d**). Reduction of the nitro group by catalytic hydrogenation with Raney nickel yielded the diaminobenzene derivatives **3.24a-d**. Because of their labile nature, these monobenzyl-protected diaminobenzenes were immediately subjected to imidazole formation by reaction with cyanogen bromide, affording compounds **3.25a-d**. Finally, condensation of compounds **3.25a-d** with ethyl 2-ethyl-4-methyl-3-oxopentanoate (**3.4d**), followed by cleavage of the benzyl protecting group using catalytic hydrogenation yielded the final compounds **3.27a-c**. Despite the fact that the 8-fluoro-benzo[4,5]imidazo[1,2-*a*]pyrimidin-4(10*H*)-one **3.26c** was synthesized successfully, the corresponding 7-fluoro regioisomer **3.26d** failed to form during the final cyclization with the keto-ester as only starting material was recovered. This can possibly be due to the inductive influence of the fluorine atom on the imidazole nitrogen lone pair.



**Scheme 3.6.** *Reagents and conditions.* a) BnBr, H<sub>2</sub>O, reflux, 48h; b) Raney Ni, H<sub>2</sub>, MeOH, rt, 3h; c) BrCN, EtOH, 50°C, overnight; d) DMF, reflux, overnight; e) H<sub>2</sub>, Pd/C, MeOH, DCM, rt, 5h.

### 3.3. Structure-activity relationship study

All synthesized compounds were evaluated for MRGPRX2 antagonism in a  $\beta$ -arrestin recruitment assay. This functional assay uses transfected CHO cells stably expressing a fusion protein, consisting of MRGPRX2 fused with a ProLink™ tag which are the first 41 amino acids of  $\beta$ -galactosidase.  $\beta$ -arrestin fused to the rest of the  $\beta$ -galactosidase enzyme is added by using retrovirus particles. Activation of MRGPRX2 by the addition of the agonist cortistatin-14 leads to the recruitment of  $\beta$ -arrestin to the



receptor and complementation of both  $\beta$ -galactosidase fragments. The activity of this active  $\beta$ -galactosidase can be measured by chemiluminescence through the decomposition of Galacton-Star™ (Figure 3.2).<sup>16</sup> In order to evaluate the MRGPRX2 antagonistic characteristics of the benzo[4,5]imidazo[1,2-*a*]pyrimidin-4(10*H*)-one analogues, the compounds were added one hour prior to addition of the agonist.

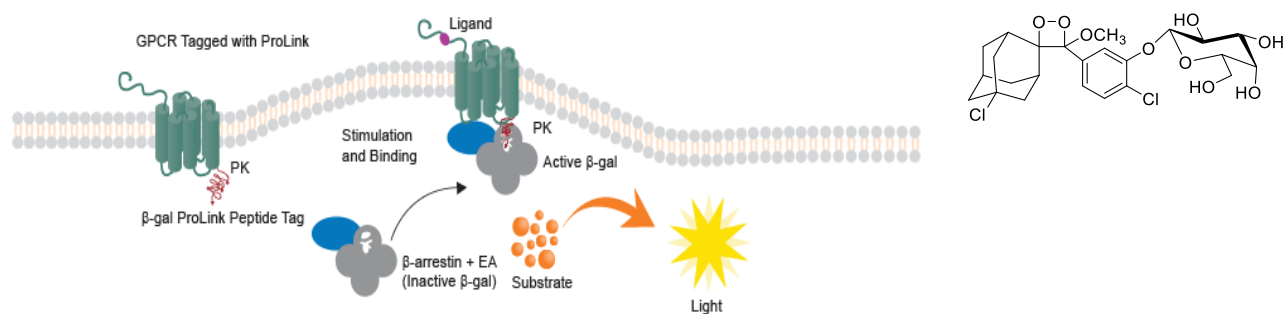
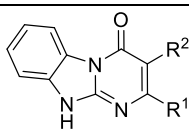


**Figure 3.2.** Principle of the  $\beta$ -arrestin recruitment assay (left) and Galacton-Star (right)

### 3.3.1. SAR of the pyrimidine moiety

The original hit compound **1.16** showed moderate antagonistic activity in the low micromolar range. A small library of compounds with structural variation of the substituents  $R^1$  and  $R^2$  at the pyrimidine moiety was synthesized. In order to define the minimal requirements for MRGPRX2 antagonism, the fully unsubstituted benzo[4,5]imidazo[1,2-*a*]pyrimidin-4(10*H*)-one **3.13** was evaluated, completely lacking activity. The effect of structural variation at position 3 (substituent  $R^2$ ) on MRGPRX2 antagonism was evaluated (Table 3.1) by fixing a methyl group at position 2 and introducing alkyl chains of varying length at position 3. The tolerable space at this position is limited but cannot be left unsubstituted as compound **3.3a** is devoid of activity. An ethyl or propyl group yielded compounds **1.18** and **1.16**, respectively, that are equipotent with  $IC_{50}$  values in the low  $\mu$ M range. The presence of a methyl or butyl group on position 3 gives rise to derivatives that are endowed with a decreased or even complete lack of activity (compounds **3.14** and **3.15**, respectively), suggesting a minimal and maximal length requirement.

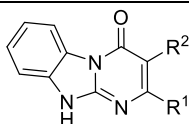


Compound	$R^1$	$R^2$	$IC_{50} \pm SEM$ ( $\mu$ M)
<b>3.13</b>	H	H	>100
<b>3.3a</b>	Me	H	>100
<b>3.14</b>	Me	Me	$11.6 \pm 11$
<b>1.18</b>	Me	Et	$3.23 \pm 0.36$

<b>1.16</b>	Me	Pr	2.42 ± 0.22
<b>3.15</b>	Me	Bu	>10

**Table 3.1.** MRGPRX2 antagonism of pyrimidine (position 3) modified benzo[4,5]imidazo[1,2-*a*]pyrimidin-4(10*H*)-ones

Evaluation of the effect on MRGPRX2 antagonism by introducing structural variation on position 2 was carried out next (**Table 3.2**). The systematic reintroduction of bulkier alkyl groups (such as propyl and isopropyl, as in compounds **3.3b** and **1.17**, respectively) at position 2 (substituent R<sup>1</sup>) allowed to regain MRGPRX2 antagonism, with especially the 2-isopropyl analogue **1.17** showing promising activity (IC<sub>50</sub> = 3.22 μM). Finally, the library was further expanded by combining two structural variations: fixing position 3 as an ethyl or propyl substituent and increasing the steric bulk at position 2. The introduction of a propyl, isopropyl, isobutyl or *tert*-butyl furnished a series of compounds that displayed IC<sub>50</sub> values in the range of 0.2-0.5 μM (compounds **3.5b-e** and **3.9a-b**) which corresponds with a 10-fold improvement over the activity of the original hit compound **1.16**. There also seems to be a limit to the increase of the steric bulk on position 2 as the introduction of a tertiary butyl or isobutyl group causes a decrease in activity. One example of a compound with a cycloaliphatic substituent at position 2 was prepared: a cyclopropyl derivative (compound **3.9c**) that shows a 5-fold decreased activity, when compared to the corresponding isopropyl analogue **3.5d**. Finally, a number of aromatic residues was inserted at position 2. The introduction of a phenyl residue gave compound **3.9d** that displayed an IC<sub>50</sub> of 0.54 μM. Surprisingly, the isosteric 2-thienyl analogue (compound **3.9e**) is completely devoid of MRGPRX2 antagonism.



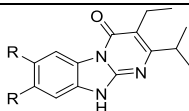
Compound	R <sup>1</sup>	R <sup>2</sup>	IC <sub>50</sub> ± SEM (μM)
<b>1.16</b>	Me	Pr	2.42 ± 0.22
<b>3.3b</b>	Pr	H	14.7 ± 1.21
<b>1.17</b>	<i>i</i> -Pr	H	3.22 ± 0.82
<b>3.5a</b>	Pr	Et	0.214 ± 0.0319
<b>3.5b</b>	Pr	Pr	0.272 ± 0.0371
<b>3.5c</b>	<i>i</i> -Pr	Pr	0.512 ± 0.107
<b>3.5d</b>	<i>i</i> -Pr	Et	0.290 ± 0.098
<b>3.9a</b>	<i>t</i> -Bu	Et	0.349 ± 0.065
<b>3.9b</b>	<i>i</i> -Bu	Et	0.458 ± 0.076

<b>3.9c</b>	cyclopropyl	Et	1.18 ± 0.065
<b>3.9d</b>	Ph	Et	0.54 ± 0.076
<b>3.9e</b>	thienyl	Et	>10

**Table 3.2.** MRGPRX2 antagonism of pyrimidine modified benzo[4,5]imidazo[1,2-*a*]pyrimidin-4(10*H*)-ones

### 3.3.2. SAR of the benzo moiety

In order to evaluate the SAR of the phenyl moiety, the substituents at positions 2 and 3 of the benzo[4,5]imidazo[1,2-*a*]pyrimidin-4(10*H*)-one scaffold were fixed as an isopropyl and ethyl group, respectively, because of the potency associated with compound **3.5d** (Table 3.3). The introduction of chlorines (**3.18b**) or bromines (**3.18c**) gave a 2- to 4-fold decreased activity, when compared to compound **3.5d**. On the other hand, the 7,8-dimethyl congener (**3.18d**) displayed excellent MRGPRX2 antagonism with an IC<sub>50</sub> value of 0.0439 μM. The 7,8-difluorobenzo[4,5]imidazo[1,2-*a*]pyrimidin-4(10*H*)-one analogue (**3.18a**), endowed with an IC<sub>50</sub> value of 0.021 μM, was the most potent derivative in this series.



Compound	R	IC <sub>50</sub> ± SEM (μM)
<b>3.5c</b>	H	0.290 ± 0.098
<b>3.18a</b>	F	0.0209 ± 0.0054
<b>3.18b</b>	Cl	0.477 ± 0.087
<b>3.18c</b>	Br	0.890 ± 0.184
<b>3.18d</b>	Me	0.0439 ± 0.0261

**Table 3.3.** MRGPRX2 antagonism of 7,8-disubstituted benzo[4,5]imidazo[1,2-*a*]pyrimidin-4(10*H*)-ones

Following the promising data associated with 7,8-disubstituted benzo[4,5]imidazo[1,2-*a*]pyrimidin-4(10*H*)-ones (especially the methylated (**3.18d**) and the fluorinated (**3.18a**) congeners), the focus was shifted to mono-substituted phenyl derivatives (Table 3.4). As mentioned above, these compounds were isolated as unseparable, regioisomeric mixtures and were evaluated as such for their antagonistic potency. Analogous to the disubstituted benzo[4,5]imidazo[1,2-*a*]pyrimidin-4(10*H*)-ones, the presence of small electron-donating groups (e.g. a methyl as in compounds **3.21c**), as well as small halogens (such as a fluorine as in compounds **3.21a**) afforded compounds that displayed potent MRGPRX2 antagonism (IC<sub>50</sub> values of 0.129 μM and 0.092 μM, respectively). On the other hand, the insertion of a cyano moiety as a mesomeric electron-withdrawing group afforded compounds **3.21e**, which is five-fold less active as the unsubstituted derivative **3.5d**. The discrepancy between the positive effect on activity of the electron negative fluorine atom versus the negative effect on activity of the mesomeric

withdrawing effect of the cyano group can be due to two reasons. The first possible explanation can be delocalization of the free electron pair of the nitrogen in the 10 position or the bridgehead nitrogen. Delocalization of the electrons of the nitrogen at position 10 gives rise to an equilibrium structure which loses its proton which can be an essential hydrogen bond donor. This is impossible with the fluorine atom whose inductive effect diminishes greatly over this distance. A second explanation can be found in the polarity of the cyano group, the nitrogen can act as polar hydrogen bond acceptor while the receptor contains a hydrophobic accommodation pocket. A methoxy group on the phenyl ring furnished compound **3.21d**, which is equally active as the unsubstituted congener **3.5d**.

Compound	R	IC <sub>50</sub> ± SEM (μM)
<b>3.5d</b>	H	0.290 ± 0.098
<b>3.21a</b>	F	0.092 ± 0.043
<b>3.21b</b>	Cl	0.169 ± 0.17
<b>3.21c</b>	Me	0.129 ± 0.087
<b>3.21d</b>	OMe	0.213 ± 0.079
<b>3.21e</b>	CN	1.260 ± 0.310

**Table 3.4.** MRGPRX2 antagonism of regioisomeric benzo[4,5]imidazo[1,2-*a*]pyrimidin-4(10*H*)-ones. As the methyl and fluorine substituted regioisomeric mixtures (compounds **3.21c** and **3.21a**, respectively) showed potent MRGPRX2 antagonism, their single regioisomers were also evaluated in the MRGPRX2 β-arrestin assay (**Table 3.5**). The 8-methyl substituted analogue **3.27b** (IC<sub>50</sub> = 0.091 μM) is slightly more potent than the 7-methyl derivative **3.27a** (IC<sub>50</sub> = 0.147 μM). The 8-fluoro derivative **3.27c** is endowed with very potent MRGPRX2 antagonism, as evidenced by an IC<sub>50</sub> value of 0.018 μM.

Compound	R <sup>1</sup>	R <sup>2</sup>	IC <sub>50</sub> ± SEM (μM)
<b>3.27a</b>	Me	H	0.147 ± 0.015
<b>3.27b</b>	H	Me	0.091 ± 0.029
<b>3.27c</b>	H	F	0.018 ± 0.004

**Table 3.5.** MRGPRX2 antagonism of 7- and 8-substituted benzo[4,5]imidazo[1,2-*a*]pyrimidin-4(10*H*)-ones

### 3.4. Conclusion

This chapter described the synthesis and biological evaluation of novel MRGPRX2 antagonists. A screening campaign identified 4 hit compounds based on a benzo[4,5]imidazo[1,2-*a*]pyrimidin-4(10*H*)-one scaffold (**1.16-1.19**) that were endowed with moderate activity in the  $\beta$ -arrestin assay. Optimization of the substitution pattern of the pyrimidine moiety led to the discovery of compounds with increased activity (**3.5a-c**). The substitution pattern of the pyrimidine moiety that conferred the strongest MRGPRX antagonism (i.e. the 2-isopropyl-3-ethyl derivative **3.5d**) was then used for structural variation of the phenyl moiety. It led to the discovery of a 8-fluoro (**3.27c**) and a 7,8-difluoro (**3.18a**) analogue with excellent potency ( $IC_{50}$  of 20 nM for both derivatives). Similarly, methyl substituted phenyl derivatives demonstrated promising MRGPRX2 antagonism. The 7,8-dimethyl congener (**3.18d**) is endowed with an  $IC_{50}$  value of 44 nM, whereas the 8-methyl analogue (**3.27b**) displayed an  $IC_{50}$  of 91 nM.

### 3.5. Experimental section

Compounds **3.13**, **3.3a-c**, **3.5a-d**, **3.18b**, **3.18d**, **3.21a-e** were synthesized by Dr. Piotr Leonczak (Lab of Medicinal Chemistry, KU Leuven). All commercial reagents were obtained from Acros Organics, Sigma-Aldrich, AK Scientific and Fluorochem and are at least 99% purity unless indicated otherwise. All dry solvents were purchased from Acros Organics with an AcroSeal system and regular solvents were obtained via Fisher Scientific at analytical grade. Thin layer chromatography (TLC) was performed on silica gel on aluminum foils with fluorescent indicator (254 nm) (60 Å pore diameter) obtained from Sigma-Aldrich and visualized using ultraviolet light (254 nm). Recording of the NMR spectra was performed using a Bruker 300 MHz, 500 MHz or 600 MHz spectrometer. The chemical shifts are reported in ppm relative to tetramethylsilane (TMS) or the residual solvent signal for  $^1H$ , the residual solvent signal for  $^{13}C$ . Spectra recorded in  $D_2O$  and for  $^{19}F$  are uncorrected. Coupling constants ( $J$ ) are reported in hertz. Mass spectra were acquired on a quadrupole orthogonal acceleration time-of-flight mass spectrometer (Synapt G2 HDMS, Waters, Milford, MA). Samples were infused at 3  $\mu L/min$  and spectra were obtained in positive or negative ionization mode with a resolution of 15000 (FWHM) using leucine enkephalin as lock mass. Purity of the compounds was determined on a Waters 600 HPLC system equipped with a Waters 2487 Dual  $\lambda$  absorbance detector set at 256 nm using a 5  $\mu m$  4.6x150 mm XBridge Reversed Phase ( $C_{18}$ ) column. The mobile phase was a gradient over 30 minutes starting from 95% A and 5% B and finishing at 5% A and 95% B with a flow rate of 1 ml per minute (solvent A: MilliQ water; solvent B: acetonitrile). All synthesized final compounds had a purity of at least 95 %.

### 3.5.1. Chemistry

#### 3.5.1.1. Synthesis of 2-alkyl-3-oxoesters

##### General procedure

To a solution of *n*-BuLi (2.3 mol equiv.) in THF (5 ml) at  $-78^{\circ}\text{C}$ , was added diisopropylamine (2.4 mol equiv.) dropwise. The mixture was stirred at  $-78^{\circ}\text{C}$  for 30 minutes. Ethyl ester (2 mol equiv.) was added dropwise via a cannula over 30 minutes and the mixture was allowed to stir further at  $-78^{\circ}\text{C}$ . Finally, the acid chloride (1 mol equiv.) was added dropwise to the reaction mixture. The reaction mixture was allowed to warm to room temperature and was stirred for another 2 hours. After reaction completion, a saturated  $\text{NH}_4\text{Cl}$  solution was added and the mixture was extracted three times with EtOAc. The combined organic layers were dried over  $\text{Na}_2\text{SO}_4$ , filtered and concentrated *in vacuo*. The crude product was purified by silica gel flash column chromatography (using a mixture of heptane and EtOAc as eluent), yielding the 2-alkyl-3-oxoesters as colorless to light yellow oils. The following compounds were made according to this procedure.

##### **Ethyl 2-ethyl-4-methyl-3-oxopentanoate (3.4d)**

The title compound was obtained from isobutyryl chloride (1.00 g, 9.39 mmol) as a colorless oil (1.70 g, 97%).  $^1\text{H}$  NMR ( $\text{CDCl}_3$ , 300 MHz):  $\delta$  0.92 (t,  $J = 7.4$  Hz, 3H), 1.11 (d,  $J = 6.9$  Hz, 3H), 1.13 (d,  $J = 6.9$  Hz, 3H), 1.26 (t,  $J = 7.1$  Hz, 3H), 1.87 (m, 2H), 2.80 (m, 1H), 3.53 (t,  $J = 7.3$  Hz, 1H), 4.18 (q,  $J = 7.1$  Hz, 2H) ppm.  $^{13}\text{C}$  NMR ( $\text{CDCl}_3$ , 75 MHz):  $\delta$  12.18, 14.22, 18.16, 18.45, 21.84, 40.72, 58.77, 61.26, 169.90, 209.26 ppm.

##### **Ethyl 2-ethyl-4,4-dimethyl-3-oxopentanoate (3.8a)**

The title compound was obtained from trimethylacetyl chloride (0.50 g, 4.15 mmol) as a colorless oil (320 mg, 38%).  $^1\text{H}$  NMR ( $\text{CDCl}_3$ , 300 MHz)  $\delta$  0.91 (t,  $J = 7.4$  Hz, 3H), 1.17 (s, 9H), 1.24 (t,  $J = 7.5$  Hz, 3H), 1.80 (m, 2H), 3.80 (t,  $J = 7.1$  Hz, 1H), 4.13 (q,  $J = 7.1$  Hz, 2H) ppm.

##### **Ethyl 2-ethyl-5-methyl-3-oxohexanoate (3.8b)**

The title compound was obtained from isovaleryl chloride (0.50 g, 4.15 mmol) as a colorless oil (490 mg, 58%).  $^1\text{H}$  NMR ( $\text{CDCl}_3$ , 300 MHz)  $\delta$  0.89 (m, 9H), 1.28 (t,  $J = 7.2$  Hz, 3H), 1.55 (m, 3H), 1.68 – 1.94 (m, 2H), 2.39 – 2.55 (m, 1H), 4.18 (dd,  $J = 8.7, 5.7$  Hz, 2H) ppm.

##### **Ethyl 2-(cyclopropanecarbonyl)butanoate (3.8c)**

The title compound was obtained from cyclopropanecarbonyl chloride (0.50 g, 4.78 mmol) as a colorless oil (320 mg, 26%).  $^1\text{H}$  NMR ( $\text{CDCl}_3$ , 300 MHz)  $\delta$  0.95 (t,  $J = 7.4$  Hz, 3H), 1.09 (m, 2H), 1.27 (t,  $J = 7.1$  Hz, 3H), 1.94 (q,  $J = 7.4$  Hz, 2H), 2.07 (m, 1H), 3.47 (t,  $J = 7.4$  Hz, 1H), 4.21 (q,  $J = 7.1$  Hz, 2H) ppm.

##### **Ethyl 2-benzoylbutanoate (3.8d)**

The title compound was obtained from benzoyl chloride (0.50 g, 3.56 mmol) and the crude compound was used in the next reaction.

**Ethyl 2-(thiophene-2-carbonyl)butanoate (3.8e)**

The title compound was obtained from thiophene-2-carbonyl chloride (0.50 g, 3.41 mmol) as a colorless oil (247 mg, 32%). <sup>1</sup>H NMR (CDCl<sub>3</sub>, 300 MHz) δ 0.81 (t, *J* = 7.5 Hz, 3H), 0.99 (t, *J* = 7.4 Hz, 3H), 2.05 (m, 2H), 2.74 (m, 1H), 4.17 (m, 2H), 7.15 (s, 1H), 7.68 (s, 1H), 7.80 (s, 1H) ppm.

**3.5.1.2. Synthesis of benzyl-protected 1,2-diaminophenyl derivatives*****N*-Benzyl-4-methyl-2-nitroaniline (3.23a)**

A mixture of 4-methyl-2-nitroaniline (1 g, 6.57 mmol) and benzyl bromide (940 μl, 7.89 mmol, 1.2 mol. eq.) in H<sub>2</sub>O (20 ml) was stirred at reflux for 1.5 h. Then, an additional amount of benzyl bromide (0.6 eq, 3.95 mmol) was added and stirring was continued at reflux for another 2 days. After cooling to room temperature, a saturated NaHCO<sub>3</sub> solution was added and the mixture was extracted with EtOAc (3x). The organic layers were combined, washed with H<sub>2</sub>O (1x) and dried over Na<sub>2</sub>SO<sub>4</sub>. After removal of drying agent and solvent, the crude residue was purified by silica gel flash column chromatography (using heptane/EtOAc 9:1 as mobile phase) affording the title compound as an orange solid (1.29 g, 81%). <sup>1</sup>H NMR (CDCl<sub>3</sub>, 300 MHz): δ 2.25 (s, 3H), 4.53 (d, 2H, *J* = 5 Hz), 6.73 (d, 1H, *J* = 7.5 Hz), 7.20 (dd, 1H, *J* = 7.5 Hz, *J* = 2.5 Hz), 7.25-7.38 (m, 5H), 7.99 (d, 1H, *J* = 2.5 Hz), 8.33 (bs, 1H) ppm. <sup>13</sup>C NMR (CDCl<sub>3</sub>, 75 MHz): δ 19.09, 46.25, 113.34, 124.42, 125.23, 126.13, 126.74, 128.01, 131.04, 136.75, 136.83, 142.63 ppm. HRMS (ESI): *m/z* [M+H]<sup>+</sup> calcd for C<sub>14</sub>H<sub>15</sub>N<sub>2</sub>O<sub>2</sub>: 265.0948, found 265.0950.

***N*-Benzyl-5-methyl-2-nitroaniline (3.23b)**

A mixture of 5-methyl-2-nitroaniline (1 g, 6.57 mmol) and benzyl bromide (940 μl, 7.89 mmol, 1.2 mol. eq.) in H<sub>2</sub>O (10 ml) was stirred at reflux for 1.5 h. Then, an additional amount of benzyl bromide (0.6 eq, 3.95 mmol) was added and stirring was continued at reflux for another 2 days. After cooling to room temperature, a saturated NaHCO<sub>3</sub> solution was added and mixture was extracted with EtOAc (3x). The combined organic layers were washed with H<sub>2</sub>O (1x) and dried over Na<sub>2</sub>SO<sub>4</sub>. After removal of drying agent and solvent, the crude residue was purified by silica gel flash column chromatography (using a mixture of heptane/EtOAc in a ratio of 9:1 as mobile phase) affording the title compound as an orange solid (1.08 g, 68%). <sup>1</sup>H NMR (DMSO-*d*<sub>6</sub>, 300 MHz) δ 2.23 (s, 3H), 4.63 (s, 2H), 6.54 (d, *J* = 10.3 Hz, 1H), 7.32 (m, 5H), 6.78 (s, 1H), 7.98 (d, *J* = 8.7 Hz, 1H), 8.64 (brs, 1H) ppm.

***N*-Benzyl-5-fluoro-2-nitroaniline (3.23c)**

A mixture of 5-fluoro-2-nitroaniline (500 mg, 3.20 mmol) and benzyl bromide (570 μl, 4.80 mmol, 1.2 mol. eq.) in H<sub>2</sub>O (10 ml) was stirred at reflux for 1.5 h. Then, an additional amount of benzyl bromide (0.6 eq, 2.40 mmol) was added and stirring was continued at reflux for another 2 days. After cooling to room temperature, a saturated NaHCO<sub>3</sub> solution was added and the mixture was extracted with EtOAc (3x). The combined organic layers were washed with H<sub>2</sub>O (1x) and dried over Na<sub>2</sub>SO<sub>4</sub>. After removal of drying agent and solvent, the residue was purified by silica gel flash column chromatography (using a mixture of heptane/EtOAc in a ratio of 9:1 as mobile phase) affording the title compound as an orange

solid (420 mg, 53%).  $^1\text{H}$  NMR (DMSO- $d_6$ , 300 MHz)  $\delta$  4.63 (d,  $J$  = 6.1 Hz, 2H), 6.54 (m, 1H), 6.71 (dd,  $J$  = 12.3, 2.6 Hz, 1H), 7.33 (m, 5H), 8.19 (m, 1H), 8.82 (br s, 1H) ppm.

#### ***N*<sup>1</sup>-Benzyl-4-fluoro-2-nitroaniline (3.23d)**

A mixture of 4-fluoro-2-nitroaniline (2 g, 12.81 mmol) and benzyl bromide (2.28 ml, 19.22 mmol, 1.5 mol. eq.) in H<sub>2</sub>O (10 ml) was stirred at reflux for 1.5 h. Then, an additional amount of benzyl bromide (0.6 eq, 2.40 mmol) was added and stirring was continued at reflux for another 2 days. After cooling to room temperature, a saturated NaHCO<sub>3</sub> solution was added and the mixture was extracted with EtOAc (3x). The combined organic layers were washed with H<sub>2</sub>O (1x) and dried over Na<sub>2</sub>SO<sub>4</sub>. After removal of drying agent and solvent, the residue was purified by silica gel flash column chromatography (using a mixture of heptane/EtOAc in a ratio of 9:1 as mobile phase) affording the title compound as an orange solid (2.40 g, 76%).  $^1\text{H}$  NMR (DMSO- $d_6$ , 300 MHz)  $\delta$  4.63 (d,  $J$  = 6.1 Hz, 2H), 6.95 (m, 1H), 7.30 (m, 7H), 7.87 (m, 1H), 8.65 (br s, 1H) ppm.

#### ***N*<sup>1</sup>-Benzyl-4-methylbenzene-1,2-diamine (3.24a)**

To a solution of **3.23a** (420 mg, 1.71 mmol) in methanol (10 ml) was added a slurry of Raney nickel (30 mg) and the mixture was stirred vigorously. The system was flushed with H<sub>2</sub> gas 3 times. The reaction was allowed to stir for 3 hours till the reaction was completely finished. The catalyst was removed by filtration through Celite<sup>®</sup> and the filtrate was concentrated *in vacuo*, yielding the title compound as a colorless oil in quantitative yield which was immediately used in the next reaction.  $^1\text{H}$  NMR (CDCl<sub>3</sub>, 300 MHz):  $\delta$  2.19 (s, 3H), 3.36 (bs, 3H), 4.23 (s, 2H), 6.50-6.58 (m, 3H), 7.22-7.34 (m, 5H) ppm.

#### ***N*<sup>1</sup>-Benzyl-5-methylbenzene-1,2-diamine (3.24b)**

To a solution of **3.23b** (420 mg, 1.71 mmol) in methanol (10 ml) was added a slurry of Raney nickel (30 mg) and the mixture was stirred vigorously. The system was flushed with H<sub>2</sub> gas 3 times. The reaction was allowed to stir for 3 hours till the reaction was completely finished. The catalyst was removed by filtration through Celite<sup>®</sup> and the filtrate was concentrated *in vacuo*, yielding the title compound as a colorless oil in quantitative yield.  $^1\text{H}$  NMR (DMSO- $d_6$ , 300 MHz)  $\delta$  2.04 (s, 3H), 4.26 (s, 4H), 4.99 (s, 1H), 6.21 (d,  $J$  = 7.2 Hz, 2H), 6.45 (d,  $J$  = 7.6 Hz, 1H), 7.32 (m, 6H) ppm.

#### ***N*<sup>1</sup>-Benzyl-5-fluorobenzene-1,2-diamine (3.24c)**

To a solution of **3.23c** (420 mg, 1.71 mmol) in methanol (10 ml) was added a slurry of Raney nickel (30 mg) and the mixture was stirred vigorously. The system was flushed with H<sub>2</sub> gas 3 times. The reaction was allowed to stir for 3 hours till the reaction was completely finished. The catalyst was removed by filtration through Celite<sup>®</sup> and the filtrate was concentrated *in vacuo*, yielding the title compound as a dark red oil in quantitative yield. The product was immediately used in the next reaction due to rapid decomposition after exposure to air.

#### ***N*<sup>1</sup>-Benzyl-4-fluorobenzene-1,2-diamine (3.24d)**

To a solution of **3.23d** (1 g, 4.06 mmol) in methanol (10 ml) was added a slurry of Raney nickel (30 mg) and the mixture was stirred vigorously. The system was flushed with H<sub>2</sub> gas 3 times. The reaction



was allowed to stir for 3 hours till the reaction was completely finished. The catalyst was removed by filtration through Celite® and the filtrate was concentrated *in vacuo*, yielding the title compound as a dark green oil in quantitative yield. The product was immediately used in the next reaction due to rapid decomposition after exposure to air.

### 3.5.1.3. Synthesis of 2-aminobenzimidazole derivatives

#### General procedure

To an appropriate diaminobenzene derivative (1 mol. equiv.) in EtOH (4.5 ml/1 mmol starting material) was added BrCN (1.2 mol. equiv.) and the resulting mixture was stirred at 50 °C till disappearance of starting material (TLC control). Then, volatiles were removed *in vacuo* and the solid residue was redissolved (or resuspended) in H<sub>2</sub>O. The aqueous mixture was extracted with EtOAc (3x). The organic layer was discarded and the pH of the aqueous layer was adjusted to 9–10 (according to universal indicator paper) using a 25% aq. NH<sub>4</sub>OH or 1 M aq. NaOH solution. The aqueous layer was extracted with EtOAc (3x). The combined organic layers were dried over MgSO<sub>4</sub>. The drying agent was filtered off. The filtrate was evaporated *in vacuo* and, if necessary, the crude residue was further purified by silica gel flash column chromatography. The following compounds were made according to this procedure.

#### **5,6-Dibromo-1*H*-benzo[d]imidazol-2-amine (3.17c)**

The title product was synthesized from 4,5-dibromo-1,2-diaminobenzene (100 mg, 0.376 mmol) according to the general procedure. The crude residue was purified by silica gel flash column chromatography (with a gradient starting from 97:3 DCM:MeOH to 9:1 DCM:MeOH as the eluent) yielding the title compound as a white solid (100 mg, 91%). <sup>1</sup>H NMR (DMSO, 300 MHz) δ 6.93 (br s, 2H), 7.46 (s, 2H) ppm.

#### **1-Benzyl-5-methyl-1*H*-benzo[d]imidazol-2-amine (3.25a)**

The title product was synthesized from **3.24a** (500 mg, 2.36 mmol) according to the general procedure affording the title compound as a white solid (294 mg, 52%). <sup>1</sup>H NMR (DMSO-*d*<sub>6</sub>, 300 MHz) δ 2.29 (s, 3H), 5.22 (s, 2H), 6.46 (s, 2H), 6.63 (d, *J* = 7.8 Hz, 1H), 6.92 (d, *J* = 18.3 Hz, 2H), 7.22 (m, 5H) ppm.

#### **1-Benzyl-6-methyl-1*H*-benzo[d]imidazol-2-amine (3.25b)**

The title product was synthesized from **3.24b** (400 mg, 1.88 mmol) according to the general procedure affording the title compound as a white solid (220 mg, 49%). <sup>1</sup>H NMR (DMSO-*d*<sub>6</sub>, 300 MHz) δ 2.27 (s, 3H), 5.22 (s, 2H), 6.40 (s, 2H), 6.74 (d, *J* = 7.9 Hz, 1H), 6.85 (s, 1H), 7.02 (d, *J* = 8.3 Hz, 1H), 7.26 (m, 5H) ppm.

#### **1-Benzyl-6-fluoro-1*H*-benzo[d]imidazol-2-amine (3.25c)**

The title product was synthesized from **3.24c** (370 mg, 1.71 mmol) according to the general procedure affording the title compound as a purple solid (251 mg, 61%). <sup>1</sup>H NMR (DMSO-*d*<sub>6</sub>, 300 MHz) δ 5.25

(s, 2H), 6.57 (s, 2H), 6.73 (m, 1H), 6.97 (dd,  $J = 9.4, 2.4$  Hz, 1H), 7.08 (dd,  $J = 8.5, 4.9$  Hz, 1H), 7.27 (m, 5H) ppm.

#### **1-Benzyl-5-fluoro-1H-benzo[d]imidazol-2-amine (3.25d)**

The title product was synthesized from **3.24d** (870 mg, 1.71 mmol) according to the general procedure affording the title compound as a purple solid (556 mg, mmol, 57%).  $^1\text{H}$  NMR (DMSO- $d_6$ , 300 MHz)  $\delta$  5.25 (s, 2H), 6.95 (m, 3H), 6.90 (m, 1H), 6.98 (m, 1H), 7.26 (m, 5H) ppm.

#### *3.5.1.4. Synthesis of 6(,7)-(di)substituted-imidazo[1,2-a]pyrimidin-5(8H)-ones and 2(,3)-(di)substituted-benzo[4,5]imidazo[1,2-a]pyrimidin-4(10H)-ones*

##### **7,8-Dibromo-3-ethyl-2-isopropylbenzo[4,5]imidazo[1,2-a]pyrimidin-4(10H)-one (3.18c)**

To a solution of **3.17c** (100 mg, 0.343 mmol) in pyridine (2 ml) was added ethyl **3.4c** (1 eq). The reaction mixture was heated to reflux and stirred for 48 hours. After reaction stagnation, the solvent was evaporated and the crude residue was purified by silica gel flash chromatography (using a mixture of heptane and EtOAc in a ratio of 5:1 as eluent) yielding the title compound as a beige solid (31.2 mg, 22%).  $^1\text{H}$  NMR (CDCl<sub>3</sub>, 300 MHz)  $\delta$  1.19 (t,  $J = 7.4$  Hz, 3H), 1.35 (d,  $J = 6.9$  Hz, 6H), 2.68 (q,  $J = 7.4$  Hz, 2H) 3.34 (m,  $J = 6.9$  Hz, 1H), 7.85 (s, 1H), 8.84 (s, 1H) ppm.  $^{13}\text{C}$  NMR (pyridine, 75 MHz)  $\delta$  14.73, 18.37, 21.18, 29.78, 54.90, 61.47, 111.23, 115.14, 118.21, 119.99, 120.59, 137.11, 160.10, 162.36 ppm. HRMS (ESI):  $m/z$  [M+H]<sup>+</sup> calcd for C<sub>15</sub>H<sub>16</sub>N<sub>3</sub>OBr<sub>2</sub>: 411.9656, found: 411.9651.

##### General procedure

To an appropriate 2-aminoimidazole derivative (1 mol. equiv.) in DMF (1–1.5 ml/1 mmol of starting material) was added the appropriate 3-oxoester (1-1.64 mol. equiv.) and the mixture was refluxed for several hours (TLC control). Upon disappearance of the starting materials or no further progress of the reaction, the mixture was cooled to room temperature. If precipitation occurred MeOH or EtOH was added, the solid was filtered off, washed with the indicated solvent and dried under vacuum. In other cases, the volatiles were removed and the crude residue was purified by silica gel column chromatography. The purity of all products was at least 95% according to analytical HPLC. The following compounds were made this way.

##### **2-(tert-Butyl)-3-ethylbenzo[4,5]imidazo[1,2-a]pyrimidin-4(10H)-one (3.9a)**

The title compound was synthesized starting from **3.1** (200 mg, 1.50 mmol) and **3.8a** (1.1 mol. equiv.). Reaction time: 16 h. After removal of the volatiles, the crude product was purified by silica gel flash column chromatography (30% of EtOAc in heptane) affording the title compound as an off-white solid (30.2 mg, 7%).  $^1\text{H}$  NMR (DMSO- $d_6$ , 300 MHz)  $\delta$  1.15 (t,  $J = 7.2$  Hz, 3H), 1.46 (s, 9H), 2.76 (q,  $J = 7.1$  Hz, 2H), 7.29 (ddd,  $J = 8.4, 5.6, 3.1$  Hz, 1H), 7.44 (m, 2H), 8.45 (d,  $J = 8.0$  Hz, 1H), 12.78 (s, 1H) ppm.  $^{13}\text{C}$  NMR (DMSO, 75 MHz)  $\delta$  13.91, 19.89, 30.48, 69.91, 110.80, 113.15, 121.40, 125.50, 126.20, 145.85, 160.54 ppm. HRMS (ESI):  $m/z$  [M+H]<sup>+</sup> calcd for C<sub>16</sub>H<sub>20</sub>N<sub>3</sub>O: 270.1601, found: 270.1595.

**3-Ethyl-2-isobutylbenzo[4,5]imidazo[1,2-*a*]pyrimidin-4(10*H*)-one (3.9b)**

The title compound was synthesized starting from **3.1** (300 mg, 2.25 mmol) and **3.8b** (1.1 mol. equiv). Reaction time: 60 h. After removal of the volatiles, the crude residue was purified by silica gel flash column chromatography (using 50% of EtOAc in heptane as mobile phase) affording an impure mixture of compounds. The mixture was suspended in a minimal amount of MeOH and the precipitate was collected by filtration. Finally, the product was purified by a second round of silica gel flash column chromatography (using a mixture of heptane and EtOAc in a ratio of 7:3 as mobile phase) yielding the title compound as a white solid (79 mg, 13%). <sup>1</sup>H NMR (pyridine, 300 MHz) δ 0.98 (d, *J* = 6.6 Hz, 6H), 1.31 (t, *J* = 7.4 Hz, 3H), 2.29 (sept, *J* = 6.9 Hz, 1H), 2.62 (d, *J* = 7.3 Hz, 2H), 2.80 (q, *J* = 7.3 Hz, 2H), 7.31 (t, *J* = 7.7 Hz, 1H), 7.43 (t, *J* = 7.7 Hz, 1H), 7.62 (d, *J* = 8.0 Hz, 1H), 8.93 (d, *J* = 7.9 Hz, 1H) ppm. <sup>13</sup>C NMR (pyridine, 75 MHz) δ 13.87, 18.68, 22.04, 28.06, 29.40, 41.53, 112.24, 113.06, 115.71, 120.76, 125.22, 136.01, 147.54, 156.38, 160.12 ppm. HRMS (ESI): *m/z* [M+H]<sup>+</sup> calcd for C<sub>16</sub>H<sub>20</sub>N<sub>3</sub>O: 270.1601, found: 270.1606.

**2-Cyclopropyl-3-ethylbenzo[4,5]imidazo[1,2-*a*]pyrimidin-4(10*H*)-one (3.9c)**

The title compound was synthesized starting from **3.1** (146 mg, 1.10 mmol) and **3.8c** (1.1 mol. equiv). Reaction time: 60 h. After removal of the volatiles, the crude product was purified twice by silica gel flash column chromatography (using 30% of EtOAc in heptane as mobile phase) affording the title product as a white solid (34 mg, 12%). <sup>1</sup>H NMR (DMSO-*d*<sub>6</sub>, 300 MHz) δ 1.02 (m, 4H), 1.12 (t, *J* = 7.4 Hz, 3H), 2.17 (m, 1H), 2.72 (q, *J* = 7.4 Hz, 2H), 7.28 (m, 1H), 7.41 (m, 2H), 8.44 (d, *J* = 7.9 Hz, 1H), 12.54 (br s, 1H) ppm. <sup>13</sup>C NMR (pyridine, 75 MHz) δ 10.17, 14.78, 19.55, 30.92, 71.79, 111.73, 114.31, 117.46, 122.46, 126.85, 132.65, 149.85, 160.95, 164.22 ppm. HRMS (ESI): *m/z* [M+H]<sup>+</sup> calcd for C<sub>15</sub>H<sub>16</sub>N<sub>3</sub>O: 254.1288, found: 254.1292.

**3-Ethyl-2-phenylbenzo[4,5]imidazo[1,2-*a*]pyrimidin-4(10*H*)-one (3.9d)**

The title compound was synthesized starting from **3.1** (232 mg, 1.75 mmol) and **3.8d** (1.1 mol. equiv). Reaction time: 60 h. After removal of the volatiles, the crude product was purified by silica gel flash column chromatography (using 30% of EtOAc in heptane as mobile phase) affording an impure mixture of compounds. This mixture was suspended in a mixture of heptane and EtOAc (ratio 7:3) and the precipitate was filtered off. This was followed by a second filtration using MeOH (10 ml), yielding the title compound as a white solid (35 mg, 7%). <sup>1</sup>H NMR (DMSO-*d*<sub>6</sub>, 300 MHz) δ 1.09 (t, *J* = 7.1 Hz, 3H), 2.45 (q, *J* = 6.9 Hz, 2H), 7.34 (m, 1H), 7.51 (m, 7H), 8.51 (d, *J* = 8.1 Hz, 1H) ppm. <sup>13</sup>C NMR (pyridine, 75 MHz) δ 14.12, 19.69, 99.66, 115.69, 121.52, 126.18, 128.27, 128.33, 128.69 ppm. HRMS (ESI): *m/z* [M+H]<sup>+</sup> calcd for C<sub>18</sub>H<sub>16</sub>N<sub>3</sub>O: 290.1288, found: 290.1292.

**3-Ethyl-2-(thiophen-2-yl)benzo[4,5]imidazo[1,2-*a*]pyrimidin-4(10*H*)-one (3.9e)**

The title compound was synthesized starting from **3.1** (300 mg, 2.25 mmol) and **3.8e** (1.1 mol. equiv). Reaction time: 60 h. After removal of the volatiles, the crude residue was purified by silica gel flash column chromatography (using 50% of EtOAc in heptane as mobile phase) affording an impure mixture of compounds. The mixture was suspended in a minimal amount of MeOH and the precipitate was

collected by filtration. Finally, the product was purified by a second round of silica gel flash column chromatography (using a mixture of heptane and EtOAc in a ratio of 7:3 as mobile phase) yielding the title compound as a white solid (79 mg, 13%). <sup>1</sup>H NMR (DMSO-*d*<sub>6</sub>, 300 MHz) δ 1.25 (t, *J* = 7.5 Hz, 3H), 2.85 (t, *J* = 7.5 Hz, 2H), 7.24 (m, 1H), 7.33 (t, *J* = 7.5 Hz, 1H), 7.45 (m, 2H), 7.60 (d, *J* = 3.3 Hz, 1H), 7.78 (d, *J* = 5.2 Hz, 1H), 8.48 (d, *J* = 7.9 Hz, 1H), 12.88 (br s, 1H) ppm. <sup>13</sup>C NMR (pyridine, 75 MHz) δ 13.46, 19.26, 110.82, 112.04, 115.69, 121.74, 125.80, 126.35, 128.25, 128.32, 129.51, 146.88, 160.19 ppm. HRMS (ESI): *m/z* [M+H]<sup>+</sup> calcd for C<sub>16</sub>H<sub>14</sub>N<sub>3</sub>OS: 296.0852, found: 296.0856.

#### **10-Benzyl-3-ethyl-2-isopropyl-7-methylbenzo[4,5]imidazo[1,2-*a*]pyrimidin-4(10*H*)-one (3.26a)**

The title compound was synthesized starting from **3.25a** (200 mg, 0.842 mmol) and **3.4c** (1.1 mol. equiv). Reaction time: 16 h. After removal of the volatiles, the crude residue was purified by silica gel flash column chromatography (using 10% of EtOAc in heptane as mobile phase) affording the title product as an off-white solid (96 mg, 32%). <sup>1</sup>H NMR (DMSO-*d*<sub>6</sub>, 300 MHz): δ 1.08 (t, *J* = 7.4 Hz, 3H), 1.24 (d, *J* = 6.6 Hz, 6H), 2.62 (m, 2H), 3.23 (m, 1H), 5.46 (s, 2H), 7.17 (t, *J* = 9.1 Hz, 1H), 7.31 (m, 3H), 7.50 (m, 2H), 7.69 (d, *J* = 9.3 Hz, 1H), 8.45 (m, 1H) ppm.

#### **10-Benzyl-3-ethyl-2-isopropyl-8-methylbenzo[4,5]imidazo[1,2-*a*]pyrimidin-4(10*H*)-one (3.26b)**

The title compound was synthesized starting from **3.25b** (260 mg, 1.10 mmol) and ethyl **3.4c** (1.1 mol. equiv). Reaction time: 16 h. After removal of the volatiles, the crude product was purified by silica gel flash chromatography (using 10% of EtOAc in heptane as mobile phase) affording the title compound as an off-white solid (183 mg, 46%). <sup>1</sup>H NMR (CDCl<sub>3</sub>, 300 MHz): δ 1.19 (t, *J* = 7.5 Hz, 3H), 1.29 (d, *J* = 6.6 Hz, 6H), 2.45 (s, 3H), 2.73 (q, *J* = 7.5 Hz, 2H), 3.25 (m, 1H), 5.39 (s, 2H), 7.02-7.44 (m, 7H), 8.49 (d, *J* = 8.1 Hz, 1H) ppm.

#### **10-Benzyl-3-ethyl-2-isopropyl-8-fluorobenzo[4,5]imidazo[1,2-*a*]pyrimidin-4(10*H*)-one (3.26c)**

The title compound was synthesized starting from **3.25c** (250 mg, 1.04 mmol) and **3.4c** (1.1 mol. equiv). Reaction time: 16 h. After removal of the volatiles, the crude product was purified by silica gel flash chromatography (using 10% of EtOAc in heptane as mobile phase) affording the title compound as a brown solid (103 mg, 27%). <sup>1</sup>H NMR (CDCl<sub>3</sub>, 300 MHz): δ 1.19 (t, *J* = 7.5 Hz, 3H), 1.29 (d, *J* = 6.6 Hz, 6H), 2.45 (s, 3H), 2.73 (q, *J* = 7.5 Hz, 2H), 3.25 (m, 1H), 5.39 (s, 2H), 7.02-7.44 (m, 7H), 8.49 (d, *J* = 8.1 Hz, 1H) ppm.

#### **10-Benzyl-3-ethyl-2-isopropyl-7-fluorobenzo[4,5]imidazo[1,2-*a*]pyrimidin-4(10*H*)-one (3.26d)**

The title compound was synthesized starting from **3.25d** (150 mg, 0.622 mmol) and **3.4c** (1.2 mol. equiv). Reaction time: 72 h. During the reaction no progress of product formation was observed and only starting material was recovered and a small amount of imine was present.

#### **3-Ethyl-2-isopropyl-7-methylbenzo[4,5]imidazo[1,2-*a*]pyrimidin-4(10*H*)-one (3.27a)**

To a solution of **3.26a** (50 mg, 0.139 mmol) in a mixture of DCM and MeOH (1:1, 5 ml) was added Pd/C catalyst (10 mol%). The reaction was flushed with H<sub>2</sub> gas and stirred for 5 hours. After reaction stagnation, the mixture was filtered through Celite® and the solvent was evaporated. The crude residue

was purified by silica gel flash column chromatography (using heptane/EtOAc in a ratio of 7:3 as mobile phase) yielding the title compound as a white solid (22 mg, 58%). <sup>1</sup>H NMR (DMSO-*d*<sub>6</sub>, 300 MHz) δ 1.07 (t, *J* = 7.4 Hz, 3H), 1.22 (d, *J* = 6.7 Hz, 6H), 2.45 (s, 3H), 2.60 (m, 2H), 3.21 (m, 1H), 7.28 (m, 2H), 8.28 (s, 1H), 12.57 (br s, 1H) ppm. <sup>13</sup>C NMR (DMSO, 75 MHz) δ 14.68, 17.89, 21.28, 21.65, 30.68, 110.95, 115.72, 126.25, 126.85, 130.61, 147.77, 159.78 ppm. HRMS (ESI): *m/z* [M+H]<sup>+</sup> calcd for C<sub>16</sub>H<sub>20</sub>N<sub>3</sub>O: 270.1601, found: 270.1606.

### 3-Ethyl-2-isopropyl-8-methylbenzo[4,5]imidazo[1,2-*a*]pyrimidin-4(10*H*)-one (3.27b)

To a solution of **3.26b** (183 mg, 0.509 mmol) in a mixture of DCM and MeOH (1:1, 5 ml) was added Pd/C catalyst (10 mol%). The reaction was flushed with H<sub>2</sub> gas and stirred for 5 hours. After reaction stagnation, the mixture was filtered through Celite® and the solvent was evaporated. The crude residue was purified by silica gel flash column chromatography (using a mixture of heptane and EtOAc in a ratio of 7:3 as mobile phase) yielding the title compound as a white solid (74 mg, 54%). <sup>1</sup>H NMR (DMSO-*d*<sub>6</sub>, 300 MHz) δ 1.07 (t, *J* = 7.0 Hz, 3H), 1.21 (d, *J* = 6.2 Hz, 6H), 2.44 (s, 3H), 2.57 (q, *J* = 6.9 Hz, 2H), 3.19 (m, 1H), 7.09 (d, *J* = 8.2 Hz, 1H) 7.21 (s, 1H), 8.29 (d, *J* = 8.1 Hz, 1H), 12.53 (br s, 1H) ppm. <sup>13</sup>C NMR (DMSO, 75 MHz) δ 14.68, 17.87, 21.44, 21.69, 30.70, 111.26, 115.20, 122.31, 135.71, 147.75, 159.61 ppm. HRMS (ESI): *m/z* [M+H]<sup>+</sup> calcd for C<sub>16</sub>H<sub>20</sub>N<sub>3</sub>O: 270.1601, found: 270.1592.

### 3-Ethyl-2-isopropyl-8-fluorobenzo[4,5]imidazo[1,2-*a*]pyrimidin-4(10*H*)-one (3.27c)

To a solution of **3.26c** (103 mg, 0.283 mmol) in a mixture of DCM and MeOH (1:1, 5 ml) was added Pd/C catalyst (10 mol%). The reaction was flushed with H<sub>2</sub> gas and stirred for 5 hours. After reaction stagnation, the mixture was filtered through Celite® and the solvent was evaporated. The crude residue was purified by silica gel flash column chromatography (using a mixture of heptane and EtOAc in a ratio of 7:3 as mobile phase) yielding the title compound as a white solid (31 mg, 40%). <sup>1</sup>H NMR (pyridine, 300 MHz) δ 1.27 (t, *J* = 7.4 Hz, 3H), 1.35 (d, *J* = 6.7 Hz, 6H), 2.82 (q, *J* = 7.3 Hz, 2H), 3.20 (m, 2H), 7.09 (m, 1H), 7.38 (dd, *J* = 9.0, 2.3 Hz, 1H), 8.81 (dd, *J* = 8.8, 5.1 Hz, 1H), 8.29 (d, *J* = 8.1 Hz, 1H) ppm. <sup>13</sup>C NMR (DMSO, 75 MHz) δ 14.68, 17.87, 21.44, 21.69, 30.70, 111.26, 115.20, 122.31, 135.71, 147.75, 159.61 ppm. HRMS (ESI): *m/z* [M+H]<sup>+</sup> calcd for C<sub>15</sub>H<sub>17</sub>N<sub>3</sub>OF: 274.1350, found: 274.1352.

## 3.5.2. β-arrestin assay

CHO cells stably expressing MRGPRX2 were seeded in a volume of 90 μL into a 96-well plate and incubated at a density of 20,000 cells/well in Opti-MEM™ for 24 h at 37 °C. After the incubation, test compounds were diluted in PBS buffer containing 10% DMSO and added to the cells in a volume of 10 μL, followed by incubation for 90 min at 37 °C. For determination of baseline luminescence, PBS buffer (containing 10% DMSO) in the absence of test compound was used. During the incubation period, the detection reagent was prepared. After the addition of 50 μL/well detection reagent to the cells, the plate was incubated for an additional 60 min at room temperature. Finally, luminescence was determined in a luminometer (TopCount NXT, Packard/Perkin-Elmer). For the determination of

antagonistic properties of tested compounds the assay was performed as described for agonists except that the test compounds were added to the cells in a volume of 5  $\mu\text{L}$ /well 60 min prior to addition of the agonist (1000 nM CST-14 final concentration, corresponding to  $\text{EC}_{80}$ , for MRGPRX2). Data were obtained from three independent experiments performed in duplicate. Data were analyzed using Graph Pad Prism, version 6.02 (San Diego, CA, U.S.A.).

### **3.5.3. General safety aspects**

In context of health and safety, documents provided by the lab of medicinal chemistry and the HSE department of the KU Leuven were signed: Binding rules – Laboratory of medicinal chemistry. Based on the European Regulation (EC) No. 1272/2008) on classification, labeling and packaging of chemicals and mixtures, chemicals are classified according to their hazardous properties to humans and the environment into 5 categories (E4+, E4, E3, E2 and E1). Chemical operations were carried out in compliance with these documents and risk analyses were created according to the template provided by the HSE department and the information retrieved from the respective material safety data sheet (MSDS) for every used chemical and solvent. Additionally, personal safety measures were enforced at all times: wearing lab coats, safety goggles, long trousers and closed shoes. Furthermore, special precautions like wearing gloves or a dust mask were taken in case of handling especially hazardous reagents or devices to guarantee optimal safety.

### 3.6. References

- (1) Manorak, W.; Idahosa, C.; Gupta, K.; Roy, S., et al., Upregulation of Mas-related G Protein coupled receptor X2 in asthmatic lung mast cells and its activation by the novel neuropeptide hemokinin-1. *Respir. Res.* **2018**, *19* (1), 1-5.
- (2) Okayama, Y.; Saito, H.; Ra, C., Targeting Human Mast Cells Expressing G-Protein-Coupled Receptors in Allergic Diseases. *Allergol. Int.* **2008**, *57* (3), 197-203.
- (3) Méndez-Enríquez, E.; Hallgren, J., Mast Cells and Their Progenitors in Allergic Asthma. *Front. Immunol.* **2019**, *10*.
- (4) Solinski, H. J.; Gudermann, T.; Breit, A., Pharmacology and Signaling of MAS-Related G Protein-Coupled Receptors. *Pharmacol. Rev.* **2014**, *66* (3), 570.
- (5) Metcalfe, D. D.; Baram, D.; Mekori, Y. A., Mast cells. *Physiol. Rev.* **1997**, *77* (4), 1033-1079.
- (6) Bader, M.; Alenina, N.; Andrade-Navarro, M. A.; Santos, R. A., Mas and Its Related G Protein-Coupled Receptors, Mrgprs. *Pharmacol. Rev.* **2014**, *66* (4), 1080-1105.
- (7) Robas, N.; Mead, E.; Fidock, M., MrgX2 Is a High Potency Cortistatin Receptor Expressed in Dorsal Root Ganglion. *J. Biol. Chem.* **2003**, *278* (45), 44400-44404.
- (8) McNeil, B. D.; Pundir, P.; Meeker, S.; Han, L., et al., Identification of a mast-cell-specific receptor crucial for pseudo-allergic drug reactions. *Nature* **2014**, *519*, 237.
- (9) Lansu, K.; Karpiak, J.; Liu, J.; Huang, X.-P., et al., In silico design of novel probes for the atypical opioid receptor MRGPRX2. *Nat. Chem. Biol.* **2017**, *13*, 529-536.
- (10) Malik, L.; Kelly, N. M.; Ma, J.-N.; Currier, E. A., et al., Discovery of non-peptidergic MrgX1 and MrgX2 receptor agonists and exploration of an initial SAR using solid-phase synthesis. *Bioorg. Med. Chem. Lett.* **2009**, *19* (6), 1729-1732.
- (11) Ogasawara, H.; Furuno, M.; Edamura, K.; Noguchi, M., Novel MRGPRX2 antagonists inhibit IgE-independent activation of human umbilical cord blood-derived mast cells. *J. Leukocyte Biol.* **2019**, 1-9.
- (12) Sirko, S. M.; Gorobets, N. Y.; Musatov, V. I.; Desenko, S. M., Generation of 500-member library of 10-alkyl-2-R(1),3-R(2)-4,10-dihydrobenzo[4,5]imidazo[1,2- $\alpha$ ]pyrimidin-4-ones. *Molecules* **2009**, *14* (12), 5223-5234.
- (13) Huang, L.; Wulff, W. D., Catalytic Asymmetric Synthesis of Trisubstituted Aziridines. *J. Am. Chem. Soc.* **2011**, *133* (23), 8892-8895.
- (14) Burke, E. D. *Stereoselective Carbon-Carbon Bond Forming Reactions*. McGill University, Montreal, 2004.
- (15) Ogura, H.; Kawano, M.; Itoh, T., Studies on Heterocyclic Compounds. XIII. Reaction of 2-Amino-benzazoles with Acetylenic Compounds. *Chem. Pharm. Bull.* **1973**, *21* (9), 2019-2025.
- (16) Olson, K. R.; Eglen, R. M.,  $\beta$  Galactosidase Complementation: A Cell-Based Luminescent Assay Platform for Drug Discovery. *ASSAY and Drug Development Technologies* **2007**, *5* (1), 137-144.





## Chapter 4: Synthesis and structure activity relationship studies of cluster chemokine receptor 8 agonists

### 4.1. Introduction

Chemokine receptors are a subclass within the superfamily of GPCRs that have a chemotactic role in both the innate and adaptive immune system and display a different expression level depending on the differentiation and activation level of the cells.<sup>1</sup> Each chemokine receptor can be activated by more than one chemokine and likewise each chemokine can activate more than one receptor.<sup>2</sup> Higher concentrations of chemokines attract CCR8 expressing cells, explaining their chemotactic role. Chemokine receptors are classified according to their first discovered ligand into four groups (CCR, CXCR, XCR and CX3CR) and contain 22 members.<sup>3</sup> This chapter focuses on CCR8, a member of the CC group with the unique property of being the sole target of chemokine CCL1.<sup>4</sup> CCR8 is mainly expressed on tumor-infiltrating T<sub>reg</sub> cells which are potent in restraining the effector T cell responses.<sup>5</sup> Furthermore, it has been demonstrated that the presence of CCR8 in the tumor environment correlates with a reduced survival of cancer patients, whereas T<sub>reg</sub> cell depletion increases the chances of survival.<sup>4,6</sup> Therefore, specific modulation of CCR8 by small molecule antagonists have potential in the treatment of various cancers.<sup>7</sup> Recently, it was reported that CCR8, also plays a pivotal role in the suppression of autoimmunity. In a mouse model of experimental autoimmune encephalomyelitis (which is a model for multiple sclerosis), administration of CCL1 and the resulting activation of CCR8 resulted in an effective suppression of the disease, confirming the immune regulating role of CCR8.<sup>5</sup> Therefore, CCR8 agonism is a promising treatment option for autoimmune diseases like multiple sclerosis, rheumatoid arthritis and Crohn's disease.<sup>8</sup> Several CCR8 agonists have been disclosed in literature<sup>2,9-11</sup> from which two (**1.9** and **4.1**) were selected as lead structure (**Figure 4.1**). To evaluate the SAR of the 3-phenoxybenzyl analogues, the molecules were subdivided into three structural parts (phenoxybenzyl, central heterocyclic ring and terminal substituent) to systematically introduce structural variation.

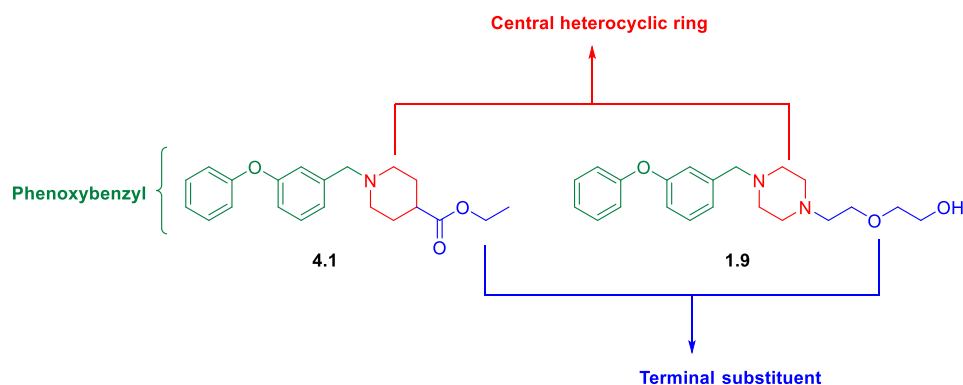
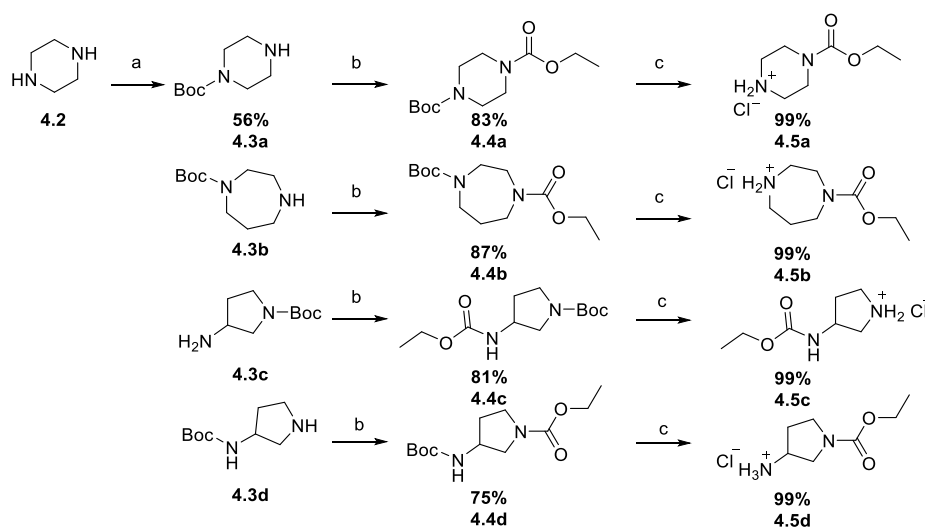


**Figure 4.1.** Subdivision of the phenoxybenzyl scaffold into three structural parts

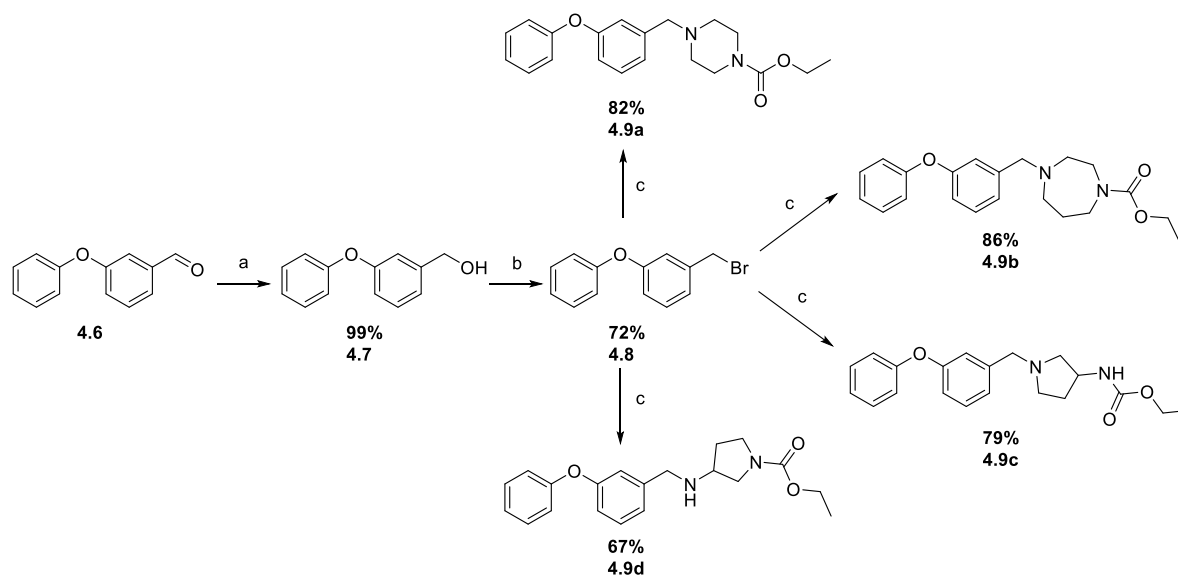
## 4.2. Synthesis of phenoxybenzyl analogues as CCR8 agonists

To gain access to potential CCR8 agonists with varying ring sizes, piperazine **4.2** was treated with *tert*-butoxycarbonyl (Boc) anhydride followed by reaction with ethyl chloroformate. Other Boc protected diamines (**4.3b-d**) were obtained commercially and were also treated with ethyl chloroformate to yield the Boc protected intermediates **4.4b-d**. The Boc protected piperazine **4.4a** was synthesized by treating piperazine (**4.2**) with Boc anhydride followed by treatment with ethyl chloroformate.<sup>12</sup> Acidic cleavage of the Boc protecting group using a 3M HCl solution in cyclopentylmethylether (CPME) yielded the desired amines **4.5a-d** as HCl salts in quantitative yield (**Scheme 4.1**).



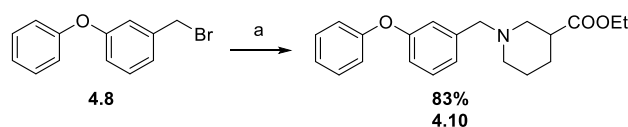
**Scheme 4.1.** *Reagents and conditions.* a)  $\text{Boc}_2\text{O}$ , NaOH, *i*-PrOH,  $\text{H}_2\text{O}$ , rt, overnight; b) ethyl chloroformate,  $\text{Et}_3\text{N}$ , DCM,  $0^\circ\text{C}$  to rt, 1.5h; c) 3M HCl in CPME, rt, overnight.

Direct coupling of the HCl salts (**4.5a-d**) with commercially available 3-phenoxybenzaldehyde **4.6** through reductive amination<sup>13</sup> using triacetoxyborohydride was unreproducible in our hands. Therefore, an alternative synthesis was devised. Reduction of 3-phenoxybenzaldehyde **4.6** with sodium borohydride gave access to 3-phenoxybenzylalcohol **4.7**. Treatment of **4.7** with phosphorus tribromide furnished key intermediate **4.8**.<sup>14</sup> Nucleophilic substitution of bromine **4.8** with amines **4.5a-d** yielded a small library (**4.9a-d**) of ring modified CCR8 agonists (**Scheme 4.2**).



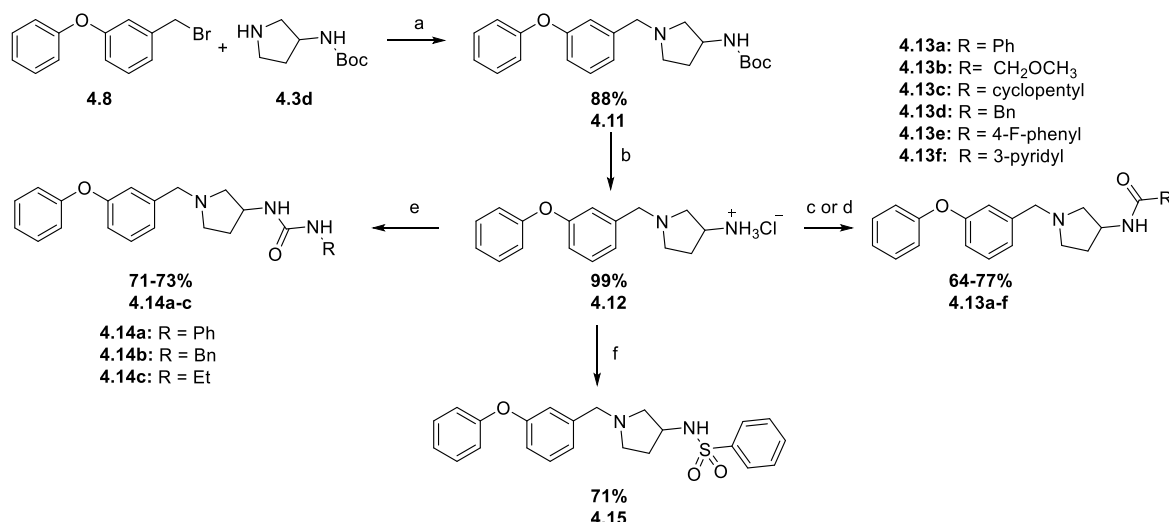
**Scheme 4.2.** *Reagents and conditions.* a) NaBH<sub>4</sub>, MeOH, 0°C to rt, 2h; b) PBr<sub>3</sub>, DCM, 0°C to rt, overnight; c) **4.5a-d**, K<sub>2</sub>CO<sub>3</sub>, DMF, rt, overnight.

The regioisomer of compound **4.1** was prepared by treating key intermediate **4.8** with ethyl piperidine-3-carboxylate furnishing congener **4.10** (Scheme 4.3).



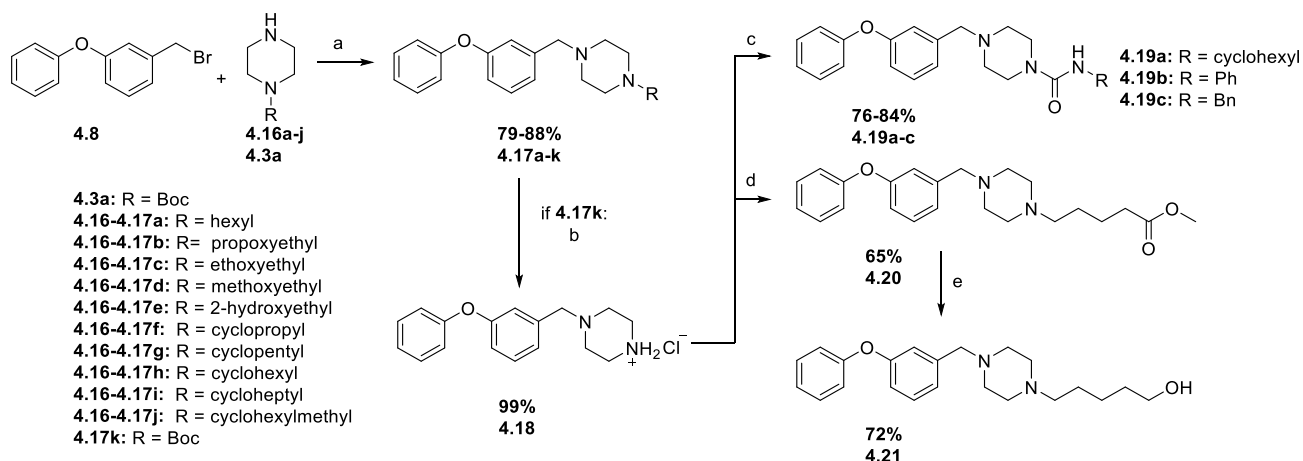
**Scheme 4.3.** *Reagents and conditions.* a) ethyl piperidine-3-carboxylate, K<sub>2</sub>CO<sub>3</sub>, DMF, rt, overnight.

A series of pyrrolidine congeners with structural variation of the terminal moiety was prepared (Scheme 4.4). Alkylation of 3-Boc-aminopyrrolidine (**4.3d**) with 3-phenoxybenzyl bromide **4.8** yielded compound **4.11**. Deprotection of the nitrogen, followed by treatment of **4.12** with acid chlorides or carboxylic acids furnished 3-(*N*-acyl)-aminopyrrolidines (**4.13a-f**).<sup>2</sup> In a similar manner, intermediate **4.12** was reacted with isocyanates<sup>15</sup> and phenylsulfonyl chloride<sup>16</sup> affording urea (**4.14a-c**) and a sulfonamide (**4.15**), respectively.



**Scheme 4.4. Reagents and conditions.** a) K<sub>2</sub>CO<sub>3</sub>, DMF, rt, overnight; b) 3M HCl in CPME, 0°C to rt, overnight; c) **4.13a-d**, RCOCl, Et<sub>3</sub>N, DCM, rt, overnight; d) **4.13a-d**, RCOOH, PyBOP, Et<sub>3</sub>N, DMF, rt, overnight; e) RNCO, Et<sub>3</sub>N, DCM, 0°C to rt, overnight; f) PhSO<sub>2</sub>Cl, Et<sub>3</sub>N, DCM, rt, overnight.

Reaction of key intermediate **4.8** with a myriad of commercially available piperazines **4.16a-j** yielded a small library with structural variety on the piperazine ring (**4.17a-j**). Treatment of key intermediate **4.8** with Boc-piperazine **4.3a** afforded **4.17k** which after acidic deprotection gave piperazine **4.18** as its hydrochloride salt. Additionally, reaction of **4.18** with three different isocyanates<sup>15</sup> furnished the urea derivatives (**4.19a-c**). To eliminate the central oxygen in the chain part, the piperazine hydrochloride salt **4.18** was treated<sup>17</sup> with methyl 5-bromovalerate **4.20** followed by reduction of the ester moiety with diisobutylaluminiumhydride (DIBAL) yielding the desired compound **4.21** (Scheme 4.5).



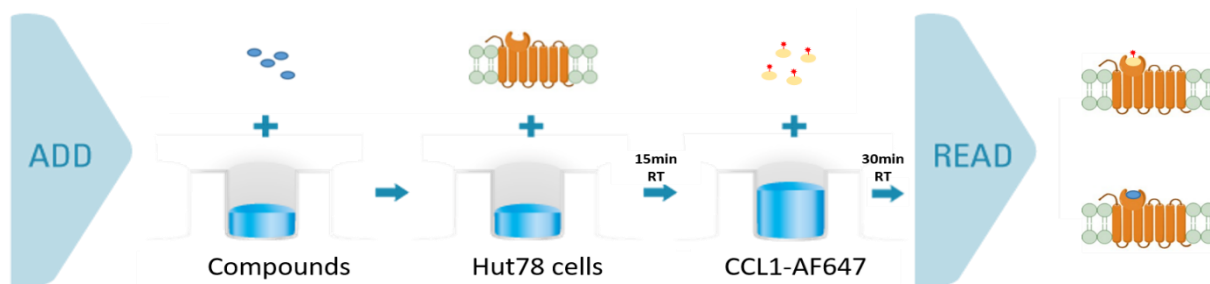
**Scheme 4.5. Reagents and conditions.** a) K<sub>2</sub>CO<sub>3</sub>, DMF, rt, overnight; b) 3M HCl in CPME, rt, overnight; c) RNCO, Et<sub>3</sub>N, DCM, 0°C to rt, overnight; d) methyl 5-bromovalerate, Et<sub>3</sub>N, EtOH, 60°C, overnight; e) DIBAL, THF, -78°C to rt, overnight.

## 4.3. Biological evaluation

### 4.3.1. Principle of the assays

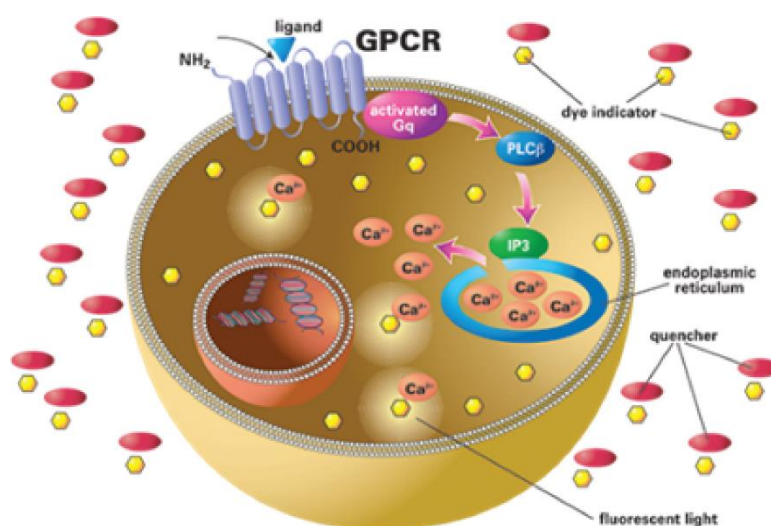
All compounds were evaluated for CCR8 agonism using a combination of two assays: a flow cytometry-based competition binding assay<sup>18</sup> and a Fluorescence Imaging Plate Reader (FLIPR™) calcium mobilization assay<sup>19</sup>. In the binding assay, HuT78 cells, that endogenously express CCR8, are exposed

to the synthesized compounds 15 minutes prior to the addition of fluorescent ligand (CCL1 fused to Alexa Fluor™ 647). The fluorescent signal arising from CCL1<sup>AF647</sup> is reduced when the phenoxybenzyl derivative disrupts the interaction between CCR8 and CCL1<sup>AF647</sup> and allows to determine IC<sub>50</sub> values (i.e. the concentration of compound that reduces the fluorescent binding signal by 50%). This assay however does not discriminate between agonists and antagonists (Figure 4.2).



**Figure 4.2.** Binding assay (Origin of figure: Schoofs et al., 2018)

Therefore, the FLIPR™ assay was used to determine the calcium mobilization after exposure of CCR8 to the compounds. In this functional assay, U87 human glioblastoma cells, stably expressing human CCR8, are charged with a calcium sensitive fluorescent dye (Calcium 6) before addition of the compounds. A dye quencher is also added to remove extracellular calcium bonding to the dye. If the compounds possess agonistic properties, calcium will be released within the cytoplasm of the cells and will bind to the dye. The resulting fluorescence is then measured using the FLIPR Tetra™ device. After comparison with the endogenous full agonist CCL1, an EC<sub>50</sub> value was calculated (Figure 4.3).

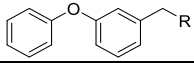
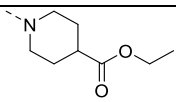
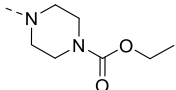
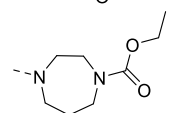
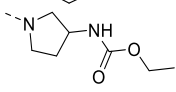
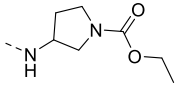
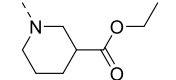


**Figure 4.3.** FLIPR™ assay (Origin of figure: Claes et al. 2018).

### 4.3.2. Structure-activity relationship study

In a first round of SAR, the importance of the central heterocycle of reference compound **4.1** was evaluated. Therefore, the phenoxybenzyl and the terminal ethyl ester moieties were kept intact and a number of five- (compounds **4.9c-d**), six- (compounds **4.9a** and **4.10**) and seven- (compound **4.9b**)

membered ring analogues were prepared. Compound **4.1** possessed moderate CCR8 activity in the micromolar range. Only the pyrrolidine congener **4.9a** displayed equipotent activity with **4.1**, whereas all other analogues were much less active in the CCR8 binding and calcium mobilization assay (**Table 4.1**).

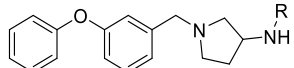
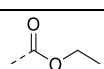
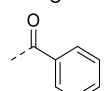
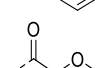
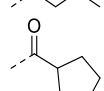
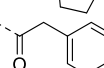
			
Compound	R	IC <sub>50</sub> ±SEM (μM) <sup>a</sup>	EC <sub>50</sub> ±SEM (μM) <sup>b</sup>
<b>4.1</b>		7.13 ± 2.47	4.09 ± 2.07
<b>4.9a</b>		66.14 ± 0.13	18.09 ± 4.14
<b>4.9b</b>		47.56 ± 3.89	8.74 ± 1.70
<b>4.9c</b>		12.09 ± 2.85	6.03 ± 2.31
<b>4.9d</b>		53.03	21.03
<b>4.10</b>		70.33 ± 3.11	25.98 ± 2.77

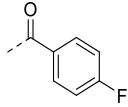
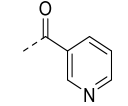
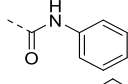
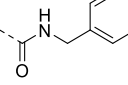
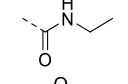
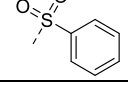
<sup>a</sup>Half maximal inhibitory concentration as obtained in the binding assay by loss of fluorescent signal

<sup>b</sup>Half maximal effective concentration as obtained in the FLIPR assay: concentration needed to release 50% of the calcium stores

**Table 4.1.** SAR of the central ring moiety

Given the promising data of the pyrrolidine congener **4.9c**, the SAR of this compound was studied further by introduction of structural variation in the terminal part. This included a series of amides (**4.13a-f**), urea (**4.14a-c**) and a sulfonamide (**4.15**). Unfortunately, all congeners within this series are much less active in the binding, as well as in the calcium mobilization assay, when compared to compound **4.9c** (**Table 4.2**).

			
Compound	R	IC <sub>50</sub> ±SEM (μM) <sup>a</sup>	EC <sub>50</sub> ±SEM (μM) <sup>b</sup>
<b>4.9c</b>		12.09 ± 2.85	6.03 ± 2.31
<b>4.13a</b>		20.06 ± 0.93	6.70 ± 2.12
<b>4.13b</b>		47.06 ± 1.27	ND
<b>4.13c</b>		47.15 ± 0.81	13.12 ± 6.41
<b>4.13d</b>		38.70±12.75	10.81 ± 5.34

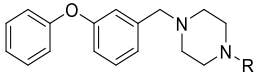
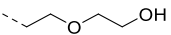
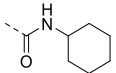
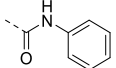
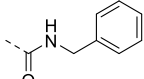
<b>4.13e</b>		$42.83 \pm 8.35$	28.65
<b>4.13f</b>		$66.70 \pm 6.40$	$8.78 \pm 5.92$
<b>4.14a</b>		$79.81 \pm 8.87$	ND
<b>4.14b</b>		$59.38 \pm 5.45$	9.60
<b>4.14c</b>		$54.78 \pm 24.42$	$5.09 \pm 2.60$
<b>4.15</b>		$23.38 \pm 0.24$	17.85

<sup>a</sup>Half maximal inhibitory concentration as obtained in the binding assay by loss of fluorescent signal

<sup>b</sup>Half maximal effective concentration as obtained in the FLIPR assay: concentration needed to release 50% of the calcium stores

**Table 4.2.** SAR of the terminal substituent of **4.9c**

As it became evident that structural modifications of pyrrolidine congener **4.9c** essentially afforded less active compounds, the focus shifted towards another series. Piperazine containing phenoxybenzyl analogues are known as CCR8 agonists. Examples include compound **1.9** (also known as ZK 756326) with an ethoxyethanol side chain and a series of phenoxybenzyl analogues with a piperazine-urea side chain.<sup>10</sup> Compound **1.9** is commercially available and the CCR8 binding and calcium mobilization data were confirmed ( $IC_{50}$  of 1.80  $\mu$ M and  $EC_{50}$  of 1.11  $\mu$ M, respectively). Piperazine urea **4.19a-b** are both reported to display low nM CCR8 agonism when evaluated in an inositol phosphate turnover assay<sup>10</sup>. Therefore, both compounds were resynthesized and evaluated along with one additional compound (**4.19b**). In our hands, the cyclohexyl derivative **4.19a** was the most active within the urea sequence, with  $IC_{50}$  and  $EC_{50}$  values in the 5  $\mu$ M range. However, this was almost 1000-fold less active than the reported values. The introduction of an aromatic residue (compounds **4.19b-c**) led to a decreased activity (**Table 4.3**).

			
Compound	R	IC <sub>50</sub> ±SEM (μM) <sup>a</sup>	EC <sub>50</sub> ±SEM (μM) <sup>b</sup>
<b>1.9</b>		1.80 ± 2.93	1.11 ± 0.51
<b>4.19a</b>		5.47 ± 1.31	7.02 ± 0.59
<b>4.19b</b>		35.68 ± 3.33	17.31
<b>4.19c</b>		22.96 ± 2.74	15.58

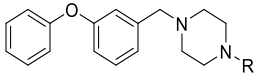
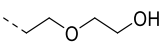
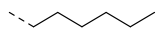
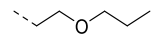
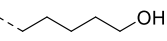
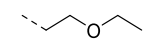
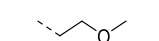
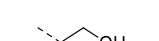
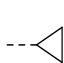
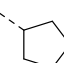
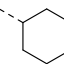
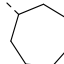
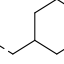
<sup>a</sup>Half maximal inhibitory concentration as obtained in the binding assay by loss of fluorescent signal

<sup>b</sup>Half maximal effective concentration as obtained in the FLIPR assay: concentration needed to release 50% of the calcium stores

**Table 4.3.** SAR of 1-(3-phenoxybenzyl)piperazine urea analogues

As, in our hands, the ethoxyethanol side chain of compound **1.9** turned out to be optimal within this piperazine series, different (cyclo)aliphatic chains were attached to 1-(3-phenoxybenzyl)piperazine (**Table 4.4**). The length of the chain was first fixed as a six atom linker, giving rise to congeners **4.17a**, **4.17b** and **4.21**. The complete removal of all oxygens furnished the *n*-hexyl analogue **4.17a**, that was completely devoid of activity, suggesting the need for a hydrogen bond acceptor or donor. The reintroduction of a single oxygen in compounds **4.17b** and **4.21** allowed to gain back CCR8 affinity and agonism with a slight preference for the presence of the ether oxygen (**4.17b**). Furthermore, the chain length was shortened from a 6 atom to a 3, 4 or 5-atom linker (compounds **4.17c**, **4.17d** and **4.17e**, respectively). The ethoxyethyl (**4.17c**) and methoxyethyl (**4.17d**) derivatives have similar activity as the reference compound **1.17**. On the other hand, the ethanol congener **4.17e** is somewhat less potent, confirming the need for an ether oxygen. In a last series of compounds, several cycloaliphatic moieties, ranging from cyclopropyl to cycloheptyl (**4.17f-j**), were inserted onto the piperazine ring. A small cyclopropyl ring (**4.17f**) is two to three-fold more active when compared to the larger rings (**4.17g-i**). The insertion of a methylene spacer between the piperazine and the cyclohexyl ring (**4.17j**) resulted in a 2-fold drop in activity.



			
Compound	R	IC <sub>50</sub> ±SEM (μM) <sup>a</sup>	EC <sub>50</sub> ±SEM (μM) <sup>b</sup>
<b>1.9</b>		1.80 ± 2.93	1.11 ± 0.51
<b>4.17a</b>		32.93 ± 3.95	>100
<b>4.17b</b>		5.12 ± 1.66	4.35 ± 1.08
<b>4.21</b>		5.77 ± 0.18	2.18
<b>4.17c</b>		3.08 ± 0.94	1.87 ± 0.09
<b>4.17d</b>		2.33 ± 0.95	3.83 ± 1.33
<b>4.17e</b>		5.79 ± 1.94	7.70 ± 0.53
<b>4.17f</b>		2.54 ± 0.46	2.91 ± 0.30
<b>4.17g</b>		6.67 ± 0.27	4.65 ± 1.45
<b>4.17h</b>		9.00 ± 2.79	13.58 ± 1.71
<b>4.17i</b>		5.90 ± 0.83	4.75 ± 1.44
<b>4.17j</b>		16.55 ± 2.72	5.68 ± 3.52

<sup>a</sup>Half maximal inhibitory concentration as obtained in the binding assay by loss of fluorescent signal

<sup>b</sup>Half maximal effective concentration in the FLIPR assay: concentration needed to release 50% of the calcium stores

**Table 4.4.** SAR of the terminal substituent of **1.9**

## 4.4. Conclusion

CCR8 agonism holds promise as strategy for the treatment of autoimmune disorders. This chapter focused on the expansion of the SAR of previously reported phenoxybenzyl analogues as CCR8 agonists. A first step in the SAR exploration dealt with variation of the central heterocyclic ring, leading to the discovery of pyrrolidine congener **4.9c** as the most potent CCR8 agonist within this series. This derivative was used further to explore the SAR of the terminal substituent. Unfortunately, the derivatization of pyrrolidine compound **4.9c** as amides, urea and sulfonamide afforded compounds that lacked CCR8 agonistic properties. Therefore, the focus shifted back to the original piperazine scaffold (**1.9**). A systematic structural variation of the terminal ethoxyethanol chain on the piperazine revealed the elements that are necessary for CCR8 agonism. Removing the central and terminal oxygens (**4.17a**) led to a complete drop in CCR8 agonism. On the other hand, retaining the ether oxygen and shortening the length of the alkyl chain (**4.17b-d**) afforded compounds that are equipotent to reference compound

1.9. This preliminary SAR study can be used as starting point for the synthesis of more potent CCR8 agonists.

## 4.5. Experimental part

### 4.5.1. Chemistry

All commercial reagents were obtained via Acros Organics, Sigma-Aldrich and TCI chemicals and were at least 99% pure unless indicated otherwise. Furthermore, all dry solvents were obtained via Acros Organics with an AcroSeal system and regular solvents were obtained via Fisher Scientific at technical grade. Thin layer chromatography (TLC) was performed on silica gel on aluminum foils (60 Å pore diameter) obtained from Sigma-Aldrich and visualized using ultraviolet light. Recording of the NMR spectra was performed using a Bruker 300 MHz, 500 MHz or 600 MHz spectrometer. The chemical shifts are reported in ppm with Me<sub>4</sub>Si as the reference and coupling constants (*J*) are reported in hertz. Mass spectra were acquired on a quadrupole orthogonal acceleration time-of-flight mass spectrometer (Synapt G2 HDMS, Waters, Milford, MA). Samples were infused at 3 µL/min and spectra were obtained in positive or negative ionization mode with a resolution of 15000 (FWHM) using leucine enkephalin as lock mass.

#### ***tert*-Butyl piperazine-1-carboxylate (4.3a)**

To a solution of **4.2** (25 g, 290 mmol) in a mixture of isopropanol and water (9:1, 100 ml) was added sodium hydroxide (4.64 g, 116 mmol) and Boc anhydride (25 g, 116 mmol). The reaction mixture was stirred overnight at room temperature. After reaction completion, the precipitate was filtered off and discarded and isopropanol was evaporated. The remaining water phase was extracted with dichloromethane. The combined organic layers were washed with water and brine and dried over MgSO<sub>4</sub>. The solvent was evaporated *in vacuo* yielding the title compound as a colorless oil that crystallized over time (12 g, 56%). <sup>1</sup>H NMR (300 MHz, CDCl<sub>3</sub>) δ 3.38 (t, *J* = 5.1 Hz, 4H), 2.80 (t, *J* = 5.1 Hz, 4H), 1.46 (s, 9H) ppm.

#### *4.5.1.1. Synthesis of Boc protected ethyl carbamates*

##### General procedure

To a solution of the Boc protected diamine (1 eq) in dry DCM (5 ml) was added Et<sub>3</sub>N (2 eq) and the mixture was cooled to 0°C. Ethyl chloroformate (2 eq) was added dropwise and the reaction was stirred for 10 minutes at 0°C after which it was warmed to room temperature and stirred for an additional hour. After reaction completion, the mixture was extracted with DCM and water three times. The combined organic layers were washed once with water and brine and dried over MgSO<sub>4</sub>. The solvent was evaporated *in vacuo* and the crude residue was purified by silica gel flash column chromatography (using a mixture of heptane and ethyl acetate in a ratio of 7:3 as mobile phase) yielding the target compounds as colorless oils. The following compounds were prepared according to this procedure.

**1-tert-Butyl 4-ethyl piperazine-1,4-dicarboxylate (4.4a)**

The title compound was synthesized from **4.3a** (500 mg, 2.68 mmol) in 83% yield. <sup>1</sup>H NMR (300 MHz, CDCl<sub>3</sub>) δ 4.13 (q, *J* = 7.1 Hz, 2H), 3.40 (m, 8H), 1.45 (s, 9H), 1.25 (t, *J* = 7.1 Hz, 3H) ppm.

**1-tert-Butyl 4-ethyl 1,4-diazepane-1,4-dicarboxylate (4.4b)**

The title compound was synthesized from **4.3b** (300 mg, 1.50 mmol) in 87% yield. <sup>1</sup>H NMR (300 MHz, CDCl<sub>3</sub>) δ 4.12 (q, *J* = 7.1 Hz, 2H), 3.40 (m, 8H), 1.83 (m, 2H), 1.44 (s, 9H), 1.25 (t, *J* = 7.1 Hz, 3H) ppm.

**tert-Butyl 3-((ethoxycarbonyl)amino)pyrrolidine-1-carboxylate (4.4c)**

The title compound was synthesized from **4.3c** (400 mg, 2.15 mmol) in 81% yield. <sup>1</sup>H NMR (300 MHz, CDCl<sub>3</sub>) δ 4.72 (br s, 1H), 4.21 (br s, 1H), 4.11 (q, *J* = 6.8 Hz, 2H), 3.59 (m, 1H), 3.40 (m, 1H), 3.20 (m, 1H), 2.12 (m, 1H), 1.82 (m, 1H), 1.44 (s, 9H), 1.23 (t, *J* = 7.1 Hz, 3H) ppm.

**Ethyl 3-((tert-butoxycarbonyl)amino)pyrrolidine-1-carboxylate (4.4d)**

The title compound was synthesized from **4.3d** (200 mg, 1.07 mmol) in 75% yield. <sup>1</sup>H NMR (300 MHz, CDCl<sub>3</sub>) δ 4.66 (br s, 1H), 4.17 (br s, 1H), 4.13 (q, *J* = 7.1 Hz, 2H), 3.62 (m, 1H), 3.45 (m, 1H), 3.22 (m, 1H), 2.11 (m, 1H), 1.82 (m, 1H), 1.45 (s, 9H), 1.25 (t, *J* = 7.2 Hz, 3H) ppm.

General procedure

Compounds **4.3a-d** were dissolved in a 3M HCl solution in cyclopentylmethylether (5 ml) and the reaction was stirred overnight. A precipitate was formed and the solvent was evaporated *in vacuo* yielding the desired compounds in quantitative yield. The following compounds were made according to this procedure.

**4-(Ethoxycarbonyl)piperazine hydrochloride (4.5a)**

The title compound was synthesized from **4.4a** (354 mg, 1.30 mmol). <sup>1</sup>H NMR (300 MHz, MeOD-*d*<sub>4</sub>) δ 4.17 (q, *J* = 7.0 Hz, 2H), 3.80 (s, 4H), 3.28 (s, 4H), 1.29 (t, *J* = 7.0 Hz, 3H) ppm.

**4-(Ethoxycarbonyl)-1,4-diazepane hydrochloride (4.5b)**

The title compound was synthesized from **4.4b** (354 mg, 1.30 mmol). <sup>1</sup>H NMR (300 MHz, MeOD-*d*<sub>4</sub>) δ 4.25 (m, 1H), 4.18 (q, *J* = 7.1 Hz, 2H), 3.79 (m, 2H), 3.63 (m, 2H), 3.34 (m, 4H), 2.12 (m, 2H), 1.30 (t, *J* = 7.1 Hz, 3H) ppm.

**3-((Ethoxycarbonyl)amino)pyrrolidine hydrochloride (4.5c)**

The title compound was synthesized from **4.4c** (354 mg, 1.30 mmol). <sup>1</sup>H NMR (300 MHz, MeOD-*d*<sub>4</sub>) δ 4.27 (m, 1H), 4.11 (q, *J* = 7.1 Hz, 2H), 3.51-3.24 (m, 5H), 2.28 (m, 1H), 2.03 (m, 1H), 1.25 (t, *J* = 7.1 Hz, 3H) ppm.

**1-(Ethoxycarbonyl)pyrrolidin-3-ammonium chloride (4.5d)**

The title compound was synthesized from **4.4d** (354 mg, 1.30 mmol). <sup>1</sup>H NMR (300 MHz, MeOD-*d*<sub>4</sub>) δ 4.14 (q, *J* = 7.1 Hz, 2H), 3.93 (m, 1H), 3.73 (m, 1H), 3.53 (m, 3H), 2.37 (m, 1H), 2.11 (m, 1H), 1.28 (t, *J* = 7.1 Hz, 3H) ppm.

### 3-Phenoxybenzylalcohol (4.7)

To a solution of **4.6** (1 g, 5.04 mmol) in methanol (10 ml) was added NaBH<sub>4</sub> (286 mg, 7.57 mmol) portionwise at 0°C. The reaction mixture was stirred for 2 hours at room temperature. The solvent was evaporated and the crude product was dissolved in water and extracted with ethyl acetate (3x). The combined organic layers were washed with water and brine, dried over MgSO<sub>4</sub> and evaporated to yield the title compound in quantitative yield as colorless oil. <sup>1</sup>H NMR (300 MHz, DMSO-*d*<sub>6</sub>) δ 7.36 (m, 3H), 7.06 (m, 5H), 6.87 (m, 1H), 5.25 (t, *J* = 5.7 Hz, 1H), 4.48 (d, *J* = 5.6 Hz, 2H) ppm.

### 3-Phenoxybenzylbromide (4.8)

To a solution of **4.7** (1 g, 4.99 mmol) in dry dichloromethane (10 ml) was added PBr<sub>3</sub> (1.49 g, 5.49 mmol) dropwise at 0°C under an inert atmosphere. The reaction mixture was stirred at 0°C for 2 hours and stirred overnight at room temperature. After reaction completion, the solvent was evaporated and the crude residue was partitioned between water and diethyl ether. After extraction, the organic phase was washed with water and brine, dried over MgSO<sub>4</sub> and evaporated *in vacuo* to yield the title compound as a colorless oil (0.942 mg, 72%). <sup>1</sup>H NMR (300 MHz, DMSO-*d*<sub>6</sub>) δ 7.40 (m, 3H), 7.18 (m, 2H), 7.05 (m, 3H), 6.94 (m, 1H), 4.68 (s, 2H) ppm.

#### 4.5.1.2. Synthesis of phenoxybenzyl-amine analogues

##### General procedure

To a solution of **4.8** (1 eq) in dry DMF (3 ml) was added K<sub>2</sub>CO<sub>3</sub> (2-3 eq) and the appropriate amine (0.9-1.2 eq) or amine hydrochloride (1.2 eq). The reaction mixture was stirred overnight at room temperature. Upon completion, water was added and the mixture was extracted with ethyl acetate (3x). The combined organic layers were washed with water (2x) and brine (1x) and dried over MgSO<sub>4</sub>. The solvent was evaporated and the crude residue was purified by silica gel flash column chromatography with an appropriate solvent system as mobile phase yielding the title compounds as colorless to yellow oils. The following compounds were made according to this procedure.

##### **Ethyl 4-(3-phenoxybenzyl)piperazine-1-carboxylate (4.9a)**

The title compound was synthesized from **4.8** (300 mg, 1.14 mmol) and **4.5a** (234 mg, 1.48 mmol). The title compound was obtained after silica gel flash column chromatography (using a mixture of dichloromethane and ethyl acetate in a ratio of 1:1) as a light yellow oil (320 mg, 82%). <sup>1</sup>H NMR (300 MHz, CDCl<sub>3</sub>) δ 7.31 (m, 3H), 7.10-6.98 (m, 5H), 6.88 (m, 1H), 4.11 (q, *J* = 7.1 Hz, 2H), 3.47 (m, 6H), 2.39 (m, 4H), 1.24 (t, *J* = 7.1 Hz, 3H) ppm. <sup>13</sup>C NMR (75 MHz, CDCl<sub>3</sub>) δ 157.61, 157.50, 155.81, 140.08, 130.04, 129.87, 124.23, 123.54, 119.78, 119.28, 119.23, 119.13, 117.92, 62.84, 61.63, 52.96, 43.88, 14.99 ppm. HRMS *m/z* [M+H]<sup>+</sup> calcd for C<sub>21</sub>H<sub>26</sub>NO<sub>3</sub> 341.1860; found 341.1859.

##### **Ethyl 4-(3-phenoxybenzyl)-1,4-diazepane-1-carboxylate (4.9b)**

The title compound was synthesized from **4.8** (175 mg, 0.663 mmol) and **4.5b** (180 mg, 0.862 mmol). The title compound was obtained after silica gel flash column chromatography (using a mixture of heptane and ethyl acetate in a ratio of 6:4) as a light yellow oil (203 mg, 86%). <sup>1</sup>H NMR (300 MHz, CDCl<sub>3</sub>) δ 7.33 (m, 3H), 7.25 (m, 5H), 6.87 (m, 1H), 4.12 (q, *J* = 7.1 Hz, 1H), 3.59 (s, 2H), 3.60-3.45

(m, 4H), 2.60 (m, 4H), 1.81 (m, 2H), 1.25 (t,  $J = 7.0$  Hz, 3H) ppm.  $^{13}\text{C}$  NMR (75 MHz,  $\text{CDCl}_3$ )  $\delta$  157.60, 157.56, 141.74, 130.02, 129.80, 123.86, 123.44, 119.43, 119.08, 117.74, 62.37, 61.43, 56.49, 56.16, 55.13, 47.00, 46.77, 46.00, 28.31, 28.18, 15.10 ppm. HRMS  $m/z$   $[\text{M}+\text{H}]^+$  calcd for  $\text{C}_{21}\text{H}_{27}\text{N}_2\text{O}_3$  355.2016; found 355.2021.

#### **Ethyl (1-(3-phenoxybenzyl)pyrrolidin-3-yl)carbamate (4.9c)**

The title compound was synthesized from **4.8** (180 mg, 0.684 mmol) and **4.5c** (200 mg, 1.03 mmol). The title compound was obtained after silica gel flash chromatography (using a mixture of dichloromethane and ethyl acetate, in a ratio of 1:1 as mobile phase) as a light yellow oil (183 mg, 79%).  $^1\text{H}$  NMR (600 MHz,  $\text{CDCl}_3$ )  $\delta$  7.33 (m, 2H), 7.25 (m, 1H), 7.09 (m, 1H), 7.04 (m, 1H), 7.00 (m, 1H), 6.99 (m, 2H), 6.88 (m, 1H), 5.06 (br s, 1H), 4.21 (br s, 1H), 4.08 (q,  $J = 6.8$  Hz, 2H), 3.57 (s, 2H), 2.81 (m, 1H), 2.56 (m, 3H), 2.25 (m, 3H), 1.59 (m, 1H), 1.22 (t,  $J = 7.1$  Hz, 3H) ppm.  $^{13}\text{C}$  NMR (150 MHz,  $\text{CDCl}_3$ )  $\delta$  157.20, 157.18, 156.01, 140.75, 129.67, 129.49, 123.50, 123.13, 119.08, 118.76, 117.43, 60.72, 60.58, 59.63, 52.48, 50.13, 32.55, 14.59 ppm. HRMS  $m/z$   $[\text{M}+\text{H}]^+$  calcd for  $\text{C}_{21}\text{H}_{26}\text{NO}_3$  341.18595; found 341.1859.

#### **Ethyl 3-((3-phenoxybenzyl)amino)pyrrolidine-1-carboxylate (4.9d)**

The title compound was synthesized from **4.8** (90 mg, 0.342 mmol) and **4.5d** (100 mg, 0.514 mmol). The title compound was obtained after silica gel flash column chromatography (using a mixture of dichloromethane and ethyl acetate, in a ratio of 1:1 as mobile phase) as a light yellow oil (78 mg, 67%).  $^1\text{H}$  NMR (600 MHz,  $\text{CDCl}_3$ )  $\delta$  7.33 (m, 2H), 7.26 (m, 1H), 7.11 (m, 1H), 7.05 (m, 1H), 7.00 (m, 3H), 6.88 (m, 1H), 4.11 (q,  $J = 7.1$  Hz, 1H), 3.78 (s, 2H), 3.60-3.48 (m, 2H), 3.38-3.33 (m, 2H), 3.23-3.12 (m, 1H), 2.03 (m, 1H), 1.75 (m, 3H), 1.25 (t,  $J = 7.1$  Hz, 3H) ppm.  $^{13}\text{C}$  NMR (150 MHz,  $\text{CDCl}_3$ )  $\delta$  157.41, 157.08, 155.22, 141.96, 129.72, 129.70, 123.23, 122.82, 118.86, 118.39, 117.44, 60.91, 56.98, 56.08, 51.78, 44.43, 44.11, 31.97, 31.23, 29.64, 14.78 ppm. HRMS  $m/z$   $[\text{M}+\text{H}]^+$  calcd for  $\text{C}_{21}\text{H}_{26}\text{NO}_3$  341.1860; found 341.1859.

#### **Ethyl 1-(3-phenoxybenzyl)piperidine-3-carboxylate (4.10)**

The title compound was synthesized from **4.8** (100 mg, 0.380 mmol) and ethyl piperidine-3-carboxylate (78 mg, 0.494 mmol). The title compound was obtained after silica gel flash column chromatography (using a mixture of dichloromethane and ethyl acetate, in a ratio of 6:4 as mobile phase) as a light yellow oil (107 mg, 83%).  $^1\text{H}$  NMR (600 MHz,  $\text{DMSO}-d_6$ )  $\delta$  7.36 (m, 3H), 7.13 (m, 1H), 7.02 (m, 2H), 6.93 (m, 1H), 6.87 (m, 1H), 4.01 (q,  $J = 7.1$  Hz, 2H) 3.44 (m, 2H), 2.75 (m, 1H), 2.27-2.02 (m, 2H), 1.77-1.46 (m, 4H), 1.13 (t,  $J = 7.0$  Hz, 3H) ppm.  $^{13}\text{C}$  NMR (150 MHz,  $\text{CDCl}_3$ )  $\delta$  173.29, 156.74, 156.67, 140.90, 130.07, 129.78, 123.73, 123.44, 118.60, 118.57, 117.13, 61.82, 59.84, 54.88, 53.23, 26.31, 23.90, 14.13 ppm. HRMS  $m/z$   $[\text{M}+\text{H}]^+$  calcd for  $\text{C}_{21}\text{H}_{26}\text{NO}_3$  340.1907; found 340.1906.

#### **tert-Butyl (1-(3-phenoxybenzyl)pyrrolidin-3-yl)carbamate (4.11)**

The title compound was synthesized from **4.8** (300 mg, 1.14 mmol) and **4.3d** (319 mg, 1.71 mmol). The title compound was obtained after silica gel flash column chromatography (using a mixture of dichloromethane and ethyl acetate, in a ratio of 6:4 as mobile phase) as a light yellow oil (368 mg,

88%).  $^1\text{H}$  NMR (300 MHz,  $\text{CDCl}_3$ )  $\delta$  7.33-7.21 (m, 3H), 7.09-6.97 (m, 5H), 6.86 (m, 1H), 5.04 (d,  $J = 6.8$  Hz, 1H), 4.14 (br s, 1H), 3.54 (s, 2H), 3.43 (m, 4H), 2.75 (m, 1H), 2.54 (m, 2H), 2.21 (m, 2H), 1.56 (m, 1H) 1.41 (s, 9H) ppm.  $^{13}\text{C}$  NMR (75 MHz,  $\text{CDCl}_3$ )  $\delta$  157.63, 157.57, 155.69, 141.26, 130.00, 129.79, 123.87, 123.44, 119.49, 119.10, 117.76, 79.44, 61.17, 60.05, 52.86, 56.19, 32.98, 28.75 ppm.

#### **1-(3-Phenoxybenzyl)pyrrolidin-3-aminium chloride (4.12)**

To a solution of HCl in cyclopentylmethylether (3M, 5 ml) was added **4.11** (1 g, 2.71 mmol). The reaction was stirred at room temperature overnight under a nitrogen atmosphere. Upon completion, the solvent was evaporated yielding the desired compound in quantitative yield.  $^1\text{H}$  NMR (300 MHz,  $\text{D}_2\text{O}$ )  $\delta$  7.45-7.35 (m, 3H), 7.22-7.14 (m, 2H), 7.10-7.00 (m, 4H), 4.37 (s, 2H), 4.15 (br s, 1H), 3.83 (br s, 1H), 3.46 (br s, 3H), 2.56 (br s, 1H), 2.16 (br s, 1H) ppm.  $^{13}\text{C}$  NMR (75 MHz,  $\text{D}_2\text{O}$ )  $\delta$  157.45, 156.02, 131.15, 131.00, 130.10, 125.18, 124.22, 120.12, 119.96, 119.10, 57.97, 55.06, 52.26, 47.58, 27.69 ppm.

#### *4.5.1.3. Synthesis of phenoxybenzylpyrrolidine-amide derivatives*

##### General Procedure A

To a suspension of **4.12** (1 eq) in dichloromethane (5 ml) was added triethylamine (4 eq), followed by dropwise addition of the appropriate acid chloride (1.5 eq). The mixture was stirred overnight at room temperature. Upon reaction completion, the solvent was evaporated and the crude residue was partitioned between and extracted with ethyl acetate and water (3x). The combined organic phases were washed with water (2x) and brine (1x), dried over  $\text{MgSO}_4$  and evaporated till dryness. The crude residue was purified by silica gel flash column chromatography employing the appropriate solvent mixture as mobile phase yielding the desired compounds.

##### General Procedure B

To a suspension of **4.12** (1 eq) in dry DMF (5 ml) was added triethylamine (3 eq) followed by an appropriate carboxylic acid (1 eq) and PyBOP (1.2 eq). The mixture was stirred overnight at room temperature. Upon reaction completion, the mixture was partitioned between ethyl acetate and water (3x). The combined organic phases were washed with water (2x) and brine (1x). The final mixture was dried over  $\text{MgSO}_4$  and evaporated till dryness. The crude residue was purified by silica gel flash column chromatography employing the appropriate solvent mixture as mobile phase, yielding the desired compounds. The following compounds were made according to this procedure.

#### ***N*-(1-(3-Phenoxybenzyl)pyrrolidin-3-yl)benzamide (4.13a)**

The title compound was synthesized according to General procedure A using **4.12** (200 mg, 0.656 mmol) and benzoyl chloride (102  $\mu\text{l}$ , 0.879 mmol). After silica gel flash column chromatography (98:2 dichloromethane:methanol) and NMR analysis, the obtained compound turned out to be the imide. Subsequent heating in methanol at reflux temperature for 2 hours and silica gel flash column chromatography (using a mixture of dichloromethane and methanol in a ratio of 96:4 as mobile phase) yielded the desired compound as a colorless oil (159 mg, 73%).  $^1\text{H}$  NMR (300 MHz,  $\text{CDCl}_3$ )  $\delta$  7.74 (m, 2H), 7.51-7.38 (m, 3H), 7.32-7.24 (m, 3H), 7.09-6.98 (m, 5H), 6.89 (m, 1H), 6.58 (m, 1H), 4.66 (m, 1H), 3.61 (s, 2H), 2.94 (m, 2H), 2.73 (m, 1H), 2.60 (m, 1H), 2.43-2.25 (m, 3H), 1.79-1.69 (m, 1H) ppm.

$^{13}\text{C}$  NMR (75 MHz,  $\text{CDCl}_3$ )  $\delta$  167.02, 157.64, 157.58, 140.92, 134.92, 131.62, 129.99, 129.88, 128.80, 127.19, 123.88, 123.47, 119.49, 119.09, 117.91, 60.99, 59.91, 52.85, 49.42, 32.96 ppm. HRMS  $m/z$   $[\text{M}+\text{H}]^+$  calcd for  $\text{C}_{24}\text{H}_{25}\text{N}_2\text{O}_2$  373.1910; found 373.1912.

#### **2-Methoxy-*N*-(1-(3-phenoxybenzyl)pyrrolidin-3-yl)acetamide (4.13b)**

The title compound was synthesized according to General procedure A using **4.12** (200 mg, 0.656 mmol) and methoxyacetyl chloride (81  $\mu\text{l}$ , 0.879 mmol). The desired compound was obtained after silica gel flash column chromatography (using a mixture of dichloromethane and methanol in a ratio of 96:4 as mobile phase) as a colorless oil (132 mg, 66%).  $^1\text{H}$  NMR (300 MHz,  $\text{CDCl}_3$ )  $\delta$  7.34-7.22 (m, 3H), 7.10-6.97 (m, 5H), 6.86 (m, 1H), 6.78 (m, 1H), 4.48 (m, 1H), 3.83 (s, 2H), 3.57 (s, 2H), 3.37 (s, 3H), 2.84 (m, 1H), 2.61-2.56 (m, 2H), 2.36-2.24 (m, 3H), 1.68-1.56 (m, 1H) ppm.  $^{13}\text{C}$  NMR (75 MHz,  $\text{CDCl}_3$ )  $\delta$  169.06, 157.63, 157.54, 141.20, 129.99, 129.81, 123.85, 123.41, 119.52, 119.02, 117.82, 72.25, 60.82, 59.89, 59.37, 52.84, 48.19, 32.71 ppm. HRMS  $m/z$   $[\text{M}+\text{H}]^+$  calcd for  $\text{C}_{20}\text{H}_{25}\text{N}_2\text{O}_3$  341.1860; found 341.1857.

#### ***N*-(1-(3-Phenoxybenzyl)pyrrolidin-3-yl)cyclopentanecarboxamide (4.13c)**

The title compound was synthesized according to General procedure A using **4.12** (180 mg, 0.591 mmol) and cyclopentanecarbonyl chloride (96  $\mu\text{l}$ , 0.791 mmol). After flash column chromatography (using a mixture of dichloromethane and methanol in a ratio of 98:2 as mobile phase) and NMR analysis, the obtained compound turned out to be the imide. Subsequent refluxing in methanol for 2 hours, followed by silica gel flash column chromatography (using a mixture of dichloromethane and methanol in a ratio of 96:4 as mobile phase) yielded the title compound as a colorless oil (136 mg, 71%).  $^1\text{H}$  NMR (300 MHz,  $\text{CDCl}_3$ )  $\delta$  7.36-7.25 (m, 3H), 7.13-6.99 (m, 5H), 6.90 (m, 1H), 5.96 (m, 1H), 4.47 (m, 1H), 3.61 (s, 2H), 2.92 (m, 1H), 2.65-2.40 (m, 3H), 2.35-2.23 (m, 2H), 1.84-1.55 (m, 9H) ppm.  $^{13}\text{C}$  NMR (75 MHz,  $\text{CDCl}_3$ )  $\delta$  175.82, 157.63, 140.58, 130.01, 129.90, 123.93, 123.49, 119.53, 119.11, 117.96, 60.99, 59.85, 52.87, 48.70, 46.12, 32.86, 30.66, 26.20 ppm. HRMS  $m/z$   $[\text{M}+\text{H}]^+$  calcd for  $\text{C}_{23}\text{H}_{29}\text{N}_2\text{O}_2$  365.2223; found 365.2220.

#### ***N*-(1-(3-Phenoxybenzyl)pyrrolidin-3-yl)-2-phenylacetamide (4.13d)**

The title compound was synthesized according to General procedure B using **4.12** (200 mg, 0.656 mmol) and phenylacetic acid (89 mg, 0.656 mmol). The desired compound was obtained after silica gel flash column chromatography (using a mixture of dichloromethane and methanol in a ratio of 96:4 as mobile phase) as a colorless oil (162 mg, 64%).  $^1\text{H}$  NMR (300 MHz,  $\text{CDCl}_3$ )  $\delta$  7.34-7.20 (m, 8H), 7.08 (m, 1H), 7.00-6.85 (m, 5H), 5.73 (m, 1H), 6.74 (m, 1H), 4.39 (m, 1H), 3.50 (m, 4H), 2.75 (m, 1H), 2.46 (m, 2H), 2.20 (m, 2H), 1.52-1.45 (m, 1H) ppm.  $^{13}\text{C}$  NMR (75 MHz,  $\text{CDCl}_3$ )  $\delta$  170.46, 157.69, 157.49, 141.27, 135.28, 130.01, 129.79, 129.61, 129.25, 127.55, 123.72, 123.41, 119.47, 118.98, 117.80, 60.70, 59.76, 52.65, 49.12, 44.11, 32.68 ppm. HRMS  $m/z$   $[\text{M}+\text{H}]^+$  calcd for  $\text{C}_{25}\text{H}_{27}\text{N}_2\text{O}_2$  387.2067; found 387.2075.

**4-Fluoro-N-(1-(3-phenoxybenzyl)pyrrolidin-3-yl)benzamide (4.13e)**

The title compound was synthesized according to General procedure B using **4.12** (200 mg, 0.656 mmol) and 4-fluorobenzoic acid (92 mg, 0.656 mmol). The desired compound was obtained after silica gel flash column chromatography (using a mixture of dichloromethane and methanol in a ratio of 96:4 as mobile phase), followed by preparative TLC (using a mixture of heptane, ethyl acetate and concentrated ammonia solution in methanol in a ratio of 79:20:1 as mobile phase) as a colorless oil (184 mg, 72%). <sup>1</sup>H NMR (600 MHz, CDCl<sub>3</sub>) δ 7.67 (m, 2H), 7.23-7.17 (m, 3H), 6.96 (m, 4H), 6.90 (m, 3H), 6.81 (m, 1H), 6.74 (m, 1H), 4.56 (m, 1H), 3.52 (s, 2H), 2.86 (m, 1H), 2.66 (m, 1H), 2.51 (m, 1H), 2.28-2.19 (m, 2H), 1.65 (m, 1H) ppm. <sup>13</sup>C NMR (150 MHz, CDCl<sub>3</sub>) δ 165.64, 164.50 (d, *J* = 250 Hz), 157.21, 157.10, 140.20, 130.55 (d, *J* = 2.5 Hz), 129.65, 129.57, 129.23 (d, *J* = 8.9 Hz), 123.60, 123.15, 119.17, 118.69, 117.61, 115.30 (d, *J* = 21.6 Hz), 60.51, 59.52, 52.52, 48.98, 32.36 ppm. HRMS *m/z* [M+H]<sup>+</sup> calcd for C<sub>24</sub>H<sub>24</sub>N<sub>2</sub>O<sub>2</sub>F 391.1816; found 391.1808.

**N-(1-(3-Phenoxybenzyl)pyrrolidin-3-yl)nicotinamide (4.13f)**

The title compound was synthesized according to General procedure B using **4.12** (200 mg, 0.656 mmol) and nicotinic acid (81 mg, 0.656 mmol). The desired compound was obtained after silica gel flash column chromatography (using a mixture of dichloromethane and methanol in a ratio of 97:3 as mobile phase) as a white solid (189 mg, 77%). <sup>1</sup>H NMR (300 MHz, CDCl<sub>3</sub>) δ 8.67 (m, 2H), 7.57 (m, 2H), 7.26 (m, 3H), 7.08-6.87 (m, 7H), 4.65 (m, 1H), 3.60 (s, 2H), 2.95 (m, 2H), 2.76 (m, 1H), 2.55 (m, 1H), 2.42-2.21 (m, 2H), 1.73 (m, 1H) ppm. <sup>13</sup>C NMR (75 MHz, CDCl<sub>3</sub>) δ 165.03, 157.57, 150.82, 141.93, 140.98, 130.02, 129.92, 123.85, 123.49, 121.14, 119.46, 119.01, 117.98, 60.80, 59.82, 52.72, 49.68, 32.80 ppm. HRMS *m/z* [M+H]<sup>+</sup> calcd for C<sub>23</sub>H<sub>24</sub>N<sub>3</sub>O<sub>2</sub> 374.1863; found 374.1858.

**4.5.1.4. Synthesis of phenoxybenzylpyrrolidine urea derivatives****General procedure**

To a solution of **4.12** (1 eq) in dichloromethane was added diisopropylethylamine (1.4 eq) and the appropriate isocyanate (0.9 eq). The reaction mixture was stirred at room temperature overnight. Upon completion of the reaction, the solvent was evaporated and the crude residue was extracted with water and ethyl acetate. The combined organic phases were washed with water and brine, dried over MgSO<sub>4</sub> and evaporated to dryness. The crude residue was purified using flash column chromatography with an appropriate solvent mixture yielding the desired compounds. The following compounds were made according to this procedure.

**1-(1-(3-Phenoxybenzyl)pyrrolidin-3-yl)-3-phenylurea (4.14a)**

The title compound was synthesized using **4.12** (300 mg, 0.984 mmol) and phenyl isocyanate (97 μl, 0.886 mmol). The desired compound was obtained after flash column chromatography (using a mixture of dichloromethane and methanol in a ratio of 96:4 as mobile phase) as a white solid (269 mg, 71%). <sup>1</sup>H NMR (300 MHz, CDCl<sub>3</sub>) δ 7.34-7.20 (m, 8H), 7.11-6.97 (m, 6H), 6.91-6.88 (m, 1H), 6.01 (d, *J* = 7.76 Hz, 1H), 4.28 (br s, 1H), 3.62 (m, 3H), 2.96 (m, 1H), 2.77 (m, 1H), 2.60 (m, 1H), 2.37-2.20 (m, 2H), 1.73 (m, 1H) ppm. <sup>13</sup>C NMR (75 MHz, CDCl<sub>3</sub>) δ 157.71, 157.40, 155.82, 139.44, 139.29, 130.07,



129.34, 124.11, 123.63, 123.46, 120.56, 119.74, 119.15, 118.18, 70.75, 60.87, 59.74, 52.94, 49.78, 32.52 ppm. HRMS  $m/z$   $[M+H]^+$  calcd for  $C_{24}H_{26}N_3O_2$  388.2019; found 388.2008.

#### **1-Benzyl-3-(1-(3-phenoxybenzyl)pyrrolidin-3-yl)urea (4.14b)**

The title compound was synthesized using **4.12** (300 mg, 0.984 mmol) and benzyl isocyanate (109  $\mu$ l, 0.886 mmol). The desired compound was obtained after flash column chromatography (using a mixture of dichloromethane and methanol in a ratio of 96:4 as mobile phase) as a white solid (287 mg, 73%).  $^1H$  NMR (600 MHz,  $CDCl_3$ )  $\delta$  7.29 (m, 1H), 7.23-7.15 (m, 6H), 7.06 (m, 1H), 6.95 (m, 3H), 6.93 (br s, 1H), 6.85 (m, 1H), 5.73 (br s, 1H), 4.21 (m, 2H), 4.10 (br s, 1H), 3.48 (s, 2H), 2.73 (m, 1H), 2.53 (m, 2H), 2.22 (m, 1H), 2.10 (m, 1H), 1.55 (m, 1H) ppm.  $^{13}C$  NMR (150 MHz,  $CDCl_3$ )  $\delta$  158.12, 157.07, 157.02, 139.96, 139.53, 129.63, 129.51, 128.33, 127.13, 126.87, 123.54, 123.10, 119.14, 118.64, 117.45, 60.64, 59.44, 52.63, 49.32, 43.93, 32.27 ppm. HRMS  $m/z$   $[M+H]^+$  calcd for  $C_{25}H_{28}N_3O_2$  402.2176; found 402.2173.

#### **1-Ethyl-3-(1-(3-phenoxybenzyl)pyrrolidin-3-yl)urea (4.14c)**

The title compound was synthesized using **4.12** (200 mg, 0.656 mmol) and ethyl isocyanate (49  $\mu$ l, 0.623 mmol). The desired compound was obtained after flash column chromatography (using a mixture of dichloromethane and methanol in a ratio of 96:4 as mobile phase) as a yellow oil (154 mg, 69%).  $^1H$  NMR (300 MHz,  $CDCl_3$ )  $\delta$  7.33-7.21 (m, 3H), 7.10-6.96 (m, 5H), 6.86 (m, 1H), 5.39 (d,  $J = 7.9$  Hz, 1H), 5.26 (m, 1H), 4.20 (br s, 1H), 3.62 (s, 1H), 3.59 (s, 2H), 3.13 (m, 2H), 2.87 (m, 1H), 2.60 (m, 2H), 2.33-2.19 (m, 2H), 1.64 (m, 1H), 1.05 (t,  $J = 7.2$  Hz, 1H) ppm.  $^{13}C$  NMR (75 MHz,  $CDCl_3$ )  $\delta$  158.33, 157.59, 157.42, 140.19, 130.08, 130.00, 124.04, 123.58, 119.60, 119.12, 117.99, 61.21, 59.94, 53.16, 49.71, 35.36, 32.74, 15.85 ppm. HRMS  $m/z$   $[M+H]^+$  calcd for  $C_{20}H_{26}N_3O_2$  340.2019; found 340.2014.

#### **N-(1-(3-Phenoxybenzyl)pyrrolidin-3-yl)benzenesulfonamide (4.15)**

To a suspension of **4.12** (200 mg, 0.656 mmol) in dichloromethane (3ml) was added triethylamine (365  $\mu$ l, 2.62 mmol), followed by dropwise addition of benzenesulfonyl chloride (113  $\mu$ l, 0.879 mmol). The mixture was stirred overnight at room temperature. Upon reaction completion, the solvent was evaporated and the crude residue was partitioned between and extracted with ethyl acetate and water. The combined organic phases were washed with water and brine, dried over  $MgSO_4$  and evaporated till dryness. The crude residue was purified by silica gel flash column chromatography (using a mixture of dichloromethane and methanol in a ratio of 96:4 as mobile phase) yielding the desired compound as a colorless oil (171 mg, 71%).  $^1H$  NMR (300 MHz,  $CDCl_3$ )  $\delta$  7.83 (m, 2H), 7.57-7.44 (m, 3H), 7.36-7.21 (m, 3H), 7.10 (m, 1H), 7.00-6.87 (m, 5H), 4.89 (m, 1H), 3.84 (m, 1H), 3.47 (m, 2H), 2.72 (m, 1H), 2.37 (m, 2H), 2.23-2.02 (m, 2H), 1.52 (m, 1H) ppm.  $^{13}C$  NMR (75 MHz,  $CDCl_3$ )  $\delta$  157.57, 140.81, 132.85, 130.04, 129.85, 129.39, 127.27, 123.74, 123.53, 119.36, 119.10, 117.84, 60.55, 59.63, 53.13, 52.26, 32.92 ppm. HRMS  $m/z$   $[M+H]^+$  calcd for  $C_{23}H_{25}N_2SO_3$  409.1580; found 409.1574

#### 4.5.1.5. Synthesis of phenoxybenzylpiperazine analogues

##### General procedure

To a solution of **4.8** (1 eq) in dry DMF (3 ml) was added  $K_2CO_3$  (2-3 eq) and the appropriate amine (0.9-1.2 eq) or amine hydrochloride (1.2 eq). The reaction mixture was stirred overnight at room temperature. Upon completion, water was added and the mixture was extracted with ethyl acetate (3x). The organic layer was washed with water (2x) and brine (1x) and dried over  $MgSO_4$ . The solvent was evaporated and the crude residue was purified by silica gel flash column chromatography with an appropriate solvent system yielding the title compounds as colorless to yellow oils. The following compounds were made according to this procedure.

##### **1-Hexyl-4-(3-phenoxybenzyl)piperazine (4.17a)**

The title compound was synthesized according to the general procedure using **4.8** (200 mg, 0.760 mmol) and **4.16a** (155 mg, 0.912 mmol). The title compound was obtained after silica gel flash column chromatography (using a mixture of dichloromethane and methanol in a ratio of 96:4 as mobile phase) as a colorless oil (226 mg, 84%).  $^1H$  NMR (300 MHz,  $CDCl_3$ )  $\delta$  7.33-7.22 (m, 3H), 7.09-6.97 (m, 5H), 6.85 (m, 1H), 3.48 (s, 2H), 2.50-2.32 (m, 10H), 1.47 (m, 2H), 1.28 (m, 6H), 0.87 (t,  $J = 6.4$  Hz, 3H) ppm.  $^{13}C$  NMR (75 MHz,  $CDCl_3$ )  $\delta$  157.63, 157.44, 140.60, 129.99, 129.73, 124.32, 123.38, 119.94, 119.02, 117.78, 62.89, 59.07, 53.47, 53.08, 32.06, 27.58, 26.96, 22.89, 14.37 ppm. HRMS  $m/z$   $[M+H]^+$  calcd for  $C_{23}H_{33}N_2O$  353.2587; found 353.2592.

##### **1-(3-Phenoxybenzyl)-4-(2-propoxyethyl)piperazine (4.17b)**

The title compound was synthesized according to the general procedure using **4.8** (200 mg, 0.760 mmol) and **4.16b** (157 mg, 0.912 mmol). The title compound was obtained after silica gel flash column chromatography (using a mixture of dichloromethane and methanol in a ratio of 96:4 as mobile phase) as a colorless oil (234 mg, 87%).  $^1H$  NMR (300 MHz,  $CDCl_3$ )  $\delta$  7.33-7.21 (m, 3H), 7.09-6.97 (m, 5H), 6.85 (m, 1H), 3.53 (t,  $J = 6.0$  Hz, 2H), 3.47 (s, 2H), 3.36 (t,  $J = 6.7$  Hz, 2H), 2.50 (m, 9H), 1.56 (m, 2H), 0.89 (t,  $J = 7.4$  Hz, 3H) ppm.  $^{13}C$  NMR (75 MHz,  $CDCl_3$ )  $\delta$  157.70, 157.45, 140.76, 129.95, 129.66, 124.28, 123.33, 119.95, 119.00, 117.74, 73.17, 68.82, 62.93, 58.14, 53.94, 53.24, 23.10, 10.84 ppm. HRMS  $m/z$   $[M+H]^+$  calcd for  $C_{22}H_{31}N_2O_2$  355.2380; found 355.2370.

##### **1-(2-Ethoxyethyl)-4-(3-phenoxybenzyl)piperazine (4.17c)**

The title compound was synthesized according to the general procedure using **4.8** (200 mg, 0.760 mmol) and **4.16c** (144 mg, 0.912 mmol). The title compound was obtained after silica gel flash column chromatography (using a mixture of dichloromethane and methanol in a ratio of 96:4 as mobile phase) as a light yellow oil (215 mg, 83%).  $^1H$  NMR (300 MHz,  $CDCl_3$ )  $\delta$  7.34-7.22 (m, 3H), 7.10-6.98 (m, 5H), 6.86 (m, 1H), 3.57-3.45 (m, 6H), 2.61-2.50 (m, 9H), 1.18 (t,  $J = 7.0$  Hz, 3H) ppm.  $^{13}C$  NMR (75 MHz,  $CDCl_3$ )  $\delta$  157.67, 157.44, 140.68, 129.97, 129.68, 124.31, 123.35, 119.96, 119.01, 117.76, 68.42, 66.70, 62.91, 58.17, 53.91, 53.15, 15.43 ppm. HRMS  $m/z$   $[M+H]^+$  calcd for  $C_{21}H_{29}N_2O_2$  341.2223; found 341.2223

**1-(2-Methoxyethyl)-4-(3-phenoxybenzyl)piperazine (4.17d)**

The title compound was synthesized according to the general procedure using **4.8** (100 mg, 0.380 mmol) and **4.16d** (82 mg, 0.570 mmol). The title compound was obtained after silica gel flash column chromatography (using a mixture of dichloromethane and methanol in a ratio of 96:4 as mobile phase) as a light yellow oil (102 mg, 82%). <sup>1</sup>H NMR (300 MHz, CDCl<sub>3</sub>) δ 7.34-7.22 (m, 3H), 7.10-6.97 (m, 5H), 6.86 (m, 1H), 3.50 (m, 4H), 3.33 (s, 3H), 2.59-2.51 (m, 9H) ppm. <sup>13</sup>C NMR (75 MHz, CDCl<sub>3</sub>) δ 157.68, 157.46, 140.64, 129.95, 129.67, 124.29, 123.34, 119.95, 119.01, 117.76, 70.45, 62.86, 59.11, 58.14, 53.86, 53.05 ppm. HRMS m/z [M+H]<sup>+</sup> calcd for C<sub>20</sub>H<sub>25</sub>N<sub>2</sub>O<sub>3</sub> 327.2067; found 327.2068.

**2-(4-(3-Phenoxybenzyl)piperazin-1-yl)ethan-1-ol (4.17e)**

The title compound was synthesized according to the general procedure using **4.8** (300 mg, 1.14 mmol) and **4.16e**. The title compound was obtained after silica gel flash column chromatography (using a mixture of dichloromethane and methanol in a ratio of 9:1 as mobile phase) as a colorless oil (197 mg, 84%). <sup>1</sup>H NMR (300 MHz, CDCl<sub>3</sub>) δ 7.34-7.23 (m, 3H), 7.10-6.97 (m, 5H), 6.87 (m, 1H), 3.99 (br s, 1H), 3.63 (t, *J* = 5.3 Hz, 2H), 3.49 (s, 2H), 2.59 (t, *J* = 5.3 Hz, 2H), 2.52 (br s, 8H) ppm. <sup>13</sup>C NMR (75 MHz, CDCl<sub>3</sub>) δ 157.56, 157.51, 140.36, 130.03, 129.81, 124.28, 123.47, 119.87, 119.06, 117.86, 62.76, 59.75, 57.89, 53.21, 52.91 ppm. HRMS m/z [M+H]<sup>+</sup> calcd for C<sub>19</sub>H<sub>23</sub>N<sub>2</sub>O<sub>2</sub> 313.1910; found 313.1904.

**1-Cyclopropyl-4-(3-phenoxybenzyl)piperazine (4.17f)**

The title compound was synthesized according to the general procedure using **4.8** (200 mg, 0.760 mmol) and the dibromide salt of **4.16f** (252 mg, 0.874 mmol). The title compound was obtained after silica gel flash column chromatography (using a mixture of heptane and ethyl acetate in a ratio of 3:2 as mobile phase) as a colorless (314 mg, 88%). <sup>1</sup>H NMR (300 MHz, CDCl<sub>3</sub>) δ 7.32-7.19 (m, 3H), 7.08-6.94 (m, 5H), 6.84 (m, 1H), 3.45 (s, 2H), 2.60 (br s, 4H), 2.41 (br s, 4H), 1.55 (m, 1H), 0.37 (m, 4H) ppm. <sup>13</sup>C NMR (75 MHz, CDCl<sub>3</sub>) δ 157.66, 157.43, 140.67, 129.99, 129.71, 124.35, 123.38, 120.00, 119.02, 117.76, 63.00, 53.60, 52.23, 38.75, 6.01 ppm. HRMS m/z [M+H]<sup>+</sup> calcd for C<sub>20</sub>H<sub>25</sub>N<sub>2</sub>O 309.1991; found 309.1996.

**1-Cyclopentyl-4-(3-phenoxybenzyl)piperazine (4.17g)**

The title compound was synthesized according to the general procedure using **4.8** (200 mg, 0.760 mmol) and **4.16g** (141 mg, 0.912 mmol). The title compound was obtained after silica gel flash column chromatography (using a mixture of heptane and ethylacetate in a ratio of 6:4 as mobile phase) as a colorless oil (202 mg, 79%). <sup>1</sup>H NMR (300 MHz, CDCl<sub>3</sub>) δ 7.34-7.22 (m, 3H), 7.10-6.97 (m, 5H), 6.86 (m, 1H), 3.49 (s, 2H), 2.45 (m, 8H), 1.85 (m, 2H), 1.67 (m, 2H), 1.52 (m, 2H), 1.38 (m, 2H) ppm. <sup>13</sup>C NMR (75 MHz, CDCl<sub>3</sub>) δ 157.67, 157.42, 140.56, 129.98, 129.70, 124.37, 123.37, 120.02, 119.02, 117.76, 67.85, 62.94, 53.22, 52.61, 30.71, 24.43 ppm. HRMS m/z [M+H]<sup>+</sup> calcd for C<sub>22</sub>H<sub>29</sub>N<sub>2</sub>O 337.2294; found 337.2316.

**1-Cyclohexyl-4-(3-phenoxybenzyl)piperazine (4.17h)**

The title compound was synthesized according to the general procedure using **4.8** (300 mg, 1.14 mmol) and **4.16h** (223 mg, 1.71 mmol). The title compound was obtained after silica gel flash column

chromatography (using a mixture of heptane and ethyl acetate in a ratio of 6:4 as mobile phase) as a colorless oil (224 mg, 81%). <sup>1</sup>H NMR (300 MHz, CDCl<sub>3</sub>) δ 7.35-7.23 (m, 3H), 7.12-6.97 (m, 5H), 6.87 (m, 1H), 3.52 (s, 2H), 2.89 (br s, 4H), 2.72 (br s, 4H), 1.84 (m, 2H), 1.65 (m, 2H), 1.30 (m, 1H), 1.15 (m, 5H) ppm. <sup>13</sup>C NMR (75 MHz, CDCl<sub>3</sub>) δ 157.65, 157.48, 139.96, 130.01, 129.87, 124.21, 123.52, 119.72, 119.10, 117.95, 64.94, 62.34, 51.54, 48.94, 28.06, 25.89, 25.72 ppm. HRMS m/z [M+H]<sup>+</sup> calcd for C<sub>23</sub>H<sub>31</sub>N<sub>2</sub>O 351.2431; found 351.2427.

#### **1-Cycloheptyl-4-(3-phenoxybenzyl)piperazine (4.17i)**

The title compound was synthesized according to the general procedure using **4.8** (200 mg, 0.760 mmol) and **4.16i** (166 mg, 0.912 mmol). The title compound was obtained after silica gel flash column chromatography (using a mixture of heptane and ethyl acetate in a ratio of 6:4 as mobile phase) as a colorless oil (224 mg, 81%). <sup>1</sup>H NMR (300 MHz, CDCl<sub>3</sub>) δ 7.31-7.19 (m, 3H), 7.07-6.97 (m, 5H), 6.83 (m, 1H), 3.45 (s, 2H), 2.50 (m, 8H), 1.78 (m, 2H), 1.62 (m, 2H), 1.43 (m, 8H) ppm. <sup>13</sup>C NMR (75 MHz, CDCl<sub>3</sub>) δ 157.70, 157.44, 140.72, 129.96, 129.67, 124.35, 123.34, 120.01, 119.01, 117.74, 65.29, 62.97, 53.66, 48.58, 30.19, 28.43, 25.99 ppm. HRMS m/z [M+H]<sup>+</sup> calcd for C<sub>24</sub>H<sub>33</sub>N<sub>2</sub>O 365.2587; found 365.2617.

#### **1-(Cyclohexylmethyl)-4-(3-phenoxybenzyl)piperazine (4.17j)**

The title compound was synthesized according to the general procedure using **4.8** (330 mg, 1.25 mmol) and **4.16j** (274 mg, 1.50 mmol). The title compound was obtained after silica gel flash column chromatography (using a mixture of heptane and ethyl acetate in a ratio of 6:4 as mobile phase) as a colorless oil (386 mg, 84%). <sup>1</sup>H NMR (300 MHz, CDCl<sub>3</sub>) δ 7.32-7.20 (m, 3H), 7.08-6.96 (m, 5H), 6.84 (m, 1H), 3.46 (s, 2H), 2.43 (m, 8H), 2.09 (d, *J* = 7.1 Hz, 2H), 1.70 (m, 5H), 1.43 (m, 1H), 1.17 (m, 3H), 0.84 (m, 2H) ppm. <sup>13</sup>C NMR (75 MHz, CDCl<sub>3</sub>) δ 157.65, 157.38, 140.77, 129.98, 129.69, 124.37, 123.36, 120.00, 119.00, 117.71, 66.02, 63.02, 53.95, 53.39, 35.30, 32.27, 27.11, 26.47 ppm. HRMS m/z [M+H]<sup>+</sup> calcd for C<sub>24</sub>H<sub>33</sub>N<sub>2</sub>O 365.25872; found 365.2616.

#### ***tert*-Butyl 4-(3-phenoxybenzyl)piperazine-1-carboxylate (4.17k)**

The title compound was synthesized according to the general procedure using **4.8** (1.50 g, 5.70 mmol) and **4.3a** (2.12 g, 11.40 mmol). The title compound was obtained after silica gel flash column chromatography (using a mixture of heptane and ethyl acetate in a ratio of 6:4 as mobile phase) as a colorless oil (1.71 g, 81%). <sup>1</sup>H NMR (300 MHz, CDCl<sub>3</sub>) δ 7.33-7.21 (m, 3H), 7.09-6.97 (m, 5H), 6.87 (m, 1H), 3.46 (s, 2H), 3.38 (m, 4H), 2.35 (m, 2H), 1.44 (s, 9H) ppm.

#### **4-(3-Phenoxybenzyl)piperazine hydrochloride (4.18)**

To a solution of HCl in cyclopentylmethylether (3M, 5 ml) was added *tert*-butyl 4-(3-phenoxybenzyl)piperazine-1-carboxylate (1 g, 2.71 mmol). The reaction was stirred at room temperature overnight under a nitrogen atmosphere. Upon completion, the solvent was evaporated yielding the desired compound in quantitative yield. <sup>1</sup>H NMR (300 MHz, MeOD) δ 7.54-7.31 (m, 5H), 7.22-7.06 (m, 4H), 4.51 (s, 2H), 3.64 (s, 8H) ppm. <sup>13</sup>C NMR (75 MHz, MeOD) δ 158.03, 156.13, 130.28, 129.51, 129.42, 125.42, 123.44, 120.60, 119.56, 118.74, 59.53, 40.25 ppm.

#### 4.5.1.6. Synthesis of phenoxybenzylpiperazine urea analogues

##### General Procedure

To a solution of **4.18** (1 eq) in dichloromethane was added diisopropylethylamine (1.4 eq) and the appropriate isocyanate (0.9 eq). The reaction mixture was stirred at room temperature overnight. Upon completion of the reaction, the solvent was evaporated and the crude mixture was partitioned between water and ethyl acetate. The water layer was extracted with ethyl acetate. The combined organic phases were washed with water and brine, dried over MgSO<sub>4</sub> and evaporated to dryness. The crude residue was purified by silica gel flash column chromatography with an appropriate solvent mixture as mobile phase yielding the desired compounds. The following compounds were made according to this procedure.

##### ***N*-Cyclohexyl-4-(3-phenoxybenzyl)piperazine-1-carboxamide (4.19a)**

The title compound was synthesized according to the general procedure using **4.18** (200 mg, 0.656 mmol) and cyclohexyl isocyanate (73 mg, 0.591 mmol). The title compound was obtained after silica gel flash column chromatography (using a mixture of dichloromethane and methanol in a ratio of 96:4 as mobile phase) as a colorless oil (208 mg, 81%). <sup>1</sup>H NMR (300 MHz, CDCl<sub>3</sub>) δ 7.34-7.23 (m, 3H), 7.11-6.97 (m, 5H), 6.87 (m, 1H), 4.31 (m, 1H), 3.61 (m, 1H), 3.48 (s, 2H), 3.32 (m, 4H), 2.40 (m, 4H), 1.91 (m, 2H), 1.69 (m, 3H), 1.33 (m, 2H), 1.11 (m, 4H) ppm. <sup>13</sup>C NMR (75 MHz, CDCl<sub>3</sub>) δ 157.55, 157.38, 140.37, 130.01, 129.81, 124.14, 123.48, 119.72, 119.07, 117.86, 62.85, 52.97, 49.70, 44.06, 34.26, 25.99, 25.38 ppm. HRMS m/z [M+H]<sup>+</sup> calcd for C<sub>21</sub>H<sub>27</sub>N<sub>2</sub>O<sub>3</sub> 394.24888; found 394.2485.

##### **4-(3-Phenoxybenzyl)-*N*-phenylpiperazine-1-carboxamide (4.19b)**

The title compound was synthesized according to the general procedure using **4.18** (200 mg, 0.656 mmol) and phenyl isocyanate (70 mg, 0.591 mmol). The title compound was obtained after silica gel flash column chromatography (using a mixture of dichloromethane and methanol in a ratio of 98:2 as mobile phase) as a white solid (194 mg, 76%). <sup>1</sup>H NMR (300 MHz, CDCl<sub>3</sub>) δ 7.36-7.23 (m, 7H), 7.12-6.99 (m, 6H), 6.89 (m, 1H), 6.46 (s, 1H), 3.50 (s, 2H), 3.56 (m, 4H), 2.44 (m, 4H) ppm. <sup>13</sup>C NMR (75 MHz, CDCl<sub>3</sub>) δ 157.67, 157.55, 157.32, 140.26, 139.35, 130.03, 129.86, 129.14, 124.12, 123.53, 123.38, 120.29, 119.71, 119.12, 117.93, 62.80, 52.97, 44.45 ppm. HRMS m/z [M+H]<sup>+</sup> calcd for C<sub>21</sub>H<sub>27</sub>N<sub>2</sub>O<sub>3</sub> 388.2019; found 388.2017.

##### ***N*-Benzyl-4-(3-phenoxybenzyl)piperazine-1-carboxamide (4.19c)**

The title compound was synthesized according to the general procedure using **4.18** (200 mg, 0.656 mmol) and benzyl isocyanate (80 mg, 0.591 mmol). The title compound was obtained after silica gel flash column chromatography (using a mixture of dichloromethane and methanol in a ratio of 96:4 as mobile phase) as a white solid (221 mg, 84 %). <sup>1</sup>H NMR (300 MHz, CDCl<sub>3</sub>) δ 7.33-7.20 (m, 8H), 7.11-6.97 (m, 5H), 6.87 (m, 1H), 4.83 (m, 1H), 4.37 (d, *J* = 5.5 Hz, 2H), 3.46 (s, 2H), 3.34 (m, 4H), 2.38 (m, 4H) ppm. <sup>13</sup>C NMR (75 MHz, CDCl<sub>3</sub>) δ 157.91, 157.64, 157.56, 140.33, 139.80, 130.02, 129.83, 128.89, 128.02, 127.57, 124.13, 123.51, 119.71, 119.11, 117.89, 62.83, 52.97, 45.28, 44.18 ppm. HRMS m/z [M+H]<sup>+</sup> calcd for C<sub>21</sub>H<sub>27</sub>N<sub>2</sub>O<sub>3</sub> 402.2176; found 402.2168.

**Methyl 5-(4-(3-phenoxybenzyl)piperazin-1-yl)pentanoate (4.20)**

To a solution of **4.18** (200 mg, 0.656 mmol) in ethanol (5 ml) was added  $K_2CO_3$  (227 mg, 1.64 mmol) and methyl 5-bromovalerate (154 mg, 0.787 mmol). The mixture was heated to 60°C and stirred overnight. Upon completion, the solvent was evaporated and the crude residue was partitioned between water and ethyl acetate. The combined organic layers were washed with water and brine, dried over  $MgSO_4$  and evaporated. The crude residue was purified by silica gel flash column chromatography (using a mixture of dichloromethane and methanol in a ratio of 96:4 as mobile phase) to yield the title compound along with its ethyl ester as a colorless oil in a ratio of 1:2 (163 mg, 65%).  $^1H$  NMR (300 MHz,  $CDCl_3$ )  $\delta$  7.34-7.22 (m, 3H), 7.10-6.97 (m, 5H), 6.87 (m, 1H), 4.11 (q,  $J = 7.1$  Hz, 1.37H, ethyl ester), 3.65 (s, 0.93H, methyl ester), 3.48 (s, 2H), 2.49 (s, 8H), 2.33 (m, 4H), 1.61 (m, 4H), 1.23 (t,  $J = 7.1$  Hz, 2.46H, ethyl ester) ppm.  $^{13}C$  NMR (75 MHz,  $CDCl_3$ )  $\delta$  173.75, 157.65, 157.47, 140.60, 129.96, 129.70, 124.27, 123.37, 119.90, 119.02, 117.77, 62.85, 60.48, 58.38, 53.40, 53.07, 51.71, 34.43, 34.15, 26.44, 23.22, 14.53 ppm.

**5-(4-(3-Phenoxybenzyl)piperazin-1-yl)pentan-1-ol (4.21)**

To a solution of **4.23** (110 mg, 0.277 mmol) in dry THF (3 ml) at -78°C was added DIBAL solution (1M in THF, 0.693 ml, 0.693 mmol) dropwise. After addition, the reaction was warmed to room temperature and stirred overnight. After reaction completion, Rochelle salt (291 mg, 1.39 mmol) was dissolved in water and added to the solution dropwise. The mixture was then extracted with ethyl acetate and the combined organics were washed with water and brine, dried using  $MgSO_4$  and evaporated to dryness. The resulting crude residue was purified by silica gel flash column chromatography (using a mixture of dichloromethane and methanol in a ratio of 92:8 as mobile phase) yielding the desired compound as a colorless oil (71 mg, 72%).  $^1H$  NMR (300 MHz,  $CDCl_3$ )  $\delta$  7.34-7.22 (m, 3H), 7.10-6.97 (m, 5H), 6.87 (m, 1H), 3.61 (t,  $J = 6.3$  Hz, 2H), 3.50 (s, 2H), 2.54 (m, 10H), 1.59 (m, 4H), 1.41 (m, 2H) ppm.  $^{13}C$  NMR (75 MHz,  $CDCl_3$ )  $\delta$  157.57, 140.16, 130.01, 129.83, 124.26, 123.48, 119.81, 119.08, 117.90, 62.57, 58.35, 53.13, 52.10, 32.41, 25.72, 23.75 ppm. HRMS  $m/z$   $[M+H]^+$  calcd for  $C_{22}H_{31}N_2O_2$  355.2380; found 355.2404.

**4.5.2. Biological assays****4.5.2.1. Cells, ligands and buffer solutions**

HuT78 cells in RPMI-1640 medium supplemented with 10% FBS and 2 mM L-glutamine were obtained from ATCC. U87CD4 cells in DMEM medium supplemented with 10% FBS, 1% of 10  $\mu$ M 4-(2-hydroxyethyl)-1-piperazineethanesulfonic acid (HEPES) solution and 200 ng/ml G418 were obtained from ATCC. The utilized ligands CCL1<sup>AF647</sup> and CCL1 were obtained from ALMAC and R&D systems respectively. The assay buffer was prepared by adding 40 ml of HEPES solution (10  $\mu$ M) to 200 ml of Hank's Balanced Salt Solution (HBSS, 10x, no phenol red, no sodium bicarbonate). Ultrapure water was added till a final volume of 2 liter was obtained after which 4g of bovine serum albumin was added. The mixture was stirred until a clear solution was obtained. The pH was adjusted to 7.4 by adding a

solution of NaOH. Final filtration of the mixture gave the assay buffer used in both the binding assay and the FLIPR® assay. FLIPR® Calcium 6 Evaluation Kit was obtained from Molecular Devices

#### 4.5.2.2. *Flow cytometry binding assay*

HuT78 cells were harvested and centrifuged at 400G for 5 min at room temperature. The supernatant was discarded and the cells were washed once with assay buffer and centrifuged once more at 400G. The supernatant was again discarded and the cells were resuspended in assay buffer at a concentration of  $2 \times 10^6$  cells/ml. Compound dilutions in 100  $\mu$ l of assay buffer were prepared in a 96-well round-bottom microtiter plate to which 50  $\mu$ l of the prepared cell suspension was added and mixed. The plates were incubated at room temperature for 15 minutes in the dark. 50  $\mu$ L of CCL1<sup>AF647</sup> (the final working concentration is 2 nM) was added to the 96-well plate and was mixed well. Further incubation for 30 minutes at room temperature in the dark was followed by washing the cells twice with 200  $\mu$ l of assay buffer. The cells were resuspended in a 1% solution of paraformaldehyde solution in 200  $\mu$ l of phosphate-buffered saline (PBS) and the fluorescence was measured by flow cytometry in a FACSCanto™ II device.

#### 4.5.2.3. *FLIPR® Calcium mobilization assay*

A 0.1% gelatin solution was prepared by adding 1 g of gelatin to 100 mL PBS to obtain a 1% solution which was diluted 10 times. This solution was used to coat black-walled polystyrene 96-well plates with clear bottom before a two hour incubation period at room temperature. The gelatin solution is removed and the plates were washed twice with 200  $\mu$ l of PBS per well. 100  $\mu$ l of cell suspension ( $2 \times 10^5$  cells/mL) per well is added. After incubating overnight at 37°C and 5% CO<sub>2</sub> atmosphere, the supernatant is removed by flipping over the plates and 80  $\mu$ l of loading dye (equal volume of cell culture medium and loading buffer, obtained by dissolving component A in 10 ml of component B from the FLIPR® Calcium 6 Evaluation Kit) is added in each well. The plates were incubated for 2 hours at 37°C and 5% CO<sub>2</sub> atmosphere. Compound dilutions were prepared in 50  $\mu$ l of assay buffer in a 96-well round-bottom plate. Likewise, a CCL1 solution (250 ng/ml) was added to 50  $\mu$ l of assay buffer in another 96-well round-bottom. Compound solution (20  $\mu$ l) and 25  $\mu$ l of CCL1 solution were added to the cell plates and fluorescence of all plates were measured in a FLIPR® Tetra Device.

### 4.5.3. **General safety aspects**

In context of health and safety, documents provided by the lab of medicinal chemistry and the HSE department of the KU Leuven were signed: Binding rules – Laboratory of medicinal chemistry. Based on the European Regulation (EC) No. 1272/2008) on classification, labeling and packaging of chemicals and mixtures, chemicals are classified according to their hazardous properties to humans and the environment into 5 categories (E4+, E4, E3, E2 and E1). Chemical operations were carried out in compliance with these documents and risk analyses were created according to the template provided by the HSE department and the information retrieved from the respective material safety data sheet (MSDS) for every used chemical and solvent. Additionally, personal safety measures were enforced at

all times: wearing lab coats, safety goggles, long trousers and closed shoes. Furthermore, special precautions like wearing gloves or a dust mask were taken in case of handling especially hazardous reagents or devices to guarantee optimal safety.



## 4.6. References

- (1) Griffith, J. W.; Sokol, C. L.; Luster, A. D., Chemokines and Chemokine Receptors: Positioning Cells for Host Defense and Immunity. *Annu. Rev. Immunol.* **2014**, *32* (1), 659-702.
- (2) Ghosh, S.; Elder, A.; Guo, J.; Mani, U., et al., Design, Synthesis, and Progress toward Optimization of Potent Small Molecule Antagonists of CC Chemokine Receptor 8 (CCR8). *J. Med. Chem.* **2006**, *49* (9), 2669-2672.
- (3) Hughes, C. E.; Nibbs, R. J. B., A guide to chemokines and their receptors. *The FEBS Journal* **2018**, *285* (16), 2944-2971.
- (4) Karin, N., Chemokines and cancer: new immune checkpoints for cancer therapy. *Curr. Opin. Immunol.* **2018**, *51*, 140-145.
- (5) Barsheshet, Y.; Wildbaum, G.; Levy, E.; Vitsenshtein, A., et al., CCR8+ FOXP3+Tregcells as master drivers of immune regulation. *Proc. Natl. Acad. Sci. U. S. A.* **2017**, *114* (23), 6086-6091.
- (6) Villarreal, D. O.; Huillier, A.; Armington, S.; Mottershead, C., et al., Targeting CCR8 induces protective antitumor immunity and enhances vaccine-induced responses in colon cancer. *Cancer Res.* **2018**, *78* (18), 5340-5348.
- (7) Iellem, A.; Mariani, M.; Lang, R.; Recalde, H., et al., Unique Chemotactic Response Profile and Specific Expression of Chemokine Receptors Ccr4 and Ccr8 by Cd4+Cd25+Regulatory T Cells. *J. Exp. Med.* **2001**, *194* (6), 847-853.
- (8) Haskell, C. A.; Horuk, R.; Liang, M.; Rosser, M., et al., Identification and Characterization of a Potent, Selective Nonpeptide Agonist of the CC Chemokine Receptor CCR8. *Mol. Pharmacol.* **2006**, *69* (1), 309-316.
- (9) Rummel, P.; Arfelt, K.; Baumann, L.; Jenkins, T., et al., Molecular requirements for inhibition of the chemokine receptor CCR8 – probe-dependent allosteric interactions. *Br. J. Pharmacol.* **2012**, *167* (6), 1206-1217.
- (10) Petersen, T. P.; Mirsharghi, S.; Rummel, P. C.; Thiele, S., et al., Multistep Continuous-Flow Synthesis in Medicinal Chemistry: Discovery and Preliminary Structure–Activity Relationships of CCR8 Ligands. *Chem. Eur. J.* **2013**, *19* (28), 9343-9350.
- (11) Onuffer, J. J.; Horuk, R., Chemokines, chemokine receptors and small-molecule antagonists: recent developments. *Trends Pharmacol. Sci.* **2002**, *23* (10), 459-467.
- (12) Brown, G. A.; Congreve, M. S.; Pickworth, M.; Tehan, B. G. Heterocyclic compounds having activity as modulators of muscarinic M1 and/or M4 receptors in the treatment of CNS diseases and pains. 2018069732, 2018.
- (13) Dou, D.; He, G.; Mandadapu, S. R.; Aravapalli, S., et al., Inhibition of noroviruses by piperazine derivatives. *Bioorg. Med. Chem. Lett.* **2012**, *22* (1), 377-379.
- (14) Fracchiolla, G.; Lavecchia, A.; Laghezza, A.; Piemontese, L., et al., Synthesis, biological evaluation, and molecular modeling investigation of chiral 2-(4-chloro-phenoxy)-3-phenyl-propanoic acid derivatives with PPAR $\alpha$  and PPAR $\gamma$  agonist activity. *Bioorg. Med. Chem.* **2008**, *16* (21), 9498-9510.
- (15) Zhu, J.; Cui, D.; Li, Y.; He, J., et al., Enantioselective amination of nitroolefins under base-free and water-rich conditions using chiral bifunctional phase-transfer catalysts. *Org. Biomol. Chem.* **2018**, *16* (16), 3012-3017.
- (16) Guandalini, L.; Martini, E.; Di Cesare Mannelli, L.; Dei, S., et al., Influence of ring size on the cognition-enhancing activity of DM235 and MN19, two potent nootropic drugs. *Bioorg. Med. Chem. Lett.* **2012**, *22* (5), 1936-1939.
- (17) Yang, L.-X. Nitrogen-based homo-camptothecin derivatives. 2003.
- (18) Schoofs, G.; Van Hout, A.; D'Huys, T.; Schols, D., et al., A Flow Cytometry-based Assay to Identify Compounds That Disrupt Binding of Fluorescently-labeled CXC Chemokine Ligand 12 to CXC Chemokine Receptor 4. *J. Vis. Exp.* **2018**, (133).
- (19) Claes, S.; D'Huys, T.; Van Hout, A.; Schols, D., et al., A Kinetic Fluorescence-based Ca<sup>2+</sup> Mobilization Assay to Identify G Protein-coupled Receptor Agonists, Antagonists, and Allosteric Modulators. *J Vis Exp* **2018**, (132).



## ***Chapter 5: General discussion and future perspectives***

### **5.1. General discussion**

In this doctoral thesis, three underexplored drug targets with therapeutic potential in the fields of virology (**Chapter 2**) and immunology (**Chapters 3 and 4**) were selected. The three projects followed the same strategy: starting from a hit (either discovered in house via a screening campaign or copied from literature), systematic structural variations were carried out in order to improve the affinity of the hits for the desired target.

**Chapter 2** described the synthesis, AAK1 affinity studies and antiviral evaluation of pyrrolo[2,3-*b*]pyridine analogues. AAK1 is a key regulator of CME by phosphorylating the  $\mu_1$ -subunit of AP2 (AP2M1) which allows this protein to recognize its cargo molecules at the cell membrane and allows the recruitment of CT to the cell membrane.<sup>1,2</sup> Previous research revealed that several unrelated viruses (such as DENV, EBOV and HCV) hijack this mechanism to enter and infect the host cell.<sup>3,4</sup> Furthermore, these viruses also exploit this host system to exit the cells.<sup>2</sup> No selective antiviral therapy is available for DENV and EBOV infections and treatment relies on general supportive care and symptomatic drug treatment.<sup>5-7</sup> The selective inhibition of AAK1 offers the possibility of a broad spectrum antiviral strategy as CCV are vital for infection and survival of various, unrelated viruses, and hence, this strategy deviates from the one-bug-one-drug approach.<sup>3</sup> Additionally, targeting a host or cellular factor provides a novel strategy for the treatment of viral infections. To start off the project a suitable hit compound was found in literature (**Figure 1.18, 1.15**)<sup>8</sup> with moderate AAK1 affinity. After confirming the AAK1 affinity ( $K_D = 120$  nM) and its antiviral activity against DENV ( $EC_{50} = 8.37$   $\mu$ M), we embarked on an optimization campaign to improve both the binding affinity and the antiviral activity against DENV, leading to the discovery of two compounds (**2.7g** and **2.20b**) that displayed low nanomolar activity in the binding assay. Additionally, they were endowed with an improved antiviral activity against DENV. The correlation of the antiviral effect and functional AAK1 inhibition was investigated by measurement of the phosphorylation level of AP2M1 after treatment with compounds **1.15**, **2.7g** and **2.20b**. Results showed that these compounds indeed reduce the amount of phosphorylated AP2M1, indicating the modulation potential of the compounds. In future work, a gain of function assay can be established to determine if the antiviral effect of the compounds can be reversed by overexpression of AAK1.

To check for the potential broad spectrum antiviral activity, compounds were also evaluated for their activity against an unrelated virus. EBOV was selected, and it was shown that, although hit compound **1.15** completely lacked anti-EBOV activity, the two potent AAK1 inhibitors **2.20b** and **2.7g** did display anti-EBOV activity in the low  $\mu$ M range ( $EC_{50}$  values of 1.59  $\mu$ M and 4.24  $\mu$ M, respectively). This slight drop compared to the anti-DENV activity can potentially be attributed to the different assay conditions used or to the compounds targeting an additional virus specific protein in the DENV assay.

Despite the promising antiviral data of both lead compounds, a number of issues are still present. First of all, the cytotoxicity of both compounds **2.7g** and **2.20b** is a point of concern, as the cell viability drops at concentrations higher than the  $EC_{90}$  values and are reported as having a  $CC_{50}$  greater than 10  $\mu$ M. However, the downward direction of the graph indicates that the exact  $CC_{50}$  values are very close to 10  $\mu$ M and low selectivity indexes are obtained. It is therefore important to evaluate the cytotoxicity of the compounds at higher concentrations in order to be able to calculate exact  $CC_{50}$  values. Moreover, the cytotoxicity can also be studied over a longer period of time (instead of a readout after 48 hours) and against a wider panel of tumor cell lines.

The most potent AAK1 inhibitor **2.20b** shows poor kinase selectivity when profiled in a panel of over four hundred kinases, although its selectivity profile is slightly better than the reference AAK1 inhibitor sunitinib. It is therefore difficult to conclude that its antiviral efficacy is ascribed to AAK1 inhibition. Multiple other cellular kinases (such as ABL1 and KIT) that are essential for the viral lifecycle are also affected by compound **2.20**.<sup>9</sup> Therefore, compound **2.20** is not an ideal tool compound to elucidate the role of AAK1 in viral infection. This needs to be addressed in future research. During writing of this PhD thesis, a potent, selective AAK1 inhibitor was published (**Figure 5.1**), although no antiviral data were reported for this compound.<sup>10</sup> It's worthwhile to investigate the antiviral properties of this compound.

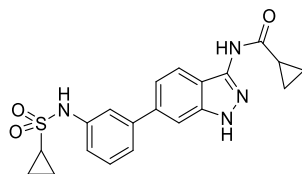


**Figure 5.1.** Selective AAK1 inhibitor ( $K_i = 8.3$  nM,  $S(10) = 0.005$ )

Another option is to improve the kinase selectivity of the current lead compounds **2.7g** and **2.20b** via molecular modelling. As the X-ray crystal structure of AAK1 and its closest kinase relatives, as well as the binding mode of **1.15** in AAK1 are known, it is possible to search for additional binding points that can be exploited to increase the selectivity and potency of the compounds.

However, there is a large difference between the AAK1 binding affinity (low nM) and antiviral activity (low  $\mu$ M). A number of reasons could explain this discrepancy. A poor cellular permeability will prevent to reach high intracellular concentrations of the compounds, having a negative impact on its antiviral activity. According to the predictions shown in **Table 5.1**, compounds **2.7g** and **2.20b** are compliant with the Lipinski rules of 5 and the extended Veber rules, suggesting that cellular permeability should not be an issue.

	<b>2.7g</b>	<b>2.20b</b>
MW*	374.40	355.40
H-bond donors	2	1
H-bond acceptors	5	4
LogP**	1.87	3.01
tPSA*** (Å <sup>2</sup> )	84.31	55.21
# of rotatable bonds	7	7

\*MW = molecular weight, \*\*LogP = partition coefficient, \*\*\*tPSA = total polar surface area.

**Table 5.1.** In silico prediction values of compounds **2.7g** and **2.20b**

To experimentally confirm this cellular permeability can be investigated either via the Caco-2 or via the parallel artificial membrane permeability assay (PAMPA). Caco-2 cells possess the unique characteristic to spread out as a monolayer, therefore they can be placed as a membrane between two compartments (a donor and acceptor). Measurement of the concentration of drug in the acceptor compartment gives an accurate estimation of the permeability *in vivo*.<sup>11</sup> A PAMPA assay uses an artificial membrane<sup>12</sup> between the two compartments and only takes into account passive diffusion making the Caco-2 assay the preferred method.

Alternatively, the inability of the AAK1 inhibitors to compete with the high, intracellular ATP concentrations might explain their rather moderate antiviral activity. To assess the influence of ATP concentration on AAK1 inhibition by the compound, the compounds can be evaluated in a kinetic, biochemical AAK1 assay, using different concentrations of the AAK1 inhibitor and radioactively labeled (<sup>32</sup>P) ATP.<sup>13</sup> For the determination of the AAK1 activity in an ATP-competitive way in cells, a NanoBRET target engagement assay can be employed. This assay is based on the ability of the inhibitor to effectively compete with a fluorescent tracer molecule bound to the ATP site. AAK1 fused with a NanoLuc luciferase produces an observable bioluminescence resonance energy transfer (BRET) signal in the absence of inhibitor. A concomitant loss of the signal occurs with increasing concentrations of an ATP-competitive AAK1 inhibitor.<sup>14</sup>

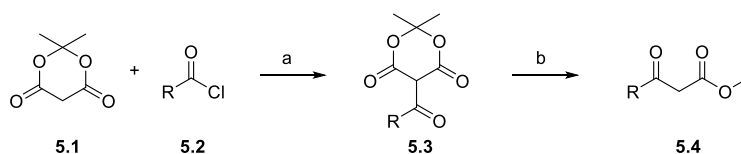
Besides its antiviral potential, AAK1 has also been associated with other disorders like neuropathic pain and Parkinson's disease.<sup>15</sup> The most active AAK1 inhibitors **2.20b** and **2.7g** deserve to be investigated as potential treatment for these diseases. In addition, it has been shown that the pyrrolo[2,3-*d*]pyridines are ATP-competitive kinase inhibitors and therefore they can be implemented into screening libraries targeting other kinases and non-kinase ATP-dependent factors.

In **Chapter 3**, the synthesis and biological evaluation of MRGPRX2 antagonists were described. MRGPRX2 is an orphan GPCR present in the central nervous system (dorsal ganglia)<sup>16</sup>, but also on mast cells (MC), and especially in the MC<sub>TC</sub> subset.<sup>17-19</sup> The MC<sub>TC</sub> subset is mainly present in the skin

as a primary protection barrier against external threats.<sup>20,21</sup> Mast cells mediate immune responses by releasing a plethora of inflammatory mediators like histamine and cytokines.<sup>22</sup> MC degranulate during allergic responses and are responsible for the discomforts experienced by an allergic reaction like itch, redness and edemas.<sup>23</sup> Therefore, MRGPRX2 antagonism is a promising strategy for the treatment of various allergic and inflammatory disorders, like asthma, urticaria and atopic dermatitis.<sup>19,22,24</sup> A small screening campaign of 1600 structurally diverse heterocycles provided a set of four hit compounds (**1.16-19**) exhibiting low  $\mu\text{M}$  activity in a  $\beta$ -arrestin assay. The common benzo[4,5]imidazo[1,2-*a*]pyrimidin-4(10*H*)-one core skeleton was taken as a suitable scaffold for further SAR investigation. It led to the discovery of three promising compounds (**3.18a**, **3.18d** and **3.27c**) with MRGPRX2 antagonism in the  $\beta$ -arrestin assay in the nanomolar range. However, the  $\beta$ -arrestin assay is a G-protein independent assay and it will be interesting to check the effect of the compounds on G-protein coupled events. This can be achieved by evaluate the compounds in a functional assay with different read-outs, such as a fluorescent calcium mobilization assay (FLIPR), as utilized in **Chapter 4**, or an AlphaScreen™ assay (both for cAMP and  $\text{IP}_3$  detection).<sup>25</sup> The AlphaScreen™ assay relies on a chemiluminescent signal produced by a biotinylated substrate (cAMP or  $\text{IP}_3$ ) when it is acting as bridge between a donor and acceptor bead. This bridge brings the two beads in close enough proximity for the donor to excite the acceptor beads by producing singlet oxygen. The disruption of the bridge by a rise in intracellular  $\text{IP}_3$  concentration results in a concomitant drop of chemiluminescence signal. Prestimulation of the cells with forskolin increases the intracellular cAMP concentration by activating adenylate cyclase and results in a signal drop. Binding of an agonist to MRGPRX2 will induce  $\text{G}_{i/o}$  and lead to an inhibition of adenylate cyclase resulting in a recovery of the signal.<sup>26</sup> Additionally, a binding assay is useful to determine the affinity of the compounds for MRGPRX2. An example can be found in the Tag-Lite™ competition assay where the GPCR is fused with a SNAP tag which can be labeled with a fluorophore. Cells expressing these labeled receptors are then incubated with a Homogeneous Time Resolved Fluorescence (HTRF) labeled ligand producing a Fluorescence resonance energy transfer (FRET) signal.<sup>27</sup> Subsequent addition of an unlabeled antagonist leads to a decrease in observed signal. A dose-response curve is used to determine the  $\text{IC}_{50}$  from which the  $K_i$  can be calculated.

A mast cell degranulation assay is essential for the proof-of-concept that MRGPRX2 antagonism inhibits mast cell degranulation. Tryptase is a protease present in all mast cells that is used to detect mast cell degranulation, by adding a *para*-nitroaniline (*pNA*) labeled protein to the medium. The tryptase will release *pNA*, which can then be measured spectrophotometrically.<sup>28</sup> In addition, no information is known about the selectivity of the compounds with respect to other members of the MRGPRX family and other GPCRs. Therefore, a selectivity profiling should be conducted with the lead compounds.

No physicochemical data of this compound class are available, but lab experience during the synthesis of benzo[4,5]imidazo[1,2-*a*]pyrimidin-4(10*H*)-one analogues indicated already the very poor solubility in common organic solvents such as methanol, dichloromethane and even DMSO. Therefore, an *in vitro* ADME profiling of the lead compounds **3.18a**, **3.18d** and **3.27c** is advisable. These assays include the determination of aqueous solubility, cellular permeability and metabolic stability. The results of these investigations will allow the medicinal chemists to address the weak points of the lead compounds. In addition, the tricyclic nature of the benzo[4,5]imidazo[1,2-*a*]pyrimidine scaffold might be problematic for its future development. Tricyclic structures are known to intercalate within the DNA leading to mutations and possibly cancer. With these issues in mind, further structural modifications should focus on improving the aqueous solubility and reducing the flat, aromatic character of the compounds. Preliminary work on structural variation indicate that this type of chemistry is not amenable to the rapid exploration of SAR indicated by the low yields of both the  $\beta$ -ketoesters and the final compounds. A way to circumvent the low yields of the  $\beta$ -ketoesters, a different approach can be used by exploiting the special characteristics of Meldrum's acid (**5.1**). This reagent, in essence a malonate ester, is more acidic than its acyclic counterpart diethyl malonate and is therefore more easily deprotonated and can subsequently act as a nucleophile towards acyl chlorides (**5.2**) generating the acyl substituted Meldrum's acids (**5.3**). When heated in the presence of methanol, transesterification and concomitant decarboxylation occur, yielding the desired  $\beta$ -ketoesters (**5.4**) (**Scheme 5.1**).



**Scheme 5.1.** *Reagents and conditions:* a) pyridine, DCM, 0°C, 3h; b) MeOH, reflux, 5h.

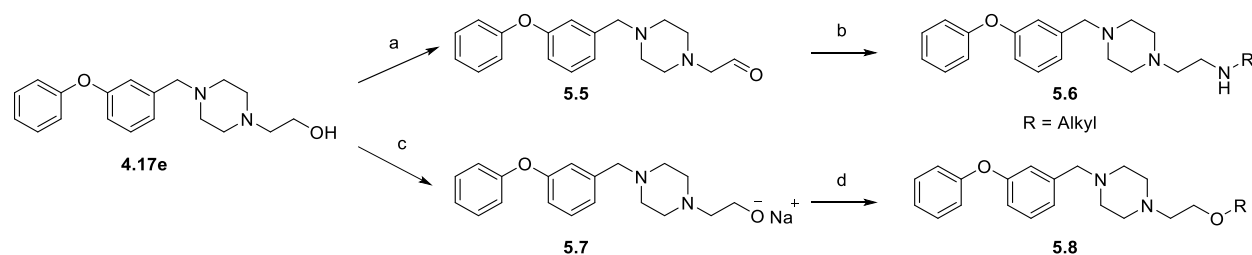
Besides working on this particular scaffold, efforts should also be directed towards the identification of alternative starting points, based on other chemotypes. This can be achieved by screening of commercial compound libraries in the MRGPRX2  $\beta$ -arrestin assay. Alternatively, a recent paper disclosed the structures of low  $\mu$ M MRGPRX2 antagonists that can be used as starting point for an optimization campaign.<sup>29</sup>

**Chapter 4** dealt with the synthesis of 3-phenoxybenzyl analogues and the evaluation of their CCR8 binding affinity and CCR8 calcium mobilization properties. Chemokines are a well-studied family of proteins involved in the migration of immune cells to infection hearths.<sup>30</sup> They are subdivided into 4 subclasses depending on the relative position of a number of cysteine residues in the conserved part of the molecule (CC, CXC, CX3C and XC).<sup>31-33</sup> Their receptors are all GPCRs that usually do not exhibit ligand selectivity, in other words one chemokine can activate multiple receptors and one receptor can be activated by multiple chemokines.<sup>32</sup> An exception to this is the ligand CCL1, as CCR8 is the only receptor known to be activated naturally by CCL1.<sup>34</sup> This fact presents an opportunity to modulate the effects of CCL1 by targeting CCR8 by small molecules. CCR8 is predominantly expressed on T<sub>reg</sub> cells and therefore plays a pivotal role in the regulation of the immune system.<sup>34,35</sup> It has been reported that

an elevated expression of CCR8 on T<sub>reg</sub> cells correlates with a poor prognosis of cancer patients.<sup>36</sup> Additionally, administration of CCL1 to mice in a model of experimental autoimmune encephalomyelitis suppresses autoimmunity.<sup>37</sup> Several CCR8 agonists based on a 3-phenoxybenzyl scaffold are known in literature.<sup>38-41</sup> After confirmation of the activity of **4.1**, obtained from literature<sup>40</sup>, in both a CCR8 binding and a calcium mobilization assay, the 3-phenoxybenzyl scaffold was taken as lead structure to further explore the SAR.

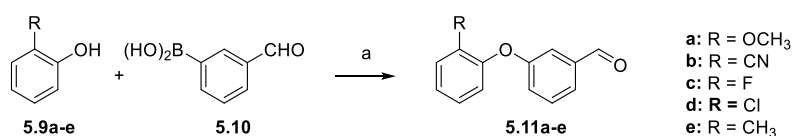
Starting from hit **4.1**, an equipotent congener **4.9c** with a pyrrolidine ring was identified. This core was therefore further exploited to evaluate the SAR of the terminal substituent. A small library of ten compounds was synthesized composed of amides, urea and a sulfonamide but all of them were completely devoid of any CCR8 agonistic activity. Despite their lack of activity as CCR8 agonists, these are drug-like compounds and worthwhile to be screened in a variety of assays. We plan to submit these compounds for a broad antiviral (retro, RNA and DNA viruses) and antitumoral screening (against 9 different cancer cell lines).

Because no increase in activity was found, focus was shifted to the SAR exploration of a second lead molecule ZK756326<sup>39</sup> (**1.9**) with a piperazine central ring. Although only a small number of compounds was prepared, some analogues were endowed with similar potency as compound **1.9**. However, it is still necessary to perform further chemistry to have access to compounds with low nanomolar CCR8 agonistic activity. New analogues can be obtained by oxidation of the terminal hydroxyl group of **4.17e** yielding an aldehyde (**5.5**). Reductive amination with various primary amines will give access to central amino derivatives (**5.6**). Another option is to alkylate the terminal alcohol group under alkaline conditions (**5.7**) with a variety of alkyl bromides to expand the structural variety of the terminal chain (**5.8**) (Scheme 5.2).



**Scheme 5.2.** Reagents and conditions. a) Dess-Martin Periodinane, DCM, rt; b) NaBH<sub>3</sub>CN, RNH<sub>2</sub>, EtOH, 50°C; c) NaH, DMF, 0°C to rt; d) RBr, DMF, 50°C.

Literature data indicate that substitution of the western ring of the 3-phenoxybenzyl moiety is favorable for CCR8 agonism.<sup>40</sup> A synthesis of the starting materials is proposed in Scheme 5.3. Ortho substituted phenols (**5.9a-e**) can be coupled via a Chan-Lam coupling to 3-formylphenylboronic acid (**5.10**), furnishing the required starting materials (**5.11a-e**).



**Scheme 5.3.** Reagents and conditions. a) Cu(OAc)<sub>2</sub>, Et<sub>3</sub>N, DCE, rt.



## 5.2. References

- (1) Pu, S.-Y.; Wouters, R.; Schor, S.; Rozenski, J., et al., Optimization of Isothiazolo[4,3-*b*]pyridine-Based Inhibitors of Cyclin G Associated Kinase (GAK) with Broad-Spectrum Antiviral Activity. *J. Med. Chem.* **2018**, *61* (14), 6178-6192.
- (2) Bekerman, E.; Neveu, G.; Shulla, A.; Brannan, J., et al., Anticancer kinase inhibitors impair intracellular viral trafficking and exert broad-spectrum antiviral effects. *J. Clin. Invest.* **2017**, *127* (4), 1338-1352.
- (3) Bekerman, E.; Einav, S., Combating emerging viral threats. *Science* **2015**, *348* (6232), 282-283.
- (4) Rodenhuis-Zybert, I. A.; Wilschut, J.; Smit, J. M., Dengue virus life cycle: viral and host factors modulating infectivity. *Cell. Mol. Life Sci.* **2010**, *67* (16), 2773-2786.
- (5) Guzman, M. G.; Gubler, D. J.; Izquierdo, A.; Martinez, E., et al., Dengue infection. *Nat. Rev. Dis. Primers* **2016**, *2*.
- (6) Gubler, D. J.; Ooi, E. E.; Vasudevan, S.; Farrar, J., *Dengue and Dengue Hemorrhagic Fever*. 2 ed.; CABI: 2014.
- (7) WHO; TDR, *Dengue: Guidelines for Diagnosis, Treatment, Prevention and Control*. WHO: France, 2009; p 147.
- (8) Bamborough, P.; Drewry, D.; Harper, G.; Smith, G. K., et al., Assessment of Chemical Coverage of Kinome Space and Its Implications for Kinase Drug Discovery. *J. Med. Chem.* **2008**, *51* (24), 7898-7914.
- (9) Clark, Margaret J.; Miduturu, C.; Schmidt, Aaron G.; Zhu, X., et al., GNF-2 Inhibits Dengue Virus by Targeting Abl Kinases and the Viral E Protein. *Cell Chem. Biol.* **2016**, *23* (4), 443-452.
- (10) Wells, C.; Couñago, R. M.; Limas, J. C.; Almeida, T. L., et al., SGC-AAK1-1: A Chemical Probe Targeting AAK1 and BMP2K. *ACS Med. Chem. Lett.* **2019**.
- (11) Van Breemen, R. B.; Li, Y., Caco-2 cell permeability assays to measure drug absorption. *Expert Opin. Drug Metab. Toxicol* **2005**, *1* (2), 175-185.
- (12) Ottaviani, G.; Martel, S.; Carrupt, P.-A., Parallel Artificial Membrane Permeability Assay: A New Membrane for the Fast Prediction of Passive Human Skin Permeability. *J. Med. Chem.* **2006**, *49* (13), 3948-3954.
- (13) Gao, L.-J.; Kovackova, S.; Šála, M.; Ramadori, A. T., et al., Discovery of Dual Death-Associated Protein Related Apoptosis Inducing Protein Kinase 1 and 2 Inhibitors by a Scaffold Hopping Approach. *J. Med. Chem.* **2014**, *57* (18), 7624-7643.
- (14) Robers, M. B.; Vasta, J. D.; Corona, C. R.; Ohana, R. F., et al., Quantitative, Real-Time Measurements of Intracellular Target Engagement Using Energy Transfer. In *Systems Chemical Biology: Methods and Protocols*, Ziegler, S.; Waldmann, H., Eds. Springer New York: New York, NY, 2019; pp 45-71.
- (15) Kostich, W.; Hamman, B. D.; Li, Y. W.; Naidu, S., et al., Inhibition of AAK1 Kinase as a Novel Therapeutic Approach to Treat Neuropathic Pain. *J. Pharmacol. Exp. Ther.* **2016**, *358* (3), 371-386.
- (16) Robas, N.; Mead, E.; Fidock, M., MrgX2 Is a High Potency Cortistatin Receptor Expressed in Dorsal Root Ganglion. *J. Biol. Chem.* **2003**, *278* (45), 44400-44404.
- (17) Bader, M.; Alenina, N.; Andrade-Navarro, M. A.; Santos, R. A., Mas and Its Related G Protein-Coupled Receptors, Mrgprs. *Pharmacol. Rev.* **2014**, *66* (4), 1080-1105.
- (18) Solinski, H. J.; Gudermann, T.; Breit, A., Pharmacology and Signaling of MAS-Related G Protein-Coupled Receptors. *Pharmacol. Rev.* **2014**, *66* (3), 570.
- (19) Manorak, W.; Idahosa, C.; Gupta, K.; Roy, S., et al., Upregulation of Mas-related G Protein coupled receptor X2 in asthmatic lung mast cells and its activation by the novel neuropeptide hemokinin-1. *Respir. Res.* **2018**, *19* (1), 1-5.
- (20) Irani, A. A.; Schechter, N. M.; Craig, S. S.; DeBlois, G., et al., Two types of human mast cells that have distinct neutral protease compositions. *Proc. Natl. Acad. Sci. U. S. A.* **1986**, *83* (12), 4464-4468.
- (21) Metcalfe, D. D.; Baram, D.; Mekori, Y. A., Mast cells. *Physiol. Rev.* **1997**, *77* (4), 1033-1079.

- (22) Méndez-Enríquez, E.; Hallgren, J., Mast Cells and Their Progenitors in Allergic Asthma. *Front. Immunol.* **2019**, *10*.
- (23) Krystel-Whittemore, M.; Dileepan, K. N.; Wood, J. G., Mast Cell: A Multi-Functional Master Cell. *Front. Immunol.* **2016**, *6*, 1-9.
- (24) Okayama, Y.; Saito, H.; Ra, C., Targeting Human Mast Cells Expressing G-Protein-Coupled Receptors in Allergic Diseases. *Allergol. Int.* **2008**, *57* (3), 197-203.
- (25) Zhang, R.; Xie, X., Tools for GPCR drug discovery. *Acta Pharmacol. Sin.* **2012**, *33* (3), 372-384.
- (26) Eglen, R. M.; Reisine, T.; Roby, P.; Rouleau, N., et al., The use of AlphaScreen technology in HTS: current status. *Curr. Chem. Genomics* **2008**, *1*, 2-10.
- (27) Degorce, F.; Card, A.; Soh, S.; Trinquet, E., et al., HTRF: A technology tailored for drug discovery - a review of theoretical aspects and recent applications. *Curr. Chem. Genomics* **2009**, *3*, 22-32.
- (28) Lavens, S. E.; Proud, D.; Warner, J. A., A sensitive colorimetric assay for the release of tryptase from human lung mast cells in vitro. *J. Immunol. Methods* **1993**, *166* (1), 93-102.
- (29) Ogasawara, H.; Furuno, M.; Edamura, K.; Noguchi, M., Novel MRGPRX2 antagonists inhibit IgE-independent activation of human umbilical cord blood-derived mast cells. *J. Leukocyte Biol* **2019**, 1-9.
- (30) Griffith, J. W.; Sokol, C. L.; Luster, A. D., Chemokines and Chemokine Receptors: Positioning Cells for Host Defense and Immunity. *Annu. Rev. Immunol.* **2014**, *32* (1), 659-702.
- (31) Koelink, P. J.; Overbeek, S. A.; Braber, S.; de Kruijf, P., et al., Targeting chemokine receptors in chronic inflammatory diseases: An extensive review. *Pharmacol. Ther.* **2012**, *133* (1), 1-18.
- (32) Hughes, C. E.; Nibbs, R. J. B., A guide to chemokines and their receptors. *The FEBS Journal* **2018**, *285* (16), 2944-2971.
- (33) Turner, M. D.; Nedjai, B.; Hurst, T.; Pennington, D. J., Cytokines and chemokines: At the crossroads of cell signalling and inflammatory disease. *Biochim. Biophys. Acta, Mol. Cell Res.* **2014**, *1843* (11), 2563-2582.
- (34) Barsheshet, Y.; Wildbaum, G.; Levy, E.; Vitenshtein, A., et al., CCR8+ FOXP3+Treg cells as master drivers of immune regulation. *Proc. Natl. Acad. Sci. U. S. A.* **2017**, *114* (23), 6086-6091.
- (35) Rummel, P.; Arfelt, K.; Baumann, L.; Jenkins, T., et al., Molecular requirements for inhibition of the chemokine receptor CCR8 – probe-dependent allosteric interactions. *Br. J. Pharmacol.* **2012**, *167* (6), 1206-1217.
- (36) Villarreal, D. O.; Huillier, A.; Armington, S.; Mottershead, C., et al., Targeting CCR8 induces protective antitumor immunity and enhances vaccine-induced responses in colon cancer. *Cancer Res.* **2018**, *78* (18), 5340-5348.
- (37) Karin, N., Chemokines and cancer: new immune checkpoints for cancer therapy. *Curr. Opin. Immunol.* **2018**, *51*, 140-145.
- (38) Onuffer, J. J.; Horuk, R., Chemokines, chemokine receptors and small-molecule antagonists: recent developments. *Trends Pharmacol. Sci.* **2002**, *23* (10), 459-467.
- (39) Haskell, C. A.; Horuk, R.; Liang, M.; Rosser, M., et al., Identification and Characterization of a Potent, Selective Nonpeptide Agonist of the CC Chemokine Receptor CCR8. *Mol. Pharmacol.* **2006**, *69* (1), 309-316.
- (40) Ghosh, S.; Elder, A.; Guo, J.; Mani, U., et al., Design, Synthesis, and Progress toward Optimization of Potent Small Molecule Antagonists of CC Chemokine Receptor 8 (CCR8). *J. Med. Chem.* **2006**, *49* (9), 2669-2672.
- (41) Petersen, T. P.; Mirsharghi, S.; Rummel, P. C.; Thiele, S., et al., Multistep Continuous-Flow Synthesis in Medicinal Chemistry: Discovery and Preliminary Structure–Activity Relationships of CCR8 Ligands. *Chem. Eur. J.* **2013**, *19* (28), 9343-9350.

## ***Chapter 6: Scientific acknowledgements, Personal contribution and Conflict of interest statement***

### **6.1. Scientific acknowledgements**

Sven Verdonck is the recipient of a doctoral fellowship of the research foundation Flanders (Grant 1S00116N). Szu-Yuan Pu is supported by the Child Health Research Institute, the Lucile Packard Foundation for Children's Health and the Stanford CSTA (grant number UL1 TR000093). This work was supported by award number W81XWH-16-1-0691 from the Department of Defense (DoD), Congressionally Directed Medical Research Programs (CDMRP), Grant 12393481 from the Defense Threat Reduction Agency (DTRA), Fundamental Research to Counter Weapons of Mass Destruction to Shirit Einav and Piet Herdewijn, and seed grant from the Stanford SPARK program. The SGC is a registered charity (number 1097737) that receives funds from AbbVie, Bayer Pharma AG, Boehringer Ingelheim, Canada Foundation for Innovation, Eshelman Institute for Innovation, Genome Canada, Innovative Medicines Initiative (EU/EFPIA) [ULTRA-DD grant no. 115766], Janssen, Merck KGaA Darmstadt Germany, MSD, Novartis Pharma AG, Ontario Ministry of Economic Development and Innovation, Pfizer, São Paulo Research Foundation-FAPESP, Takeda, and Wellcome [106169/ZZ14/Z]. Furthermore, the authors are indebted to Prof. Jef Rozenski for providing the HRMS data and to Luc Baudemprez and Prof. Eveline Lescrinier for their help in NMR spectra recordings.

### **6.2. Personal contribution**

Dr. Szu-Yuan Pu and Prof. Shirit Einav contributed to the evaluation of all compounds mentioned in **Chapter 2** against DENV. Their extensive research in correlating AAK1 inhibition with antiviral efficacy led to a shared first authorship. The US army (Laura I. Prugar, Dr. Danielle E. Dorosky, Dr. Jennifer M. Brannan, Dr. John M. Dye) performed the antiviral assays against EBOV described in **Chapter 2**. Dr. Fiona J. Sorrell, Dr. Jon M. Elkins and Prof. Stefan Knapp performed the cocrystallisation of compound **1.15** with AAK1. The evaluation of AAK1 affinity of all compounds was performed by DiscoverX and ThermoFisher based on a fee-for-service. In **Chapter 3**, all compounds were investigated for MRGPRX2 antagonism in a  $\beta$ -arrestin assay performed by Yvonne Riedel, Dr. Mohamad Wessam Alnouri, Dr. Dominik Thimm and Prof. Christa Müller. Dr. Piotr Leonczak synthesized MRGPRX2 antagonists **3.13**, **3.3a-c**, **3.5a-d**, **3.18b**, **3.18d** and **3.21a-e** prior to the start of this thesis. The CCR8 flow cytometry binding assay and FLIPR calcium mobilization assay described in **Chapter 4** were carried out by Libao Liu, Dr. Tom Van Loy and Prof. Dominique Schols. Finally, Dr. Steven De Jonghe contributed in all aspects of this PhD thesis and in extensively proofreading this manuscript.

### **6.3. Conflict of interest statement**

No conflict of interest are declared

## CV and publications

Sven Verdonck was born in Diest, Belgium in 1991. He graduated as a master degree in drug development with distinction in 2015 at the KU Leuven. In August of the same year he started his PhD research at the Laboratory of Medicinal Chemistry at the Rega Institute for Medical Research, KU Leuven under supervision of Piet Herdewijn.

### Publications

---

**Verdonck, S\***; Pu, S.-Y\*.; Sorrell, F. J.; Elkins, J. M., Froeyen, Mathy, Gao, Ling-Jie, Prugar, Laura I., Dorosky, Danielle E., Brannan, Jennifer M., Barouch-Bentov, Rina, Knapp, Stefan, Dye, John M., Herdewijn, Piet, Einav, Shirit, De Jonghe, Steven. Synthesis and Structure–Activity Relationships of 3,5-Disubstituted-pyrrolo[2,3-b]pyridines as Inhibitors of Adaptor-Associated Kinase 1 with Antiviral Activity. *J. Med. Chem.* **2019**, *62* (12), 5810-5831.

\* Joint first author

### Scholarships

---

2016-2019 PhD Fellowship - Strategic basic research scholarship from the Research Foundation Flanders (FWO-SB Grant: 1S00116N)

### Attended Conferences

---

VIII EFMC International Symposium on Advances in Synthetic and Medicinal Chemistry (EFMC-ASMC 2019), Athens, Greece – September 1-5, 2019 – Poster Presentation